
Electronic Thesis and Dissertation Repository

4-28-2017 12:00 AM

The CDK-resistant pRB-E2F1 complex recruits chromatin-organizing proteins to repetitive DNA sequences

Charles A. Ishak
The University of Western Ontario

Supervisor
Dr. Fred Dick
The University of Western Ontario

Graduate Program in Biochemistry
A thesis submitted in partial fulfillment of the requirements for the degree in Doctor of Philosophy
© Charles A. Ishak 2017

Follow this and additional works at: <https://ir.lib.uwo.ca/etd>



Part of the [Molecular Biology Commons](#), [Molecular Genetics Commons](#), and the [Neoplasms Commons](#)

Recommended Citation

Ishak, Charles A., "The CDK-resistant pRB-E2F1 complex recruits chromatin-organizing proteins to repetitive DNA sequences" (2017). *Electronic Thesis and Dissertation Repository*. 4532.
<https://ir.lib.uwo.ca/etd/4532>

This Dissertation/Thesis is brought to you for free and open access by Scholarship@Western. It has been accepted for inclusion in Electronic Thesis and Dissertation Repository by an authorized administrator of Scholarship@Western. For more information, please contact wlsadmin@uwo.ca.

Abstract

This thesis investigates mechanistic links between genome integrity and the recruitment of chromatin organizing proteins to repetitive DNA sequences mediated by the retinoblastoma tumor suppressor protein (pRB). I demonstrate that a CDK-resistant interaction between the pRB C-terminus and the E2F1 coiled-coil marked box (CM) domain establishes a scaffold that facilitates recruitment of multiple chromatin-organizing proteins to repetitive sequences across the genome throughout the cell cycle. Specifically, pRB recruits the enhancer-of-zeste-homologue 2 (EZH2) histone methyltransferase to establish repressive facultative heterochromatin at repetitive sequences, and the Condensin II complex to ensure proper DNA replication and mitotic progression. To disrupt the CDK-resistant pRB-E2F1 interaction *in vivo*, a gene-targeted mutant mouse strain bearing a germline F832A substitution (RbI^S) is generated. Viable homozygous mutants permit exploration of CDK-resistant pRB-E2F1 functions in cell culture and *in vivo*. $RbI^{S/S}$ MEFs and adult splenocytes exhibit pronounced misregulation of endogenous retroviruses (ERVs), long interspersed nuclear elements (LINEs) and major satellites (MaSats). Misexpression is associated with reduced co-occupancy of pRB and EZH2, along with reduced H3K27me3 at repetitive genomic regions but not developmental H3K27me3 targets. Furthermore, $RbI^{S/S}$ MEFs exhibit increased γ H2AX, aneuploidy, ppRPA32, and chromosome segregation errors. γ H2AX accumulates specifically at major satellites that exhibit reduced co-occupancy of pRB and Condensin II. Collectively, the consequences of perturbed EZH2 and Condensin II recruitment contribute to a state of genomic instability in $RbI^{S/S}$ cells that likely underlie the onset of spontaneous lymphomas that arise from the spleen or mesenteric lymph nodes of aged homozygous mutant mice. Finally, I explore whether the pRB-E2F1 scaffold provides an opportunity for therapeutic exploitation, and whether these properties directly alter tumor phenotypes in combination with p53 inactivation. Overall, this work suggests that chromatin-organization mediated through the CDK-resistant pRB-E2F1 complex underscores a previously unknown facet of pRB-mediated tumor suppression.

Keywords

Retinoblastoma protein, genome instability, repetitive DNA, chromatin, enhancer-of-zeste-homologue 2, Condensin II.

Co-Authorship Statement

All chapters were written by Charles Ishak and edited by Dr. Fred Dick.

For chapter 2, Charles Ishak and Dr. Fred Dick conceived experiments. Charles Ishak executed all experiments with assistance as follows: Dr. Fred Dick, Dr. Matt Cecchini, and Dr. Daniel Passos generated the genetically engineered mouse model as depicted in Figure 2.2B-C. Aren Marshall generated the bioinformatics pipeline and guided Charles Ishak through all NGS analysis. Sara Ferwati used this pipeline to generate Figure 2.6A. Seung June Kim conducted the IP shown in Figure 2.3D. Dr. Carlee White conducted bisulfite sequencing with primers designed by Dr. William MacDonald for Figure 2.10A-B. Dr. Daniel Passos harvested RNA for qRT-PCR shown in Figure 2.6C, 2.12H, and 2.13A-B. Dr. Cecchini, Dr. Welch, and Dr. Howlett conducted pathological analysis for Figure 2.14B-C.

For chapter 3, Charles Ishak and Dr. Fred Dick conceived experiments. Charles Ishak executed all experiments with assistance as follows: Michael Roes assisted with IF staining and quantification in Figure 3.2B-C. Dr. Courtney Coschi generated transduced cell stocks and conducted live cell microscopy depicted in Figure 3.4C-D.

For chapter 4, Charles Ishak and Dr. Fred Dick conceived experiments. Charles Ishak executed all experiments with assistance as follows: Dr. Daniel Passos conducted IP injections and harvested RNA for qRT-PCR shown in Figure 4.3. David Carter of the London Regional Genomics Center used Partek to conduct the ANOVA and GO analysis to generate Figure 4.5. Dr. Matt Cecchini conducted histological analysis for Figure 4.7B-C, and Figure 4.8B.

Dedication

To my family who taught me to persevere

To Giulianna who reminds me about what matters most

Acknowledgments

I would like to thank my supervisor Dr. Fred Dick who provided me with more opportunities, resources, and training experiences than I could have possibly ever asked for. His dedication to scientific progress is matched by his dedication to trainee development. His patient guidance, mentorship, and encouragement created an environment that was conducive to engaging bold scientific lines of questioning through ambitious experimental undertakings. As a result of his mentorship, I have a permanent example of how to transition to become an independent investigator to hopefully pass on the mentorship that was provided to me.

I would like to thank my supervisory committee members Dr. Joe Torchia, Dr. Gabe DiMattia, and Dr. Rodney DeKoter. I am grateful for their frequent discussions and investment in my development throughout my tenure as a graduate student.

I would like to thank all past and present members of the Dick lab for their lasting positive impact on my time as a graduate student. Mike for his contagious scientific curiosity and friendship that were indispensable to my graduate experience. Aren for both her friendship and her patient guidance in teaching me skills that significantly elevated the work in this thesis. Daniel and James for their mentorship and consistent attentiveness to my development as a trainee. Piru and Joon for their friendship and frequent discussions that keep a positive environment in the lab. Finally, I would like to thank Matt, Courtney, and Srikanth who welcomed me into the lab, and mentored me through my steepest learning curves at the bench.

I would like to thank the people whose intangible support outside of the lab directly impacted my professional trajectory. To my parents and siblings, I am grateful for their constant support in every aspect of my life. My frequent trips back home were necessary to rejuvenate my motivation and ambition. Finally, I would like to thank Giulianna Misasi. I am grateful for your patience for all of the times that my work followed me well into the evenings and weekends. I am grateful for your unwavering love and support that were the foundation of my progress. Thank you for always being there for me.

Abbreviations

γ H2AX: Phosphorylation of H2AX at Serine 193

BrdU: 5-bromo-2-deoxyuridine

CAP-D3: chromosome associated protein D3

CD: cluster of differentiation

CDK: Cyclin-dependent kinase

ChIP: Chromatin immunoprecipitation

CKI: CDK inhibitor

C-terminal: carboxyterminal

DAPI: 4',6-Diamidino-2-Phenylindole

DNMT: DNA methyltransferase

DP: differentiation-regulated transcription factor 1 polypeptide

DRTF1: differentiation-regulated transcription factor 1

E2F: E2a-binding factor

ERV: endogenous retrovirus

ESC: embryonic stem cell

EZH2: enhancer-of-zeste-homologue 2

G1: gap 1 phase

G2: gap 2 phase

GST: glutathione S-transferase

H&E: hematoxylin and eosin

HAT: histone acetyltransferase

HDAC: histone deacetylase

HMT: Histone methyltransferase

IAP: intracisternal A-particle

IF: immunofluorescence

IFN: interferon

IgG: immunoglobulin G

INK4: inhibitor of CDK4

IP: immunoprecipitation

ISG: IFN-stimulated gene

kDa: kilodalton

KIP: kinase inhibitory protein

LINE: long interspersed nuclear element

LTR: long terminal repeat

LxCxE: Leucine-any amino acid-cysteine-any amino acid-glutamate

M: mitosis

MaSat: major satellite

MBD: marked box domain

MEF: mouse embryonic fibroblast

NGS: next generation sequencing

PcG: polycomb group

PI: propidium iodide

pRB: retinoblastoma tumor suppressor protein

PRC: polycomb repressor complex

RBI: retinoblastoma susceptibility gene

RBL1: retinoblastoma-like-1

RBL2: retinoblastoma-like-2

RBLP: pRB large pocket

RPA: replication protein A

S: DNA synthesis phase

seq: sequencing

SINE: short interspersed nuclear element

SMC: structural maintenance of chromosomes

TP53: tumor protein 53

UTR: untranslated region

Table of Contents

Abstract.....	i
Keywords.....	ii
Co-Authorship Statement.....	iii
Dedication.....	iv
Acknowledgments.....	v
Abbreviations.....	vi
Table of Contents.....	ix
List of Tables.....	xv
List of Figures.....	xvi
List of Appendices.....	xviii
Chapter 1.....	1
1 Introduction.....	1
1.1 Tandem repetitive elements.....	4
1.2 Interspersed repetitive elements.....	6
1.2.1 Type I transposable elements.....	7
1.2.2 Type II transposable elements.....	10
1.3 Host responses to repetitive elements.....	10
1.3.1 Host exaptation of genomic parasites.....	10
1.3.2 Host epigenetic silencing of repetitive elements.....	13
1.4 Genome instability is associated with repetitive element activation.....	23
1.5 Retinoblastoma onset reveals the existence of a tumor suppressor gene.....	24
1.6 The pocket domain defines the pRB pocket protein family.....	26
1.7 E2F transcription factors recruit pocket proteins to DNA.....	28
1.8 Cyclin Dependent Kinases govern cell cycle entry and progression.....	29

1.9	CDK-induced structural alterations govern pRB-E2F association dynamics.....	32
1.10	E2F1 binds the pRB C-terminus independent of small pocket interactions	34
1.11	Distinct biochemical properties underlie the alternate pRB-E2F1 interaction	35
1.12	Biochemical properties suggest cell cycle-independent functions of pRB-E2F1.	38
1.13	Rationale	42
1.14	Objectives	43
1.15	References.....	45
Chapter 2.....		61
2	An RB-EZH2 complex mediates cell cycle independent silencing of repetitive DNA sequences	61
2.1	Abstract.....	61
2.2	Introduction.....	61
2.3	Experimental Procedures	65
2.3.1	Cell Culture and Mice.....	65
2.3.2	Chromatin immunoprecipitation.....	65
2.3.3	RNA expression	65
2.3.4	Analysis of ChIP-seq and RNA-seq experiments.....	66
2.3.5	Generation of gene targeted mice	66
2.3.6	Cell cycle analysis.....	67
2.3.7	Cell extracts	67
2.3.8	Chromatin Fractionation	68
2.3.9	GST pulldowns	69
2.3.10	Immunoprecipitation.....	69
2.3.11	Splenocyte ChIP.....	69
2.3.12	ChIP-reChIP.....	70
2.3.13	ChIP-seq and Read Alignment.....	70

2.3.14	Peak Calling and annotation	71
2.3.15	deepTools enrichment analysis	71
2.3.16	RNA-sequencing.....	72
2.3.17	Expression microarray analysis	72
2.3.18	RNA-seq read alignment and analysis	73
2.3.19	Bisulfite sequencing.....	73
2.3.20	qRT-PCR analysis of expression	74
2.4	Results.....	75
2.4.1	The RB protein associates with repetitive genomic sequences	75
2.4.2	Loss of a CDK-resistant pRB-E2F1 interaction disrupts repeat association	78
2.4.3	pRB-repeat association is required for silencing of repetitive sequence expression.	89
2.4.4	H3K27me3 enrichment at repetitive sequences is pRB-dependent.....	94
2.4.5	pRB-chromatin association is required for EZH2 recruitment to repetitive sequences.	101
2.4.6	<i>Rbl</i> ^{S/S} mice succumb to spontaneous lymphoma.....	106
2.5	Discussion.....	110
2.6	References.....	114
Chapter 3	120
3	Disruption of CDK-resistant chromatin association by pRB causes DNA damage, mitotic errors, and reduces Condensin II recruitment.....	120
3.1	Abstract.....	120
3.2	Introduction.....	120
3.3	Experimental Procedures	122
3.3.1	Cell culture.....	122
3.3.2	Fluorescence microscopy.....	123
3.3.3	Flow cytometry	124

3.3.4	Detection of RNA and protein levels.....	124
3.3.5	Chromatin immunoprecipitation and ChIP-seq analysis	124
3.3.6	Video Microscopy.....	126
3.4	Results.....	126
3.4.1	The <i>Rbl</i> ^S mutation causes defects in genome integrity	126
3.4.2	Rb1S mutant cells exhibit defects in mitosis.	133
3.4.3	pRB-E2F1 recruits Condensin II to major satellites to mitigate DNA damage.	136
3.5	Discussion.....	141
3.6	References.....	143
Chapter 4.....		147
4	Disruption of the CDK-resistant pRB-E2F1 scaffold up-regulates L1 ORF2p, interferon response genes, and shifts tumor spectrum of <i>Trp53</i>^{-/-} mice	147
4.1	Introduction.....	147
4.2	Experimental Procedures	149
4.2.1	Cell culture and mouse colonies	149
4.2.2	Determination of protein and RNA expression	149
4.2.3	EZH2 inhibition	150
4.2.4	Retrotransposition Assay	151
4.2.5	Expression Microarray.....	151
4.2.6	CD4 CD8 thymocyte quantification	152
4.3	Results.....	152
4.3.1	Disruption of the CDK-resistant pRB-E2F1 interaction deregulates L1 ORF2p expression.....	152
4.3.2	GSK343 treatment de-represses repetitive elements in MEFs	153
4.3.3	GSK343 treatment de-represses repetitive elements in splenocytes.....	153
4.3.4	The CDK-resistant pRB-E2F1 complex suppresses retrotransposition of LINE1 reporters	157

4.3.5	Disruption of the CDK-resistant pRB-E2F1 interaction activates innate immune components	162
4.3.6	Disruption of the CDK-resistant pRB-E2F1 interaction does not alter thymocyte maturation	165
4.3.7	Disruption of the CDK-resistant pRB-E2F1 complex decreases tumor-free survival of <i>Trp53</i> ^{-/-} mice.	166
4.4	Discussion.....	171
4.5	References.....	175
Chapter 5	177
5	Discussion	177
5.1	Summary of findings.....	177
5.2	The CDK-resistant pRB-E2F1 scaffold recruits multiple complexes to repetitive sequences.	180
5.3	Do E2F-consensus motifs underlie pRB-E2F1 recruitment to repetitive elements? 182	
5.4	pRB-E2F1 repeat-recruitment independent of E2F consensus motifs?.....	186
5.5	pRB-E2F1 functions may underlie phenotypes associated with both regulated and unregulated repetitive element reactivation	188
5.6	Exploitation of pRB functions at repetitive elements	189
5.7	Summary of pRB-E2F1 functions at repetitive elements	193
5.8	References.....	194
Appendix A:	Permissions from Molecular Cell.....	199
Appendix B:	Permissions from Cancer Discovery	200
Appendix C:	Haploinsufficiency of an RB-E2F1-Condensin II complex leads to aberrant replication and aneuploidy	201
Appendix D:	List of primers used.....	215
Appendix E:	List of plasmids used	218
Appendix F:	List of antibodies used	218
Appendix G:	PCR Conditions.....	220

Curriculum Vitae 221

List of Tables

Table 1.1: Epigenetic alterations at repetitive elements in methyltransferase knockout models	17
---	----

List of Figures

Figure 1.1: Classification of repetitive elements.	3
Figure 1.2: Structural features underlie expansion strategies of repetitive elements.	5
Figure 1.3: DNA and histone modifications underlie chromatin accessibility.	14
Figure 1.4: pRB-E2F dissociation dynamics at the G1/S transition	37
Figure 2.1: pRB associates with genomic repeats in murine and human fibroblasts	76
Figure 2.2: <i>In vivo</i> disruption of the CDK-resistant pRB-E2F1 interaction.	79
Figure 2.3: The <i>Rbl^{S/S}</i> mutant maintains pRB cell cycle regulatory functions in primary mouse fibroblasts.	82
Figure 2.4: Cell cycle independent pRB-repeat association.	84
Figure 2.5: Occupancy of repetitive sequences by pRB and E2F1.....	87
Figure 2.6: pRB silences repetitive element expression.	90
Figure 2.7: Distinct transcript expression patterns in <i>Rbl^{S/S}</i> cells.	93
Figure 2.8: The <i>Rbl^{S/S}</i> mutant maintains normal H3K9 and H4K20 lysine methylation at repeats.	95
Figure 2.9: H3K27me3 enrichment at repetitive elements is pRB-dependent.	97
Figure 2.10: <i>Rbl^{S/S}</i> mutant cells retain DNA methylation at repetitive elements.....	100
Figure 2.11: pRB-chromatin association mediates EZH2 recruitment to repetitive DNA. ..	102
Figure 2.12: pRB-E2F1 dependent and independent roles for EZH2.....	104
Figure 2.13: Altered chromatin and repeat expression in <i>Rbl^{S/S}</i> splenocytes.....	107
Figure 2.14: Aged <i>Rbl^{S/S}</i> mice are tumor-prone.....	109

Figure 3.1: Disruption of pRB association with repetitive sequences.	127
Figure 3.2: Loss of genome integrity in <i>Rb1^{S/S}</i> mutant cells.	129
Figure 3.3: Normal expression of DNA replication targets of pRB-E2F.	132
Figure 3.4: Defective mitosis in <i>Rb1^{S/S}</i> mutant cells.	134
Figure 3.5: Normal expression of mitotic pRB-E2F target genes.	137
Figure 3.6: Recruitment of CAP-D3 by pRB mitigates DNA damage at pericentromeric major satellite repeats.	139
Figure 4.1: Disruption of the CDK-resistant pRB-E2F1 interaction de-represses L1 ORF2p.	154
Figure 4.2: GSK343 inhibition of EZH2 de-represses repetitive elements in MEFs.	155
Figure 4.3: GSK343 inhibition of EZH2 de-represses repetitive elements in splenocytes. .	158
Figure 4.4: pRB suppresses retrotransposition.	160
Figure 4.5: Upregulation of innate immune components upon loss of the CDK-resistant pRB-E2F1 interaction.	163
Figure 4.6: Disruption of the CDK-resistant pRB-E2F1 interaction does not alter thymocyte maturation.	167
Figure 4.7: Disruption of the CDK-resistant pRB-E2F1 interaction accelerates onset of tumorigenesis in a <i>Trp53^{-/-}</i> background.	169
Figure 4.8: Disruption of the CDK-resistant pRB-E2F1 interaction accelerates onset of thymic lymphomas in a <i>Trp53^{-/-}</i> background.	172
Figure 5.1: The CDK-resistant pRB-E2F1 scaffold recruits chromatin-organizing complexes to repetitive sequences.	179

List of Appendices

Appendix A: Permissions from Molecular Cell.....	199
Appendix B: Permissions from Cancer Discovery	200
Appendix C: Haploinsufficiency of an RB-E2F1-Condensin II complex leads to aberrant replication and aneuploidy	201
Appendix D: List of primers used.....	215
Appendix E: List of plasmids used	218
Appendix F: List of antibodies used	218
Appendix G: PCR Conditions.....	220

Chapter 1

1 Introduction

Recent advancements in sequencing capabilities have illuminated the sheer magnitude of repetitive sequences within the human genome. Nearly half of the mammalian genome is comprised of repetitive sequences, while single copy protein-coding sequences account for only 1-2% of total sequence content (Lander et al., 2001). Current models of the molecular genetics that underlie disease and development are predominantly based upon extensive characterizations of protein-coding sequences and the interactions of their protein products. In contrast, the contributions of repetitive sequences remain poorly understood and largely unaccounted for within these models.

This omission is especially surprising upon consideration that investigations of repetitive elements have yielded seminal concepts within the field of eukaryotic genetics, many of which earned Nobel Prizes. For example, Barbara McClintock's discovery of maize colour patterns driven by 'controlling elements' that could transpose to different chromosomal regions demonstrated that transposable elements existed and could regulate overt phenotypes of the individual (McClintock, 1950). A mechanism of transposition would emerge following the discovery that serologic tests against viral Gag proteins of the avian leukosis virus (ALV) could produce a positive signal in uninfected individuals (Dougherty and Di Stefano, 1966; Dougherty et al., 1967). The presence of viral-encoded proteins in the genome of uninfected individuals suggested that RNA viruses must integrate as DNA proviruses into the host germline. The discovery of reverse transcriptase by David Baltimore and Howard Temin provided a mechanism to explain

how RNA tumor viruses could ‘endogenize’ within the host (Baltimore, 1970; Temin and Mizutani, 1970). It also provided an explanation for the presence of the *src* viral oncogene (*v-src*) of the Rous Sarcoma Virus (RSV) within the genomes of uninfected chickens. Reactivation of endogenized RSV facilitated acquisition of *src* from the infected host (Stehelin et al., 1976). Thus, the concepts of mobile endogenous retroviruses that could regulate host phenotypes emerged.

Characterization of endogenous retroviruses revealed multiple repeating instances of their sequences within various eukaryotic genomes. Numerous classes and structural features of these repeating sequences were uncovered (Figure 1.1) (Weiss, 2006). Due to the mutagenic potential of mobilization, and homology of endogenous retroviruses to RNA tumor viruses, early investigations focused on potential links between repetitive sequence activity and genome instability (Mager and Stoye, 2015).

This thesis explores potential links between genome integrity and the recruitment of chromatin organizing proteins to repetitive DNA sequences. Propagation strategy underlies two possible genomic distribution patterns used to classify repetitive elements: tandem or interspersed (Wicker et al., 2007). Understanding the structural features and propagation strategies of tandem and interspersed repeats is fundamental to understanding how host responses to repetitive sequences create vulnerabilities that may underlie genome instability. Following this review, a survey of structure-function characteristics suggests that the retinoblastoma tumor suppressor protein may provide a link between genome instability and chromatin organization at repetitive sequences. The data chapters that follow present the results from experimental exploration of this hypothesis.

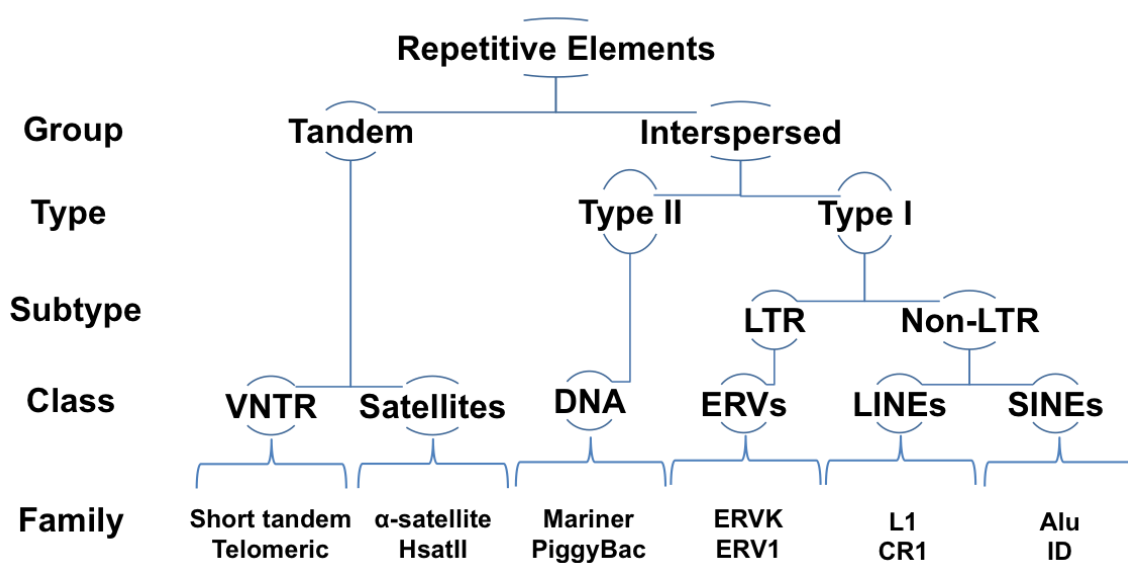


Figure 1.1: Classification of repetitive elements.

Repetitive elements are generally classified based upon genomic arrangement, expansion mechanism, and structural components. Only select families are listed for each repetitive element class.

1.1 Tandem repetitive elements

Tandem repetitive elements are characterized by sequential adjacent ‘head-to-tail’ recurrences of a particular sequence that most often accumulate at either end of a chromosome arm. Tandem repeats are further sub-classified based on the length of a single element that repeats sequentially (Gemayel et al., 2010). Tandem repeats have long been hypothesized to expand through strand slippage replication, in which either the template or nascent DNA strand denatures during replication and re-anneals such that one of the strands is ‘looped out’ and then re-anneals to another part of the repeat on the other strand. If the template strand is looped out, contraction occurs on the nascent strand, while looping out of the nascent strand results in expansion of the repeat (Levinson and Gutman, 1987; Tachida and Iizuka, 1992).

The visible accessory bands formed from density gradient centrifugation of genomic DNA were coined as ‘satellite’ DNA (Meselson et al., 1957). These bands were discovered to be comprised of the tandem DNA repeats that are primarily found at or near chromosome centromeres (Figure 1.2) (Walker, 1971). A satellite element that ranges from 1-10 nucleotides is classified as a microsatellite, also known as a simple sequence repeat, while elements that range from 10-60 nucleotides are minisatellites. Elements greater than this threshold are referred to as ‘satellites’ until 135bp in length, beyond which they are classified as megasatellites. Human centromeres and pericentromeres are both comprised of 171 bp α -satellites. In contrast, mouse

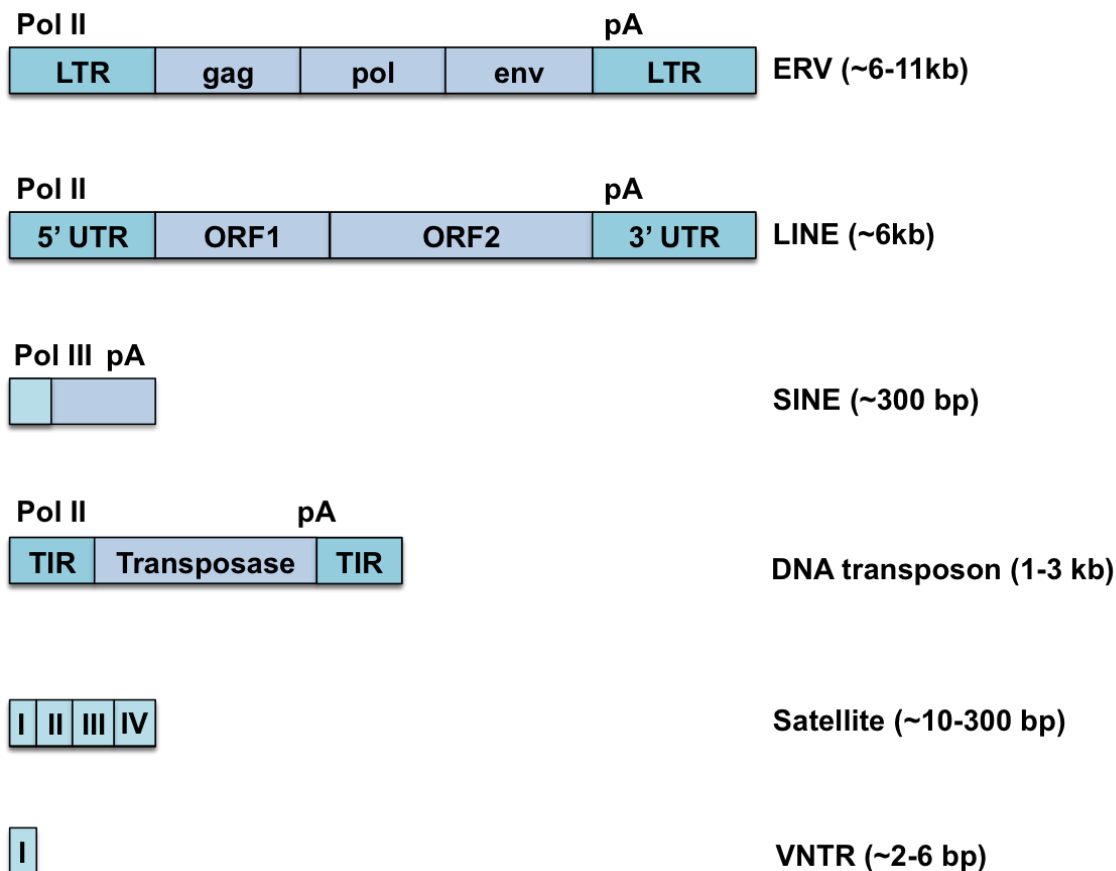


Figure 1.2: Structural features underlie expansion strategies of repetitive elements.

Structural features reveal whether repetitive elements encode machinery required for autonomous transposition. Full-length endogenous retroviruses (ERVs) are flanked by long terminal repeats and encode machinery required for autonomous retrotransposition. The two open reading frames (ORFs) of long interspersed nuclear elements (LINEs) encode machinery required for autonomous retrotransposition, and transposition of short interspersed nuclear elements (SINEs). In contrast to retrotransposons, DNA transposons are flanked by terminal inverted repeats (TIRs) and encode a transposase that facilitates transposition that is inherently non duplicative. Tandem repetitive elements may be comprised of as few as a single repeating subunit arranged in tandem as a result of replication errors. Relative RNA polymerase and polyadenylation sites are shown.

centromeres are comprised of 123-bp minor satellites, while their pericentromeres are comprised of 234-bp major satellites (Gemayel et al., 2010).

Satellite expansion occurs through replication machinery errors characterized as strand-slippage. However, recent evidence demonstrates that mammalian centromeric and pericentromeric repeats can also expand through an RNA intermediate that is reverse transcribed prior to re-integration into the host genome (Bersani et al., 2015). This provides a putative explanation for the identification of tandem repeat units found interspersed in isolation.

While satellites constitute their own class of tandem repeats, certain satellites are segregated within the ‘variable number of tandem repeat’ (VNTR) class. This includes microsatellites that are also called short tandem repeats or simple sequence repeats. Opposite to the centromere are another family of VNTRs. Vertebrate telomeric chromosome ends are comprised of tandem ‘TTAGG’ sequences that repeat from a few to over 100 kb depending on organism and age (Figure 1.2). These repeats extend into subtelomeric regions as well that encode G-rich transcripts known as telomere repeat-containing RNA (TERRA) that range from 0.1-10kb (Ye et al., 2014).

1.2 Interspersed repetitive elements

In contrast to tandem repetitive elements, interspersed repetitive elements are predominantly dispersed throughout the intergenic regions of the genome. Structural features and expansion strategies define classification systems of interspersed repeats. Unlike tandem repeats that expand primarily through replication errors, interspersed repeats expand through variations of transposition. For this reason, interspersed repeats

are alternatively referred to as transposable elements (Kazazian, 2004). Intact transposable elements encode machinery required to transpose and propagate autonomously throughout the host genome, and facilitate non-autonomous mobilization of partial elements. Mechanisms of propagation distinguish transposable element type and class (Jurka et al., 2007).

1.2.1 Type I transposable elements

Type I transposable elements undergo reverse-transcription during duplicative retrotransposition and are thus commonly referred to as retrotransposons (Boeke et al., 1985; Garfinkel et al., 1985; Kazazian and Moran, 1998). These elements are commonly flanked by target site duplications as a result of staggered nicks at the integration site that are ‘filled in’ upon repair. Sub-classifications of Type I elements are based on the presence or absence of long terminal repeat (LTR) elements (Figure 1.1) (Mager and Stoye, 2015). Non-LTR retrotransposons account for approximately 30-35% of the mammalian genome, and are further distinguished by the absence of an encoded envelope protein (Treangen and Salzberg, 2012).

The most abundant and active non-LTR retrotransposons are long interspersed nuclear elements (LINEs) that comprise ~21% of the human genome and were first characterized in human haemophilia (Dombroski et al., 1991; Kazazian et al., 1988; Rogan et al., 1987; Treangen and Salzberg, 2012). LINEs are believed to originate from host RNAs that were retrotransposed by active retrotransposons. The majority of the 1.5 million LINEs within the human genome are thought to reside as inactive fragments that often lack the promoter element due to 5' end truncations, however, approximately 80-100 full-length LINEs are thought to remain active (Beck et al., 2011). Full-length LINEs

possess a 5'UTR composed of tandem repeats with an internal RNA pol II promoter, followed by two open reading frames that encode machinery sufficient for autonomous retrotransposition, and finally a 3'UTR (Figure 1.2). ORF1 encodes an RNA-binding protein, while ORF2 encodes an endonuclease and reverse transcriptase (Kazazian and Moran, 1998). Structural variations of these modular domains distinguish phylogeny of LINE families into groups that are subdivided into clades. LINE ORF products are used to execute the mechanism of LINE retrotransposition called target-primed reverse transcription (TPRT) (Levin and Moran, 2011).

Short-interspersed nuclear elements (SINEs) represent the second most abundant group of non-LTR retrotransposons. SINEs comprise ~13% of the mammalian genome, and are derived from small functional RNAs transcribed by RNA pol III such as transfer RNAs (tRNAs) or 7S or 5S ribosomal RNAs (rRNAs) (Treangen and Salzberg, 2012). Thus due to their origins, SINEs contain 5' internal RNA pol III promoters. The 3' ends contain poly(A) tails that can be recognized by LINE ORF products (Figure 1.2). SINEs utilize machinery encoded by LINES to achieve non-autonomous retrotransposition. SINEs also contribute to SVA retrotransposons that can contain LTR sequences (Slotkin and Martienssen, 2007).

LTR-containing retrotransposons, more commonly referred to as endogenous retroviruses (ERVs), comprise approximately 8% of the human genome and 10% of the mouse genome (Treangen and Salzberg, 2012). These elements derive from ancient exogenous retroviruses that infected germ cells or progenitors of germ cells and lost the potential for extracellular mobility and infection following host integration. Replication-competent full-length ERVs contain 300-1000 bp LTRs flanking open reading frames

that collectively range from 6-9kb and encode Gag, Pol, and Env proteins to facilitate autonomous retrotransposition. More specifically, the Pol protein possesses a reverse transcriptase, endonuclease, and aspartyl protease domains (Figure 1.2). *Gag* encodes a ‘group-specific’ retroviral antigen, while *env* encodes an envelope protein (Göke and Ng, 2016). In addition, these elements contain an internal RNA polymerase II promoter sequence in the 5'LTR, an RNA polyadenylation sequence in the 3'LTR, signals for splicing, packaging, a tRNA primer-binding site, and a polypurine tract. Today, ERVs are more commonly found missing some ORFs, or missing all ORFs. Approximately 90% simply exist as solo LTRs. Phylogenetic analysis of the conserved regions of the *pol* gene dictates classification of ERVs into one of three classes that are further stratified into families (Thompson et al., 2016).

Beyond LINEs, SINEs, and ERVs, NGS-based exploration continues to uncover retrotransposons that do not meet all criteria for existing Type I transposable element categories. For example, Penelope retrotransposons possess a single ORF that encodes a protein with reverse transcriptase and endonuclease activity, are flanked by LTR-like inverted terminal repeats, but lack LTRs. However, phylogenetic analysis of the Penelope reverse transcriptase groups it closer to telomerases than reverse-transcriptases of other non-LTR retrotransposons. Thus, structural and phylogenetic divergence underlies classification of Penelope as a separate class of retrotransposons (Jurka et al., 2007). Likewise analysis of reverse-transcriptase domains suggests *Dictyostelium* intermediate repeat sequence (DIRS) retrotransposons derive from the ancestor of an LTR retrotransposon currently in the mammalian genome. However the endonuclease domain

most resembles analogous domains found in DNA transposon-like elements found in species of fungi and other ciliates (Wicker et al., 2007).

1.2.2 Type II transposable elements

Type II transposable elements, also known as DNA transposons, are most distinct from Type I counterparts based upon their mechanism of mobilization throughout the host genome. DNA transposons encode a transposase that recognizes flanking 10-400 bp long terminal inverted repeats (Figure 1.2). Upon recognition, the transposase excises the DNA element, and nicks a new target site to integrate the element into new 'acceptor' site. At no point is an RNA intermediate generated. The gap left at the original 'donor' site is repaired. Colloquially, this approach is referred to as 'cut-and-paste' transposition, and is distinct from the 'copy-and-paste' transposition approaches of Type I elements (Munoz-Lopez and García-Pérez, 2010). Differences in transposase homology primarily distinguish DNA transposase superfamilies. In addition to a transposase, some DNA transposon superfamilies also encode for DNA-binding proteins. Multiple instances of the same DNA transposon suggests that duplication of DNA transposons must occur despite the fact that DNA 'cut-and-paste' mobilization is not inherently duplicative. One model by which this can occur is transposition during replication. If a template element has been replicated and then transposes to a region that is yet to be replicated, the result is duplication of the element (Jurka et al., 2007).

1.3 Host responses to repetitive elements

1.3.1 Host exaptation of genomic parasites

The potential mutagenic consequences of indiscriminate repetitive element mobilization threaten host genome stability. Therefore the host adopts strategies that

reduce mobilization potential of these elements. Over evolutionary time, this results in the accumulation of relatively dormant repetitive sequences that eventually fragment to varying degrees. Host genomes co-opt portions of these fragments to serve as novel genes or transcriptional regulatory elements. This co-option is referred to as exaptation (Cowley and Oakey, 2013). Utility for host exaptation may underlie the long-term success of particular elements in host colonization. Such repeat-derived genes and regulatory elements are commonly utilized in a cell type-specific and temporal manner. Review of how repetitive elements have become intricate components of host regulatory networks illuminates the vulnerabilities associated with this dependence.

Repetitive element ORF sequences can be exapted as exons, or even full length genes. Up to 100 mammalian genes are believed to have evolved from repetitive elements. Over 50 protein-coding genes derive from the LTR retrotransposon *gag* protein, more than half of which reside on the X-chromosome (Thompson et al., 2016). Host dependence on such genes is most evident in the evolution of regulatory networks. For example in placental development, the human syncytin-1 and syncytin-2 proteins required for placental trophoblast formation derive from HERV ENV genes. Knock out of the mouse homologues syncytin-A and syncytin-B disrupts placental formation and impedes trophoblast fusion (Blaise et al., 2003).

Exaptation of repetitive elements is more frequently employed towards maximizing transcriptional regulatory control for existing host genes. Intact ERV LTRs are particularly favourable for exaptation since recombination between the 5' and 3' LTRs removes the internal ERV ORFs but preserves a residual 'solo' LTR for the host genome to utilize. These LTRs contain promoters, enhancers, transcription factor binding sites,

and can provide polyadenylation sites for host mRNA. Evolutionary exaptation of such elements now confers tissue-specific control over entire regulatory networks that are active within the mammalian placenta, the developing embryo, germ cells, and erythroid cells (Chuong et al., 2017).

Screening the 5' ends of host mRNA for evidence of LTR sequence identifies ERV LTRs that serve as functional host promoters. As promoters, ERV LTRs contribute functional binding sites for an expanding list of transcription factors that include p53, CTCF, ER α , c-Myc, and the pluripotency transcription factors NANOG, OCT4, and SOX2. Overall, 30% of all mammalian transcriptional start sites intersect with retrotransposons. The ability to direct pluripotency transcription factors in embryonic stem cells (ESCs) illustrates the prevalent exaptation of ERV LTRs by the host genome as tissue and cell type-specific promoters (Thompson et al., 2016).

ChIP-seq profiling has identified numerous repetitive sequences that bear the epigenetic marks associated with enhancer elements, such as H3K4me3, H3K27Ac, H3K9Ac. DNase-seq demonstrates that accessibility of these repetitive element-derived enhancers varies in a cell-type specific and tissue specific manner. ChIP-seq also reveals that these enhancers are extensively bound by pluripotency transcription factors in ESCs, germ cells, the placenta, and tissues that participate in sexual reproduction (Göke and Ng, 2016). While prediction of enhancer function is largely based upon gene proximity and epigenetic mark enrichment, direct loss-of-function approaches continue to confirm enhancer activity of these elements (Chuong et al., 2016).

1.3.2 Host epigenetic silencing of repetitive elements

Prior to repetitive sequence exaptation, the host modulates accessibility of repetitive sequences through alterations to the structural organization of DNA to render these elements dormant (Groh and Schotta, 2017). In the nucleus of a eukaryotic cell, the entire genome is wrapped around histone proteins in a compact arrangement referred to as chromatin. This arrangement consists of a repeating nucleosome core that possesses approximately 147 base pairs of DNA wrapped around a core histone protein octamer comprised of two H3-H4 dimers bound to two H2A-H2B dimers. The nucleosome base possesses an H1 'linker' histone involved in higher order compaction. Adjacent nucleosomes are connected by 10 - 80 bp of free 'linker' DNA (Venkatesh and Workman, 2015). Nucleosome compaction broadly distinguishes two general states of DNA accessibility. De-condensed chromatin establishes a 'relaxed' state referred to as 'euchromatin' in which nucleosome-wrapped DNA is most accessible. In contrast, the most compact form of chromatin, referred to as 'heterochromatin', characterizes the least accessible state (Figure 1.3) (Mozzetta et al., 2015).

Modulation of structure to regulate accessibility is achieved through a series of chemical modifications that do not alter DNA sequence. These modifications target the association between DNA and histones. Histones contain positively charged residues in their protruding tails that interact with the negatively charged double-stranded DNA backbone to facilitate an electrostatic interaction that maintains wrapped DNA around the nucleosome (Mozzetta et al., 2015). Covalent modifications imposed on histone tails or DNA alter the strength of the interaction with the double-stranded DNA backbone, leading to altered states of DNA accessibility. Through a combination of different

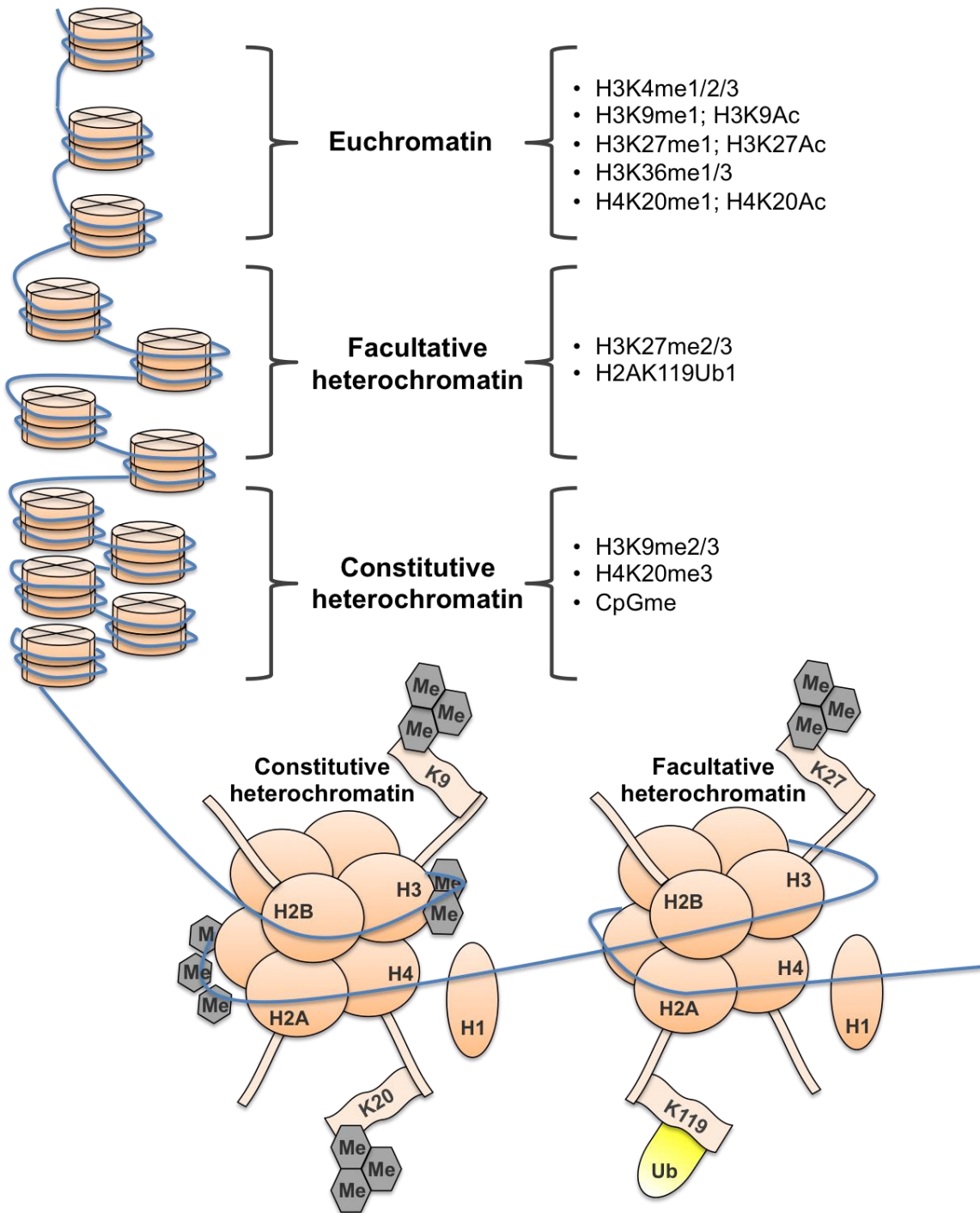


Figure 1.3: DNA and histone modifications underlie chromatin accessibility.

Relative DNA accessibility per chromatin state is indicated along with typically associated epigenetic modifications. Representative nucleosomes depict arrangements of modifications associated with constitutive or facultative heterochromatin.

modifications, repression can be achieved through establishment of ‘constitutive’ heterochromatin, or the more readily reversible and dynamic ‘facultative’ heterochromatin.

1.3.2.1 Constitutive heterochromatin through lysine methylation

Constitutive heterochromatin is characterized by a combination of epigenetic marks to both histone tails and DNA, and enrichment of the heterochromatin protein HP1. The most prevalent of these modifications consist of histone methylation (Saksouk et al., 2015). Histone methylation occurs primarily on the side-chains of lysines and arginines of histone H3 and histone H4. Methylation does not alter the charge of the histone, and can occur in successive magnitude as mono-, di-, or tri- methylation. When certain residues are methylated they hold DNA together strongly and restrict access to various enzymes. Since histone methylation can either compact or loosen chromatin, an empirically derived ‘histone code’ has emerged to classify the effects of differential methylation (Mozzetta et al., 2015).

Constitutive heterochromatin is most concentrated over centromeric and telomeric tandem repeats. In mice, pericentric heterochromatin can be readily visualized as DAPI-dense foci (Peters et al., 2003). H3K9me3 enrichment defines the fundamental H3 lysine methylation mark that distinguishes constitutive heterochromatin from facultative heterochromatin (Figure 1.3). In mammals, H3K9 residues are methylated by the suppressor of variegation 3-9 homolog (SUV39h) and SET domain bifurcated (SETDB1) histone methyltransferases (HMTs) (Martens et al., 2005). Dependence of either HMT depends on chromosome region, developmental context, and cell type. At pericentric heterochromatin, SUV39h HMTs are the dominant HMTs. Individual knockout of either

Suv39h1 or *Suv39h2* does not perturb viability and causes minimal changes to global H3K9me3 levels. In contrast, *Suv39h1/2* double knock out mice are viable at sub-mendelian ratios, and succumb to B-cell lymphomas with ~30% penetrance. *Suv39h1/2* double-knockout MEFs and ESCs exhibit pronounced reductions of H3K9me3 at pericentric major satellites and telomeric repeats (Table 1.1) (Lehnertz et al., 2003; Peters et al., 2001; Peters et al., 2003).

Unlike SUV39h HMTs, the role of SETDB1 at tandem repeats remains poorly understood. While ChIP-seq suggests that SETDB1 accumulates at pericentric repeats, other techniques fail to detect this accumulation (Dejardin and Kingston, 2009). Loss of SETDB1 diminishes H3K9me3 at pericentric repeats, indicating some degree of non-redundancy with SUV39h HMTs at these regions (Bulut-Karslioglu et al., 2012; Matsui et al., 2010). SETDB1 also targets interspersed repetitive elements. In mESCs, early embryos, and during gametogenesis, SETDB1 trimethylates H3K9 at repeats that include LINEs, and ERV classes I and II (Table 1.1) (Karimi et al., 2011; Liu et al., 2014; Matsui et al., 2010; Sharif et al., 2016). Following nucleation at interspersed repeats, H3K9me3 spreads across the retrotransposon gene body to extend into neighbouring genes, a phenomenon referred to as position effect variegation (Allis and Jenuwein, 2016).

Constitutive heterochromatin is also characterized by methylation of H4 lysine 20 (Figure 1.3) (Schotta et al., 2004). The SUV4-20H1 and 2 HMTs catalyze H4K20me2/3 deposition at centromeric, pericentric, and telomeric repeats (Jørgensen et al., 2013). Since recruitment is dependent on HP1 which itself recognizes H3K9me3, this is thought to be a downstream event relative to H3K9me3 (Schotta et al., 2004). Surprisingly, germline deletion of either *Suv4-20h1* or *Suv4-20h2* is not embryonic lethal

Table 1.1: Epigenetic alterations at repetitive elements in methyltransferase knockout models.

Murine model	Alteration	Cell type	Repeats affected
<i>Dnmt1</i> ^{-/-}	↓ CpGme	ESCs	Minor satellites, certain IAP LTRs
<i>Dnmt3a</i> ^{-/-}	↓ CpGme	ESCs	N/A
<i>Dnmt3b</i> ^{-/-}	↓ CpGme	ESCs	Minor satellites
<i>Dnmt3l</i> ^{-/-}	↓ CpGme	ESCs	Certain IAP LTRs and L1 elements
<i>Dnmt3c</i> ^{IAP/IAP}	↓ CpGme	P20 testis	Certain ERV-K and L1 elements
<i>Setdb1</i> ^{-/-}	↓ H3K9me3	ESCs	Major satellites, select LINEs and ERV-I/II elements
<i>Suv39h1</i> ^{-/-} ; <i>Suv39h2</i> ^{-/-}	↓ H3K9me3	ESCs, MEFS	Major satellites, telomeres
<i>Suv4-20h1</i> ^{-/-}	↓ H4K20me2	MEFS	Major satellites
<i>Suv4-20h2</i> ^{-/-}	↓ H4K20me3	MEFS	Major satellites

in mice, and *Suv4-20h*-double knockout mice are born at sub-mendelian ratios. *Suv4-20h1^{-/-}* MEFs exhibit modestly reduced H3K20me2 at pericentric repeats, while *Suv4-20h1^{-/-}* reduces H3K20me3 at pericentric repeats (Table 1.1). Ablation of both HMTs results in monomethylation at H4K20 residues normally di- or tri-methylated (Schotta et al., 2008).

1.3.2.2 Constitutive heterochromatin through hypoacetylation

Another epigenetic feature of constitutive heterochromatin is the absence of modifications that neutralize electrostatic interactions between DNA and histones (Jeppesen and Turner, 1993). Histone acetylation and phosphorylation both neutralize the positive charge of histone tails to diminish affinity for proximal negatively charged DNA strands (Brehove et al., 2015; Saksouk et al., 2015). This leads to a less compact chromatin structure that facilitates DNA accessibility. Examples of phosphorylation marks that achieve this include phosphorylation of H2A.X at serine 129 during DNA damage (Brehove et al., 2015). However, for the context of constitutive heterochromatin, regulation of histone acetylation is more pertinent.

Acetylation marks on histone tail lysines are commonly enriched at enhancer elements and gene promoters to facilitate access for transcription factors (Figure 1.3). Histone acetyl transferases (HATs) catalyze the transfer of acetyl groups from acetyl-coenzyme A (acetyl CoA) to positively charged lysines on histone tails such as H3K9, H3K18, and H3K27 (Verdin and Ott, 2015). Conversely, histone de-acetylases (HDACs) catalyze the removal of acetyl groups from histone tails to re-compact chromatin (Taunton et al., 1996). Thus constitutive heterochromatin is also characterized by hypoacetylated histones due to HDAC activity. Accordingly, disruption of HDAC

activity using HDAC inhibitors can suffice to de-repress repetitive elements silenced by constitutive heterochromatin (Garcia-Perez et al., 2010).

1.3.2.3 Constitutive heterochromatin through DNA methylation

DNA methylation describes the addition of a methyl (CH₃) group predominantly to carbon 5 of a cytosine residue adjacent to a guanosine that forms the repetitive unit of CpG dinucleotides. The addition of the methyl group reduces DNA accessibility to proteins that bind chromatin (Jones, 2012). This reduced accessibility contributes to the suppressive properties of constitutive heterochromatin used to silence repetitive DNA sequences (Smith and Meissner, 2013). DNA methyltransferases (DNMTs) methylate target cytosines. In mammalian cells, DNMT3A and DNMT3B catalyze *de novo* methylation, while DNMT1 is required for the maintenance of DNA methylation in particular during genome replication when passive demethylation can occur (Okano et al., 1999) (Li et al., 1992). The recently discovered DNMT3C also imparts *de novo* DNA methylation, however its activity is exclusive to male germ cells (Barau et al., 2016). The DNMT3 homologue DNMT3L lacks catalytic activity but enhances DNA binding and activity of the *de novo* DNMTs (Hata et al., 2002).

DNA methylation is enriched at centomeric and subtelomeric tandem repeats in addition to interspersed repetitive sequences. Surprisingly, individual ablation of *de novo* DNMTs results in minimal CpG methylation reductions at repetitive sequences. *Dnmt3a*^{-/-} mice are viable up to four weeks of age, while *Dnmt3b*^{-/-} mice are embryonic lethal at E9.5 (Okano et al., 1999). Examination of E9.5 ESCs from either model reveals that notable CpG methylation reductions are limited to minor satellites in *Dnmt3b*^{-/-} cells (Table 1.1) (Okano et al., 1999). Likewise, disruption of DNMT3C activity has limited

effects on methylation of repetitive sequences. The *Dnmt3c*^{IAP} allele disrupts expression of the full length *Dnmt3c* transcript due to an IAP insertion that results in exclusion of the last exon. This exclusion diminishes CpG methylation at a select number of ERV-K and L1 members only in the testes of day 20 homozygous mutant animals (Table 1.1) (Barau et al., 2016).

Analogous to *Dnmt3c* inactivation, deletion of *Dnmt3l* in murine models does not induce embryonic lethality (Hata et al., 2002). *Dnmt3l*^{-/-} cells exhibit loss of *de novo* cytosine methylation at specific IAP LTRs and certain LINE1s but not centromeric or pericentric satellites (Table 1.1) (Bourc'his and Bestor, 2004; Hata et al., 2002). *Dnmt1*^{-/-} mice are embryonic lethal at E9, and exhibit reductions of CpG methylation at IAP and centromeric satellites in ESCs (Table 1.1) (Colum et al., 1998; Li et al., 1992). A germline *Dnmt1* hypomorphic murine model exhibits reductions of CpG methylation at IAPs in MEFs, with novel MMTV integrations detectable in a subset of the resulting T-cell lymphomas in adult mice (Gaudet et al., 2003; Howard et al., 2008).

1.3.2.4 Facultative heterochromatin dynamics at repetitive sequences

In contrast to constitutive heterochromatin, facultative heterochromatin establishes a more readily reversible form of chromatin compaction (Trojer and Reinberg, 2007). Facultative heterochromatin is distinguished by H3 methylation at K27 by the enhancer-of-zeste homologue (EZH) HMTs, EZH1 and EZH2 (Figure 1.3). Each HMT belongs to multi-subunit complexes referred to as Polycomb Group (PcG) complexes that were originally identified and characterized in *D.melanogaster* (Abel et al., 1996; Hobert et al., 1996; Jones and Gelbart, 1990, 1993). H3K27me2/H3K27me3 is largely

established by polycomb repressive complex 2 (PRC2) that contain suppressor of zeste 12 homologue (SUZ12), embryonic ectoderm development (EED), and either retinoblastoma-associated protein 46 (RBAP46) or retinoblastoma-associated protein 48 (RBAP48) (O'Carroll et al., 2001; Su et al., 2003; van der Vlag and Otte, 1999). Distinct PRC2 complexes contain either EZH1 or EZH2, however EZH2-containing PRC2 complexes are most prevalent in mammalian cells. PRC2 establishes facultative heterochromatin in concert with polycomb repressor complex 1 (PRC1) that deposits H2AK119Ub1 (Figure 1.3) (Hauri et al., 2016; Margueron et al., 2008). In contrast to constitutive heterochromatin, the contribution of facultative heterochromatin-based repeat silencing remains poorly understood in mammalian ESCs, and relatively uninvestigated in somatic cells (Casa and Gabellini, 2012; Leeb et al., 2010). Expression patterns of repetitive elements in germline knockouts for effectors of constitutive heterochromatin provide some indication of possible roles of facultative heterochromatin and polycomb contributions towards repetitive element silencing.

Redundancy of repetitive sequence silencing has been most characterized within the context of embryogenesis, during which successive rounds of DNA methylation and demethylation occur. Despite reductions of DNA methylation, silencing of repetitive elements is maintained through modification of histone tails (Leung and Lorincz, 2012; Rowe and Trono, 2011). This phenomenon is recapitulated in *Dnmt1*, *Dnmt3a*, and *Dnmt3b* triple-knockout ESCs that exhibit proper silencing of repetitive elements (Karimi et al., 2011). In these cells, pronounced reductions in CpG methylation and H3K9me2/3 precede compensatory recruitment of PRC2 and H3K27me3 deposition at pericentric repeats (Saksouk et al., 2014). In contrast to germline knockouts that may be confounded

by long-term adaptation, acute loss of DNA methylation can be modeled through the ‘2i+VitC’ treatment in which GSK2 β and Mek1/2 inhibitors are used to ensure passive demethylation, while vitamin C stimulates TET enzymes that engage in active demethylation (Walter et al., 2016). In ESCs treated with 2i+VitC, H3K9me2 levels decrease, H3K9me3 levels remain constant, but H3K27me3 increases to maintain repetitive element silencing (Walter et al., 2016).

The sensitivity of H3K9me2/3 deposition to CpG methylation loss in *Dnmt* triple-knockout ESCs suggests that facultative heterochromatinization may compensate for loss of H3K9me3 alone (Déjardin, 2015). Indeed, in SUV39h1/2-deficient ESCs, PRC2 and H3K27me3 are recruited to repetitive sequences (Cooper et al., 2014). Pronounced misregulation of repetitive elements is only achieved upon 2i+VitC treatment of SUV39h1/2-deficient ESCs in combination with *Eed* knockout to disrupt PRC2 function (Walter et al., 2016). Likewise, depletion of all three HP1 isoforms in ESCs does not result in strong de-repression of repetitive elements (Maksakova et al., 2011). Even in MEFs, SETDB1 ablation results in minimal ERV de-repression, indicating presence of compensatory silencing in more differentiated cells (Maksakova et al., 2011). This suggests that facultative heterochromatin provides a sensitive and dynamic compensatory response to maintain repetitive element silencing upon disruption of constitutive heterochromatin marks. Its contributions towards silencing in normal somatic cells remain unknown.

1.4 Genome instability is associated with repetitive element activation

Despite redundancy and compensatory potential of epigenetic silencing mechanisms, associations between repetitive element misregulation and genomic instability are well established (Belancio et al., 2010; Dombroski et al., 1991; Ionov et al., 1993; Kazazian et al., 1988; Miki et al., 1992; Strand et al., 1993). Consequences of this misregulation are directly related to host strategies of repetitive element exaptation and silencing. For instance, alleviation of epigenetic silencing permits cis- or trans- regulatory activation by repetitive elements of adjacent genes (Lau et al., 2014). This has been observed for the MaLR THE solo LTR that activates the normally silenced CSF1R in Hodgkin lymphoma (Lamprecht et al., 2010). Furthermore, re-integration of tandem or interspersed repeats can drive mutagenesis by ablating expression, causing hypomorphic expression, or conferring oncogenic gain-of-function by providing alternate splice sites within gene bodies. This has been observed most frequently with mobile centromeric satellite repeats or LINE elements in human colorectal tumors (Bersani et al., 2015; Doucet-O'Hare et al., 2015; Miki et al., 1992; Rodic et al., 2015; Shukla et al., 2013). In addition, the meiotic and mitotic defects that accompany repetitive element misregulation suggest a yet unidentified connection between repeat-derived organization of chromosome structure and chromosome segregation (Ionov et al., 1993). Evidence that these may be early events in human cancer appears to be corroborated by NGS-based characterizations of pre-malignant lesions that harbor active repetitive elements (Ewing et al., 2015; Rodic et al., 2015).

Disruption of broad mechanisms that regulate chromatin structure likely underlie frequent resurrection of repetitive elements under conditions of genomic instability. While the effectors of these marks have been characterized to varying degrees, mechanisms of recruitment to repeats remain poorly understood. An unexplored link between the organization of heterochromatin at repetitive sequences and cancer-initiating mechanisms may be the RB tumor suppressor protein (pRB). Thorough review of known pRB activities illuminates multiple connections that position pRB as a likely candidate to mediate recruitment to repetitive elements for broad organizers of chromatin structure.

1.5 Retinoblastoma onset reveals the existence of a tumor suppressor gene

Loss of growth control through tumor suppressor inactivation is a universal ‘hallmark’ of every human cancer (Hanahan and Weinberg, 2011). The concept of tumor suppressor inactivation in cancer originates from studies of fusions between normal and cancer cells, and analyses of retinoblastoma incidence (Harris and Miller, 1969; Knudson, 1971). By the early 1970s, multiple studies suggested that cancers likely arose through multistage accumulation of mutations (Ashley, 1969). However, in 1971, Dr. Alfred Knudsen’s statistical analysis suggested that retinoblastomas arose through a minimum of two ‘events’. This analysis noted that bilateral inherited cases of retinoblastoma occurred at a younger age than unilateral non-inherited retinoblastoma. David Comings proposed that differences in time of cancer onset and tumor frequency amongst the two groups must be caused by ‘loss-of-function’ mutations to both alleles of a single critical ‘tumor-suppressive’ gene (Comings, 1973).

Assuming a constant rate of mutation for this gene, individual differences in complete inactivation must be due to a difference in the number of functional copies inherited. Individuals who inherit a germline mutation in one allele simply require the acquisition of a single inactivating mutation in the remaining functional allele to completely inactivate the gene. This would decrease tumor latency and increase tumor burden relative to patients that must acquire two independent inactivating somatic mutations (Comings, 1973; Knudson, 1971). This conclusion would be coined the 'two-hit' hypothesis. Subsequent genetic studies of retinoblastomas identified that loss of the q14 segment of chromosome 13 was associated with the appearance of retinoblastoma (Cavenee et al., 1984; Cavenee et al., 1983; Cavenee et al., 1985; Dryja et al., 1986; Godbout et al., 1983). In 1986, a single gene mapped from this segment of chromosome 13 was cloned and confirmed to be deleted in retinoblastomas and sarcomas (Friend et al., 1986; Lee et al., 1987). This gene became known as the retinoblastoma susceptibility gene, abbreviated as *RBI*.

Today, the *RBI* gene product, pRB, is recognized as one of the most frequently inactivated tumor suppressors in human cancer, and has been the center of intense investigation within the field of cancer biology (Dyson, 1998; Weinberg, 1995). Homozygous deletion of murine *Rb1* results in embryonic lethality, while *Rb1*^{+/-} mice succumb to pituitary tumors in concert with loss of the remaining wild-type allele (Clarke et al., 1992; Jacks et al., 1992; Lee et al., 1992). Therefore, early loss-of-function molecular investigations were predominantly limited to cell culture experiments with *Rb1*^{-/-} MEFs, or characterizations of patient-derived cancer cells with *RBI* deficiency (DeCaprio et al., 1989; Ewen et al., 1991; Goodrich et al., 1991; Hannon et al., 1993;

Horowitz et al., 1989; Muncaster et al., 1992; Williams et al., 1994). These early investigations identified two more *RBI*-like genes, p107 and p130, and characterized numerous pRB functions that would prove advantageous if disabled in cancer (Dyson, 1998; Ewen et al., 1991; Hannon et al., 1993; Weinberg, 1995). Notably, pRB was observed to impart negative growth control through restriction of G1 exit. However, identification of a single indispensable tumor suppressor activity remains an area of contention, and currently appears to be multifaceted (Dyson, 2016). The known functions of pRB have emerged in tandem with discovery of the pRB interactome. Therefore, understanding of pRB function requires understanding of the structural underpinnings that govern the pRB interactome.

1.6 The pocket domain defines the pRB pocket protein family

The structural feature that defines the pRB-family is the hydrophobic small pocket domain that consists of two cyclin-like folds, referred to as the A and B subdomains respectively, separated by an unstructured linker region (Chow and Dean, 1996; Huang et al., 1993; Qin et al., 1992). For this reason, pRB and the pRB homologues p107 and p130 are collectively referred to as the ‘pocket protein’ family. The small pocket domain contains the minimal segment required to interact with viral oncoproteins that include adenovirus E1A, human papilloma virus E7, and Simian vacuolating virus 40 large T antigen (DeCaprio et al., 1988; Dyson et al., 1989; Huang et al., 1993; Whyte et al., 1988). This minimal segment harbors a shallow hydrophobic binding cleft found within the B subdomain referred to as the LxCxE binding cleft since oncoproteins found to bind this region possess a conserved LxCxE peptide motif (Kaelin

et al., 1990; Lee et al., 1998). Discovery that DNA tumor viruses targeted pocket proteins and that the interaction appeared necessary for transformation proved amongst the earliest evidence for a tumor suppressive role for pRB family proteins.

Downstream of the small pocket domain of pocket proteins is the intrinsically unstructured carboxy-terminus (C-terminus). Within human pRB, the small pocket and C-terminus encompass a region from residues 379-928 and are referred to as the large pocket. This region was originally defined as the minimal region required to maintain negative growth control (Qin et al., 1992). Early mechanistic investigations attributed this restriction to an interaction with the differentiation-regulated transcription factor 1 (DRTF1) that was determined to be the E2a-binding factor (E2F) (Bandara and La Thangue, 1991; Chellappan et al., 1991; Kovesdi et al., 1987). This transcription factor was found to bind DRTF1-polypeptide-1 (DP1) to form a functional heterodimeric transcription factor (Girling et al., 1993). Through the use of tumor-derived *RBI* mutants, viral oncoprotein-induced inactivation, and E2F interaction studies, an emerging model of mammalian cell cycle control proposed that pRB-family proteins associated with E2F/DP transcription factors to silence genes involved in cell cycle progression. These genes were discovered to contain an E2F-consensus or recognition motif within their promoters that were responsive to E2F-dependent transcription in transfection-based reporter assays (Boeuf et al., 1990; Kovesdi et al., 1987; Yee et al., 1987). Temporal signals governed dissociation of pRB proteins from E2F/DP to permit the transcription of these genes in a controlled manner (DeCaprio et al., 1989; Hurford et al., 1997). DNA tumor virus proteins could bind the pRB-family small pocket to perturb this temporal control and prevent negative growth control in cancer.

1.7 E2F transcription factors recruit pocket proteins to DNA

Since pocket proteins were discovered to lack intrinsic DNA binding activity, the discovery of E2F-mediated pocket protein recruitment to cell cycle promoters presented a starting point to investigate differential transcriptional properties of pocket proteins. In mammals, the pocket protein-E2F network expanded considerably to eventually consist of eight *E2F* genes that encode 9 protein products, as E2F3a and E2F3b are generated by the use of alternative promoters (Johnson and Degregori, 2006). E2Fs are defined by their ability to bind to a sequence element that was originally identified in the adenovirus E2 promoter (Boeuf et al., 1990; Kovesdi et al., 1987; Yee et al., 1987).

With respect to structure, all E2F family members possess a highly conserved DNA binding domain (Morgunova et al., 2015; Zheng et al., 1999). A highly conserved dimerization domain allows E2F1-6 to interact with DP family members to confer specificity of DNA binding. As with the E2Fs, the DP family has expanded to consist of four members that exhibit differential preference for endogenous association with E2Fs. In contrast, E2F7 and E2F8 do not dimerize with DP family members, but instead bind as homodimers or E2F7-E2F8 heterodimers (Morgunova et al., 2015). E2F1-5 possess a transactivation domain required for activation of respective gene targets. Embedded within the E2F transactivation domain is a highly conserved segment that mediates binding of E2F1-4 to the pRB small pocket. E2F4 and E2F5 interact with p107, and p130. E2F6, E2F7, and E2F8 do not interact with any pocket proteins (Dimova and Dyson, 2005; van den Heuvel and Dyson, 2008).

Historically, the E2F transcription factors have been classified into two distinct functional categories based upon their observed ability to either activate or repress

transcription of simple reporter constructs possessing multiple E2F-binding sites in cell culture-based assays. E2F1, E2F2, and E2F3a, comprise one subfamily referred to as ‘activator E2Fs’, while the remaining E2F family members are classified as ‘repressor E2Fs’. This historical classification appears to be an oversimplification as large-scale expression studies demonstrate that ‘activator E2Fs’ repress almost as many targets as they activate (Henley and Dick, 2012).

1.8 Cyclin Dependent Kinases govern cell cycle entry and progression

As the rudimentary model of pRB-mediated E2F repression emerged, a family of serine/threonine kinases, called the cyclin-dependent kinases (CDKs), were identified as likely determinants of cell-cycle dependent pRB-E2F dissociation (Bremner et al., 1995; DeCaprio et al., 1992; DeCaprio et al., 1989). CDK-consensus sites were discovered throughout the pRB protein, and over expression of Cyclin E or Cyclin A was discovered to allow cells to escape pRB-mediated cell cycle arrest (Bandara et al., 1991). These observations appeared to complement early observations that pRB became heavily modified during the G1-to-S transition (DeCaprio et al., 1989). However, the nature of these modifications and their effects on proliferative control would emerge in tandem with elucidation of the cyclin-CDK signaling network.

Cyclin dependent kinases comprise the core components of eukaryotic cell cycle regulatory machinery. In mammals, there are currently 20 members of the CDK family, each of which possess a conserved catalytic core comprised of an ATP-binding pocket, a PSTAIRE-like cyclin-binding domain, and an activating T-loop motif (Malumbres, 2014). CDK activity depends on association with regulatory subunits called cyclins that

are defined by a conserved sequence involved in CDK-binding and activation. While endogenous CDK levels remain relatively consistent, cyclin protein levels fluctuate in accordance with cell cycle stage (Evans et al., 1983). Upon stabilization of a certain cyclin, association with the appropriate CDK forms a cyclin-CDK complex in which the cyclin enhances CDK activity, and directs the complex to the appropriate target protein. Activation of the kinase requires phosphorylation of a conserved threonine residue on the activating CDK T-loop. In metazoans, CDK7 binds cyclin H to initiate CDK T-loop activation (Tassan et al., 1994).

Cell cycle entry begins with an increase in D-type cyclins (D1, D2, and D3) that bind CKD4 and CDK6 to initiate progression past the G1 'restriction point', a crucial point at which the cell irreversibly commits to cell cycle entry (Hochegger et al., 2008). Different D-type cyclins are activated in response to extracellular signals that stimulate different surface receptors. For example, mitogenic growth factors activate receptor tyrosine kinases on the cell surface to induce signalling cascades that ultimately result in the AP-1 transcription factor binding to and activating the cyclin D1 promoter, resulting in rapid accumulation of cyclin D1 (Donjerkovic and Scott, 2000).

After the restriction point in late G1, E-type cyclins (E1 and E2) associate with CDK2. Cyclin E-CDK2 complexes phosphorylate substrates to promote entry into S-phase, upon which A-type cyclins (A1 and A2) replace E-type cyclins to form cyclin A-CDK2 complexes. As S-phase progresses, CDK1 becomes the most abundant CDK associated with the A-type cyclins (Bertoli et al., 2013). In late G2 phase, B-type cyclins (B1 and B2) replace A-type cyclins to form Cyclin B-CDK1 complexes required for mitotic entry and progression. Rapid increase of one type of cyclin just prior to cyclin-

CDK complex formation occurs in accordance with rapid degradation of the preceding prominent cyclin (Glotzer et al., 1991). Thus, beyond the G1 restriction point, cyclin-CDK complex formation and activation occurs in an autonomous manner to ensure completion of the cell cycle.

Just as mitogenic signals positively regulate cyclin-CDK activity, antimitogenic signals exert antagonistic effects through endogenous CDK inhibitors (CKIs) (Sherr and Roberts, 1995). CDK inhibitors are generally classified within two families. The first is an abbreviation based on originally observed functions towards inhibiting CDK4. The **in**hibitors of **CDK4**, or INK4, family of CKIs target G1 cyclin-CDK4/CDK6 complexes. The four INK4 proteins, p16^{INK4A}, p15^{INK4B}, p18^{INK4C}, and p19^{INK4D} bind and distort the cyclin-binding site and the ATP-binding site of CDK4/6 to compromise catalytic activity through allosteric inhibition of cyclin and ATP binding. The **CDK interacting protein/Kinase inhibitory protein**, or Cip/Kip, family of CKIs consists of p21^{Cip1/Waf1}, p27^{Kip1}, and p57^{Kip2}. Like INK4 CKIs, Cip/Kip CKIs obstruct the ATP-binding site of their target CDKs to achieve allosteric inhibition. However, Cip/Kip CKIs typically target cyclin-CDK complexes active in late G1 and S-phase, specifically CDK4 and CDK2. As negative regulators of cell cycle entry and progression, both Ink4 and Cip/Kip CKIs are frequently inactivated in human cancers (Asghar et al., 2015).

Despite the emergence of a complex cyclin-CDK regulatory network, viable CDK knock out mouse models suggest a high degree of redundancy amongst CDKs involved in mammalian cell cycle progression. In contrast to cell cycle regulation, CDK members involved in transcriptional control function non-redundantly as ablation results in embryonic lethality for knockouts of CDK7, CDK8, and CDK11. Likewise, viable CKI

knockout models reveal a high degree of functional redundancy, with overt phenotypes most apparent in compound mutant backgrounds. The exception to this is p57^{Kip2} knockout that causes embryonic lethality (Malumbres, 2014).

1.9 CDK-induced structural alterations govern pRB-E2F association dynamics

The elucidation of the cyclin-CDK network has proven crucial to understanding determinants of pRB-E2F association and function throughout the mammalian cell cycle. Prior to the G1-S transition, hypophosphorylated pRB binds E2Fs at E2F cell cycle promoters. Inhibition of E2F-dependent transactivation depends on a direct physical interaction between the A-B interface of the pRB large pocket (RBLP) domain (residues 379-928) and the C-terminal transcriptional activation domain of E2Fs (Qin et al., 1992) (Chow and Dean, 1996; Dick et al., 2000; Huang et al., 1993). Co-crystallization studies of the pRB small pocket and the E2F2 transactivation domain identify molecular contact points which occur primarily through basic residues of the A region of RBLP, and acidic residues of the E2F transactivation domain (Lee et al., 2002). However, stable binding and full repression of E2F activity requires the pRB C-terminus as well (Burke et al., 2013; Sengupta et al., 2015). This binding and physical masking of the E2F transactivation domain is thought to be one of the mechanisms by which pRB renders E2Fs transcriptionally inactive.

Alleviation of E2F transcriptional repression occurs in tandem with CDK-mediated phosphorylation of pRB at the G1-S transition. This is initiated by cyclin D-CDK4/6 followed by cyclin E-CDK2 complexes (Calbó et al., 2002). Consensus mapping identifies 16 potential CDK phosphorylation sites on human pRB, 13 of which have been

confirmed *in vivo*. The majority of these sites occur in pairs distributed primarily throughout the intrinsically disordered regions of the protein (Rubin, 2013). A minimal docking site mapped within pRB-C-terminus mediates competitive association with either CDKs or the PP1 phosphatase (Hirschi et al., 2010). The conformational effects of CDK-induced phosphorylation ultimately dissociates pRB from E2Fs (Burke et al., 2012). The elucidation of a CDK phosphorylation code on pRB has evolved through structural and functional investigations.

The current model of how particular CDK phosphorylation events displace E2Fs from the small pocket is based upon structural investigation that utilized pRB and E2F fragments with truncated or absent linker regions and phosphomimetic residue substitutions. These investigations conclude that phosphorylation at S608/S612 within the linker region between the cyclin-like folds of the small pocket causes a sequence within the linker to bind the pocket as a helix that competes with the E2F transactivation domain (Burke et al., 2010). Furthermore, phosphorylation at T356/T373 causes regions of the pRB N-terminus to dock against the pocket subdomains, widening the E2F-binding site between the cyclin-like folds to a degree that allosterically inhibits E2F transactivation domain binding to the pocket. This also occludes protein binding to the LxCxE binding cleft. This effect can be recapitulated to a lesser extent with phosphorylation of T373 alone (Burke et al., 2012). Phosphorylation of S788/S795 induces an association between a region within the pRB-C-terminus, and the pocket domain to disrupt pocket contact points with the most upstream residues of the E2F transactivation domain (Burke et al., 2013). Collectively, multiple CDK phosphorylations induce intramolecular interactions between both pRB termini into the pocket region to achieve an additive effect that

enhances disruption between the pRB pocket and E2F transactivation domain (Dick and Rubin, 2013).

1.10 E2F1 binds the pRB C-terminus independent of small pocket interactions

The model of CDK-induced conformational changes suffices to explain association and dissociation dynamics of most of the ‘activator’ E2Fs with pRB. However, synthetic pRB mutants designed to disrupt RBLP-E2F complexes led to the discovery of a second E2F1 binding site outside of the A-B interface within the C-terminal region of pRB (Dick and Dyson, 2003). Subsequently, GST-tagged recombinant protein fragments were used in pulldown assays to map minimal interaction domains on both the pRB C-terminus and E2F1. Within the pRB C-terminus, residues 825-860 were found to be indispensable to this interaction (Julian et al., 2008). Within E2F1, a minimal fragment from residues 1-374 that encompasses a region termed the ‘marked box’ domain (MBD), but excludes the transactivation domain, was required for the pRB C-terminus interaction (Dick and Dyson, 2003). Substitution of the E2F1 MBD into E2F3 could confer pRB C-terminal binding, while the analogous domain swap into E2F1 abrogated the pRB C-terminus interaction with E2F1 (Julian et al., 2008). Conversely, pulldowns with GST-tagged recombinant C-terminal fragments of the pocket proteins demonstrate that this interaction is exclusive to the pRB C-terminus (Cecchini and Dick, 2011).

Although highly conserved amongst the E2Fs, the marked box domains of other activator E2Fs fail to bind the pRB C-terminus due to a proline located at a critical binding interface between the E2F MBD and pRB. The MBD of E2F1 is distinguished by

a valine instead of a proline at residue 276 that suffices to allow for the unique interaction when substituted for the analogous proline in E2F3 (Cecchini and Dick, 2011). Since E2F1 can utilize two distinct binding sites on pRB, the two binding interfaces are named according to E2F-binding specificity. The A-B interface of the pRB large pocket is referred to as the ‘general’ E2F binding site because it shows no preference for binding between E2F1-4, while the C-terminal binding surface is referred to as the E2F1-‘specific’ binding site (Dick and Dyson, 2003).

Co-crystallization studies of a pRB C-terminal fragment and a fragment of the E2F1-DP1 heterodimer identified specific molecular contact points between pRB-C and the E2F1 marked box domain and the DP1 coiled-coil domain (Rubin et al., 2005). These crucial residues would be used to generate a panel of pRB C-terminus mutants to be utilized in interaction assays with E2F1 (Cecchini and Dick, 2011; Julian et al., 2008). Ultimately, this screen yielded several pRB mutants that could disrupt the E2F1-pRB C-terminus interaction with considerably fewer substitutions as compared to the original pRB mutant used to discover the interaction that harbored 11 amino acid substitutions.

1.11 Distinct biochemical properties underlie the alternate pRB-E2F1 interaction

Initial biochemical characterizations yielded curious properties of this alternate pRB-E2F1 conformation. Electromobility shift assays demonstrate that within this conformation, pRB-E2F1 exhibit reduced affinity for a probe with the E2F consensus sequence (Dick and Dyson, 2003). Accordingly, luciferase reporters under the control of E2F promoters are not repressed by this alternate pRB-E2F1 conformation (Julian et al., 2008). Consistent with these properties, pRB mutants that disrupt small pocket E2F

interactions but retain the C-terminal interaction with E2F1 fail to induce a complete G1 cell cycle arrest upon overexpression in SaOS-2 cells (Dick and Dyson, 2003).

Perhaps the most striking feature of this alternate pRB-E2F1 interaction is its resistance to classic pRB-E2F dissociation signals. The first of these signals to be investigated was competitive binding between pRB and adenoviral oncoprotein E1A. Viral oncoproteins that bind the pRB LxCxE binding cleft dissociate the E2F transactivation domain from the pRB small pocket. Through utilization of the pRB C-terminal interaction, pRB-E2F1 complexes are resistant to this disruption by either the 12S or 13S forms of E1A. In contrast, both forms of E1A competitively displace other E2Fs, such as E2F4, that rely predominantly on the pRB small pocket interaction (Seifried et al., 2008).

However, the biochemical property that has provided the most insight into the potential endogenous functions of this alternate conformation has been its behavior in response to CDK phosphorylation. Overexpression of cyclin D-CDK4 and cyclin E-CDK2 in T98G cells enriches for a hyperphosphorylated pRB species that no longer associates with E2Fs that primarily bind pRB through the small pocket. In contrast, pRB-E2F1 complexes are resistant to CDK phosphorylation of pRB due to utilization of the C-terminal pRB interaction (Figure 1.4). This phenomenon is recapitulated with endogenous IPs in which E2F1 co-immunoprecipitates with both hypo and hyperphosphorylated pRB (ppRB) enriched from synchronized extracts. In contrast, E2F3 only associates with hypophosphorylated pRB (Cecchini and Dick, 2011). This complements observations of endogenous ppRB-E2F1 complexes by multiple

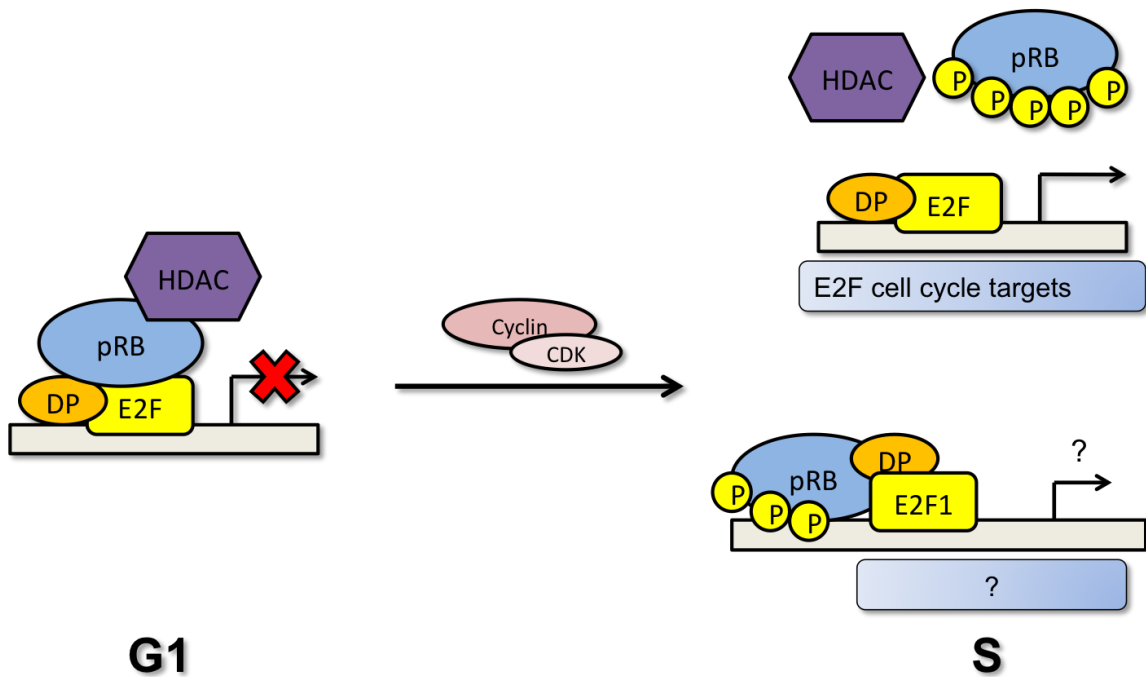


Figure 1.4: pRB-E2F dissociation dynamics at the G1/S transition

During the G1 phase of the cell cycle, pRB binds heterodimeric E2F/DP transcription factors and recruits co-repressor complexes to render the transcription factors transcriptionally inactive. This interaction forms in part through the pRB ‘small pocket’ domain that binds the E2F transactivation domain. Upon cell cycle entry, activated cyclin/CDK complexes phosphorylate pRB to dissociate interactions between the pRB small pocket and the E2F transactivation domain. Unbound E2Fs activate transcription of genes required for DNA synthesis. An alternate interaction between the pRB C-terminus and the E2F1 marked box domain exhibits resistance to CDK phosphorylation. The biological relevance of CDK-resistant pRB-E2F1 association remains largely unknown.

independent groups (Calbó et al., 2002; Cecchini and Dick, 2011; Ianari et al., 2009; Wells et al., 2003).

1.12 Biochemical properties suggest cell cycle-independent functions of pRB-E2F1

The unique biochemical properties of this CDK-resistant pRB-E2F1 interaction dictated initial investigations of potential endogenous functions. Since this complex does not recognize or suppress classic E2F cell cycle promoters and is resistant to CDK phosphorylation, cell cycle-independent functions of pRB or E2F1 provided a logical starting point to initiate exploration. An extended repertoire of transcriptional regulatory functions distinguishes E2F1 from other E2Fs. For instance, DNA damage activates transcription of machinery involved in DNA repair or induction of pro-apoptotic caspase cascades (Wu et al., 2009). E2F1 loss-of-function models reveal that E2F1 functions extensively in cell cycle-independent transcriptional regulation of components involved in either process (Irwin et al., 2000; Lin et al., 2001).

Overexpression of pRB mutants in pRB-null C33A cell cultures suggest that the pRB C-terminus binds the E2F1 MBD to negatively regulate E2F1-induced apoptosis (Dick and Dyson, 2003). This complements reports that the E2F1 MBD activates pro-apoptotic effectors independent of the transactivation domain (Hallstrom and Nevins, 2003). DNA damage investigations suggest that the post-translational modifications imposed on both pRB and E2F1 following etoposide treatment establish populations of E2F1 which are resistant to pRB-binding, and others that form an pRB-E2F1 complex with hyperphosphorylated pRB, presumably through the pRB C-terminus. Paradoxically,

both populations localize to and activate the same pro-apoptotic E2F1 targets following DNA damage (Carnevale et al., 2011). Nevertheless, this provides evidence that alternate pRB-E2F1 conformations bind promoters devoid of E2F consensus motifs to regulate transcription of non-cell cycle genes in a cell cycle-independent manner. Whether this complex imparts transcriptional control at other non-cell cycle targets remains unknown.

Beyond transcriptional control at the G1-S interface, pRB maintains genome integrity through transcription-independent activities on chromatin post-G1. While a post-G1 pRB recruitment mechanism has remained elusive, the CDK-resistant pRB-E2F1 interaction provides a possible mechanism that may underlie these functions. For instance, the pRB N-terminus interacts with Mcm7, DNA polymerase α and Ctf4 to restrict initiation of DNA replication (Borysov et al., 2015). Upon S-phase entry, Orc1 bound to pRB is displaced by E2F1 (Mendoza-Maldonado et al., 2010). This event regulates firing of the *Lamin B2* and *GM-CSF* replication origins (Avni et al., 2003). To halt progression of the replication fork, pRB displaces PCNA (Braden et al., 2006).

pRB also associates with chromatin post-G1 to ensure proper mitotic entry and progression (Bourgo et al., 2011). Mitotic defects in pRB-deficient cells were originally attributed to misregulation of E2F target genes involved in mitotic control, such as *MAD2* (Srinivasan et al., 2007). However, the use of synthetic pRB mutants demonstrates that pRB mediates mitotic regulation through transcription-independent means as well. Cells from a gene-targeted mouse model encoding alanine substitutions at I746, N750, and M754 residues within the pRB LxCxE binding cleft exhibit discrete loss of pRB interactions that form through the LxCxE binding cleft. This mutant is referred to as the pRB^{LXCXE} or pRB^L mutant (Isaac et al., 2006). The majority of proteins that bind pRB

through this cleft exhibit enzymatic activities used to alter chromatin structure, and often lack the LxCxE motif present in the original viral oncoproteins found to bind the cleft (Talluri and Dick, 2012). In this regard, it appears surprising that all of these interactions are largely dispensable for certain aspects of proliferative control as *Rb1^{L/L}* mice are viable, and *Rb1^{L/L}* cells exhibit proper induction of quiescence, with anomalies most apparent within the context of senescence and mammary gland development (Francis et al., 2009; Isaac et al., 2006; Talluri et al., 2010). Amongst the repertoire of pRB-interactors that bind this cleft, the mitotic defects in *Rb1^{L/L}* cells have largely been attributed to loss of pRB binding to the Condensin II complex (Coschi et al., 2014).

pRB-Condensin interactions were first noted in *D.melanogaster* where chromatin loading of the dCAPD3 subunit of the Condensin complex appeared to be dependent on the *D.melanogaster* pRB homologue RBF1 (Longworth et al., 2008). In mammals, two multimeric Condensin complexes exist, both of which contain SMC2 and SMC4 subunits that bind to form a hinge that connects two protruding coiled-coil arms that form a ring (Uhlmann, 2016). In Condensin I, this ring is completed by the CAPH subunit bound to CAPD2 and CAPG, while the SMC ring of Condensin II is connected by CAPH2 bound to CAPD3 and CAPG2. Condensin II associates with interphase chromosomes, and facilitates chromosome condensation during prophase (Hirano, 2012). As mitosis progresses, nuclear envelope breakdown permits entry of cytoplasmic Condensin I complexes that bind and further condense mitotic chromosomes during prometaphase and metaphase (Hirano, 2016).

The mitotic functions of Condensins appear to underlie the overt aberrations present in *Rb1^{L/L}* cells. These cells exhibit slightly increased G2/M content accompanied by

lagging chromosomes, centromere fusions, and aneuploidy (Isaac et al., 2006). Further inspection of mitotic progression reveals chromosome condensation and segregation errors characterized by a diffuse metaphase plate and prolonged anaphase. Upon inspection of Condensin loading onto chromatin as a possible underlying mechanism, chromatin fractions reveal reduced enrichment of Condensin II subunits, but not Condensin I (Coschi et al., 2010). Collectively, this suggests that pRB recruits Condensin II to ensure proper chromosome condensation and segregation. Condensin II subunits are particularly enriched at pericentric heterochromatin. However, the mechanism by which pRB recruits Condensin II to pericentric satellite repeats during mitosis remains unknown.

Collectively, misregulation of pRB functions during replication and mitosis likely contribute to the pronounced endoreduplication, aneuploidy, replication stress, and segregation defects that characterize a state of genomic instability in pRB-deficient cells. A common feature that underlies these activities is the ability of pRB to function as an adapter that recruits a diverse spectrum of machinery to modulate local chromatin structure. Indeed, pRB deficient cells exhibit defective heterochromatinization of pericentric and telomeric repeats (Gonzalo et al., 2005; Isaac et al., 2006; Manning et al., 2014). However, since the mechanism of post-G1 pRB chromatin recruitment remains poorly understood, it remains unknown whether defective heterochromatinization is directly due to perturbed pRB function, or simply a by product of perturbed replication and mitotic progression. The CDK-resistance coupled with altered DNA binding specificity merits investigation into whether the CDK-resistant pRB-E2F1 interaction

exists endogenously and whether it may underlie the aforementioned post-G1 functions of pRB.

1.13 Rationale

Next-generation sequencing approaches detect repetitive element activation in premalignant lesions (Lee et al., 2012). A mechanistic basis for why misregulation is an early event in the initiation of tumorigenesis remains elusive. Mechanisms of repetitive element silencing provide a starting point to identify cancer-susceptible aspects of silencing. Knockout models for epigenetic silencers of repeats demonstrate extensive compensatory effects exerted by facultative heterochromatin (Déjardin, 2015). This suggests that disruption of facultative heterochromatin is likely a rate-limiting event that underlies constitutive misregulation of repetitive elements in cancer.

The retinoblastoma tumor suppressor protein provides a potential mechanistic link between repetitive element misregulation upon initiation of tumorigenesis. Epigenetic writers that silence repetitive elements in ESCs are recruited to particular genes in a pRB-dependent manner. This includes DNMTs, H3K9me3 HMTs, H3K27me3 HMTs, and HDACs (Kotake et al., 2007; Robertson et al., 2000). Whether this recruitment occurs at repeats has remained largely unexplored. More direct evidence comes from investigation of triple-knockout (TKO) MEFs that lack expression of all three pocket proteins. Extracts from proliferating TKO MEFs exhibit pronounced expression of L1 ORF2p (Montoya-Durango et al., 2009). Whether this misexpression can be attributed to a single pocket protein remains unexplored.

Since repetitive element expression remains suppressed throughout the cell cycle, a repeat-silencing mechanism must be resistant to fluctuations in cell cycle phase. An interaction between the pRB C-terminus and the E2F1 marked box domain exhibits resistance to CDK-mediated phosphorylation that dissociates other pRB-E2F interactions that form primarily through the pRB small pocket (Cecchini and Dick, 2011). Within this conformation, pRB and E2F1 demonstrate altered DNA binding sensitivity (Carnevale et al., 2011; Dick and Dyson, 2003; Julian et al., 2008). Whether this altered DNA binding sensitivity underlies recruitment to repetitive sequences remains unexplored. If this is the case, this justifies investigation into whether post-G1 pRB-Condensin II recruitment to pericentric satellite repeats occurs through this mechanism. Overall, this work focuses on whether a CDK-resistant pRB-E2F1 interaction underlies both known and yet-unknown post G1 functions of pRB that are required to maintain genome integrity through recruitment of chromatin remodelers to repetitive genomic regions.

1.14 Objectives

In chapter 2, a novel gene targeted mouse model encoding an F832A substitution in the *Rb1* gene, called *Rb1^S*, is generated to disrupt the CDK-resistant pRB-E2F1 interaction in order to investigate its endogenous functions. I hypothesized that the CDK-resistant pRB-E2F1 complex functions as a scaffold to mediate epigenetic silencing of repeats genome-wide. To test this hypothesis, I mapped pRB occupancy at repeats across the genome using chromatin-immunoprecipitation-sequencing (ChIP-seq) and ChIP-qPCR. To determine whether occupancy was functional, I performed RNA-seq and microarray analysis using mutant cells. DNA methylation and histone tail modifications were also compared at repetitive elements in order to determine potential epigenetic

regulatory roles of pRB at repetitive sequences. Finally, homozygous mutant animals were aged until animal protocol endpoints to determine whether loss of this interaction resulted in any overt phenotypes.

In both chapter 3 and the appended paper (Coschi, Ishak, *et. al* 2014), I used *Rb1^{S/S}* MEFs to investigate contributions of the CDK-resistant pRB-E2F1 interaction to the maintenance of genome integrity. I hypothesized that pRB-E2F1 were required to ensure proper replication and mitotic progression independent of transcriptional regulation of E2F cell cycle target genes. In order to test this hypothesis, γ H2AX foci and $>4N$ DNA content were compared as overt indicators of genome stability. Microarray analysis and western blots were conducted to assess expression of E2F targets involved in replication and mitosis. To assess whether certain post-G1 functions of pRB utilized this scaffold, ppRPA accumulation, chromosome congression, chromosome segregation, and micronuclei frequency were assessed. Finally, we investigated whether this pRB-E2F1 scaffold recruits the Condensin II complex to particular repetitive sequences, and whether such sequences were enriched for γ H2AX foci upon loss of this recruitment.

In chapter 4, the pRB-EZH2 complex was assessed as a potential target for drug-induced epigenetic modulation. Specifically, acute EZH2 inhibition was assessed as a means of activating repetitive elements silenced by pRB-EZH2 in cell culture and *in vivo*. To determine how constitutive alleviation of multiple tumor suppressor-based chromatin-organizing mechanisms affects tumorigenesis, *Rb1^{S/S}* mice were crossed into a *Trp53^{-/-}* background, and characterized upon animal protocol endpoints for evidence of altered cancer phenotypes.

1.15 References

- Abel, K.J., Brody, L.C., Valdes, J.M., Erdos, M.R., McKinley, D.R., Castilla, L.H., Merajver, S.D., Couch, F.J., Friedman, L.S., Ostermeyer, E.A., *et al.* (1996). Characterization of EZH1, a Human Homolog of *Drosophila* Enhancer of zeste near BRCA1. *Genomics* 37, 161-171.
- Allis, C.D., and Jenuwein, T. (2016). The molecular hallmarks of epigenetic control. *Nat Rev Genet* 17, 487-500.
- Asghar, U., Witkiewicz, A.K., Turner, N.C., and Knudsen, E.S. (2015). The history and future of targeting cyclin-dependent kinases in cancer therapy. *Nat Rev Drug Discov* 14, 130-146.
- Ashley, D.J. (1969). The two "hit" and multiple "hit" theories of carcinogenesis. *British Journal of Cancer* 23, 313-328.
- Avni, D., Yang, H., Martelli, F., Hofmann, F., ElShamy, W.M., Ganesan, S., Scully, R., and Livingston, D.M. (2003). Active localization of the retinoblastoma protein in chromatin and its response to S phase DNA damage. *Mol Cell* 12, 735-746.
- Baltimore, D. (1970). RNA-dependent DNA polymerase in virions of RNA tumour viruses. *Nature* 226, 1209-1211.
- Bandara, L.R., Adamczewski, J.P., Hunt, T., and La Thangue, N.B. (1991). Cyclin A and the retinoblastoma gene product complex with a common transcription factor. *Nature* 352, 249-251.
- Bandara, L.R., and La Thangue, N.B. (1991). Adenovirus E1a prevents the retinoblastoma gene product from complexing with a cellular transcription factor. *Nature* 351, 494-497.
- Barau, J., Teissandier, A., Zamudio, N., Roy, S., Nalesso, V., Héroult, Y., Guillou, F., and Bourc'his, D. (2016). The DNA methyltransferase DNMT3C protects male germ cells from transposon activity. *Science* 354, 909.
- Beck, C.R., Garcia-Perez, J.L., Badge, R.M., and Moran, J.V. (2011). LINE-1 Elements in Structural Variation and Disease. *Annual Review of Genomics and Human Genetics* 12, 187-215.
- Belancio, V.P., Roy-Engel, A.M., and Deininger, P.L. (2010). All y'all need to know 'bout retroelements in cancer. *Seminars in Cancer Biology* 20, 200-210.
- Bersani, F., Lee, E., Kharchenko, P.V., Xu, A.W., Liu, M., Xega, K., MacKenzie, O.C., Brannigan, B.W., Wittner, B.S., Jung, H., *et al.* (2015). Pericentromeric satellite repeat expansions through RNA-derived DNA intermediates in cancer. *Proc Natl Acad Sci U S A* 112, 15148-15153.

- Bertoli, C., Skotheim, J.M., and de Bruin, R.A.M. (2013). Control of cell cycle transcription during G1 and S phases. *Nat Rev Mol Cell Biol* 14, 518-528.
- Blaise, S., de Parseval, N., Benit, L., and Heidmann, T. (2003). Genomewide screening for fusogenic human endogenous retrovirus envelopes identifies syncytin 2, a gene conserved on primate evolution. *Proc Natl Acad Sci U S A* 100, 13013-13018.
- Boeke, J.D., Garfinkel, D.J., Styles, C.A., and Fink, G.R. (1985). Ty elements transpose through an RNA intermediate. *Cell* 40, 491-500.
- Boeuf, H., Reimund, B., Jansen-Durr, P., and Kédinger, C. (1990). Differential activation of the E2F transcription factor by the adenovirus Ela and EIV products in F9 cells. *Proceedings of the National Academy of Sciences of the United States of America* 87, 1782-1786.
- Borysov, S.I., Nepon-Sixt, B.S., and Alexandrow, M.G. (2015). The N Terminus of the Retinoblastoma Protein Inhibits DNA Replication via a Bipartite Mechanism Disrupted in Partially Penetrant Retinoblastomas. *Mol Cell Biol* 36, 832-845.
- Bourc'his, D., and Bestor, T.H. (2004). Meiotic catastrophe and retrotransposon reactivation in male germ cells lacking Dnmt3L. *Nature* 431, 96-99.
- Bourgo, R.J., Ehmer, U., Sage, J., and Knudsen, E.S. (2011). RB deletion disrupts coordination between DNA replication licensing and mitotic entry in vivo. *Molecular Biology of the Cell* 22, 931-939.
- Braden, W.A., Lenihan, J.M., Lan, Z., Luce, K.S., Zagorski, W., Bosco, E., Reed, M.F., Cook, J.G., and Knudsen, E.S. (2006). Distinct Action of the Retinoblastoma Pathway on the DNA Replication Machinery Defines Specific Roles for Cyclin-Dependent Kinase Complexes in Prereplication Complex Assembly and S-Phase Progression. *Mol. Cell Biol.* 26, 7667-7681.
- Brehove, M., Wang, T., North, J., Luo, Y., Dreher, S.J., Shimko, J.C., Ottesen, J.J., Luger, K., and Poirier, M.G. (2015). Histone Core Phosphorylation Regulates DNA Accessibility. *Journal of Biological Chemistry*.
- Bremner, R., Cohen, B.L., Sopta, M., Hamel, P.A., Ingles, C.J., Gallie, B.L., and Phillips, R.A. (1995). Direct transcriptional repression by pRB and its reversal by specific cyclins. *Molecular and Cellular Biology* 15, 3256-3265.
- Bulut-Karslioglu, A., Perrera, V., Scaranaro, M., de la Rosa-Velazquez, I.A., van de Nobelen, S., Shukeir, N., Popow, J., Gerle, B., Opravil, S., Pagani, M., *et al.* (2012). A transcription factor-based mechanism for mouse heterochromatin formation. *Nature structural & molecular biology* 19, 1023-1030.
- Burke, J.R., Deshong, A.J., Pelton, J.G., and Rubin, S.M. (2010). Phosphorylation-induced conformational changes in the retinoblastoma protein inhibit E2F transactivation domain binding. *J Biol Chem* 285, 16286-16293.

- Burke, J.R., Hura, G.L., and Rubin, S.M. (2012). Structures of inactive retinoblastoma protein reveal multiple mechanisms for cell cycle control. *Genes & Development*.
- Burke, J.R., Liban, T.J., Restrepo, T., Lee, H.-W., and Rubin, S.M. (2013). Multiple Mechanisms for E2F Binding Inhibition by Phosphorylation of the Retinoblastoma Protein C-Terminal Domain. *Journal of Molecular Biology*.
- Calbó, J., Parreño, M., Sotillo, E., Yong, T., Mazo, A., Garriga, J., and Graña, X. (2002). G1 Cyclin/Cyclin-dependent Kinase-coordinated Phosphorylation of Endogenous Pocket Proteins Differentially Regulates Their Interactions with E2F4 and E2F1 and Gene Expression. *Journal of Biological Chemistry* 277, 50263-50274.
- Carnevale, J., Palander, O., Seifried, L.A., and Dick, F.A. (2011). DNA damage signals through differentially modified E2F1 molecules to induce apoptosis. *Molecular and Cellular Biology*.
- Casa, V., and Gabellini, D. (2012). A repetitive elements perspective in Polycomb epigenetics. *Frontiers in genetics* 3, 199.
- Cavenee, W., Leach, R., Mohandas, T., Pearson, P., and White, R. (1984). Isolation and regional localization of DNA segments revealing polymorphic loci from human chromosome 13. *American journal of human genetics* 36, 10-24.
- Cavenee, W.K., Dryja, T.P., Phillips, R.A., Benedict, W.F., Godbout, R., Gallie, B.L., Murphree, A.L., Strong, L.C., and White, R.L. (1983). Expression of recessive alleles by chromosomal mechanisms in retinoblastoma. *Nature* 305, 779-784.
- Cavenee, W.K., Hansen, M.F., Nordenskjold, M., Kock, E., Maumenee, I., Squire, J.A., Phillips, R.A., and Gallie, B.L. (1985). Genetic origin of mutations predisposing to retinoblastoma. *Science* 228, 501-503.
- Cecchini, M.J., and Dick, F.A. (2011). The biochemical basis of CDK phosphorylation-independent regulation of E2F1 by the retinoblastoma protein. *Biochem J*.
- Chellappan, S.P., Hiebert, S., Mudryj, M., Horowitz, J.M., and Nevins, J.R. (1991). The E2F transcription factor is a cellular target for the RB protein. *Cell* 65, 1053-1061.
- Chow, K.N., and Dean, D.C. (1996). Domains A and B in the Rb pocket interact to form a transcriptional repressor motif. *Molecular and Cellular Biology* 16, 4862-4868.
- Chuong, E.B., Elde, N.C., and Feschotte, C. (2016). Regulatory evolution of innate immunity through co-option of endogenous retroviruses. *Science* 351, 1083-1087.
- Chuong, E.B., Elde, N.C., and Feschotte, C. (2017). Regulatory activities of transposable elements: from conflicts to benefits. *Nat Rev Genet* 18, 71-86.

- Clarke, A.R., Maandag, E.R., van Roon, M., van der Lugt, N.M.T., van der Valk, M., Hooper, M.L., Berns, A., and te Rielef, H. (1992). Requirement for a functional Rb-1 gene in murine development. *Nature* 359, 328-330.
- Colum, P.W., J., R.C., and Timothy, H.B. (1998). Transcription of IAP endogenous retroviruses is constrained by cytosine methylation. *Nature Genetics* 20, 116 - 117.
- Comings, D.E. (1973). A general theory of carcinogenesis. *Proceedings of the National Academy of Sciences* 70, 3324-3328.
- Cooper, S., Dienstbier, M., Hassan, R., Schermelleh, L., Sharif, J., Blackledge, N.P., De Marco, V., Elderkin, S., Koseki, H., Klose, R., *et al.* (2014). Targeting polycomb to pericentric heterochromatin in embryonic stem cells reveals a role for H2AK119u1 in PRC2 recruitment. *Cell Rep* 7, 1456-1470.
- Coschi, C.H., Ishak, C.A., Gallo, D., Marshall, A., Talluri, S., Wang, J., Cecchini, M.J., Martens, A.L., Percy, V., Welch, I., *et al.* (2014). Haploinsufficiency of an RB–E2F1–Condensin II Complex Leads to Aberrant Replication and Aneuploidy. *Cancer Discovery* 4, 840-853.
- Coschi, C.H., Martens, A.L., Ritchie, K., Francis, S.M., Chakrabarti, S., Berube, N.G., and Dick, F.A. (2010). Mitotic chromosome condensation mediated by the retinoblastoma protein is tumor-suppressive. *Genes & Development* 24, 1351-1363.
- Cowley, M., and Oakey, R.J. (2013). Transposable Elements Re-Wire and Fine-Tune the Transcriptome. *PLoS Genet* 9, e1003234.
- DeCaprio, J.A., Furukawa, Y., Ajchenbaum, F., Griffin, J.D., and Livingston, D.M. (1992). The retinoblastoma-susceptibility gene product becomes phosphorylated in multiple stages during cell cycle entry and progression. *Proceedings of the National Academy of Sciences of the United States of America* 89, 1795-1798.
- DeCaprio, J.A., Ludlow, J.W., Figge, J., Shew, J.-Y., Huang, C.-M., Lee, W.-H., Marsilio, E., Paucha, E., and Livingston, D.M. (1988). SV40 large tumor antigen forms a specific complex with the product of the retinoblastoma susceptibility gene. *Cell* 54, 275-283.
- DeCaprio, J.A., Ludlow, J.W., Lynch, D., Furukawa, Y., Griffin, J., Piwnica-Worms, H., Huang, C.M., and Livingston, D.M. (1989). The product of the retinoblastoma susceptibility gene has properties of a cell cycle regulatory element. *Cell* 58, 1085-1095.
- Déjardin, J. (2015). Switching between Epigenetic States at Pericentromeric Heterochromatin. *Trends in Genetics* 31, 661-672.
- Dejardin, J., and Kingston, R.E. (2009). Purification of proteins associated with specific genomic Loci. *Cell* 136, 175-186.

Dick, F.A., and Dyson, N. (2003). pRB Contains an E2F1 Specific Binding Domain that Allows E2F1 Induced Apoptosis to be Regulated Separately from other E2F Activities. *Mol Cell* 12, 639-649.

Dick, F.A., and Rubin, S.M. (2013). Molecular mechanisms underlying RB protein function. *Nat Rev Mol Cell Biol* 14, 297-306.

Dick, F.A., Sailhamer, E., and Dyson, N.J. (2000). Mutagenesis of the pRB pocket reveals that cell cycle arrest functions are separable from binding to viral oncoproteins. *Mol Cell Biol* 20, 3715-3727.

Dimova, D.K., and Dyson, N.J. (2005). The E2F transcriptional network: old acquaintances with new faces. *Oncogene* 24, 2810-2826.

Dombroski, B.A., Mathias, S.L., Nanthakumar, E., Scott, A.F., and Kazazian, H.H. (1991). Isolation of an active human transposable element. *Science* 254, 1805.

Donjerkovic, D., and Scott, D.W. (2000). Regulation of the G1 phase of the mammalian cell cycle. *Cell Res* 10, 1-16.

Doucet-O'Hare, T.T., Rodic, N., Sharma, R., Darbari, I., Abril, G., Choi, J.A., Young Ahn, J., Cheng, Y., Anders, R.A., Burns, K.H., *et al.* (2015). LINE-1 expression and retrotransposition in Barrett's esophagus and esophageal carcinoma. *Proc Natl Acad Sci U S A* 112, E4894-4900.

Dougherty, R.M., and Di Stefano, H.S. (1966). Lack of relationship between infection with avian leukosis virus and the presence of COFAL antigen in chick embryos. *Virology* 29, 586-595.

Dougherty, R.M., Di Stefano, H.S., and Roth, F.K. (1967). Virus particles and viral antigens in chicken tissues free of infectious avian leukosis virus. *Proc Natl Acad Sci U S A* 58, 808-817.

Dryja, T.P., Rapaport, J.M., Joyce, J.M., and Petersen, R.A. (1986). Molecular detection of deletions involving band q14 of chromosome 13 in retinoblastomas. *Proc Natl Acad Sci U S A* 83, 7391-7394.

Dyson, N. (1998). The regulation of E2F by pRB-family proteins. *Genes Dev* 12, 2245-2262.

Dyson, N., Howley, P.M., Munger, K., and Harlow, E. (1989). The human papilloma virus-16 E7 oncoprotein is able to bind to the retinoblastoma gene product. *Science* 243, 934.

Dyson, N.J. (2016). RB1: a prototype tumor suppressor and an enigma. *Genes & Development* 30, 1492-1502.

Evans, T., Rosenthal, E.T., Youngblom, J., Distel, D., and Hunt, T. (1983). Cyclin: A protein specified by maternal mRNA in sea urchin eggs that is destroyed at each cleavage division. *Cell* 33, 389-396.

Ewen, M.E., Xing, Y., Lawrence, J.B., and Livingston, D.M. (1991). Molecular cloning, chromosomal mapping, and expression of the cDNA for p107, a retinoblastoma gene product-related protein. *Cell* 66, 1155-1164.

Ewing, A.D., Gacita, A., Wood, L.D., Ma, F., Xing, D., Kim, M.S., Manda, S.S., Abril, G., Pereira, G., Makohon-Moore, A., *et al.* (2015). Widespread somatic L1 retrotransposition occurs early during gastrointestinal cancer evolution. *Genome research* 25, 1536-1545.

Francis, S.M., Bergsied, J., Isaac, C.E., Coschi, C.H., Martens, A.L., Hojilla, C.V., Chakrabarti, S., Dimattia, G.E., Khoka, R., Wang, J.Y., *et al.* (2009). A functional connection between pRB and transforming growth factor beta in growth inhibition and mammary gland development. *Mol Cell Biol* 29, 4455-4466.

Friend, S.H., Bernards, R., Rogelj, S., Weinberg, R.A., Rapaport, J.M., Albert, D.M., and Dryja, T.P. (1986). A human DNA segment with properties of the gene that predisposes to retinoblastoma and osteosarcoma. *Nature* 323, 643-646.

Garcia-Perez, J.L., Morell, M., Scheys, J.O., Kulpa, D.A., Morell, S., Carter, C.C., Hammer, G.D., Collins, K.L., O'Shea, K.S., Menendez, P., *et al.* (2010). Epigenetic silencing of engineered L1 retrotransposition events in human embryonic carcinoma cells. *Nature* 466, 769-773.

Garfinkel, D.J., Boeke, J.D., and Fink, G.R. (1985). Ty element transposition: Reverse transcriptase and virus-like particles. *Cell* 42, 507-517.

Gaudet, F., Hodgson, J.G., Eden, A., Jackson-Grusby, L., Dausman, J., Gray, J.W., Leonhardt, H., and Jaenisch, R. (2003). Induction of Tumors in Mice by Genomic Hypomethylation. *Science* 300, 489-492.

Gemayel, R., Vinces, M.D., Legendre, M., and Verstrepen, K.J. (2010). Variable tandem repeats accelerate evolution of coding and regulatory sequences. *Annu Rev Genet* 44, 445-477.

Girling, R., Partridge, J.F., Bandara, L.R., Burden, N., Totty, N.F., Hsuan, J.J., and La Thangue, N.B. (1993). A new component of the transcription factor DRTF1/E2F. *Nature* 362, 83-87.

Glotzer, M., Murray, A.W., and Kirschner, M.W. (1991). Cyclin is degraded by the ubiquitin pathway. *Nature* 349, 132-138.

Godbout, R., Dryja, T.P., Squire, J., Gallie, B.L., and Phillips, R.A. (1983). Somatic inactivation of genes on chromosome 13 is a common event in retinoblastoma. *Nature* 304, 451-453.

- Göke, J., and Ng, H.H. (2016). CTRL+INSERT: retrotransposons and their contribution to regulation and innovation of the transcriptome. *EMBO reports* *17*, 1131-1144.
- Gonzalo, S., Garcia-Cao, M., Fraga, M.F., Schotta, G., Peters, A.H.F.M., Cotter, S.E., Eguia, R., Dean, D.C., Esteller, M., Jenuwein, T., *et al.* (2005). Role of the RB1 family in stabilizing histone methylation at constitutive heterochromatin. *Nat Cell Biol* *7*, 420-428.
- Goodrich, D.W., Wang, N.P., Qian, Y.-W., Lee, E.Y.H.P., and Lee, W.-H. (1991). The retinoblastoma gene product regulates progression through the G1 phase of the cell cycle. *Cell* *67*, 293-302.
- Groh, S., and Schotta, G. (2017). Silencing of endogenous retroviruses by heterochromatin. *Cellular and Molecular Life Sciences*, 1-11.
- Hallstrom, T.C., and Nevins, J.R. (2003). Specificity in the activation and control of transcription factor E2F-dependent apoptosis. *Proceedings of the National Academy of Sciences* *100*, 10848-10853.
- Hanahan, D., and Weinberg, Robert A. (2011). Hallmarks of Cancer: The Next Generation. *Cell* *144*, 646-674.
- Hannon, G.J., Demetrick, D., and Beach, D. (1993). Isolation of the Rb-related p130 through its interaction with CDK2 and cyclins. *Genes & Development* *7*, 2378-2391.
- Harris, H., and Miller, O. (1969). Suppression of malignancy by cell fusion. *Nature* *223*, 363-368.
- Hata, K., Okano, M., Lei, H., and Li, E. (2002). Dnmt3L cooperates with the Dnmt3 family of de novo DNA methyltransferases to establish maternal imprints in mice. *Development* *129*, 1983.
- Hauri, S., Comoglio, F., Seimiya, M., Gerstung, M., Glatter, T., Hansen, K., Aebersold, R., Paro, R., Gstaiger, M., and Beisel, C. (2016). A High-Density Map for Navigating the Human Polycomb Complexome. *Cell Reports* *17*, 583-595.
- Henley, S., and Dick, F. (2012). The retinoblastoma family of proteins and their regulatory functions in the mammalian cell division cycle. *Cell Division* *7*, 10.
- Hirano, T. (2012). Condensins: universal organizers of chromosomes with diverse functions. *Genes & Development* *26*, 1659-1678.
- Hirano, T. (2016). Condensin-Based Chromosome Organization from Bacteria to Vertebrates. *Cell* *164*, 847-857.
- Hirschi, A., Cecchini, M., Steinhardt, R.C., Schamber, M.R., Dick, F.A., and Rubin, S.M. (2010). An overlapping kinase and phosphatase docking site regulates activity of the retinoblastoma protein. *Nature structural & molecular biology* *17*, 1051-1057.

Hobert, O., Sures, I., Ciossek, T., Fuchs, M., and Ullrich, A. (1996). Isolation and developmental expression analysis of *Enx-1*, a novel mouse Polycomb group gene. *Mechanisms of Development* 55, 171-184.

Hochegger, H., Takeda, S., and Hunt, T. (2008). Cyclin-dependent kinases and cell-cycle transitions: does one fit all? *Nat Rev Mol Cell Biol* 9, 910-916.

Horowitz, J.M., Yandell, D.W., Park, S.H., Canning, S., Whyte, P., Buchkovich, K., Harlow, E., Weinberg, R.A., and Dryja, T.P. (1989). Point mutational inactivation of the retinoblastoma antioncogene. *Science* 243, 937-940.

Howard, G., Eiges, R., Gaudet, F., Jaenisch, R., and Eden, A. (2008). Activation and transposition of endogenous retroviral elements in hypomethylation induced tumors in mice. *Oncogene* 27.

Huang, P.S., Patrick, D.R., Edwards, G., Goodhart, P.J., Huber, H.E., Miles, L., Garsky, V.M., Oliff, A., and Heimbrook, D.C. (1993). Protein domains governing interactions between E2F, the retinoblastoma gene product, and human papillomavirus type 16 E7 protein. *Mol Cell Biol* 13, 953-960.

Hurford, R.K., Jr., Cobrinik, D., Lee, M.H., and Dyson, N. (1997). pRB and p107/p130 are required for the regulated expression of different sets of E2F responsive genes. *Genes Dev* 11, 1447-1463.

Ianari, A., Natale, T., Calo, E., Ferretti, E., Alesse, E., Screpanti, I., Haigis, K., Gulino, A., and Lees, J.A. (2009). Proapoptotic function of the retinoblastoma tumor suppressor protein. *Cancer Cell* 15, 184-194.

Ionov, Y., Peinado, M.A., Malkhosyan, S., Shibata, D., and Perucho, M. (1993). Ubiquitous somatic mutations in simple repeated sequences reveal a new mechanism for colonic carcinogenesis. *Nature* 363, 558-561.

Irwin, M., Marin, M.C., Phillips, A.C., Seelan, R.S., Smith, D.I., Liu, W., Flores, E.R., Tsai, K.Y., Jacks, T., Vousden, K.H., *et al.* (2000). Role for the p53 homologue p73 in E2F-1-induced apoptosis. *Nature* 407, 645-648.

Isaac, C.E., Francis, S.M., Martens, A.L., Julian, L.M., Seifried, L.A., Erdmann, N., Binne, U.K., Harrington, L., Sicinski, P., Berube, N.G., *et al.* (2006). The retinoblastoma protein regulates pericentric heterochromatin. *Mol Cell Biol* 26, 3659-3671.

Jacks, T., Fazeli, A., Schmitt, E., Bronson, R., Goodell, M., and Weinberg, R. (1992). Effects of an Rb mutation in the mouse. *Nature* 359, 295-300.

Jeppesen, P., and Turner, B.M. (1993). The inactive X chromosome in female mammals is distinguished by a lack of histone H4 acetylation, a cytogenetic marker for gene expression. *Cell* 74, 281-289.

- Johnson, D.G., and Degregori, J. (2006). Putting the Oncogenic and Tumor Suppressive Activities of E2F into Context. *Curr Mol Med* 6, 731-738.
- Jones, P.A. (2012). Functions of DNA methylation: islands, start sites, gene bodies and beyond. *Nat Rev Genet* 13, 484-492.
- Jones, R.S., and Gelbart, W.M. (1990). Genetic analysis of the enhancer of zeste locus and its role in gene regulation in *Drosophila melanogaster*. *Genetics* 126, 185.
- Jones, R.S., and Gelbart, W.M. (1993). The *Drosophila* Polycomb-group gene Enhancer of zeste contains a region with sequence similarity to trithorax. *Molecular and Cellular Biology* 13, 6357-6366.
- Jørgensen, S., Schotta, G., and Sørensen, C.S. (2013). Histone H4 Lysine 20 methylation: key player in epigenetic regulation of genomic integrity. *Nucleic acids research* 41, 2797-2806.
- Julian, L.M., Palander, O., Seifried, L.A., Foster, J.E., and Dick, F.A. (2008). Characterization of an E2F1-specific binding domain in pRB and its implications for apoptotic regulation. *Oncogene* 27, 1572-1579.
- Jurka, J., Kapitonov, V.V., Kohany, O., and Jurka, M.V. (2007). Repetitive sequences in complex genomes: structure and evolution. *Annu Rev Genomics Hum Genet* 8, 241-259.
- Kaelin, W.G., Ewen, M.E., and Livingston, D.M. (1990). Definition of the minimal simian virus 40 large T antigen- and adenovirus E1A-binding domain in the retinoblastoma gene product. *Molecular and Cellular Biology* 10, 3761-3769.
- Karimi, Mohammad M., Goyal, P., Maksakova, Irina A., Bilenky, M., Leung, D., Tang, Jie X., Shinkai, Y., Mager, Dixie L., Jones, S., Hirst, M., *et al.* (2011). DNA Methylation and SETDB1/H3K9me3 Regulate Predominantly Distinct Sets of Genes, Retroelements, and Chimeric Transcripts in mESCs. *Cell Stem Cell* 8, 676-687.
- Kazazian, H.H. (2004). Mobile Elements: Drivers of Genome Evolution. *Science* 303, 1626.
- Kazazian, H.H., and Moran, J.V. (1998). The impact of L1 retrotransposons on the human genome. *Nat Genet* 19, 19-24.
- Kazazian, H.H., Wong, C., Yousoufian, H., Scott, A.F., Phillips, D.G., and Antonarakis, S.E. (1988). Haemophilia A resulting from de novo insertion of L1 sequences represents a novel mechanism for mutation in man. *Nature* 332, 164-166.
- Knudson, A.G., Jr. (1971). Mutation and cancer: statistical study of retinoblastoma. *Proc Natl Acad Sci U S A* 68, 820-823.
- Kotake, Y., Cao, R., Viatour, P., Sage, J., Zhang, Y., and Xiong, Y. (2007). pRB family proteins are required for H3K27 trimethylation and Polycomb repression complexes

binding to and silencing p16INK4a tumor suppressor gene. *Genes & Development* 21, 49-54.

Kovesdi, I., Reichel, R., and Nevins, J.R. (1987). Role of an adenovirus E2 promoter binding factor in E1A-mediated coordinate gene control. *Proceedings of the National Academy of Sciences of the United States of America* 84, 2180-2184.

Lamprecht, B., Walter, K., Kreher, S., Kumar, R., Hummel, M., Lenze, D., Kochert, K., Bouhleh, M.A., Richter, J., Soler, E., *et al.* (2010). Derepression of an endogenous long terminal repeat activates the CSF1R proto-oncogene in human lymphoma. *Nat Med* 16, 571-579.

Lander, E.S., Linton, L.M., Birren, B., Nusbaum, C., Zody, M.C., Baldwin, J., Devon, K., Dewar, K., Doyle, M., FitzHugh, W., *et al.* (2001). Initial sequencing and analysis of the human genome. *Nature* 409, 860-921.

Lau, C.-C., Sun, T., Ching, Arthur K.K., He, M., Li, J.-W., Wong, Alissa M., Co, Ngai N., Chan, Anthony W.H., Li, P.-S., Lung, Raymond W.M., *et al.* (2014). Viral-Human Chimeric Transcript Predisposes Risk to Liver Cancer Development and Progression. *Cancer Cell* 25, 335-349.

Lee, C., Chang, J.H., Lee, H.S., and Cho, Y. (2002). Structural basis for the recognition of the E2F transactivation domain by the retinoblastoma tumor suppressor. *Genes Dev* 16, 3199-3212.

Lee, E., Iskow, R., Yang, L., Gokcumen, O., Haseley, P., Luquette, L.J., 3rd, Lohr, J.G., Harris, C.C., Ding, L., Wilson, R.K., *et al.* (2012). Landscape of somatic retrotransposition in human cancers. *Science* 337, 967-971.

Lee, E.Y., Chang, C.Y., Hu, N., Wang, Y.C., Lai, C.C., Herrup, K., Lee, W.H., and Bradley, A. (1992). Mice deficient for Rb are nonviable and show defects in neurogenesis and haematopoiesis. *Nature* 359, 288-294.

Lee, J.-O., Russo, A.A., and Pavletich, N.P. (1998). Structure of the retinoblastoma tumour-suppressor pocket domain bound to a peptide from HPV E7. *Nature* 391, 859-865.

Lee, W.H., Bookstein, R., Hong, F., Young, L.J., Shew, J.Y., and Lee, E.Y. (1987). Human retinoblastoma susceptibility gene: cloning, identification, and sequence. *Science* 235, 1394-1399.

Leeb, M., Pasini, D., Novatchkova, M., Jaritz, M., Helin, K., and Wutz, A. (2010). Polycomb complexes act redundantly to repress genomic repeats and genes. *Genes & Development* 24, 265-276.

Lehnertz, B., Ueda, Y., Derijck, A.A.H.A., Braunschweig, U., Perez-Burgos, L., Kubicek, S., Chen, T., Li, E., Jenuwein, T., and Peters, A.H.F.M. (2003). Suv39h-

Mediated Histone H3 Lysine 9 Methylation Directs DNA Methylation to Major Satellite Repeats at Pericentric Heterochromatin. *Current Biology* 13, 1192-1200.

Leung, D.C., and Lorincz, M.C. (2012). Silencing of endogenous retroviruses: when and why do histone marks predominate? *Trends in Biochemical Sciences* 37, 127-133.

Levin, H.L., and Moran, J.V. (2011). Dynamic interactions between transposable elements and their hosts. *Nat Rev Genet* 12, 615-627.

Levinson, G., and Gutman, G.A. (1987). Slipped-strand mispairing: a major mechanism for DNA sequence evolution. *Molecular biology and evolution* 4, 203-221.

Li, E., Bestor, T.H., and Jaenisch, R. (1992). Targeted mutation of the DNA methyltransferase gene results in embryonic lethality. *Cell* 69, 915-926.

Lin, W.C., Lin, F.T., and Nevins, J.R. (2001). Selective induction of E2F1 in response to DNA damage, mediated by ATM-dependent phosphorylation. *Genes Dev* 15, 1833-1844.

Liu, S., Brind'Amour, J., Karimi, M.M., Shirane, K., Bogutz, A., Lefebvre, L., Sasaki, H., Shinkai, Y., and Lorincz, M.C. (2014). Setdb1 is required for germline development and silencing of H3K9me3-marked endogenous retroviruses in primordial germ cells. *Genes Dev* 28, 2041-2055.

Longworth, M.S., Herr, A., Ji, J.-Y., and Dyson, N.J. (2008). RBF1 promotes chromatin condensation through a conserved interaction with the Condensin II protein dCAP-D3. *Genes & Development* 22, 1011-1024.

Mager, D.L., and Stoye, J.P. (2015). Mammalian Endogenous Retroviruses. *Microbiology spectrum* 3, Mdna3-0009-2014.

Maksakova, I.A., Goyal, P., Bullwinkel, J., Brown, J.P., Bilenky, M., Mager, D.L., Singh, P.B., and Lorincz, M.C. (2011). H3K9me3-binding proteins are dispensable for SETDB1/H3K9me3-dependent retroviral silencing. *Epigenetics & Chromatin* 4, 12-12.

Malumbres, M. (2014). Cyclin-dependent kinases. *Genome biology* 15, 122-122.

Manning, Amity L., Yazinski, Stephanie A., Nicolay, B., Bryll, A., Zou, L., and Dyson, Nicholas J. (2014). Suppression of Genome Instability in pRB-Deficient Cells by Enhancement of Chromosome Cohesion. *Molecular Cell*.

Margueron, R., Li, G., Sarma, K., Blais, A., Zavadil, J., Woodcock, C.L., Dynlacht, B.D., and Reinberg, D. (2008). Ezh1 and Ezh2 maintain repressive chromatin through different mechanisms. *Mol Cell* 32, 503-518.

Martens, J.H.A., O'Sullivan, R.J., Braunschweig, U., Opravil, S., Radolf, M., Steinlein, P., and Jenuwein, T. (2005). The profile of repeat-associated histone lysine methylation states in the mouse epigenome. *Embo J* 24, 800-812.

- Matsui, T., Leung, D., Miyashita, H., Maksakova, I.A., Miyachi, H., Kimura, H., Tachibana, M., Lorincz, M.C., and Shinkai, Y. (2010). Proviral silencing in embryonic stem cells requires the histone methyltransferase ESET. *Nature* 464, 927-931.
- McClintock, B. (1950). The origin and behavior of mutable loci in maize. *Proceedings of the National Academy of Sciences* 36, 344-355.
- Mendoza-Maldonado, R., Paolinelli, R., Galbiati, L., Giadrossi, S., and Giacca, M. (2010). Interaction of the Retinoblastoma Protein with Orc1 and Its Recruitment to Human Origins of DNA Replication. *PLoS ONE* 5, e13720.
- Meselson, M., Stahl, F.W., and Vinograd, J. (1957). EQUILIBRIUM SEDIMENTATION OF MACROMOLECULES IN DENSITY GRADIENTS. *Proceedings of the National Academy of Sciences of the United States of America* 43, 581-588.
- Miki, Y., Nishisho, I., Horii, A., Miyoshi, Y., Utsunomiya, J., Kinzler, K.W., Vogelstein, B., and Nakamura, Y. (1992). Disruption of the APC gene by a retrotransposal insertion of L1 sequence in a colon cancer. *Cancer Res* 52, 643-645.
- Montoya-Durango, D.E., Liu, Y., Teneng, I., Kalbfleisch, T., Lacy, M.E., Steffen, M.C., and Ramos, K.S. (2009). Epigenetic control of mammalian LINE-1 retrotransposon by retinoblastoma proteins. *Mutation Research/Fundamental and Molecular Mechanisms of Mutagenesis* 665, 20-28.
- Morgunova, E., Yin, Y., Jolma, A., Dave, K., Schmierer, B., Popov, A., Eremina, N., Nilsson, L., and Taipale, J. (2015). Structural insights into the DNA-binding specificity of E2F family transcription factors. *Nature communications* 6, 10050.
- Mozzetta, C., Boyarchuk, E., Pontis, J., and Ait-Si-Ali, S. (2015). Sound of silence: the properties and functions of repressive Lys methyltransferases. *Nat Rev Mol Cell Biol* 16, 499-513.
- Muncaster, M.M., Cohen, B.L., Phillips, R.A., and Gallie, B.L. (1992). Failure of RB1 to reverse the malignant phenotype of human tumor cell lines. *Cancer Res* 52, 654-661.
- Munoz-Lopez, M., and García-Pérez, J.L. (2010). DNA transposons: nature and applications in genomics. *Current genomics* 11, 115.
- O'Carroll, D., Erhardt, S., Pagani, M., Barton, S.C., Surani, M.A., and Jenuwein, T. (2001). The Polycomb-Group Gene *Ezh2* Is Required for Early Mouse Development. *Molecular and Cellular Biology* 21, 4330-4336.
- Okano, M., Bell, D.W., Haber, D.A., and Li, E. (1999). DNA Methyltransferases *Dnmt3a* and *Dnmt3b* Are Essential for De Novo Methylation and Mammalian Development. *Cell* 99, 247-257.

- Peters, A.H., O'Carroll, D., Scherthan, H., Mechtler, K., Sauer, S., Schofer, C., Weipoltshammer, K., Pagani, M., Lachner, M., Kohlmaier, A., *et al.* (2001). Loss of the Suv39h histone methyltransferases impairs mammalian heterochromatin and genome stability. *Cell* *107*, 323-337.
- Peters, A.H.F.M., Kubicek, S., Mechtler, K., O'Sullivan, R.J., Derijck, A.A.H.A., Perez-Burgos, L., Kohlmaier, A., Opravil, S., Tachibana, M., Shinkai, Y., *et al.* (2003). Partitioning and Plasticity of Repressive Histone Methylation States in Mammalian Chromatin. *Molecular Cell* *12*, 1577-1589.
- Qin, X.Q., Chittenden, T., Livingston, D.M., and Kaelin, W.G., Jr. (1992). Identification of a growth suppression domain within the retinoblastoma gene product. *Genes Dev* *6*, 953-964.
- Robertson, K.D., Ait-Si-Ali, S., Yokochi, T., Wade, P.A., Jones, P.L., and Wolffe, A.P. (2000). DNMT1 forms a complex with Rb, E2F1 and HDAC1 and represses transcription from E2F-responsive promoters. *Nat Genet* *25*, 338-342.
- Rodic, N., Steranka, J.P., Makohon-Moore, A., Moyer, A., Shen, P., Sharma, R., Kohutek, Z.A., Huang, C.R., Ahn, D., Mita, P., *et al.* (2015). Retrotransposon insertions in the clonal evolution of pancreatic ductal adenocarcinoma. *Nat Med* *21*, 1060-1064.
- Rogan, P.K., Pan, J., and Weissman, S.M. (1987). L1 repeat elements in the human epsilon-G gamma-globin gene intergenic region: sequence analysis and concerted evolution within this family. *Molecular biology and evolution* *4*, 327-342.
- Rowe, H.M., and Trono, D. (2011). Dynamic control of endogenous retroviruses during development. *Virology* *411*, 273-287.
- Rubin, S.M. (2013). Deciphering the retinoblastoma protein phosphorylation code. *Trends in Biochemical Sciences*.
- Rubin, S.M., Gall, A.L., Zheng, N., and Pavletich, N.P. (2005). Structure of the Rb C-terminal domain bound to E2F1-DP1: a mechanism for phosphorylation-induced E2F release. *Cell* *123*, 1093-1106.
- Saksouk, N., Barth, T.K., Ziegler-Birling, C., Olova, N., Nowak, A., Rey, E., Mateos-Langerak, J., Urbach, S., Reik, W., Torres-Padilla, M.E., *et al.* (2014). Redundant mechanisms to form silent chromatin at pericentromeric regions rely on BEND3 and DNA methylation. *Mol Cell* *56*, 580-594.
- Saksouk, N., Simboeck, E., and Déjardin, J. (2015). Constitutive heterochromatin formation and transcription in mammals. *Epigenetics & Chromatin* *8*, 3.
- Schotta, G., Lachner, M., Sarma, K., Ebert, A., Sengupta, R., Reuter, G., Reinberg, D., and Jenuwein, T. (2004). A silencing pathway to induce H3-K9 and H4-K20 trimethylation at constitutive heterochromatin. *Genes Dev* *18*, 1251-1262.

- Schotta, G., Sengupta, R., Kubicek, S., Malin, S., Kauer, M., Callén, E., Celeste, A., Pagani, M., Opravil, S., De La Rosa-Velazquez, I.A., *et al.* (2008). A chromatin-wide transition to H4K20 monomethylation impairs genome integrity and programmed DNA rearrangements in the mouse. *Genes & Development* 22, 2048-2061.
- Seifried, L.A., Talluri, S., Cecchini, M., Julian, L.M., Mymryk, J.S., and Dick, F.A. (2008). pRB-E2F1 complexes are resistant to adenovirus E1A-mediated disruption. *J Virol* 82, 4511-4520.
- Sengupta, S., Lingnurkar, R., Carey, T.S., Pomaville, M., Kar, P., Feig, M., Wilson, C.A., Knott, J.G., Arnosti, D.N., and Henry, R.W. (2015). The Evolutionarily Conserved C-terminal Domains in the Mammalian Retinoblastoma Tumor Suppressor Family Serve as Dual Regulators of Protein Stability and Transcriptional Potency. *Journal of Biological Chemistry* 290, 14462-14475.
- Sharif, J., Endo, Takaho A., Nakayama, M., Karimi, Mohammad M., Shimada, M., Katsuyama, K., Goyal, P., Brind'Amour, J., Sun, M.-A., Sun, Z., *et al.* (2016). Activation of Endogenous Retroviruses in Dnmt1^{-/-} ESCs Involves Disruption of SETDB1-Mediated Repression by NP95 Binding to Hemimethylated DNA. *Cell Stem Cell*.
- Sherr, C.J., and Roberts, J.M. (1995). Inhibitors of mammalian G1 cyclin-dependent kinases. *Genes & Development* 9, 1149-1163.
- Shukla, R., Upton, Kyle R., Muñoz-Lopez, M., Gerhardt, Daniel J., Fisher, Malcolm E., Nguyen, T., Brennan, Paul M., Baillie, J.K., Collino, A., Ghisletti, S., *et al.* (2013). Endogenous Retrotransposition Activates Oncogenic Pathways in Hepatocellular Carcinoma. *Cell* 153, 101-111.
- Slotkin, R.K., and Martienssen, R. (2007). Transposable elements and the epigenetic regulation of the genome. *Nat Rev Genet* 8, 272-285.
- Smith, Z.D., and Meissner, A. (2013). DNA methylation: roles in mammalian development. *Nat Rev Genet* 14, 204-220.
- Srinivasan, S.V., Mayhew, C.N., Schwemberger, S., Zagorski, W., and Knudsen, E.S. (2007). RB loss promotes aberrant ploidy by deregulating levels and activity of DNA replication factors. *J Biol Chem* 282, 23867-23877.
- Stehelin, D., Varmus, H.E., Bishop, J.M., and Vogt, P.K. (1976). DNA related to the transforming gene(s) of avian sarcoma viruses is present in normal avian DNA. *Nature* 260, 170-173.
- Strand, M., Prolla, T.A., Liskay, R.M., and Petes, T.D. (1993). Destabilization of tracts of simple repetitive DNA in yeast by mutations affecting DNA mismatch repair. *Nature* 365, 274-276.

- Su, I.H., Basavaraj, A., Krutchinsky, A.N., Hobert, O., Ullrich, A., Chait, B.T., and Tarakhovskiy, A. (2003). Ezh2 controls B cell development through histone H3 methylation and Igh rearrangement. *Nat Immunol* 4, 124-131.
- Tachida, H., and Iizuka, M. (1992). Persistence of Repeated Sequences That Evolve by Replication Slippage. *Genetics* 131, 471-478.
- Talluri, S., and Dick, F.A. (2012). Regulation of transcription and chromatin structure by pRB: here, there and everywhere. *Cell Cycle* 11, 3189-3198.
- Talluri, S., Isaac, C.E., Ahmad, M., Henley, S.A., Francis, S.M., Martens, A.L., Bremner, R., and Dick, F.A. (2010). A G1 checkpoint mediated by the retinoblastoma protein that is dispensable in terminal differentiation but essential for senescence. *Mol Cell Biol* 30, 948-960.
- Tassan, J.P., Schultz, S.J., Bartek, J., and Nigg, E.A. (1994). Cell cycle analysis of the activity, subcellular localization, and subunit composition of human CAK (CDK-activating kinase). *The Journal of cell biology* 127, 467.
- Taunton, J., Hassig, C.A., and Schreiber, S.L. (1996). A mammalian histone deacetylase related to the yeast transcriptional regulator Rpd3p. *Science* 272, 408-411.
- Temin, H.M., and Mizutani, S. (1970). RNA-dependent DNA polymerase in virions of Rous sarcoma virus. *Nature* 226, 1211-1213.
- Thompson, P.J., Macfarlan, T.S., and Lorincz, M.C. (2016). Long Terminal Repeats: From Parasitic Elements to Building Blocks of the Transcriptional Regulatory Repertoire. *Mol Cell* 62, 766-776.
- Treangen, T.J., and Salzberg, S.L. (2012). Repetitive DNA and next-generation sequencing: computational challenges and solutions. *Nat Rev Genet* 13, 36-46.
- Trojer, P., and Reinberg, D. (2007). Facultative Heterochromatin: Is There a Distinctive Molecular Signature? *Molecular Cell* 28, 1-13.
- Uhlmann, F. (2016). SMC complexes: from DNA to chromosomes. *Nat Rev Mol Cell Biol* 17, 399-412.
- van den Heuvel, S., and Dyson, N.J. (2008). Conserved functions of the pRB and E2F families. *Nat Rev Mol Cell Biol* 9, 713-724.
- van der Vlag, J., and Otte, A.P. (1999). Transcriptional repression mediated by the human polycomb-group protein EED involves histone deacetylation. *Nat Genet* 23, 474-478.
- Venkatesh, S., and Workman, J.L. (2015). Histone exchange, chromatin structure and the regulation of transcription. *Nat Rev Mol Cell Biol* 16, 178-189.

- Verdin, E., and Ott, M. (2015). 50 years of protein acetylation: from gene regulation to epigenetics, metabolism and beyond. *Nat Rev Mol Cell Biol* *16*, 258-264.
- Walker, P.M.B. (1971). "Repetitive" DNA in higher organisms. *Progress in Biophysics and Molecular Biology* *23*, 145-190.
- Walter, M., Teissandier, A., Perez-Palacios, R., and Bourc'his, D. (2016). An epigenetic switch ensures transposon repression upon dynamic loss of DNA methylation in embryonic stem cells. *eLife* *5*.
- Weinberg, R.A. (1995). The retinoblastoma protein and cell cycle control. *Cell* *81*, 323-330.
- Weiss, R.A. (2006). The discovery of endogenous retroviruses. *Retrovirology* *3*, 67.
- Wells, J., Yan, P.S., Cechvala, M., Huang, T., and Farnham, P.J. (2003). Identification of novel pRb binding sites using CpG microarrays suggests that E2F recruits pRb to specific genomic sites during S[thinsp]phase. *Oncogene* *22*, 1445-1460.
- Whyte, P., Buchkovich, K.J., Horowitz, J.M., Friend, S.H., Raybuck, M., Weinberg, R.A., and Harlow, E. (1988). Association between an oncogene and an anti-oncogene: the adenovirus E1A proteins bind to the retinoblastoma gene product. *Nature* *334*, 124-129.
- Wicker, T., Sabot, F., Hua-Van, A., Bennetzen, J.L., Capy, P., Chalhoub, B., Flavell, A., Leroy, P., Morgante, M., Panaud, O., *et al.* (2007). A unified classification system for eukaryotic transposable elements. *Nat Rev Genet* *8*, 973-982.
- Williams, B.O., Schmitt, E.M., Remington, L., Bronson, R.T., Albert, D.M., Weinberg, R.A., and Jacks, T. (1994). Extensive contribution of Rb-deficient cells to adult chimeric mice with limited histopathological consequences. *Embo j* *13*, 4251-4259.
- Wu, Z., Zheng, S., and Yu, Q. (2009). The E2F family and the role of E2F1 in apoptosis. *The International Journal of Biochemistry & Cell Biology* *41*, 2389-2397.
- Ye, J., Renault, V.M., Jamet, K., and Gilson, E. (2014). Transcriptional outcome of telomere signalling. *Nat Rev Genet* *15*, 491-503.
- Yee, A.S., Reichel, R., Kovesdi, I., and Nevins, J.R. (1987). Promoter interaction of the E1A-inducible factor E2F and its potential role in the formation of a multi-component complex. *The EMBO Journal* *6*, 2061-2068.
- Zheng, N., Fraenkel, E., Pabo, C.O., and Pavletich, N.P. (1999). Structural basis of DNA recognition by the heterodimeric cell cycle transcription factor E2F-DP. *Genes Dev* *13*, 666-674.

Chapter 2

2 **An RB-EZH2 complex mediates cell cycle independent silencing of repetitive DNA sequences**

2.1 Abstract

Repetitive genomic regions include tandem sequence repeats, and interspersed repeats such as endogenous retroviruses and LINE-1 elements. Repressive heterochromatin domains silence expression of these sequences through mechanisms that remain poorly understood. Here, we present evidence that the retinoblastoma protein (pRB) utilizes a cell cycle-independent interaction with E2F1 to recruit enhancer of zeste homologue 2 (EZH2) to diverse repeat sequences. These include simple repeats, satellites, LINEs and endogenous retroviruses, as well as transposon fragments. We generate a mutant mouse strain carrying an F832A mutation in *Rb1* that is defective for recruitment to repetitive sequences. Loss of pRB-EZH2 complexes from repeats disperses H3K27me3 from these genomic locations and permits repeat expression. Consistent with maintenance of H3K27me3 at the *Hox* clusters, these mice are developmentally normal. However, susceptibility to lymphoma suggests that pRB-EZH2-recruitment to repetitive elements may be cancer relevant.

2.2 Introduction

Repetitive genomic regions comprise approximately 50% of the human genome (Lander et al., 2001). These repetitive elements include tandem repeats, such as satellite sequences that underpin the heterochromatin at centromeres, in addition to interspersed repeats that are capable of transposition (Slotkin and Martienssen, 2007). Expression of

repetitive elements poses a mutagenic threat to the host through multiple possible aberrations (Mager and Stoye, 2015). For example, de-repression of satellite repeats disrupts organization of centromeric heterochromatin and coincides with defects in chromosome segregation and meiosis (Slotkin and Martienssen, 2007). At the transcriptional level, de-repressed repeat sequences can serve as alternate enhancers or promoters that permit 'read-through' transcription and cis-activation of proximal genes, including proto-oncogenes that have been established as initiating events in human lymphomas (Lamprecht et al., 2010). More recently, sequencing-based studies demonstrate that re-integration of activated mobile repetitive elements can generate cancer-relevant mutations in pre-malignant lesions that precede various human cancers (Helman et al., 2014; Iskow et al., 2010; Lamprecht et al., 2010; Lee et al., 2012; Lock et al., 2014). Likewise, re-integration of activated satellites expands centromere repeats and can fuel cancer cell growth (Bersani et al., 2015). The frequent co-occurrence of repetitive element reactivation with genome instability suggests that the antagonism of repeat silencing may be achieved through mechanisms commonly employed to initiate tumorigenesis. Recent evidence of p53-mediated transposon repression indicates that this may indeed be the case (Leonova et al., 2013; Wylie et al., 2016). Thus, any potential contribution of repetitive sequences to cancer initiation must ultimately be mitigated through transcriptional silencing. Understanding how silencing is achieved is fundamental to understanding how cancer-initiating mechanisms may circumvent this facet of genome regulation.

Repetitive elements are transcriptionally repressed by DNA methylation and histone tail modifications (Schlesinger and Goff, 2015). Sustained repression of repetitive

elements during periods of genome-wide DNA hypomethylation in early embryogenesis has stimulated investigation of histone-dependent repression mechanisms in ES cells (Leung and Lorincz, 2012; Levin and Moran, 2011). Repetitive sequences in ES cells are enriched for H3K9me_{2/3}, H4K20me₃, and H3K27me₃ (Day et al., 2010). Upon loss of DNA methylation, H3K27me₃ expands to maintain silencing of interspersed and tandem repeat sequences (Walter et al., 2016). Following genetic ablation of H3K9 histone methyl transferases, H3K27me₃ compensates for H3K9me₃ loss at interspersed and pericentromeric repeats (Peters et al., 2003). However, additional deletion of the Polycomb repressor complex 2 (PRC2) subunit EED can de-regulate these repetitive sequences indicating redundancy of repressive mechanisms (Walter et al., 2016). Proteomic analysis of ES cells indicates that 60% of histone H3 proteins are comprised of H3K27me_{2/3} modifications (Peters et al., 2003). Collectively, these data suggest H3K27me₃-based heterochromatinization provides a dynamic epigenetic mechanism that silences repeat sequence expression in response to alterations in other silencing mechanisms, and likely contributes extensively on its own (Bulut-Karslioglu et al., 2014; Karimi et al., 2011; Liu et al., 2014). Despite this fundamental contribution to genome-wide repeat silencing, little is known about the mechanism of H3K27me₃ deposition and expansion at repetitive sequences, as investigation of Polycomb at non-unique genomic regions primarily concerns the regulation of neighbouring genes (Bauer et al., 2015; Casa and Gabellini, 2012). Beyond ES cells, investigation of repetitive DNA silencing by PRC2 remains even less understood.

Dynamic response to various genomic alterations positions Polycomb as a robust barrier to reactivation of repeat sequences. Thus, disruption of genome stability through

repeat sequence resurrection likely requires disruption of Polycomb-mediated heterochromatin. A surprising link between Polycomb, repetitive sequences, and cancer-initiating mechanisms may be the RB tumor suppressor protein (pRB). While pRB is best known as a repressor of E2F transcription factors at cell cycle genes during the G1 phase of the cell cycle, pRB family proteins also direct H3K27me3 to repress transcription during differentiation and stress (Blais et al., 2007; Bracken et al., 2007; Karetka et al., 2015; Kotake et al., 2007). In addition, RB cell cycle-independent interactions with chromatin (Avni et al., 2003; Wells et al., 2003) have been observed, but genome-wide analysis of pRB at repeat sequences is lacking (Coschi et al., 2014; Montoya-Durango et al., 2009). In addition, there is no evidence pRB-mediated regulation of H3K27me3 is sufficiently widespread to match the magnitude of H3K27me3 abundance and distribution at repeats.

In this study we demonstrate that pRB and EZH2 form a complex that directs H3K27me3 deposition at most repeat element types from simple sequence repeats and satellites, to DNA transposons, LINEs, SINEs, and endogenous retroviruses. We report the generation of a new strain of mice carrying a targeted point mutation, F832A (called *Rb1^S*), that is specifically defective for recruitment of EZH2 to repetitive sequences. In the absence of pRB recruitment, EZH2 no longer directs H3K27me3 to these elements, leading to dispersion or loss of heterochromatin. *Rb1^{S/S}* fibroblast cells and splenocytes express diverse repeat sequences, including tandem and interspersed elements, and aged *Rb1^{S/S}* mice develop spontaneous lymphomas. Collectively, these data suggest that silencing of repetitive elements contributes to pRB's function as a tumor suppressor.

2.3 Experimental Procedures

2.3.1 Cell Culture and Mice

Mouse embryonic fibroblasts (MEFs) were generated from E13.5 embryos using standard procedures and cultured as previously described (Coschi et al., 2014). Cells were typically arrested by serum starvation for at least 3 days.

2.3.2 Chromatin immunoprecipitation

ChIP methods were based on previously published work (Cecchini et al., 2014). Briefly, cells were cross-linked with 2mM ethylene glycol bissuccinimidylsuccinate (EGS) and 1% formaldehyde. Chromatin was sonicated to ≤ 400 bp in length and normalized between experimental groups. Samples were pre-cleared with protein G Dynabeads and ChIP antibodies were added to immunoprecipitate proteins. Samples had their cross-links reversed at 65°C and were treated with RNase and proteinase K. DNA was isolated for qPCR or library preparation followed by single-end sequencing using Illumina HiSeq2500. See supplemental tables for list of ChIP-qPCR primers. Further details of ChIP-reChIP and ChIP-seq are available in supplemental experimental procedures.

2.3.3 RNA expression

Total RNA was isolated using Trizol reagent, treated with DNaseI, and reverse-transcribed to generate cDNA using random primers and Superscript III reverse transcriptase (Invitrogen). qRT-PCR was performed using iQ SYBR green Super Mix (Bio-Rad) using a CFX96 Real-Time PCR Detection System (Bio-Rad). Relative changes in gene expression were calculated by normalizing to *β -actin*. Primer sequences are

described in supplemental materials. Some expression microarray experiments have been reported previously (Cecchini et al., 2014), or can be found in GEO (GSE85640).

2.3.4 Analysis of ChIP-seq and RNA-seq experiments

Sequence reads from ChIP experiments were mapped to the mm9 genome assembly without allowing mismatches as previously reported (Bulut-Karslioglu et al., 2014).

Reads with more than one exact match were randomly assigned amongst these locations.

RNA-seq reads were mapped to a custom repeat index (Day et al., 2010), assigning reads to their best match allowing up to two sequence mismatches. Further details on computational analyses are available in supplemental materials. Sequence data is available in GEO (accession number GSE85640).

2.3.5 Generation of gene targeted mice

A targeting vector encoding a floxed PGK-Neomycin cassette and an F832A missense point mutation in exon 24 of the *Rbl* gene was generated and electroporated into mouse R1 embryonic stem (ES) cells in the London Regional Transgenic and Gene-Targeting facility. After G418 selection, positive clones were identified by Southern blotting and microinjected into blastocysts to generate chimeric males that were intercrossed with *EIIa-Cre* transgenic females essentially as we have reported previously (Isaac et al., 2006). Primers designed to flank the floxed Neomycin cassette amplified a product approximately 80 bp larger than the wild-type product, indicating presence of a residual LoxP site after successful Cre-mediated excision of the floxed marker in targeted F1 offspring. DNA sequencing confirmed germline transmission of the targeted allele. Targeted F1 progeny were intercrossed to generate mice that did not express the Cre-

recombinase. Heterozygous F2 crosses produced offspring genotypes according to expected Mendelian frequencies, with viable, fertile, homozygous mutant mice that developed into adulthood without overt developmental defects. Animals were housed and handled as approved by the Canadian Council on Animal Care.

2.3.6 Cell cycle analysis

Asynchronous or serum-starved MEFs were pulse-labeled with bromodeoxyuridine (BrdU; Amersham Biosciences) for 2 hours, detached with 3 mM EDTA, and ethanol-fixed. Cells were then permeabilized with 2 N HCl and 0.5% TritonX-100, neutralized with 0.1M NaB₄O₇ (pH 8.5), immunostained with anti-BrdU (BD Biosciences), followed by FITC-conjugated secondary (Vector laboratories), then stained with propidium iodide. Cells were treated with RNase, strained, and analyzed by flow cytometry on a Beckman-Coulter EPICS XL-MCL (Cecchini et al., 2012).

2.3.7 Cell extracts

Nuclear extracts were generated according to methods described by Cecchini and Dick (Cecchini and Dick, 2011). Briefly, cells were washed twice and collected in 1 ml of PBS. Cells were then re-suspended in three times cell volume of hypotonic lysis buffer (20 mM Tris-HCl, pH 7.5, 10 mM KCl, 3 mM MgCl₂, 1 mM EDTA) supplemented with protease inhibitors. After 5 minutes on ice, 0.05% Nonidet P40 was added, extracts were iced 5 minutes before nuclei were pelleted by centrifugation at 1700 g for 10 minutes at 4°C and washed twice with hypotonic lysis buffer containing 0.05% Nonidet P40. Nuclei were re-suspended in Gel Shift Extract (GSE) buffer (20mM Tris pH 7.5, 420 mM NaCl, 1.5mM MgCl₂, 0.2mM EDTA, 25% glycerol) and frozen at -80°C. Extracts were

thawed, cellular debris was cleared by centrifugation, and extracts were quantified for interaction assays. To generate whole-cell lysates, cells were washed twice with PBS, and scraped in ice-cold RIPA buffer (50 mM Tris-HCl [pH 8.0], 150 mM NaCl, 1% Triton X-100, 0.5% sodium deoxycholate, and 0.1% SDS) supplemented with protease inhibitors. After 20 minutes on ice, lysates were centrifuged at 20800 g for 20 min at 4°C. Supernatant was isolated, quantified, boiled 5 minutes in Laemmli sample buffer, and then resolved by SDS-PAGE (Yu et al., 2012). See appendix F for antibodies used.

2.3.8 Chromatin Fractionation

Chromatin isolation method was adapted from Mendez and Stillman (Méndez and Stillman, 2000). Briefly, cells were resuspended in buffer A (10 mM Tris [pH 8.0], 10 mM KCl, 1.5 mM MgCl₂, 0.34 M sucrose, 10% glycerol, 1 mM DTT) supplemented with protease inhibitors at 4×10^7 cells/ml, and incubated on ice for 5 minutes. Equal volume of 0.3mg/ml digitonin in buffer A was added, and the cells were further incubated for 10 minutes on ice in the presence of detergent. Approximately 5-10% of this total volume was stored to preserve a whole-cell extract fraction. Centrifugation at 1300 xg for 5 minutes at 4°C pelleted nuclei, and supernatant containing the cytoplasmic fraction was collected. Nuclei were washed in buffer A, then lysed 30 minutes on ice in buffer B (3 mM EDTA, 0.2 mM EGTA, 1 mM DTT) supplemented with protease inhibitors using a volume ~2x that of the pellet. Insoluble chromatin was pelleted by centrifugation at 1,700 xg for 5 minutes at 4°C, and supernatant containing the nucleoplasmic fraction was collected. The chromatin pellet was resuspended in DNaseI buffer (20mM Tris [pH 7.5], 10 mM MgCl₂) at a volume ~2x that of the pellet, supplemented with 200U of DNaseI (Sigma), and incubated 1 hour on ice. All fractions were quantified, boiled in Laemmli

buffer, resolved by SDS-PAGE, and coomassie stained to assess fraction purity and histone normalization. Fractions were then used for western blotting. See Appendix F for antibodies used.

2.3.9 GST pulldowns

GST-fusion proteins were expressed in and purified from 500 ml cultures of BL21-DE3-Gold *Escherichia coli* (Stratagene) using glutathione–Sepharose beads according to standard protocols. Purified GST-fusion protein (4 µg) was incubated with 400µg of nuclear extract diluted with low salt GSE buffer (20 mM Tris-HCl pH 7.5, 200 mM NaCl, 1.5 mM MgCl₂, 0.2 mM EDTA, 1 mM DTT and 0.1% Nonidet P40), and rocked 1-2 hours at 4°C. GST–protein complexes were collected with glutathione–Sepharose, washed twice with low salt GSE buffer, and eluted with Laemmli sample buffer for western blot analysis (Dick et al., 2000). See table S1 for antibodies used.

2.3.10 Immunoprecipitation

For immunoprecipitations, nuclear extract was diluted 1:1 in IP wash buffer (20mM Tris pH 7.5, 200 mM NaCl, 1.5 mM MgCl₂, 0.2 mM EDTA, 25 mM DTT and 0.1% NP-40). Protein complexes were immunoprecipitated overnight at 4°C with antibodies pre-bound to washed protein G Dynabeads. Antibody-protein complexes were washed twice with IP wash buffer, then eluted in Laemmli sample buffer for western blot analysis. See table S1 for antibodies used (Cecchini and Dick, 2011).

2.3.11 Splenocyte ChIP

Splenocyte ChIP experiments were conducted following splenocyte isolation from 6-week old adult mice. Briefly, spleens were isolated from freshly sacrificed mice, and mashed through a 40µm sterile cell strainer in a 10cm dish containing 3-4ml of media.

Cells were then isolated, pelleted at 4°C, and incubated 5 minutes in 1x RBC lysis buffer (0.15M NH₄Cl, 10mM KHCO₃, 0.1mM EDTA) to lyse erythrocytes. Splenocytes were washed twice in 1x PBS, rocked 1 hour at room temperature in 10ml of 2mM EGS-PBS, then supplemented with formaldehyde to a final concentration of 1% and rocked for another 15 minutes at room temperature before fixation was quenched with 2.5M glycine for 15 minutes. Fixed splenocytes were pelleted, and processed in ChIP buffers 1-3 as described in methods. Splenocytes were resuspended in a final volume of 200μL of ChIP lysis buffer and sonicated to ≤400 bp before ChIP experiments were conducted as per MEF ChIP experiments.

2.3.12 ChIP-reChIP

For ChIP-reChIP experiments, we adapted methods from Thillainadesan and colleagues (Thillainadesan et al., 2012). Protein-DNA complexes were eluted 30 minutes at 37°C in 10 mM DTT with 5 mM β-mercaptoethanol. Eluted DNA was diluted 10x in reChIP buffer (1% Triton X-100, 2 mM EDTA, 20 mM Tris-HCl pH 8.1, 150 mM NaCl), and incubated with second antibody overnight at 4°C. Antibody-protein complexes were immunoprecipitated with washed protein G Dynabeads for 2 hours at 4°C, then washed with low salt buffer, high salt buffer, and TE. Reverse-crosslinking and purification were done as described in ChIP methods section. See table S1 for antibodies used.

2.3.13 ChIP-seq and Read Alignment

ChIP was conducted as described in methods according to protocols adapted from Cecchini *et al.* (Cecchini et al., 2014). DNA from multiple replicates per genotype were pooled to achieve DNA yield required for library preparation (Illumina TruSeq). For pRB ChIP-seq in proliferating MEFs, 6 IPs were pooled, while 11-18 IPs were pooled in

arrested MEFs. For H3K27me3 ChIP-seq in proliferating MEFs, 9 IPs were pooled, while 12 IPs were pooled for IPs in arrested MEFs. For EZH2 ChIP-seq in proliferating MEFs, 9 IPs were pooled. Libraries were sequenced using an Illumina HiSeq 2500. Resulting FASTQ reads were aligned to mouse genome build mm9 using Bowtie version 2.2.3 (Langmead and Salzberg, 2012). Reads aligning to multiple locations of a particular repeat element were distributed randomly to these positions, while reads mapping to the same location were retained as previously described (Bulut-Karslioglu et al., 2014). The following command was used: `bowtie2 -t -p 24 -D 15 -R 2 -L 32 -i S,1,0.75 -x mm9 -U reads.fastq -S output.SAM`.

2.3.14 Peak Calling and annotation

Peaks were identified using MACS1.4 or MACS2 version 2.0.10 according to parameters stated below, and the options to detect broad peak distributions for histone marks (Feng et al., 2012; Zhang et al., 2008). The results from this peak calling were stored as BED files. The following commands were used:

```
macs14 -t ChIP.sam -c input.sam -n output -g mm -p 0.01 -m 5,50 --bw 180 --keep-dup all -B -S -w; MACS2 callpeak -t ChIP.sam -c input.sam -n output -g mm -q 0.05 --broad -keep-dup all -B (q 0.01 for histones). Peak enrichment per genomic region was determined using HOMER (Heinz et al., 2010). Peak intersection and enrichment at repetitive elements was determined using BEDintersect of MACS peaks against repeat indices derived from UCSC RepeatMasker (Quinlan and Hall, 2010).
```

2.3.15 deepTools enrichment analysis

`bamCompare` was used generate bigWig files of ChIP reads normalized to input (Ramirez et al., 2014). `computeMatrix` was used to calculate read enrichment scores at wild-type

repeat peak intersects or promoter regions. heatMapper was used to plot enrichment at each repeat element per repeat family +/-1kb of wild-type repeat peak intersect locations (Ramirez et al., 2014).

2.3.16 RNA-sequencing

Total RNA from quiescent MEFs was isolated using TRIzol reagent protocol (Invitrogen). rRNA was depleted from total RNA using RiboMinus Euk System V2 (Life technologies). rRNA-depleted RNA samples were submitted for picoanalyzer analysis to determine concentration, purity, and rRNA content. Samples with <10% rRNA remaining were submitted for library construction at the Sick Kids/TCAG (Toronto) facility followed by paired end sequencing on an Illumina HiSeq 2500.

2.3.17 Expression microarray analysis

Total RNA was extracted according to Trizol manufacturer protocol, and quality control tested using an Agilent 2100 Bioanalyzer. Preparations that met quality control standards were used to prepare biotin end-labeled single strand cDNA. 5.5 ug of prepared cDNA was hybridized for 16 hours at 45°C on GeneChip Mouse Gene 1.0 ST Arrays that were subsequently washed, stained, and scanned using the Affymetrix GeneChip Scanner 3000 7G. RMA expression values derived from CEL files were log-transformed prior to ANOVA analysis using Partek Genomics Suite. Log₂ values of mutant/wild-type were plotted as heatmaps using matrix to PNG at chibi.ubc.ca/matrix. Annotations were derived from Affymetrix MoGene-1 0-st-v1 Transcript Cluster Annotations, CSV, Release 32.

2.3.18 RNA-seq read alignment and analysis

Single end sequence reads were aligned using Bowtie v1.0.0 to indices of repeats derived from Repbase and Tandem Repeats Databases (Day et al., 2010). Bowtie parameters were established to report the single best alignment per read, with a default value of 2 for the maximum number of mismatches; the following Bowtie v1.0.0 parameters were used: `bowtie -S -best -k 1 -chunkmbs 500 -p24 -t -un`. Read enrichments were binned using the `awk` command according to functional categories, based on RepeatMasker's annotation. Residual rRNA reads were subtracted from the total number aligned reads reported for each sample. The number of reads for each category were then normalized to the corrected number of total aligned reads per sample. Expression per biological replicate relative to the control average was compared between repFamily categories as a LOG_2 ratio, and plotted as a heatmap using `matrix` to PNG at chibi.ubc.ca/matrix.

2.3.19 Bisulfite sequencing

Bisulfite sequencing was conducted as previously described (Denomme et al., 2012; White et al., 2015). Briefly, P4 MEFs were trypsinized, washed and re-suspended in 1 ml of 1X PBS. 1 μL of cell suspension was embedded into a 2:1 3% low melting point (LMP) agarose (Sigma) and lysis [100 mM Tris-HCl, pH 7.5 (Bioshop), 500 mM LiCl (Sigma), 10 mM EDTA, pH 8.0 (Sigma), 1% LiDS (Bioshop), and 5 mM DTT (Sigma), 1 μL of 2 mg/ml proteinase K (Sigma), and 1 μL 10% Igepal (Sigma)] solution for bisulfite mutagenesis. This mixture was iced 10 minutes, then lysed 20 hours overnight in 500 μL of SDS lysis buffer (450 μL TE pH 7.5, 50 μL 10% SDS, 1 μL proteinase K) at 50°C. Lysis buffer was replaced with 300 μL of mineral oil, and samples were processed for bisulfite mutagenesis or stored at -20°C 1-5 days, then processed for bisulfite to

amplify IAP (Lane, 2003) and LINE1 sequences as previously described (Denomme et al., 2012; White et al., 2015). Briefly, proteinase K was inactivated at 90°C, then samples were iced 10 minutes, incubated 15 minutes at 37°C with 0.1 M NaOH solution to denature DNA, and covered with 300 µL of mineral oil. Following addition of 500 µL of 2.5 M bisulfite solution, samples were incubated 3.5 hours at 50°C, then desulfonated 15 minutes in 1 mL of 0.3 M NaOH at 37°C. Samples were washed twice in TE pH 7.5 then water. Negative controls were processed in parallel. For first round PCR, 10 µL of agarose bead with bisulfite converted DNA was added to Hot Start Ready-To-Go (RTG) (GE Healthcare) PCR beads hydrated with 0.5 µL of 10 µM IAP (Lane, 2003)_F1/R1 or L1_F/R1 external primers, 1 µL of 240 ng/mL transfer RNA and 13 µL water with a 25 µL mineral oil overlay. 5 µL of amplicon was added to 20 µL of RTG beads mixed with 0.5 µL of each 10 µM IAP (Lane, 2003)_F2/R2 or L1_F/R2 internal primer and 19 µL water for nested PCR. PCR amplification was performed as follows: 94°C for 3 minutes, followed by 35 cycles of 94°C for 1 minute, 53°C (IAP)/56°C (L1) for 1 minute, 72°C for 1 minute, and a final extension of 72°C for 5 minutes.

2.3.20 qRT-PCR analysis of expression

Tissues from 6-8 week-old mice were harvested and processed for RNA isolation using the SIGMA GenElute mammalian total RNA kit. RNA was DNaseI (SIGMA) treated and reverse transcribed to cDNA using the BIO-RAD iScript RT Supermix kit. Isolated cDNA was used in qRT-PCR reactions. Resulting target C_q values were normalized to *β-actin*, then expressed as fold change relative to the global wild-type mean. Normalized fold change was plotted as a heatmap using matrix to PNG at chibi.ubc.ca/matrix.

2.4 Results

2.4.1 The RB protein associates with repetitive genomic sequences

To explore emerging chromatin regulatory functions beyond cell cycle control, we compared pRB association with chromatin in arrested and proliferating mouse embryonic fibroblasts (MEFs). While noticeably reduced, pRB retains some chromatin binding in proliferating cells (Figure 2.1A). We sought to further investigate genome wide distribution of pRB across growth conditions by chromatin immunoprecipitation-sequence analysis (ChIP-seq). We used a stringent sequence alignment approach that prohibited mismatches. We also randomized read assignments where more than one exact match existed to enhance potential alignments to repetitive regions of the genome (see methods and (Bulut-Karslioglu et al., 2014)). Analysis of peak distribution across broad genomic regions reveals a dramatic abundance of peaks in introns and intergenic locations (Figure 2.1B). The proportion of peaks that localize to introns and intergenic regions remains unaltered by proliferative status, suggesting that even though pRB occupancy on chromatin may be reduced in proliferating cells, this distribution pattern displays cell cycle-independence for pRB at these regions. Comparison of enrichment at wild type peak locations within promoters to the same genomic locations in *Rb1*^{-/-} controls confirms a high degree of stringency in peak assignment (Figure 2.1C). Since an abundance of peaks localize to non-coding regions, we next annotated peaks based on categories of repetitive sequences (Figure 2.1D). Analysis of peak distribution reveals pRB association with SINEs, long terminal repeat (LTR)-containing endogenous retroviruses (ERVs), LINEs, and simple repeat sequences among others. Importantly, these surprising findings are mirrored in a meta-analysis of a recently published human

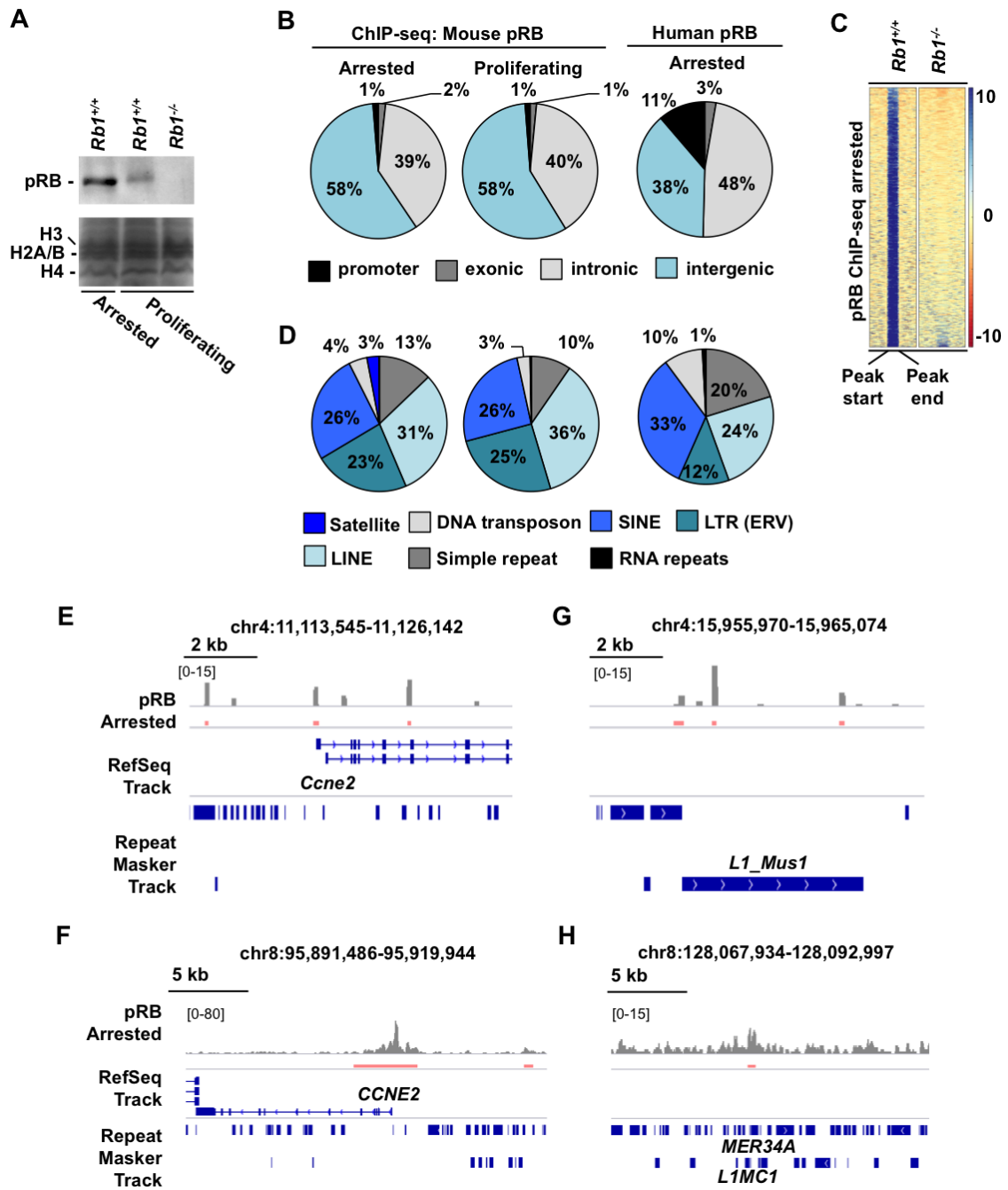


Figure 2.1: pRB associates with genomic repeats in murine and human fibroblasts

Figure 2.1: pRB associates with genomic repeats in murine and human fibroblasts

(A) pRB western blots of MEF chromatin fractions. Coomassie stained histones indicate relative chromatin quantities per lane. (B) Overall genomic distribution of pRB ChIP-seq peaks. Growth conditions are indicated above the pie charts; n=424588 peaks and n=77809 peaks for mouse pRB in arrested and proliferating MEFs respectively; n=71511 peaks for human pRB in arrested IMR90 cells. (C) Heat maps display scaled pRB ChIP-seq read build ups from the indicated genotypes at proximal promoter regions occupied by wild type pRB peaks. Each row contains ± 1 kb of flanking sequence. The intensity scale indicates magnitude of read enrichment (D) Percent distribution of pRB ChIP-seq peaks amongst indicated repeat sequence classes; n=321892 peaks for mouse pRB arrested, n=49210 peaks for mouse pRB proliferating, and n=99186 peaks for human pRB arrested. RNA repeats include tRNA, snRNA and others. (E) Genome browser tracks display mouse pRB ChIP-seq reads at *Ccne2*. Genomic co-ordinates are indicated above the tracks. Repeat Masker and RefSeq tracks are shown below. Red bars denote regions of pRB enrichment (peaks) determined with MACS. (F) The analogous region of human *CCNE2* is shown and labeled akin to panel D. (G) Example of mouse pRB occupancy at a LINE-1 element 3' of the *Ccne2* gene. (H) Example of a human pRB peak 5' of *CCNE2* that simultaneously overlaps multiple repeat elements.

pRB ChIP-seq study, although promoter occupancy is noticeably greater in human data (Figure 2.1B and 2.1D)(Ferrari et al., 2014).

The RB protein is best known for its regulation of E2F-responsive cell cycle genes, and our mapping of ChIP-seq reads detects these promoter occupancy events in mouse and human data sets (Figure 2.1E and 2.1F). Repeat occupying peaks are also found in neighboring regions of the same chromosomes (Figure 2.1 G and 2.1H). Our analysis of peak distribution in murine cells demonstrates that at least two thirds of pRB occupying peaks map to repetitive sequences (Figure 2.1B and 2.1D). It is difficult to draw a similar conclusion in human data because many pRB peaks contain multiple repetitive elements in the same peak (Figure 2.1H). Collectively these data indicate that pRB associates with diverse repetitive elements in mouse and human fibroblasts. We describe this pattern of pRB distribution as cell cycle independent because it is similar between growth states, but recognize that its magnitude is altered.

2.4.2 Loss of a CDK-resistant pRB-E2F1 interaction disrupts repeat association

We previously identified an interaction between pRB and E2F1 that confers reduced binding to consensus E2F sequence elements and resistance to disruption by CDK phosphorylation(Cecchini and Dick, 2011; Dick and Dyson, 2003). We sought to determine whether the properties of this interaction could underlie the cell-cycle independent pRB occupancy observed in our ChIP-seq. We generated a targeted mutant mouse strain bearing a single F832A substitution to disrupt the unique interaction between pRB and E2F1, and named this allele *Rb1^{S/S}* (Figure 2.2A-D). *Rb1^{S/S}* mice are indistinguishable from their littermates (Figure 2.2E&F), and cells isolated from these mice exhibit ostensibly normal pRB expression levels with no indication of

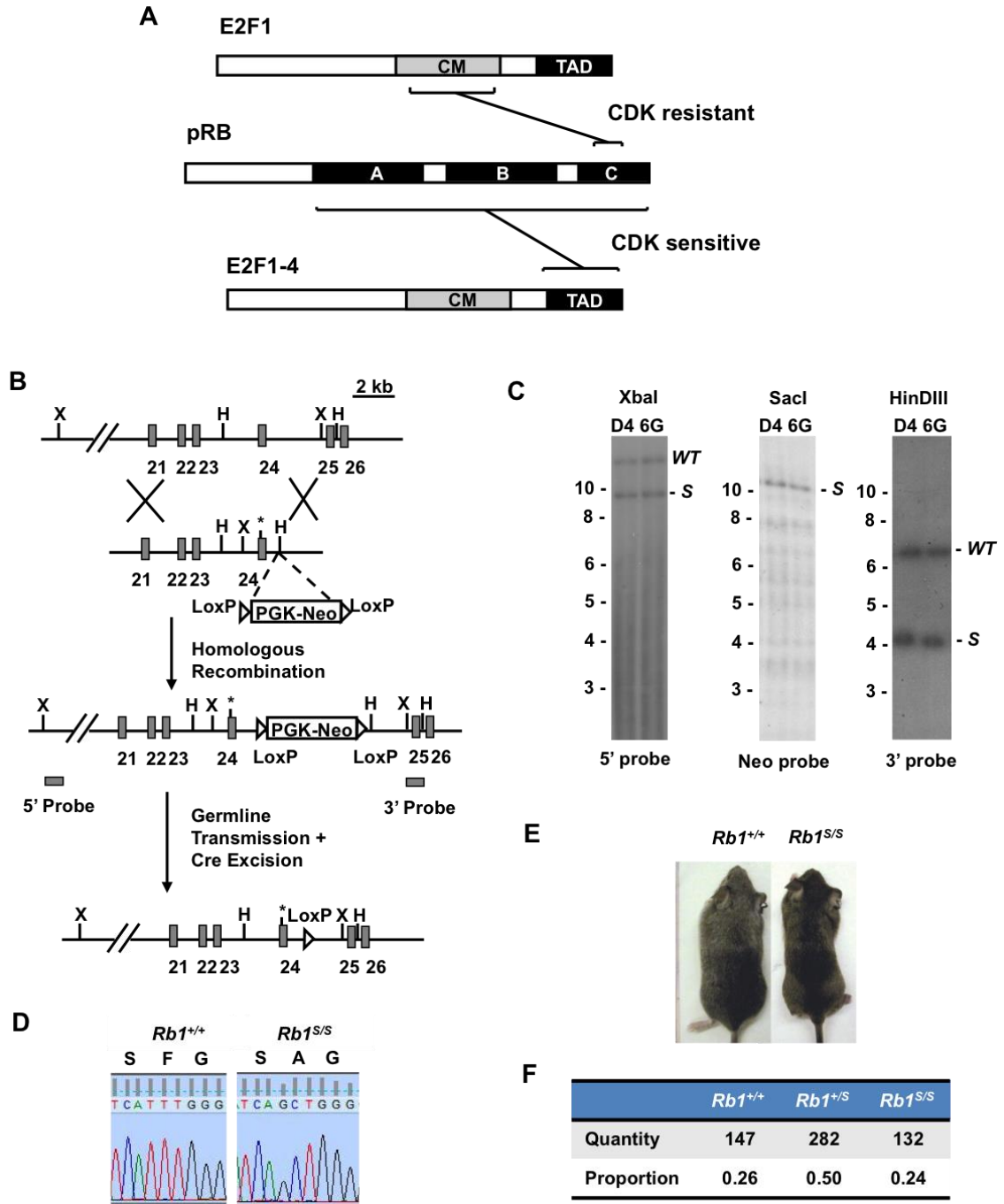


Figure 2.2: *In vivo* disruption of the CDK-resistant pRB-E2F1 interaction.

Figure 2.2: *In vivo* disruption of the CDK-resistant pRB-E2F1 interaction.

(A) Schematic diagram showing the minimal interaction regions for the different pRB-E2F interactions. E2F1-4 transactivation domains (TAD) bind the pRB large pocket domain, while the E2F1 coiled coil and marked-box domain (CM) binds a minimal interaction surface mapped to the pRB-C-terminus. (B) Diagram of the *Rb1* locus along with the targeting vector encoding the F832A missense point mutation in exon 24. Gene structure of a correctly targeted locus is shown with the PGK-neo cassette and the structure of the *Rb1*^S gene following excision of the PGK-neo cassette. Locations of probes used in Southern blots are shown. (C) Southern blots of two correctly targeted ES clones are shown. The left most blot shows the banding pattern from the 5' probe, the neo probe shows a single band corresponding to recombination of the targeting vector, and the right most blot shows the expected fragment sizes from hybridization with the 3' probe. (D) DNA sequencing of *Rb1* exon 24 codon from genomic DNA of the indicated genotypes of mice. (E) Photographs of 6-8 week old wild type and *Rb1*^{S/S} mice. (F) Genotype frequencies from heterozygous intercrosses.

compensatory expression of RB-related family members p107 and p130 (Figure 2.4A). Furthermore, analysis of the F832A substitution in pRB demonstrates a specific defect in binding the E2F1 coiled coil and marked box domain, without effects on E2F transcriptional activation domain binding to pRB (Figure 2.3A-D). Consistent with these biochemical properties, cell cycle regulation and E2F target gene expression are indistinguishable from wild type controls (Figure 2.3E and 2.3G).

Western blots of chromatin fractions reveal diminished pRB^S association with chromatin under both proliferating and arrested conditions (Figure 2.4A). ChIP-qPCR was performed to assess pRB recruitment in arrested and proliferating growth conditions at the cell cycle responsive *Mcm3* promoter. In addition to *Rb1^{S/S}* cells, we utilized the previously characterized *Rb1^G* mutant that disrupts canonical pRB-E2F transcriptional control through R461E and K542E substitutions for comparison (Cecchini et al., 2014)(Figure 2.4B). Under arrested conditions, the pRB^S protein exhibits similar association with the *Mcm3* transcriptional start site (TSS) as wild type pRB, while the pRB^G mutant exhibits reduced occupancy. Under proliferating conditions, wild type and pRB^S occupancy of the *Mcm3* promoter diminishes, consistent with CDK-dependent regulation of pRB-E2F interactions at this genomic location.

Given the retention of pRB^S at E2F cell cycle targets, but the clear loss of chromatin association revealed by fractionation, we conducted ChIP-seq for pRB in *Rb1^{S/S}* cells to discover genomic locations that require this pRB-E2F1 interaction. Since pRB^S chromatin association was globally reduced in Figure 2.4A, we focused our analysis on wild type locations lost in *Rb1^{S/S}* cells. Under both growth conditions, ChIP-

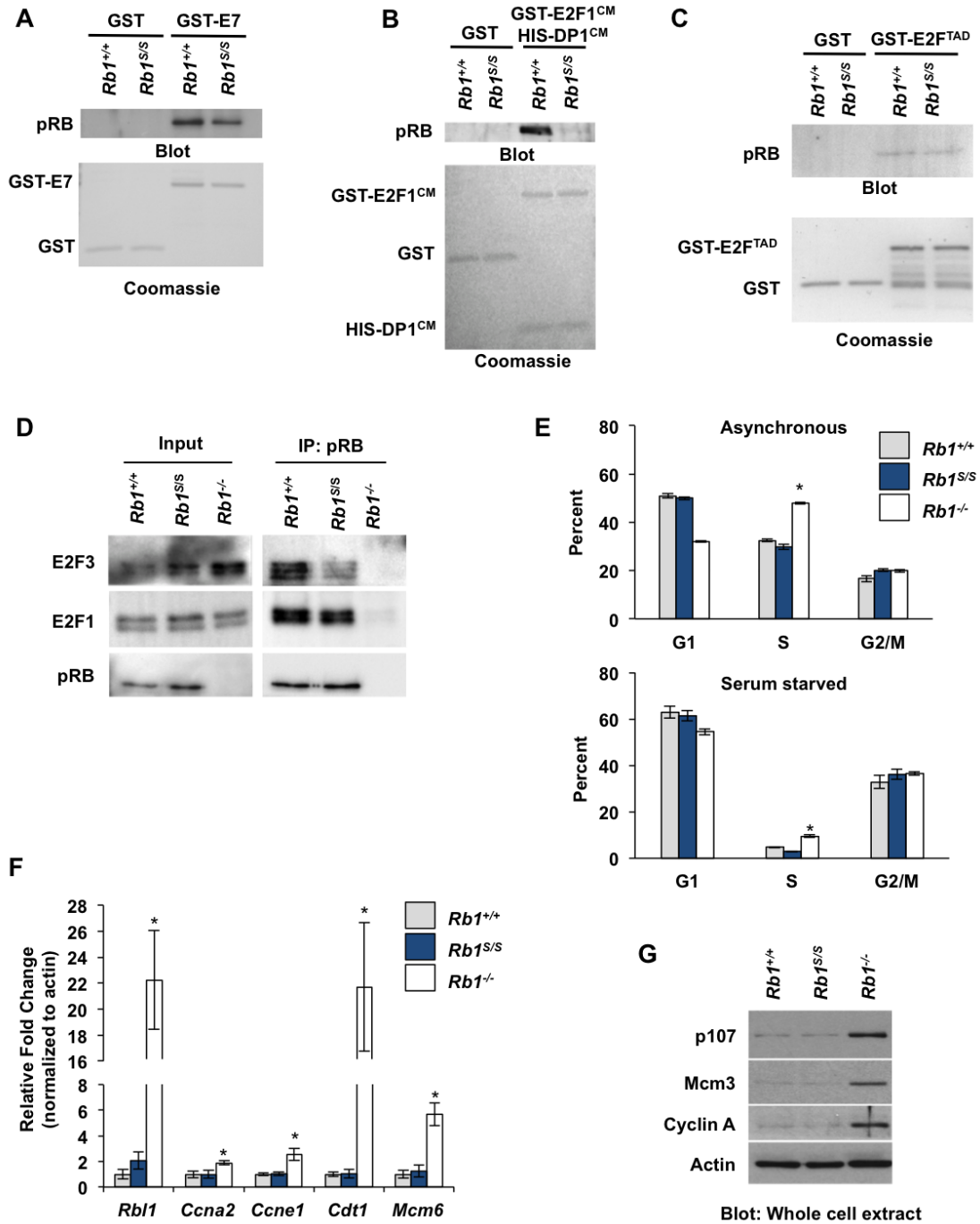


Figure 2.3: The *Rb1*^{S/S} mutant maintains pRB cell cycle regulatory functions in primary mouse fibroblasts.

Figure 2.3: The *Rb1*^{S/S} mutant maintains pRB cell cycle regulatory functions in primary mouse fibroblasts.

(A) Nuclear extracts were prepared from wild type and *Rb1*^{S/S} primary mouse embryonic fibroblasts (MEFs) and pRB was isolated using a GST-E7 pulldown. A western blot demonstrates pRB binding to E7 and a coomassie stained gel shows the loading levels of GST proteins. (B) Western blotting and coomassie stained gels of GST-pulldowns using GST-E2F1^{CM} (aa 200-301) in complex with HIS-DP1^{CM} (aa 198-350) to isolate pRB from nuclear extracts using its unique interaction with E2F1. (C) GST-E2F1-TAD pulldowns were performed to assess binding at the canonical pRB-E2F interaction site. (D) IP-western blotting experiment using extracts from the indicated genotypes of MEFs. The left most blots show levels of pRB, E2F1, and E2F3 present in extracts and pRB associated levels of E2F1 and E2F3 are shown to the right. (E) Asynchronous or 72-hour serum-starved passage 4 MEFs were BrdU pulse-labeled for 2 hours, ethanol-fixed, immunostained, and PI-stained for signal quantification via flow cytometry. Graphs show the proportions of each cell cycle phase from this analysis. (F) qRT-PCR of cDNA from total RNA of 72-hour serum-starved P4 MEFs for indicated targets in pRB mutant MEFs. (G) Western blots of the indicated cell cycle and E2F regulated proteins from whole cell extracts of 72-hour serum-starved P4 MEFs of the indicated genotypes. For all graphs, error bars indicate +/- 1 standard deviation; an asterisk represents a significant difference from the wild type control $P \leq 0.05$ by t-test.

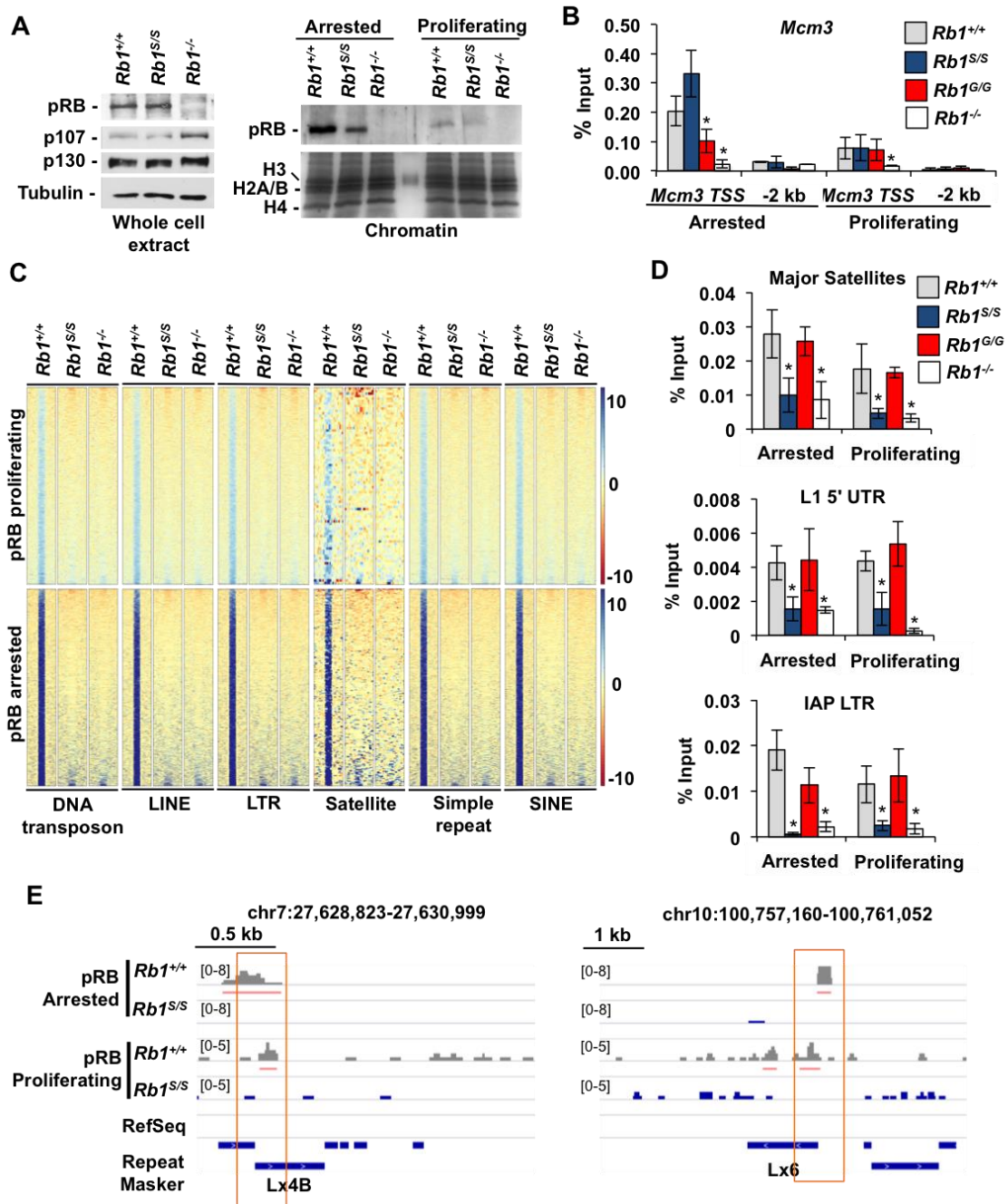


Figure 2.4: Cell cycle independent pRB-repeat association.

Figure 2.4: Cell cycle independent pRB-repeat association.

(A) Western blots of whole cell extracts display expression levels of wild type and the F832A mutant (*Rb1^S*) pRB, as well as related family members p107 and p130. Western blot detects pRB association with chromatin fractions from arrested and proliferating cells. Coomassie stained histones serve as a loading control. (B) pRB ChIP-qPCR at the *Mcm3* transcriptional start site (TSS) and 2 kb 5' of *Mcm3* for the indicated genotypes under arrested and proliferating conditions. (C) Heat maps of pRB ChIP-seq read enrichment per repClass for the indicated growth conditions and genotypes. Each row represents one scaled wild type peak location at an element within the repClass and includes ± 1 kb of flanking sequence. The intensity scale indicates magnitude of read enrichment. (D) ChIP-qPCR for pRB at the indicated repetitive elements conducted in proliferating and arrested MEFs. (E) Two representative genomic regions depict wild type and mutant pRB repeat association at LINE-1 fragments across growth conditions. Red bars mark regions of pRB enrichment (peaks). For all graphs, error bars indicate one standard deviation from the mean and an asterisk represents a significant difference from wild type ($P \leq 0.05$ by *t*-test).

seq in *Rb1^{S/S}* fibroblasts uncovers a dramatic loss of pRB enrichment at repetitive elements occupied by wild type pRB that is equally evident by ChIP-qPCR (Figure 2.4C-E). Comparison of read build-ups at wild type peak locations reveals that pRB localization is disrupted by the F832A substitution at the vast majority of elements in these repClass groups, and resembles *Rb1^{-/-}* controls at these locations (Figure 2.4C). Quantitatively, greater than 80% of wild type pRB peak intersections at repetitive elements are lost in *Rb1^{S/S}* chromatin under both growth conditions (Figure 2.5A).

In contrast to repetitive elements, the pRB^S enrichment profile at E2F cell cycle genes parallels that of wild type pRB (Figure 2.5B). Interestingly, pRB localizes extensively to repeat-containing regions within 1kb of non-E2F target genes, and indeed, pRB^S exhibits a loss of enrichment at these regions under both growth conditions (Figure 2.5C). ChIP-qPCR for pRB at major satellites, LTR-containing, and non-LTR retrotransposon repeat classes confirms diminished pRB^S occupancy at repetitive elements, while the pRB^G mutant parallels the cell cycle independent occupancy displayed by wild type pRB at these elements (Figure 2.4D). Genome browser tracks show two examples of pRB peak loss in *Rb1^{S/S}* cells at fragments of LINE-1 elements (Figure 2.4E). Lastly, ChIP-qPCR detects E2F1 at these repetitive sequences, consistent with a model of E2F1 contributing to pRB localization to repeats (Figure 2.5D).

Collectively, these data indicate that disrupting pRB's CDK-resistant binding site for E2F1 prevents its localization to repetitive regions of the genome. Analysis of mutant forms of pRB with distinct defects for E2F interaction type across different growth conditions further supports the conclusion that pRB possesses a cell cycle independent

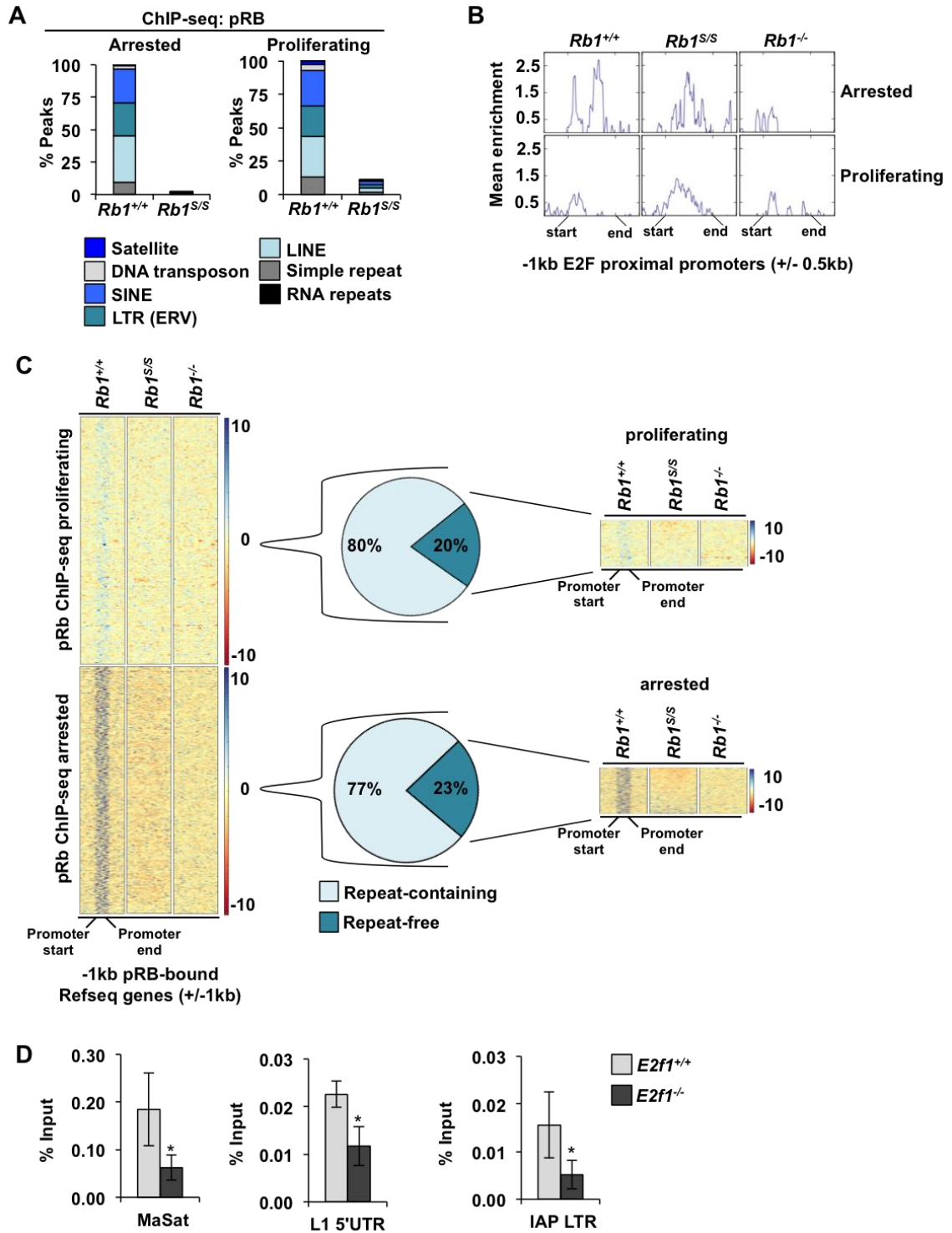


Figure 2.5: Occupancy of repetitive sequences by pRB and E2F1.

(A) Peak retention relative to wild type-repeat intersections was determined using BEDintersect. Bar graphs show peak location by repeat element class using the indicated color scheme. RNA repeats include tRNA, snRNA and others. The frequency of peak retention in *Rb1^{S/S}* mutant cells compared with wild-type at these repeat elements is shown for both growth conditions. N=321892 peaks for wild-type pRB in arrested cells, n=49210 peaks for mouse pRB in proliferating cells. (B) Average pRB ChIP-seq enrichment profiles across the 1kb upstream region of pRB regulated E2F cell cycle target genes for the indicated genotypes visualized using deepTools profiler. (C) Heat maps of pRB ChIP-seq read enrichment within 1kb regions that contain wild type pRB peaks upstream of RefSeq genes. The intensity scale indicates the magnitude of read enrichment. Pie charts indicate relative repeat content of such regions, followed by enrichment profiles at the repeat-void regions within this category. (D) ChIP-qPCR assays were performed to detect E2F1 at the indicated repetitive sequences. Error bars indicated one standard deviation from the mean. An asterisk indicates a significant difference compared to wild type $P \leq 0.05$ by t-test.

mechanism for repeat occupancy that is distinct from its transcriptional regulatory role during the G1-S phase transition.

2.4.3 pRB-repeat association is required for silencing of repetitive sequence expression.

To investigate the functional role of repeat occupancy by pRB, we performed RNA-seq on arrested wild type and *Rb1^{S/S}* MEFs. Total RNA was depleted of rRNA prior to library construction, and reads were aligned to repeat indices and binned according to repeat classification and family. The number of reads in each category was normalized to the total number of aligned reads per sample. Columns display expression from three separate *Rb1^{S/S}* MEF preparations as a log₂ ratio normalized to the average of three wild type samples (Figure 2.6A). *Rb1^{S/S}* MEFs exhibit increased expression of type I and type II transposable elements (e.g. Gypsy, Mariner/Tc2, LINE_other, RTE, and SINE/ID), satellites, and simple repeats in all three biological replicates. In two samples, many families of LTR containing repeats, DNA transposons, LINEs, and SINEs show widespread de-regulation in mutant MEFs. Collectively, this demonstrates transcriptional misregulation of repeats that matches the occupancy pattern of pRB among repetitive sequences. We note variability of expression in sample C5137_E3, however, broad differences between biological replicates are common to investigations of repeat sequence expression (Howard et al., 2008; Muotri et al., 2010; Wylie et al., 2016), and limited misregulation appears specific to this MEF preparation alone.

Representative elements from highly deregulated repeat classes were selected to further explore pRB-repeat regulation. Mapping sequence reads to instances of LINE-1, IAP, and major satellite sequences confirms increased read abundance across these

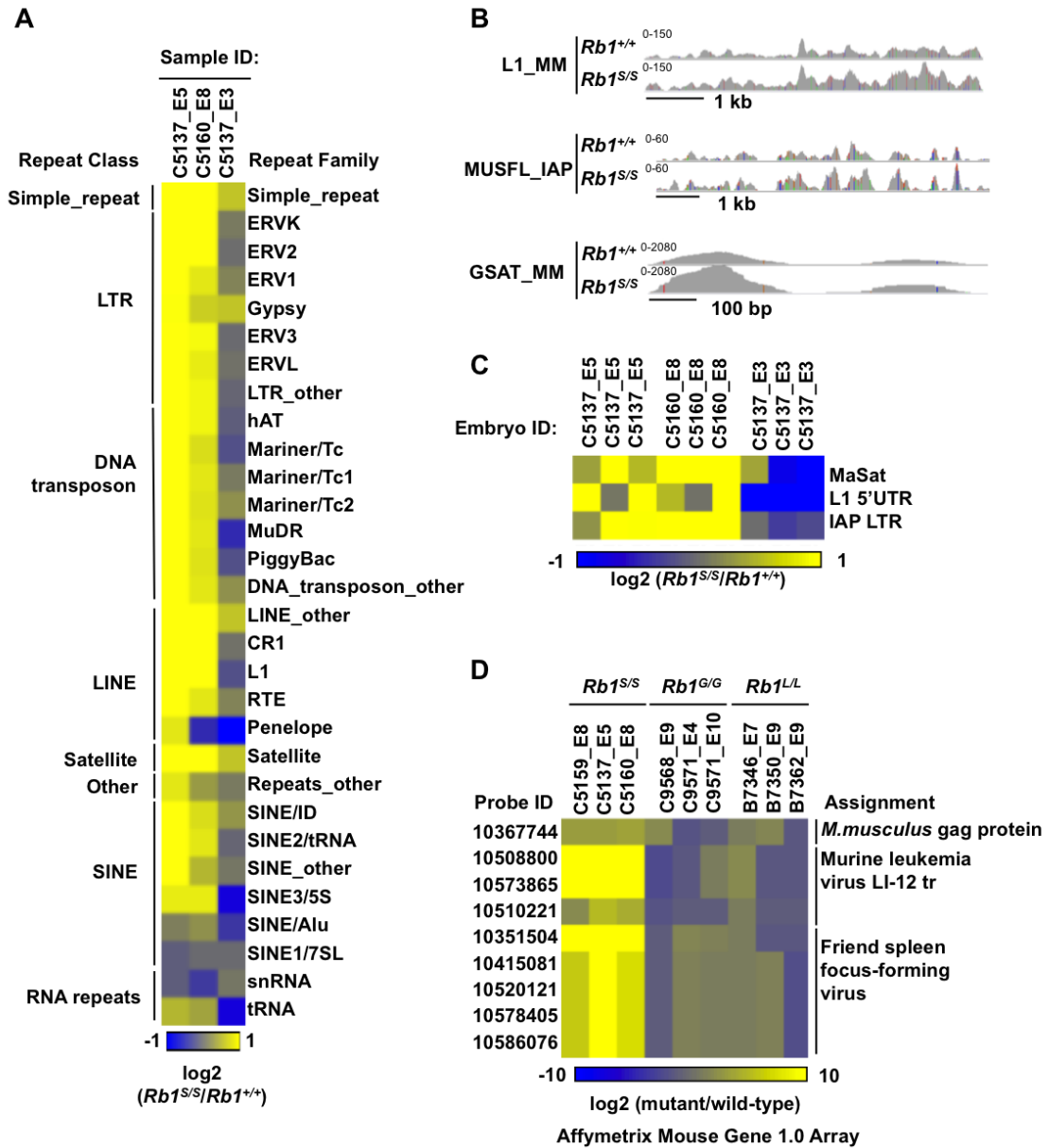


Figure 2.6: pRB silences repetitive element expression.

Figure 2.6: pRB silences repetitive element expression.

(A) Heat map of repeat expression from three *Rbl*^{S/S} MEF preparations relative to the average of three wild type replicates. RNA-seq reads were aligned to repeat indices, binned according to repClass and repFamily, and normalized to the total number of aligned reads in the sample. Expression was quantified as a log₂ ratio relative to the average of three wild type replicates. (B) RNA-seq reads aligned to instances of LINE, IAP endogenous retrovirus, and major satellite repeats. (C) qRT-PCR of the indicated repetitive elements in proliferating MEFs plotted as log₂ of the ratio with wild type, using actin as an internal control. Each MEF pair was cultured independently three times and expression levels for each replicate is shown to illustrate variability in expression between culture and genotypes. (D) Expression microarrays performed with RNA from arrested MEFs of the indicated genotypes. Log₂ values of mutant/wild type are shown as a heat map to depict expression levels of endogenous retrovirus detecting probe sets on the arrays.

elements (Figure 2.6B). Furthermore, elevated transcript levels from major satellites, LINE-1 elements, and IAP endogenous retroviruses are readily detectable in arrested and proliferating cultures of *Rb1^{S/S}* MEFs by qRT-PCR (Figure 2.6C and 2.7A). Elevated LINE-1 5' UTR and IAP LTR-containing transcript levels are consistent with full length element expression (Figures 2.6B and 2.6C). Again, we note that MEFs from embryo C5137_E3 are refractory to expression in three separate analyses of these cells (Figure 2.6C). Microarray analysis was performed to compare the specificity of endogenous retroviral expression in *Rb1^{S/S}* cells with other structure-function mutants of pRB that disrupt binding to the E2F transactivation domain (*Rb1^{G/G}*) or to LXCXE motif containing proteins (*Rb1^{L/L}*). This analysis reveals increased expression of repeats specifically in the *Rb1^{S/S}* mutant and not the other genotypes (Figure 2.6D). Importantly, expression of canonical E2F target genes appears increased only in *Rb1^{G/G}* and *Rb1^{L/L}* cells (Figure 2.7B), further emphasizing the unique alteration in gene expression found in *Rb1^{S/S}* mutants.

These experiments demonstrate that pRB occupancy of repetitive sequences is functionally important for their silencing, as loss of binding correlates with increased expression of a wide array of repeats that are detectable using a number of expression profiling methods. Curiously, many examples of pRB occupancy in Figures 2.1 and 2.4 are fragments of repetitive elements that may not be capable of autonomous expression. This suggests that this pRB-dependent silencing mechanism is broad and indiscriminate both in the elements that it silences and their potential for expression.

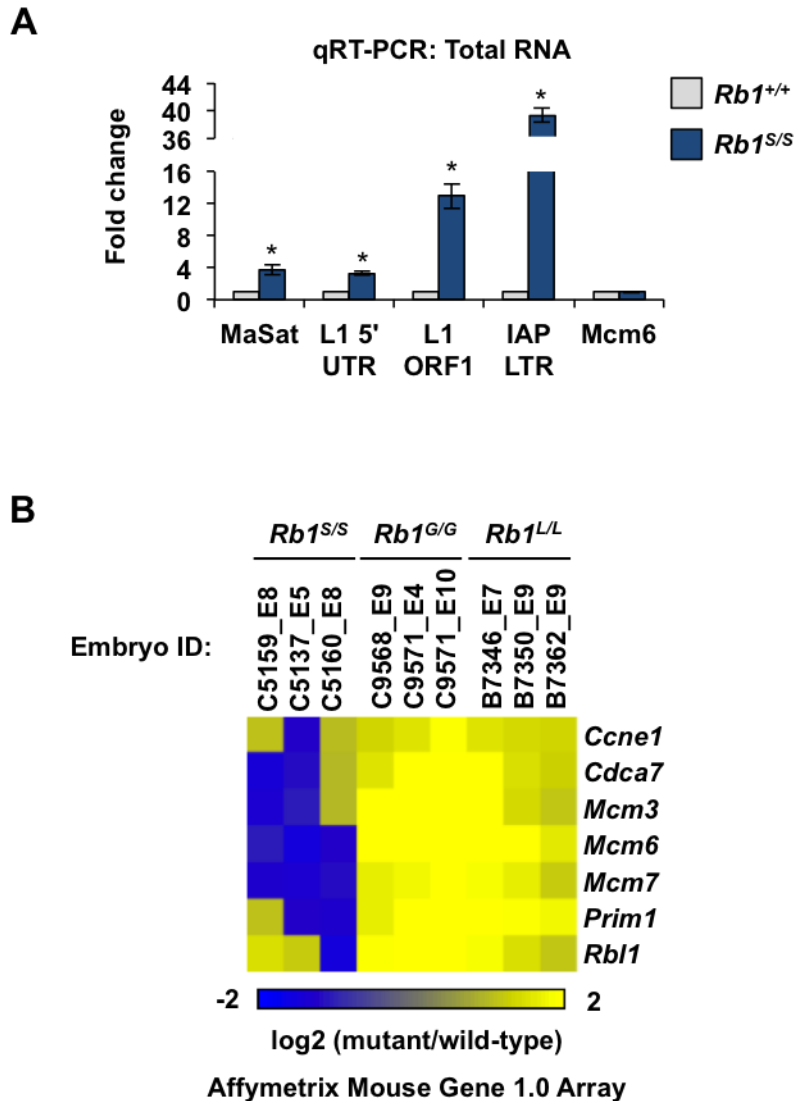


Figure 2.7: Distinct transcript expression patterns in *Rb1*^{S/S} cells.

(A) Expression levels of the indicated repetitive elements was determined by qRT-PCR in serum starved wild type and *Rb1*^{S/S} MEFs. Error bars indicate +/- 1 standard deviation from the mean and an asterisk indicates a significant difference (*t*-test, $P < 0.05$). (B) Expression microarrays were performed with RNA isolated from arrested MEFs of the indicated genotypes. Log₂ values of mutant/wild type are shown as a heat map to depict expression levels of known pRB-E2F target genes.

2.4.4 H3K27me3 enrichment at repetitive sequences is pRB-dependent

DNA methylation and histone modifications contribute to both redundant and non-redundant silencing of repetitive elements. The contribution of each was assessed in fibroblasts from our mutant mice. ChIP was used to detect histone tail modifications regulated by pRB and present at repetitive elements in ES cells. While H4K20me3 and H3K9me3 enrichment remain unchanged between genotypes at major satellites, LINEs, and LTR-containing endogenous retroviruses (Figure 2.8A and 2.8B), a prominent reduction of H3K27me3 appears evident (Figure 2.9A). Beyond methylation, *Rbl*^{S/S} cells exhibit elevated H3K9Ac enrichment at these repetitive elements, and derepression by Trichostatin A further suggests that histone deacetylation functionally contributes to this regulation (Figure 2.8C). In contrast, *H19* and *Gapdh* maintain equivalent enrichment of these histone tail modifications between genotypes.

We performed ChIP-seq for H3K27me3 to expand upon the pRB-dependence observed at repetitive elements by ChIP-qPCR. Similar to pRB, the vast majority of wild type H3K27me3 peaks reside within intronic and intergenic regions, irrespective of proliferative status (Figure 2.9B). A number of distinct effects of the *Rbl*^{S/S} mutation on H3K27me3 distribution emerge from this data. H3K27me3 reductions are readily observed in sequence tracks over repeat-rich intergenic regions (Figure 2.9C). Many canonical genes regulated by H3K27me3, such as in *Hox* clusters, *Cdkn2a*, and *Sox2*, retain normal H3K27me3 enrichment in *Rbl*^{S/S} MEFs (Figure 2.9D and 2.8D). Comparison of H3K27me3 read build-up at wild type peak locations across repeat classes reveals diminished enrichment in *Rbl*^{S/S} cells, particularly under arrested growth

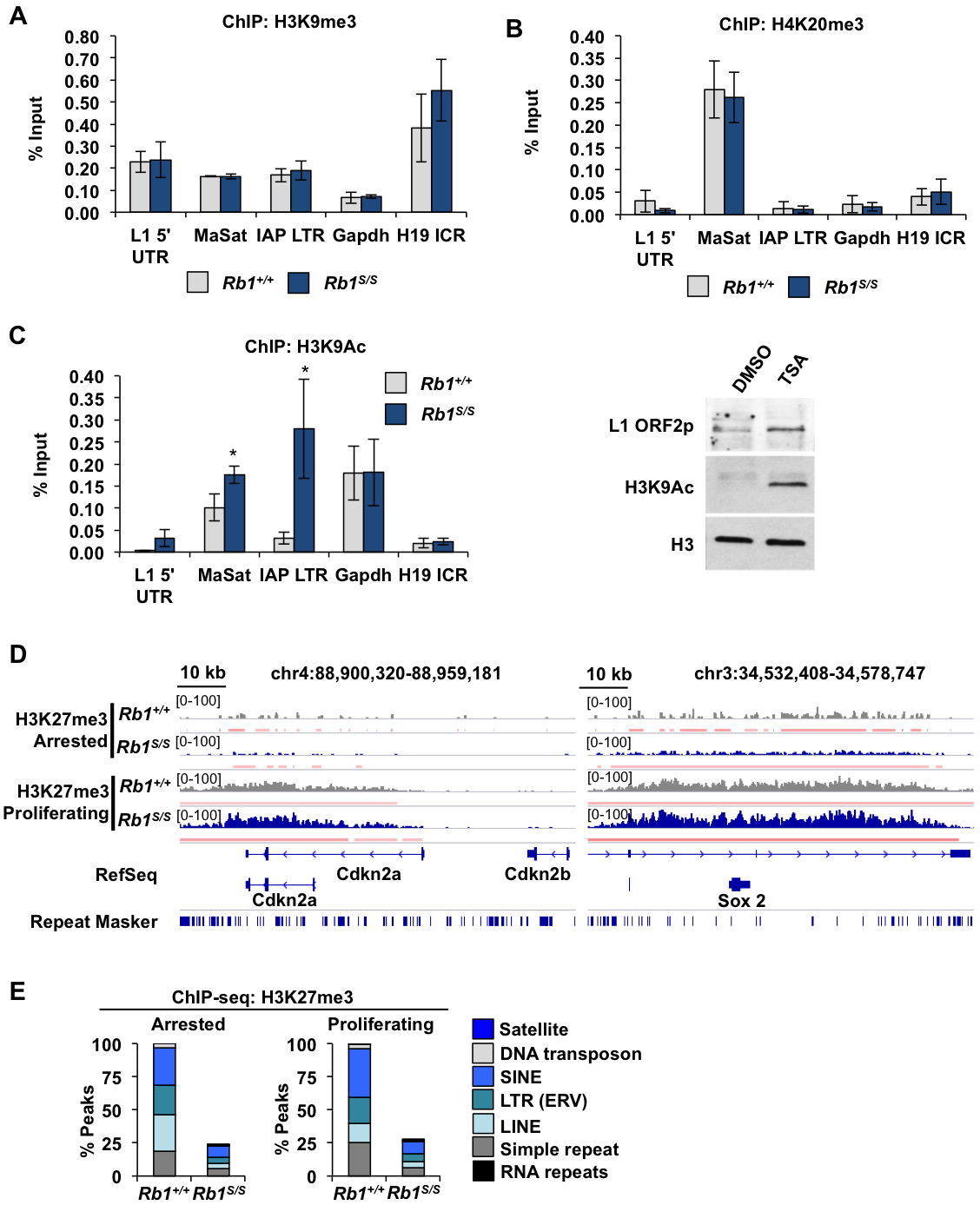


Figure 2.8: The *Rb1*^{S/S} mutant maintains normal H3K9 and H4K20 lysine methylation at repeats.

Figure 2.8: The *Rb1*^{S/S} mutant maintains normal H3K9 and H4K20 lysine methylation at repeats.

(A) H3K9me3 ChIP-qPCR was performed using chromatin from wild type and *Rb1*^{S/S} MEFs for the indicated repetitive families and unique location controls under arrested conditions. (B) H4K20me3 ChIP-qPCR of the same repetitive element families in arrested MEFs. (C) H3K9Ac ChIP-qPCR at the indicated repetitive sequences in arrested MEFs. For all graphs, error bars indicate +/- 1 standard deviation, an asterisk indicates a significant difference compared to wild type $P \leq 0.05$ by t-test. Wild-type MEFs were treated with 2.5 μ M Trichostatin A for 24 hours and extracts were prepared for western blotting. Blots show expression of L1 Orf2p and H3K9Ac respectively. (D) Genome browser tracks display mouse H3K27me3 ChIP-seq reads at *Cdkn2a* and *Sox2* loci. Genomic co-ordinates are indicated above the tracks. Repeat Masker and RefSeq tracks are shown below. Red bars denote regions of pRB enrichment (peaks) determined with MACS. (E) Overall genomic distribution of H3K27me3 ChIP-seq peaks at repetitive elements is shown for wild type MEFs, and peak retention frequency for *Rb1*^{S/S} is shown for both growth conditions. RNA repeats include tRNA, snRNA and others. N=622358 peaks for H3K27me3 in arrested cells, n=539696 peaks for H3K27me3 in proliferating MEFs.

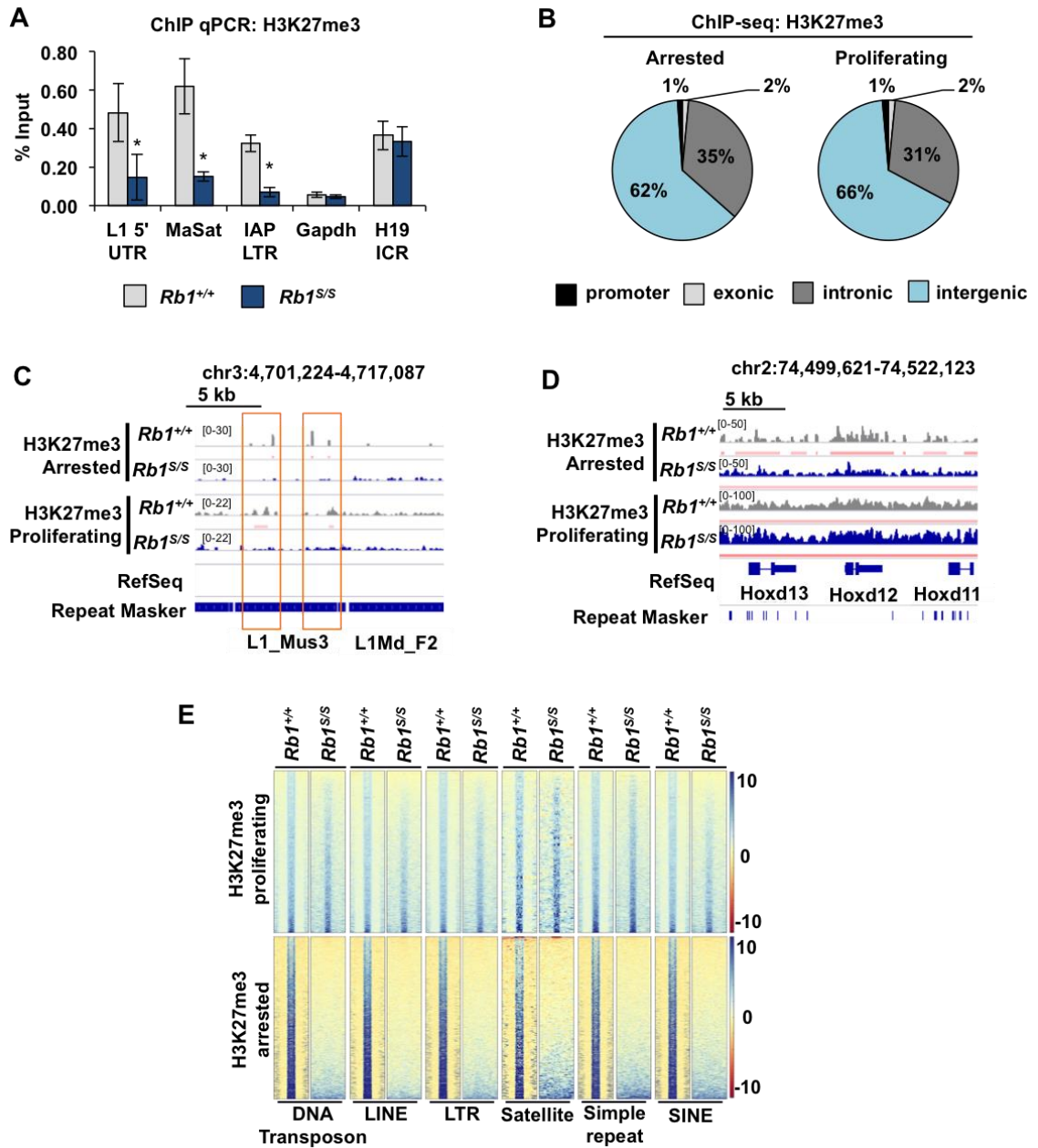


Figure 2.9: H3K27me3 enrichment at repetitive elements is pRB-dependent.

Figure 2.9: H3K27me3 enrichment at repetitive elements is pRB-dependent.

(A) ChIP-qPCR for H3K27me3 at the indicated repetitive and unique targets in arrested MEFs. Error bars indicate one standard deviation from the mean and an asterisk represents a significant difference from wild type ($P \leq 0.05$ using a *t*-test). (B) Overall genomic distribution of H3K27me3 ChIP-seq peaks. Growth conditions are indicated above pie charts; $n=656342$ peaks in arrested cells, $n=143252$ peaks in proliferating cells. (C) Genome viewer tracks depict H3K27me3 read build up at L1 elements (highlighted by red boxes). Genomic co-ordinates and scale are indicated above peak tracks. (D) H3K27me3 distribution at a *Hox* gene cluster. (E) Heat maps of H3K27me3 read enrichment per repClass for the indicated growth conditions. Each row represents one scaled wild type peak location at an element within the repClass and includes ± 1 kb of flanking region. The intensity scale indicates magnitude of read enrichment.

conditions (Figure 2.9E). However, some individual repeat elements disperse or broaden their H3K27me3 distribution, and this is more common in proliferating cells. Comparison of peak intersections at repetitive elements reveals that 75% of wild type H3K27me3 peaks in repeat regions are lost in *Rb1*^{S/S} chromatin in both arrested and proliferating conditions (Figure 2.8E). The retention of reads at many repeats in proliferating *Rb1*^{S/S} cells (Figure 2.9E) at magnitudes below the threshold of peak calling suggests that H3K27me3 becomes dispersed, but not altogether lost under proliferating conditions. This is important because elevated expression levels of repeats in proliferating *Rb1*^{S/S} cells (Figure 2.6C) suggests silencing by H3K27me3 is compromised.

These data demonstrate an extremely broad mechanism of heterochromatin establishment among many distinct repeat element types. To our knowledge, DNA methylation is perhaps the only other mechanism that is as indiscriminate in its choice of sequences to silence. Therefore, we investigated the status of DNA methylation in *Rb1*^{S/S} MEFs by bisulfite sequencing (Figure 2.10A and 2.10B), to determine if H3K27me3 and DNA methylation may be functionally related by pRB. Amplification of the same families of LINE-1 and IAP LTR viruses as in Figure 2.4D and 2.6C bears no obvious DNA methylation differences. We also cultured wild type and *Rb1*^{S/S} fibroblasts in the presence of 5-aza-cytidine to inhibit DNA methylation, and analyzed repeat expression by qPCR (Figure 2.10C). As expected, repeat sequence expression increases in *Rb1*^{+/+} cells but not *Rb1*^{S/S} MEFs, suggesting that they are already derepressed.

Our data reveals a dramatic loss of H3K27me3 organization at repetitive genomic sequences. The loss of H3K27me3 is similar in magnitude to loss of pRB recruitment to

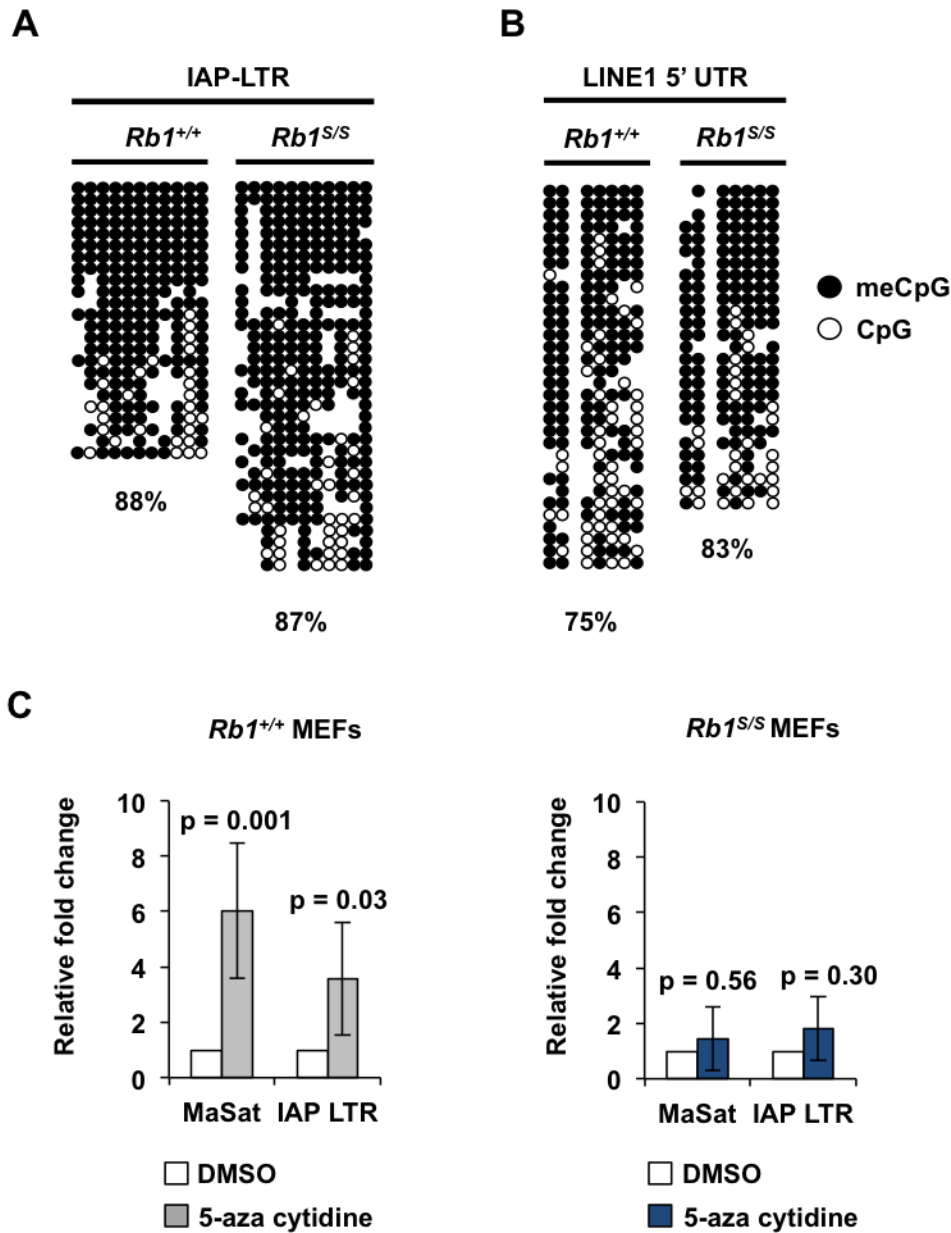


Figure 2.10: *Rb1*^{S/S} mutant cells retain DNA methylation at repetitive elements.

(A&B) Bisulfite sequencing of MEF DNA for IAP-LTR and LINE-1 families of repeats. Each row of circles represents a separate clone sequence. Lack of a circle in a particular row represents the absence of a CpG detected at that position in the clone. Black circles represent meCpG. (C) qRT-PCR of cDNA from total RNA of vehicle- or 5-aza-cytidine-treated MEFs for the indicated repeat targets. Error bars indicate +/- 1 standard deviation, with t-test p-value indicated.

repeat sequences in *Rb1^{SS}* fibroblasts. Our data further suggests that alterations to DNA methylation do not underlie widespread changes to heterochromatin in *Rb1^{SS}* cells. For this reason, we interpret our experiments to be indicative of a mechanism for silencing repetitive DNA sequences that acts in parallel to DNA methylation in primary fibroblasts.

2.4.5 pRB-chromatin association is required for EZH2 recruitment to repetitive sequences.

The polycomb repressor 2 complex (PRC2) contains the enhancer of zeste homologue 2 (EZH2) histone methyltransferase that methylates H3K27 to establish the trimethylation mark. We explored whether pRB-dependent regulation of EZH2 might underlie epigenetic and transcriptional changes observed in *Rb1^{SS}* cells.

ChIP-seq was used to determine whether EZH2 association at repeat elements was affected in growth arrested *Rb1^{SS}* cells. This analysis reveals that EZH2 also displays primarily intronic and intergenic distribution (Figure 2.11A). Across all repeat classes, wild type locations of EZH2 enrichment diminish in *Rb1^{SS}* MEFs (Figure 2.11B), with more than 80% of wild type peak intersections at repetitive elements lost in *Rb1^{SS}* fibroblasts (Figure 2.12A). ChIP-qPCR confirms pRB-dependent EZH2 association with chromatin at major satellites, LINEs, and endogenous retroviral sequences (Figure 2.11C). Since pRB and E2Fs control EZH2 expression (Bracken et al., 2003; Jung et al., 2010), we confirm that EZH2 levels remain unchanged in *Rb1^{SS}* MEFs, and therefore do not mislead our investigation of function or localization (Figure 2.12B). pRB-dependent EZH2 localization suggests regulation beyond transcriptional control of EZH2 at repetitive sequences. Indeed, ChIP-reChIP indicates that EZH2 and pRB co-localize at LINE-1 and IAP LTRs, while chromatin association in *Rb1^{SS}* MEFs is comparable to background (Figure 2.12D). Co-immunoprecipitation demonstrates that

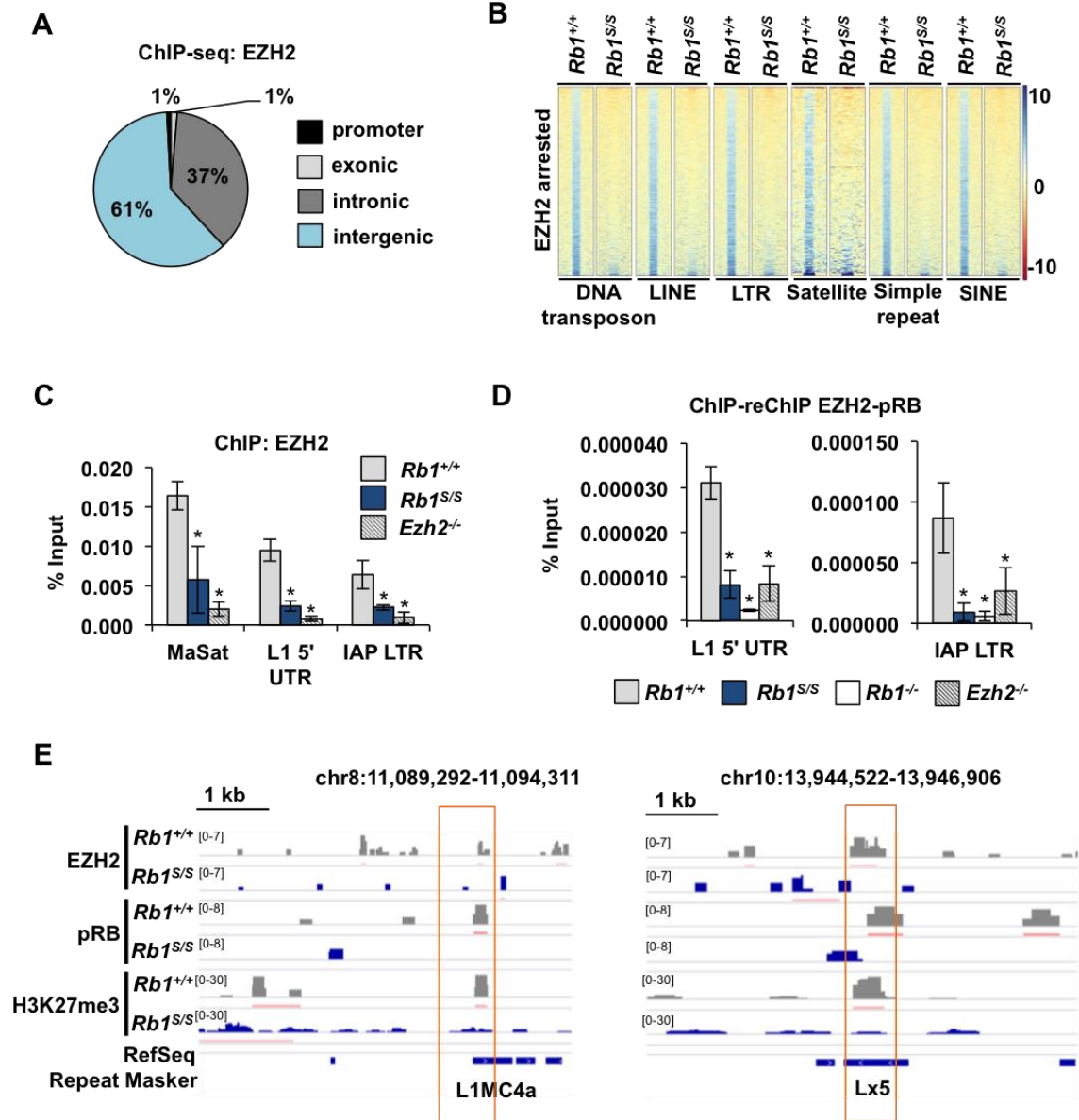


Figure 2.11: pRB-chromatin association mediates EZH2 recruitment to repetitive DNA.

Figure 2.11: pRB-chromatin association mediates EZH2 recruitment to repetitive DNA.

(A) Overall genomic distribution of EZH2 ChIP-seq peaks in arrested wild type MEFs; n= 840543 peaks. (B) Heat maps of EZH2 read enrichment per repClass. Each row represents one scaled wild type peak location at an element within the repClass that includes ± 1 kb of flanking region. Intensity scale indicates magnitude of read enrichment. (C) ChIP-qPCR for EZH2 at the indicated repetitive elements. (D) ChIP-reChIP for EZH2 followed by pRB, quantified at the indicated repetitive elements with genetic knockouts as controls. (E) Two representative genomic regions depict ChIP-seq tracks for EZH2, pRB, and H3K27me3 in arrested MEFs. Genomic co-ordinates and scale are indicated above peak tracks. Red boxes highlight peak overlaps across datasets. For all graphs, error bars indicate one standard deviation from the mean and an asterisk represents a significant difference from wild type ($P \leq 0.05$ using a *t*-test).

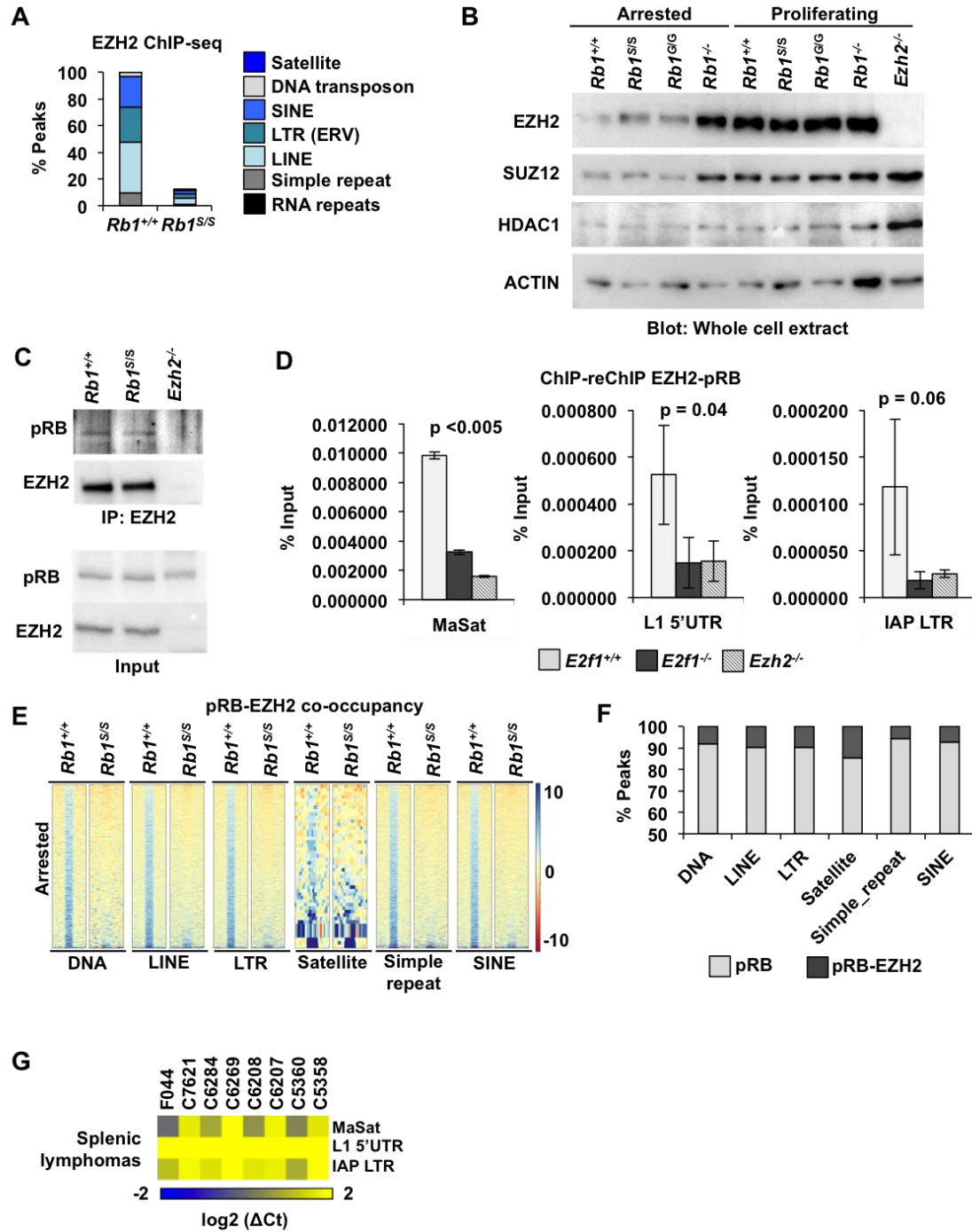


Figure 2.12: pRB-E2F1 dependent and independent roles for EZH2.

Figure 2.12: pRB-E2F1 dependent and independent roles for EZH2.

(A) Peak distribution of EZH2 ChIP-seq peaks at repetitive elements is shown for wild type MEFs, and peak retention frequency for *Rbl*^{S/S} is shown for both growth conditions. RNA repeats include tRNA, snRNA and others. N=465495 peaks analyzed. (B) Western blots of the indicated Polycomb proteins from whole cell extract of P4 MEFs of the indicated genotypes under the indicated growth conditions. (C) IP-western blot analysis to detect pRB associated with EZH2 in nuclear cell extracts from the indicated genotypes of MEFs. (D) ChIP-reChIP for EZH2 followed by pRB quantified at the indicated repetitive elements. Chromatin was derived from the indicated genotypes. Error bars indicate one standard deviation from the mean and an asterisk represents a significant difference from wild type ($P \leq 0.05$ using a *t*-test). (E) Heat maps of EZH2 read enrichment per repClass that intersect with pRB peaks. Each row represents one scaled wild-type peak location at an element within the repClass that includes ± 1 kb of flanking region. Intensity scale indicates magnitude of read enrichment. (F) Graph depicting the percentage peak intersection between pRB and EZH2 as a proportion of total pRB peaks in wild type chromatin for the indicated repClass categories. (G) Graph showing $\log_2 \Delta ct$ values for qRT-PCR of repetitive sequence expression in tumor samples isolated from *Rbl*^{S/S} mice.

both wild type and pRB^S bind EZH2 (Figure 2.12C). In addition, ChIP-reChIP reveals that E2F1 deficiency prevents pRB and EZH2 co-localization to LINE-1, IAP, and major satellite repeats (Figure 2.12D). Collectively, this suggests a model whereby pRB^S can bind EZH2, but fails to localize to repetitive sequences because of its deficiency for binding E2F1, while wild type pRB is capable of both EZH2 and E2F1 interactions, leading to H3K27me3 deposition at repetitive locations (Figure 2.11E).

Our data indicates that pRB, E2F1, and EZH2 are capable of forming a complex at repetitive genomic regions. However, while peak intersections between pRB and EZH2 at repetitive sequences in *Rb1*^{S/S} cells indicate a genetic requirement for pRB to recruit EZH2, they do not co-localize stoichiometrically (Figure 2.12E and 2.12F). This suggests that pRB and E2F1 may recruit EZH2 initially, but subsequent spreading of EZH2 and H3K27me3 may occur independent of pRB.

2.4.6 *Rb1*^{S/S} mice succumb to spontaneous lymphoma

In order to determine where this repeat silencing mechanism is most relevant, we assessed repeat expression in tissues of adult mice using qRT-PCR (Figure 2.13A). For most tissues, expression varies between individuals with no consistent trend relative to wild type controls. However, four of eight *Rb1*^{S/S} mice display elevated levels of all repeats tested in the spleen (F241, F242, F248, and F307), while only one of eight wild type mice expresses repeats in this tissue (F233). This suggests that pRB dependent silencing may be most relevant in the spleen. However, a survey of major tissues in these mice, including the spleen, reveals no obvious histological differences. Given that expression of repetitive sequences stimulates an immune response to eliminate these cells, we searched for evidence of interferon activation. Figure 2.13B shows qRT-PCR

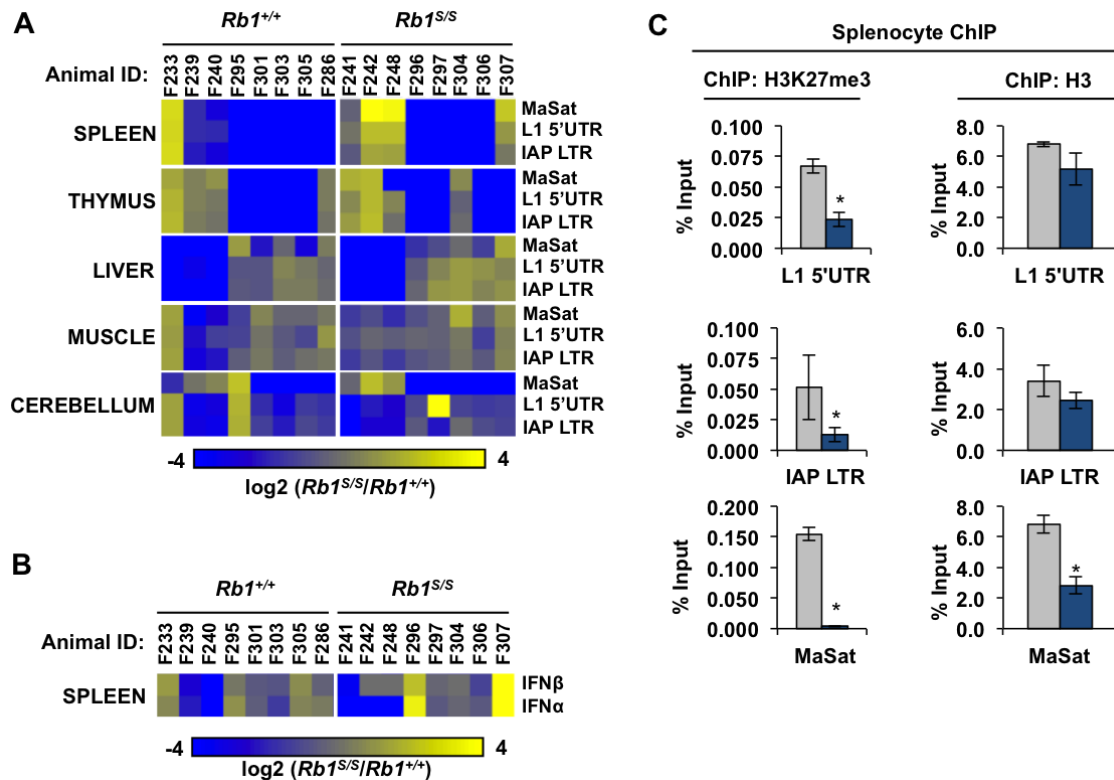


Figure 2.13: Altered chromatin and repeat expression in *Rb1*^{S/S} splenocytes.

(A) Heat map of repeat element expression in tissues of 6-8 week old wild type and *Rb1*^{S/S} mutant mice quantified by qRT-PCR. Log₂ ratio of expression is displayed relative to the average of all wild type measurements for a given element in each tissue. (B) Heat map of interferon gene expression in splenocytes from the same mice analyzed above. (C) H3K27me3 and H3 ChIP from freshly harvested splenocytes of 6 week-old wild type and *Rb1*^{S/S} mutant mice. Enrichment at the indicated repeat element families was determined by qPCR. Error bars indicate one standard deviation from the mean (n=3, an asterisk indicates $P < 0.05$, *t*-test).

analysis of *Ifn- α* and *Ifn- β* expression in splenocytes. Again, expression varies between individuals, but we note that two *Rbl^{S/S}* mice display high level expression of both (F296 and F307), further suggesting that *Rbl^{S/S}* mice are responding to abnormal repeat expression in their splenocytes. Conversely, this magnitude of interferon response is largely absent from wild type mice. Since normal mammalian immune function seeks to eliminate repeat misexpressing cells, we further sought evidence of altered repression by investigating H3K27me3 deposition at repetitive sequences in splenocytes. ChIP-qPCR assays demonstrate that H3K27me3 is reduced at IAP ERVs, LINE-1 elements, and major satellites, but H3 levels remain comparable between genotypes (Figure 2.13C). These experiments suggest that H3K27me3 is altered in chromatin from *Rbl^{S/S}* splenocytes, and that repeats can be misexpressed, but these cells are likely unable to accumulate in young adult mice with a functional immune system.

To determine the long-term consequences of the *Rbl^S* mutation, we generated cohorts of *Rbl^{S/S}* mutant mice and wild type siblings to monitor over the course of their lifetime for the manifestation of pathology. Mutant mice exhibit a significantly reduced tumor free survival with a median lifespan of 576 days (Figure 2.14A). Necropsy and histopathological analysis reveals that the majority of mice succumb to lymphomas, particularly in the spleen and mesenteric lymph node (Figure 2.14B). Examples of lesions evident upon necropsy are shown in Figure 7C as well as the normal abdominal cavity of an unaffected wild type mouse at 2 years of age. The corresponding histology for each example is shown (Figure 2.14D). In addition, qRT-PCR of RNA derived from these tumor samples indicates that diverse repetitive sequences are expressed in these malignancies (Figure 2.12G). This suggests that pRB's ability to form complexes with

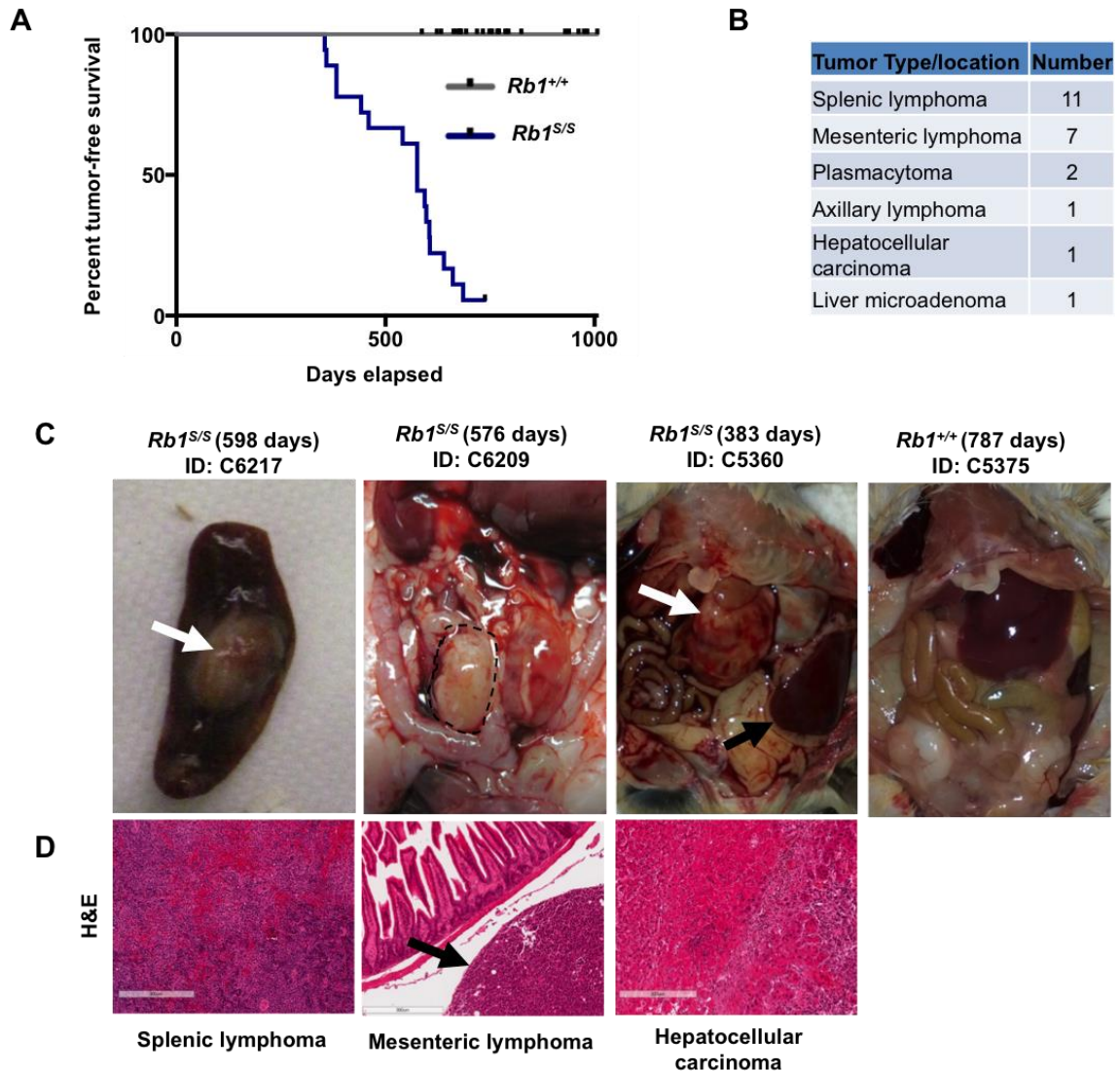


Figure 2.14: Aged *Rb1^{S/S}* mice are tumor-prone.

(A) Kaplan-Meier plot of tumor free survival for mice of the indicated genotypes aged until animal protocol endpoints. Tick marks indicate animals necropsied at intermediate ages. Mutant mice are significantly more cancer prone than wild type (log rank test, $P < 0.05$). (B) The table indicates anatomical location and cancer type listed by frequency of occurrence. (C) Images of the peritoneal cavity upon necropsy for the indicated animals. A white arrow indicates an abnormal mass in the spleen of mouse C6217. A dashed line highlights the mesenteric lymph node of mouse C6209. A white arrow indicates abnormal liver and a black arrow indicates a normal lobe in mouse C5360. (D) H&E staining of tissue sections from the abnormality indicated in the mutant animals above. A black arrow indicates the lymph node in mouse C6209. The scale bars indicate 300 μ m.

E2F1 at repetitive sequences and establish H3K27me3 dependent silencing is highly relevant to its tumor suppressive functions.

Collectively, our work suggests a model in which pRB recruits EZH2 to repeat sequences where it catalyzes H3K27me3 to silence expression, and a point mutation in pRB that blocks localization to these sequences prevents recruitment of EZH2 and causes dispersion of H3K27me3. Endogenously, this mechanism is important in splenocytes where deregulated expression of repeats is most detectable, and these cells eventually give rise to lymphomas in older *Rb1^{SS}* mice.

2.5 Discussion

Our data reveals a mechanism in which pRB and EZH2 co-operate to establish H3K27me3 that silences expression of genomic repeat sequences. This mechanism is largely indiscriminate as it silences tandem repeats, such as simple sequence repeats and satellites, in addition to retrotransposons. These characteristics indicate that pRB-EZH2 dependent silencing of repeats plays a broad but previously unappreciated role in genome organization.

Investigation of Polycomb-based repeat regulation by H3K27me3 in mammals primarily concerns critical steps of early embryonic development (Leeb et al., 2010; Macfarlan et al., 2012). Misregulation typically manifests in defects that prevent embryonic development before implantation (Leeb et al., 2010; Macfarlan et al., 2012), or that have overt consequences in adult mice (Li et al., 2015). Lack of developmental impediments in *Rb1^{SS}* mice, and retention of H3K27me3 at developmentally regulated loci, such as *Hox* genes and *Sox2*, suggests the pRB-EZH2 complex must be recruited to

repeats through a mechanism that is distinct from previous studies, or this pRB dependent mechanism is not functional in cells during early development.

Comprehensive understanding of Polycomb function requires detailed elucidation of chromatin recruitment mechanisms (Bauer et al., 2015; Casa and Gabellini, 2012). Previous studies demonstrate that non-coding transcripts can target Polycomb repressor complexes to specific loci, as observed upon X-chromosome inactivation (Blackledge et al., 2015). Based on the co-immunoprecipitation of pRB and EZH2 and their co-occupancy of repeats by CHIP-reCHIP, it is likely that pRB directly recruits EZH2 to repeats. Diminished pRB binding to repeats in *Rb1^{S/S}* cells resulted in loss of EZH2 and H3K27me3 peaks, but our data also suggests that EZH2 may not stably associate with pRB at all of these locations and may spread H3K27me3 heterochromatin without it.

Beyond non-coding RNAs, sequence specific transcription factors can recruit Polycomb to specific genomic locations to initiate such nucleation and spreading (Bauer et al., 2015; Casa and Gabellini, 2012). Our study indicates that E2F1 can fulfill this role, and while some repeats contain consensus E2F elements (Montoya-Durango et al., 2009), E2F1 site selection appears increasingly diverse in the post-genomic era. Early CHIP-chip experiments revealed considerable heterogeneity in binding sites (Bieda et al., 2006), and sequence-independent roles in DNA damage recognition and repair further suggest that E2F1 is not simply a sequence specific transcription factor (Biswas and Johnson, 2012). Our initial identification of pRB's unique interaction with E2F1 was based on the inability of this complex to recognize a consensus E2F promoter element (Dick and Dyson, 2003). Major satellite repeats exemplify this *in vivo* where GC-rich consensus E2F elements are missing, but pRB and E2F1 bind cooperatively such that E2F1 binding

is greatly diminished without pRB (Coschi et al., 2014). Therefore, pRB-E2F1 interactions underlie recruitment of Polycomb to repeats, however a recognition mechanism for E2F1 at the variety of repeat sequences identified remains unclear and is highly reminiscent of searches for Polycomb response elements in mammalian gene promoters (Bauer et al., 2015)

The cancer susceptibility of *Rb1^{S/S}* mice suggests a role for pRB-EZH2 in genome maintenance and tumor suppression. This begs the question of how this mechanism functions endogenously, particularly since up regulation of repeat sequences in the spleen appeared quite variable. We note that elevated repetitive elements are detectable in splenocytes from cancer prone *Tlr3*, *Tlr7*, and *Tlr9* triple deficient mice (Yu et al., 2012), even though chromatin dependent repression mechanisms are wild type. This implies that immune surveillance acts to eliminate wild type cells that sporadically express repetitive elements on an ongoing basis, even if their repressive mechanisms are normal. This may explain the high degree of variability in repeat expression found in cells deficient for DNA methylation or histone methylation dependent repressive mechanisms (Howard et al., 2008; Muotri et al., 2010; Wylie et al., 2016). In this way, splenocytes of *Rb1^{S/S}* mice may be poised to over express repeats, but are eliminated by immune detection mechanisms, preventing their accumulation and consistent detection of repeat expression.

It is difficult to conclude that repeat expression alone causes cancer in *Rb1^{S/S}* mice. However, there are a number of reasons to expect that a pRB-E2F1-EZH2 complex has cancer relevant properties. First, the preference for lymphomas and age of onset in *Rb1^{S/S}* mice phenotypically parallels *E2f1^{-/-}* mice (Yamasaki et al., 1996). Missense alleles in human *RBI* are rare, so it is not surprising that the *Rb1^S* allele is absent from

cancer genome datasets. However, a low penetrance *RBI* family has been reported to possess exon 24 and 25 deletions (Bremner et al., 1997) that eliminate pRB's unique binding domain for E2F1 (Cecchini and Dick, 2011; Julian et al., 2008). Similarly, multiple instances of D295 substitutions in DP1 (Munro et al., 2014) indicate that the unique contact point for E2F1/DP1 with pRB is directly targeted in human cancers. Lastly, other *Rb1* targeted strains that compromise E2F transcriptional control at canonical cell cycle target genes, such as *Rb1*^{G/G} (Cecchini et al., 2014), or that are prone to unstable genomes related to defective chromatin condensation, as in *Rb1*^{L/L} and *Rb1*^{NF/NF} mice (Coschi et al., 2010; Vormer et al., 2014), are not spontaneously cancer prone. Since only *Rb1*^{S/S} cells misexpress repeat sequences among these genotypes, and repeat expression is most pronounced in the cancer prone tissue of *Rb1*^{S/S} mice, these data point to a very strong correlation between defective pRB-EZH2 repeat suppression and cancer incidence.

Likely the most significant implication for our work is the relationship between *RBI* status and the effects of new EZH2 inhibitors. We anticipate that EZH2 inhibitors will cause widespread derepression of repetitive sequences in pRB positive cancers as reported for inhibitors of DNA methylation (Chiappinelli et al., 2015; Roulois et al., 2015), and this may offer a new pathway to sensitize tumors to immunotherapy. Furthermore, our work suggests EZH2 inhibitors may have activity as anti-viral agents as they may awaken latent viral genomes. This manuscript reveals an exciting new connection between a canonical tumor suppressor and heterochromatin formation that further supports repetitive element silencing as a cancer relevant process.

2.6 References

- Avni, D., Yang, H., Martelli, F., Hofmann, F., ElShamy, W.M., Ganesan, S., Scully, R., and Livingston, D.M. (2003). Active localization of the retinoblastoma protein in chromatin and its response to S phase DNA damage. *Mol Cell* *12*, 735-746.
- Bauer, M., Trupke, J., and Ringrose, L. (2015). The quest for mammalian Polycomb response elements: are we there yet? *Chromosoma*.
- Bersani, F., Lee, E., Kharchenko, P.V., Xu, A.W., Liu, M., Xega, K., MacKenzie, O.C., Brannigan, B.W., Wittner, B.S., Jung, H., *et al.* (2015). Pericentromeric satellite repeat expansions through RNA-derived DNA intermediates in cancer. *Proc Natl Acad Sci U S A* *112*, 15148-15153.
- Bieda, M., Xu, X., Singer, M.A., Green, R., and Farnham, P.J. (2006). Unbiased location analysis of E2F1-binding sites suggests a widespread role for E2F1 in the human genome. *Genome Res* *16*, 595-605.
- Biswas, A.K., and Johnson, D.G. (2012). Transcriptional and nontranscriptional functions of E2F1 in response to DNA damage. *Cancer Res* *72*, 13-17.
- Blackledge, N.P., Rose, N.R., and Klose, R.J. (2015). Targeting Polycomb systems to regulate gene expression: modifications to a complex story. *Nat Rev Mol Cell Biol* *16*, 643-649.
- Blais, A., van Oevelen, C.J., Margueron, R., Acosta-Alvear, D., and Dynlacht, B.D. (2007). Retinoblastoma tumor suppressor protein-dependent methylation of histone H3 lysine 27 is associated with irreversible cell cycle exit. *J Cell Biol* *179*, 1399-1412.
- Bracken, A.P., Kleine-Kohlbrecher, D., Dietrich, N., Pasini, D., Gargiulo, G., Beekman, C., Theilgaard-Monch, K., Minucci, S., Porse, B.T., Marine, J.C., *et al.* (2007). The Polycomb group proteins bind throughout the INK4A-ARF locus and are disassociated in senescent cells. *Genes Dev* *21*, 525-530.
- Bracken, A.P., Pasini, D., Capra, M., Prosperini, E., Colli, E., and Helin, K. (2003). EZH2 is downstream of the pRB-E2F pathway, essential for proliferation and amplified in cancer. *EMBO J* *22*, 5323-5335.
- Bremner, R., Du, D.C., Connolly-Wilson, M.J., Bridge, P., Ahmad, K.F., Mostachfi, H., Rushlow, D., Dunn, J.M., and Gallie, B.L. (1997). Deletion of RB exons 24 and 25 causes low-penetrance retinoblastoma. *Am J Hum Genet* *61*, 556-570.
- Bulut-Karslioglu, A., De La Rosa-Velazquez, I.A., Ramirez, F., Barenboim, M., Onishi-Seebacher, M., Arand, J., Galan, C., Winter, G.E., Engist, B., Gerle, B., *et al.* (2014). Suv39h-dependent H3K9me3 marks intact retrotransposons and silences LINE elements in mouse embryonic stem cells. *Mol Cell* *55*, 277-290.

- Casa, V., and Gabellini, D. (2012). A repetitive elements perspective in Polycomb epigenetics. *Frontiers in genetics* 3, 199.
- Cecchini, M.J., Amiri, M., and Dick, F.A. (2012). Analysis of cell cycle position in mammalian cells. *Journal of visualized experiments : JoVE*.
- Cecchini, M.J., and Dick, F.A. (2011). The biochemical basis of CDK phosphorylation-independent regulation of E2F1 by the retinoblastoma protein. *Biochem J*.
- Cecchini, M.J., Thwaites, M., Talluri, S., Macdonald, J.I., Passos, D.T., Chong, J.L., Cantalupo, P., Stafford, P., Saenz-Robles, M.T., Francis, S.M., *et al.* (2014). A retinoblastoma allele that is mutated at its common E2F interaction site inhibits cell proliferation in gene targeted mice. *Molecular and cellular biology* 34, 2029-2045.
- Chiappinelli, K.B., Strissel, P.L., Desrichard, A., Li, H., Henke, C., Akman, B., Hein, A., Rote, N.S., Cope, L.M., Snyder, A., *et al.* (2015). Inhibiting DNA Methylation Causes an Interferon Response in Cancer via dsRNA Including Endogenous Retroviruses. *Cell* 162, 974-986.
- Coschi, C., Ishak, C., Gallo, D., Marshall, A., Talluri, S., Wang, J., Cecchini, M., Martens, A., Percy, V., Welch, I., *et al.* (2014). Haploinsufficiency of an RB-E2F1-Condensin II complex leads to aberrant replication and aneuploidy. *Cancer Discov* 4, 840-853.
- Coschi, C.H., Martens, A.L., Ritchie, K., Francis, S.M., Chakrabarti, S., Berube, N.G., and Dick, F.A. (2010). Mitotic chromosome condensation mediated by the retinoblastoma protein is tumor-suppressive. *Genes Dev* 24, 1351-1363.
- Day, D.S., Luquette, L.J., Park, P.J., and Kharchenko, P.V. (2010). Estimating enrichment of repetitive elements from high-throughput sequence data. *Genome biology* 11, R69.
- Denomme, M.M., Zhang, L., and Mann, M.R. (2012). Single oocyte bisulfite mutagenesis. *Journal of visualized experiments : JoVE*.
- Dick, F.A., and Dyson, N. (2003). pRB contains an E2F1-specific binding domain that allows E2F1-induced apoptosis to be regulated separately from other E2F activities. *Mol Cell* 12, 639-649.
- Dick, F.A., Sailhamer, E., and Dyson, N.J. (2000). Mutagenesis of the pRB pocket reveals that cell cycle arrest functions are separable from binding to viral oncoproteins. *Mol Cell Biol* 20, 3715-3727.
- Feng, J., Liu, T., Qin, B., Zhang, Y., and Liu, X.S. (2012). Identifying ChIP-seq enrichment using MACS. *Nature protocols* 7, 10.1038/nprot.2012.1101.
- Ferrari, R., Gou, D., Jawdekar, G., Johnson, S.A., Nava, M., Su, T., Yousef, A.F., Zemke, N.R., Pellegrini, M., Kurdistani, S.K., *et al.* (2014). Adenovirus small E1A employs the

lysine acetylases p300/CBP and tumor suppressor Rb to repress select host genes and promote productive virus infection. *Cell host & microbe* *16*, 663-676.

Heinz, S., Benner, C., Spann, N., Bertolino, E., Lin, Y.C., Laslo, P., Cheng, J.X., Murre, C., Singh, H., and Glass, C.K. (2010). Simple combinations of lineage-determining transcription factors prime cis-regulatory elements required for macrophage and B cell identities. *Molecular cell* *38*, 576-589.

Helman, E., Lawrence, M.S., Stewart, C., Sougnez, C., Getz, G., and Meyerson, M. (2014). Somatic retrotransposition in human cancer revealed by whole-genome and exome sequencing. *Genome Res* *24*, 1053-1063.

Howard, G., Eiges, R., Gaudet, F., Jaenisch, R., and Eden, A. (2008). Activation and transposition of endogenous retroviral elements in hypomethylation induced tumors in mice. *Oncogene* *27*, 404-408.

Isaac, C.E., Francis, S.M., Martens, A.L., Julian, L.M., Seifried, L.A., Erdmann, N., Binne, U.K., Harrington, L., Sicinski, P., Berube, N.G., *et al.* (2006). The retinoblastoma protein regulates pericentric heterochromatin. *Mol Cell Biol* *26*, 3659-3671.

Iskow, R.C., McCabe, M.T., Mills, R.E., Torene, S., Pittard, W.S., Neuwald, A.F., Van Meir, E.G., Vertino, P.M., and Devine, S.E. (2010). Natural mutagenesis of human genomes by endogenous retrotransposons. *Cell* *141*, 1253-1261.

Julian, L.M., Palander, O., Seifried, L.A., Foster, J.E., and Dick, F.A. (2008). Characterization of an E2F1-specific binding domain in pRB and its implications for apoptotic regulation. *Oncogene* *27*, 1572-1579.

Jung, J.W., Lee, S., Seo, M.S., Park, S.B., Kurtz, A., Kang, S.K., and Kang, K.S. (2010). Histone deacetylase controls adult stem cell aging by balancing the expression of polycomb genes and jumonji domain containing 3. *Cell Mol Life Sci* *67*, 1165-1176.

Kareta, M.S., Gorges, L.L., Hafeez, S., Benayoun, B.A., Marro, S., Zmoos, A.F., Cecchini, M.J., Spacek, D., Batista, L.F., O'Brien, M., *et al.* (2015). Inhibition of pluripotency networks by the Rb tumor suppressor restricts reprogramming and tumorigenesis. *Cell Stem Cell* *16*, 39-50.

Karimi, M.M., Goyal, P., Maksakova, I.A., Bilenky, M., Leung, D., Tang, J.X., Shinkai, Y., Mager, D.L., Jones, S., Hirst, M., *et al.* (2011). DNA methylation and SETDB1/H3K9me3 regulate predominantly distinct sets of genes, retroelements, and chimeric transcripts in mESCs. *Cell Stem Cell* *8*, 676-687.

Kotake, Y., Cao, R., Viatour, P., Sage, J., Zhang, Y., and Xiong, Y. (2007). pRB family proteins are required for H3K27 trimethylation and Polycomb repression complexes binding to and silencing p16INK4alpha tumor suppressor gene. *Genes Dev* *21*, 49-54.

Lamprecht, B., Walter, K., Kreher, S., Kumar, R., Hummel, M., Lenze, D., Kochert, K., Bouhrel, M.A., Richter, J., Soler, E., *et al.* (2010). Derepression of an endogenous long

terminal repeat activates the CSF1R proto-oncogene in human lymphoma. *Nat Med* 16, 571-579.

Lander, E.S., Linton, L.M., Birren, B., Nusbaum, C., Zody, M.C., Baldwin, J., Devon, K., Dewar, K., Doyle, M., FitzHugh, W., *et al.* (2001). Initial sequencing and analysis of the human genome. *Nature* 409, 860-921.

Langmead, B., and Salzberg, S.L. (2012). Fast gapped-read alignment with Bowtie 2. *Nat Meth* 9, 357-359.

Lee, E., Iskow, R., Yang, L., Gokcumen, O., Haseley, P., Luquette, L.J., 3rd, Lohr, J.G., Harris, C.C., Ding, L., Wilson, R.K., *et al.* (2012). Landscape of somatic retrotransposition in human cancers. *Science* 337, 967-971.

Leeb, M., Pasini, D., Novatchkova, M., Jaritz, M., Helin, K., and Wutz, A. (2010). Polycomb complexes act redundantly to repress genomic repeats and genes. *Genes Dev* 24, 265-276.

Leonova, K.I., Brodsky, L., Lipchick, B., Pal, M., Novototskaya, L., Chenchik, A.A., Sen, G.C., Komarova, E.A., and Gudkov, A.V. (2013). p53 cooperates with DNA methylation and a suicidal interferon response to maintain epigenetic silencing of repeats and noncoding RNAs. *Proc Natl Acad Sci U S A* 110, E89-98.

Leung, D.C., and Lorincz, M.C. (2012). Silencing of endogenous retroviruses: when and why do histone marks predominate? *Trends Biochem Sci* 37, 127-133.

Levin, H.L., and Moran, J.V. (2011). Dynamic interactions between transposable elements and their hosts. *Nat Rev Genet* 12, 615-627.

Li, W., Lee, M.H., Henderson, L., Tyagi, R., Bachani, M., Steiner, J., Campanac, E., Hoffman, D.A., von Geldern, G., Johnson, K., *et al.* (2015). Human endogenous retrovirus-K contributes to motor neuron disease. *Sci Transl Med* 7, 307ra153.

Liu, S., Brind'Amour, J., Karimi, M.M., Shirane, K., Bogutz, A., Lefebvre, L., Sasaki, H., Shinkai, Y., and Lorincz, M.C. (2014). Setdb1 is required for germline development and silencing of H3K9me3-marked endogenous retroviruses in primordial germ cells. *Genes Dev* 28, 2041-2055.

Lock, F.E., Rebollo, R., Miceli-Royer, K., Gagnier, L., Kuah, S., Babaian, A., Sistiaga-Poveda, M., Lai, C.B., Nemirovsky, O., Serrano, I., *et al.* (2014). Distinct isoform of FABP7 revealed by screening for retroelement-activated genes in diffuse large B-cell lymphoma. *Proc Natl Acad Sci U S A* 111, E3534-3543.

Macfarlan, T.S., Gifford, W.D., Driscoll, S., Lettieri, K., Rowe, H.M., Bonanomi, D., Firth, A., Singer, O., Trono, D., and Pfaff, S.L. (2012). Embryonic stem cell potency fluctuates with endogenous retrovirus activity. *Nature* 487, 57-63.

- Mager, D.L., and Stoye, J.P. (2015). Mammalian Endogenous Retroviruses. *Microbiology spectrum* 3, Mdna3-0009-2014.
- Méndez, J., and Stillman, B. (2000). Chromatin Association of Human Origin Recognition Complex, Cdc6, and Minichromosome Maintenance Proteins during the Cell Cycle: Assembly of Prereplication Complexes in Late Mitosis. *Molecular and Cellular Biology* 20, 8602-8612.
- Montoya-Durango, D.E., Liu, Y., Teneng, I., Kalbfleisch, T., Lacy, M.E., Steffen, M.C., and Ramos, K.S. (2009). Epigenetic control of mammalian LINE-1 retrotransposon by retinoblastoma proteins. *Mutat Res* 665, 20-28.
- Munro, S., Oppermann, U., and La Thangue, N.B. (2014). Pleiotropic effect of somatic mutations in the E2F subunit DP-1 gene in human cancer. *Oncogene* 33, 3594-3603.
- Muotri, A.R., Marchetto, M.C., Coufal, N.G., Oefner, R., Yeo, G., Nakashima, K., and Gage, F.H. (2010). L1 retrotransposition in neurons is modulated by MeCP2. *Nature* 468, 443-446.
- Peters, A.H., Kubicek, S., Mechtler, K., O'Sullivan, R.J., Derijck, A.A., Perez-Burgos, L., Kohlmaier, A., Opravil, S., Tachibana, M., Shinkai, Y., *et al.* (2003). Partitioning and plasticity of repressive histone methylation states in mammalian chromatin. *Mol Cell* 12.
- Quinlan, A.R., and Hall, I.M. (2010). BEDTools: a flexible suite of utilities for comparing genomic features. *Bioinformatics* 26, 841-842.
- Ramirez, F., Dundar, F., Diehl, S., Gruning, B.A., and Manke, T. (2014). deepTools: a flexible platform for exploring deep-sequencing data. *Nucleic acids research* 42, W187-191.
- Roulois, D., Loo Yau, H., Singhania, R., Wang, Y., Danesh, A., Shen, S.Y., Han, H., Liang, G., Jones, P.A., Pugh, T.J., *et al.* (2015). DNA-Demethylating Agents Target Colorectal Cancer Cells by Inducing Viral Mimicry by Endogenous Transcripts. *Cell* 162, 961-973.
- Schlesinger, S., and Goff, S.P. (2015). Retroviral transcriptional regulation and embryonic stem cells: war and peace. *Mol Cell Biol* 35, 770-777.
- Slotkin, R.K., and Martienssen, R. (2007). Transposable elements and the epigenetic regulation of the genome. *Nat Rev Genet* 8, 272-285.
- Thillainadesan, G., Chitilian, Jennifer M., Isovich, M., Ablack, Jailal Nicholas G., Mymryk, Joe S., Tini, M., and Torchia, J. (2012). TGF- β -Dependent Active Demethylation and Expression of the p15ink4b Tumor Suppressor Are Impaired by the ZNF217/CoREST Complex. *Molecular Cell* 46, 636-649.
- Vormer, T.L., Wojciechowicz, K., Dekker, M., de Vries, S., van der Wal, A., Delzenne-Goette, E., Naik, S.H., Song, J.Y., Dannenberg, J.H., Hansen, J.B., *et al.* (2014). RB

family tumor suppressor activity may not relate to active silencing of E2F target genes. *Cancer Res* 74, 5266-5276.

Walter, M., Teissandier, A., Perez-Palacios, R., and Bourc'his, D. (2016). An epigenetic switch ensures transposon repression upon dynamic loss of DNA methylation in embryonic stem cells. *Elife* 5.

Wells, J., Yan, P.S., Cechvala, M., Huang, T., and Farnham, P.J. (2003). Identification of novel pRb binding sites using CpG microarrays suggests that E2F recruits pRb to specific genomic sites during S phase. *Oncogene* 22, 1445-1460.

White, C.R., Denomme, M.M., Tekpetey, F.R., Feyles, V., Power, S.G., and Mann, M.R. (2015). High Frequency of Imprinted Methylation Errors in Human Preimplantation Embryos. *Scientific reports* 5, 17311.

Wylie, A., Jones, A.E., D'Brot, A., Lu, W.J., Kurtz, P., Moran, J.V., Rakheja, D., Chen, K.S., Hammer, R.E., Comerford, S.A., *et al.* (2016). p53 genes function to restrain mobile elements. *Genes Dev* 30, 64-77.

Yamasaki, L., Jacks, T., Bronson, R., Goillot, E., Harlow, E., and Dyson, N. (1996). Tumor induction and tissue atrophy in mice lacking E2F-1. *Cell* 85, 537-548.

Yu, P., Lübben, W., Slomka, H., Gebler, J., Konert, M., Cai, C., Neubrandt, L., Prazeres da Costa, O., Paul, S., Dehnert, S., *et al.* (2012). Nucleic Acid-Sensing Toll-like Receptors Are Essential for the Control of Endogenous Retrovirus Viremia and ERV-Induced Tumors. *Immunity* 37, 867-879.

Zhang, Y., Liu, T., Meyer, C.A., Eeckhoute, J., Johnson, D.S., Bernstein, B.E., Nusbaum, C., Myers, R.M., Brown, M., Li, W., *et al.* (2008). Model-based analysis of ChIP-Seq (MACS). *Genome biology* 9, R137.

Chapter 3

3 Disruption of CDK-resistant chromatin association by pRB causes DNA damage, mitotic errors, and reduces Condensin II recruitment

3.1 Abstract

Organization of chromatin structure is indispensable to the maintenance of genome integrity. The retinoblastoma tumor suppressor protein (pRB) mediates both transcriptional repression and chromatin organization, but the independent contributions of these functions have been difficult to study. Here, we utilize a synthetic *Rb1* mutant allele (F832A) that maintains pRB association at cell cycle gene promoters, but disrupts a cyclin-dependent kinase (CDK)-resistant interaction with E2F1 to reduce occupancy of pRB on intergenic chromatin. Reduced pRB chromatin association increases spontaneous γ H2AX deposition and aneuploidy. Our data indicates that the CDK-resistant pRB-E2F1 scaffold recruits Condensin II to major satellite repeats to stabilize chromatin structure in interphase and mitosis. In its absence, pericentromeric major satellite repeats are enriched with γ H2AX, but LINE and ERV repeats remain free of this DNA damage marker. This suggests that DNA damage phenotypes in *Rb1* F832A mutant cells are mechanistically distinct from silencing of repetitive sequence expression.

3.2 Introduction

Regulated alterations in chromatin structure during the cell cycle ensure coordination of transcription, DNA replication, and segregation of chromosomes in mitosis. Perturbations to broad mechanisms of chromatin organization that disrupt the careful coordination of these processes are often observed in concert with genome instability

(Papamichos-Chronakis and Peterson, 2013). This state of instability, characterized by persistent DNA damage, often precedes tumorigenesis (Jackson and Bartek, 2009). In this regard, it is not surprising that genes encoding broad organizers of chromatin structure are often classified as tumor suppressors.

In human cancer, a frequent target for disruption or misregulation is the retinoblastoma protein (pRB) (Dyson, 2016). Primary fibroblasts deficient for pRB exhibit relaxed chromatin structure (Herrera et al., 1996), along with replication defects and reduced chromatin compaction in prophase and chromosome segregation errors (Coschi et al., 2014; Coschi et al., 2010; Longworth et al., 2008; Manning et al., 2010; Manning et al., 2014). These changes are often accompanied by manifestations of genome instability, such as aneuploidy and widespread DNA damage (Coschi et al., 2014; Manning et al., 2014; van Harn et al., 2010). However, since pRB exerts transcriptional control over S- and M- phase cell cycle targets through E2Fs (Hernando et al., 2004; Schwartzman et al., 2011), genetic models of pRB deficiency may not distinguish the mechanistic contributions of pRB chromatin regulation from pRB-E2F transcriptional control in the maintenance of genome integrity. Thus, the ability to determine contributions of pRB chromatin organization to maintenance of genome stability requires specific loss-of-function models that maintain E2F transcriptional control and cell cycle regulation.

To regulate chromatin structure, pRB serves as a scaffold for a number of regulatory complexes that methylate DNA, modify histone tails, or mediate topological remodeling of nucleosomes (Longworth and Dyson, 2010). DNA-binding proteins, such as transcription factors, mediate region-specific pRB-chromatin association (Talluri and

Dick, 2012). This recruitment is predominantly mediated by E2F transcription factors. However, pRB-E2F complexes dissociate at the G1-S transition in response to cyclin-dependent kinase (CDK) phosphorylation. Recent evidence indicates that pRB uses an alternate CDK-resistant interaction with E2F1 to associate with repetitive elements (Calbo et al., 2002; Cecchini and Dick, 2011; Coschi et al., 2014; Ianari et al., 2009; Ishak et al., 2016). Germline disruption of this interaction abrogates EZH2-mediated facultative heterochromatinization at repetitive elements in concert with repeat misexpression and lymphomagenesis in mice (Ishak et al., 2016). The cancer susceptibility observed upon loss of CDK-resistant pRB-chromatin association merits investigation into whether this pRB-E2F1 interaction might underlie other pRB-dependent activities that impact genome integrity.

Here, we report that disruption of pRB's unique interaction with E2F1 causes the accumulation of γ H2AX foci, aneuploidy, increased RPA phosphorylation, and mitotic defects. Importantly, E2F target genes involved in DNA replication and mitosis remain at normal expression levels. We demonstrate that cells bearing an F832A mutation in *Rb1* (*Rb1^S*) exhibit impaired chromatin recruitment of the Condensin II complex specifically at genomic locations where γ H2AX accumulates. This mechanism further suggests that chromatin organization is an indispensable facet of pRB-mediated tumor suppression.

3.3 Experimental Procedures

3.3.1 Cell culture

Gene targeted mouse strains bearing a null allele of *Rb1* (*Rb1^{tm1Tyj}*) and an F832A point mutation to disrupt pRB's unique interaction with E2F1 (*Rb1^S*, or *Rb1^{tm3Fad}*) have been

previously described (Ishak et al., 2016; Jacks et al., 1992). Primary murine embryonic fibroblasts (MEFs) were isolated and cultured from E13.5 embryos of the desired genotypes according to established procedures (Thwaites et al., 2016). All experiments were performed on passage 4 (P4) cells.

3.3.2 Fluorescence microscopy

Immunofluorescence was conducted as previously described (Coschi et al., 2014).

Briefly, 2.5×10^5 MEFs were seeded per confocal dish, incubated 24h, washed 3x for 5 minutes in 1x PBS, fixed by incubation with 4% paraformaldehyde in 1x PBS for 10 minutes at room temperature, then washed and stored at 4°C. To immunostain, cells were permeabilized for 10 minutes with 0.3% Triton X-1000 in 1xPBS (PBS-T), blocked for 1 hour at room temperature with 5% goat serum in PBS-T, incubated one hour with mouse anti-Phospho histone H2A.X Ser139 (05-636, Millipore) diluted 1:400 in PBS-T, washed, and incubated one hour in goat anti-mouse Alexa Fluor 594 secondary antibody diluted 1:800 in PBS-T. Cells were washed 3x for 5 minutes with PBS-T, then incubated 5 minutes with DAPI in PBS-T. Stained MEFs were washed 3x with PBS-T, twice with 1x PBS, then mounted with a coverslip using SlowFade® Gold antifade reagent (S36937, Life Technologies). Fluorescence was visualized using an Olympus Fluoview FV1000 confocal microscope system, with images compiled using Olympus Fluoview FV1000 Viewer. γ H2AX foci were quantified using the focinator program (Oeck et al., 2015) with fixed thresholds and parameters maintained across all groups in a given experiment.

3.3.3 Flow cytometry

Asynchronous or serum starved MEFs were ethanol-fixed, stained with propidium iodide, treated with RNase, strained, and analyzed by flow cytometry on a Beckman-Coulter EPICS XL-MCL (Cecchini et al., 2012).

3.3.4 Detection of RNA and protein levels

RNA levels were determined by Affymetrix Mouse Gene 1.0 Array as previously described using rRNA-depleted total RNA from serum starved P4 MEFs (Cecchini et al., 2014) (Ishak et al., 2016). Log₂ values of mutant/wild-type expression determined with Partek Genomics Suite were plotted as heat maps using matrix to PNG at chibi.ubc.ca/matrix. Array CEL files are available at GSE85640 and GSE54924. To assess protein levels, whole-cell lysates and chromatin fractions were generated as previously described (Ishak et al., 2016), resolved by SDS-PAGE, and immunoblotted using the following antibodies: RPA32 (A300-244A, Bethyl labs), RPA32 pSer33 (A300-246A, Bethyl labs), H3, (ab1791, Abcam), Actin (A2066, Sigma), PCNA (F-2 Santa Cruz), Mcm3 (4012S, Cell Signaling), Mcm7 (H-5, Santa Cruz), BubR1 (C-20, Santa Cruz), Cdk1 (ab7953 abcam), Mad2 (C-19, Santa Cruz), CAP-D3 (Coschi et al., 2010), SMC2 (Coschi et al., 2014).

3.3.5 Chromatin immunoprecipitation and ChIP-seq analysis

Chromatin immunoprecipitation experiments and analyses were conducted as previously described (Ishak et al., 2016). Briefly, cross-linked chromatin fragments were pre-cleared with protein G Dynabeads for immunoprecipitation with ChIP antibodies. Cross-links

were reversed at 65°C followed by DNA isolation. For ChIP-reChIP experiments, crosslinks were maintained following the first immunoprecipitation. Protein-DNA complexes were eluted, and subjected to a second immunoprecipitation with a different antibody. DNA was isolated as described for single-IP ChIP. deepTools was used to generate heat maps depicting ChIP-seq read enrichment at wild-type peak locations. bamCompare was used to normalize ChIP to input reads, then computeMatrix was used to determine read enrichment at wild-type repeat peak intersects with the mm9 RepeatMasker index from UCSC Table Browser. heatMapper was used to plot enrichment per peak location (Ramirez et al., 2014). Reads are available at GSE85640. ChIP antibodies used were anti-phospho histone H2A.X Ser139 (07-164, Millipore), anti-CAP-D3 (Coschi et al., 2010), and a previously described cocktail of pRB antibodies (Cecchini et al., 2014). ChIP-qPCR primer sources have been previously described (Cecchini 2014, Ishak 2016 references). Sequences 5- to 3' are as follows: PCNA_E2F_F CAGAGTAAGCTGTACCAAGGAGAC, PCNA_E2F_R CGTTCCTCTTAGAGTAGCTCTCATC, PCNA_-2kb_F CATCAGTGAATACGTCTCTGTTCCA, PCNA_-2kb_R CTGCTTCTCAGTTGTTTTAGGAAGG, Maj_F GACGACTTGAAAAATGACGAAATC, Maj_R CATATTCCAGGTCCTTCAGTGTGC, L1 5' UTR_F CTGCCTTGCAAGAAGAGAGC, L1 5' UTR_R AGTGCTGCGTTCTGATGATG, IAP LTR_F CTGACAGCTGTGTTCTAAGTGGTAAACAAA, IAP LTR_R AGAACACCACAGACCAGAATCTTCTGC

3.3.6 Video Microscopy

Video microscopy was conducted as previously described (Coschi et al., 2010). Briefly, MEFs infected with ecotropic retroviruses carrying pBABE-H2B-GFP packaged in Bosc23 cells were plated into glass-bottom tissue culture dishes in phenol-free DMEM with 5% FBS, penicillin, streptomycin, and glutamine. Cells were maintained at 37°C with 5% CO₂ as phase-contrast and fluorescent images were captured every 3 minutes for 15 hours by a DMI 6000b Leica microscope. Images were assembled into movies and analyzed for mitotic errors.

3.4 Results

3.4.1 The *Rb1^S* mutation causes defects in genome integrity

To assess the contribution of pRB-E2F1 interactions in chromatin association and its effects on genome stability, we utilized a previously described mutation (F832A, called *Rb1^S*) that disrupts pRB's unique C-terminal interaction with the E2F1 marked box domain (Cecchini and Dick, 2011; Coschi et al., 2014; Ishak et al., 2016). ChIP-sequence of pRB from wild type and *Rb1^{S/S}* cells was analyzed. Alignment of pRB ChIP-seq reads reveals locations of pRB enrichment within repetitive elements throughout the genome and these are lost in ChIP-seq using pRB^S (Figure 3.1A). Strikingly, this pattern of repeat occupancy by pRB is relatively preserved under proliferating conditions. In contrast, pRB ChIP-qPCR demonstrates that pRB^S retains occupancy at cell cycle and E2F regulated promoters, such as *Pcna*, at levels comparable to that of wild-type pRB (Figure 3.1B) (Ishak et al., 2016). Therefore, in contrast to previous models of pRB-deficiency,

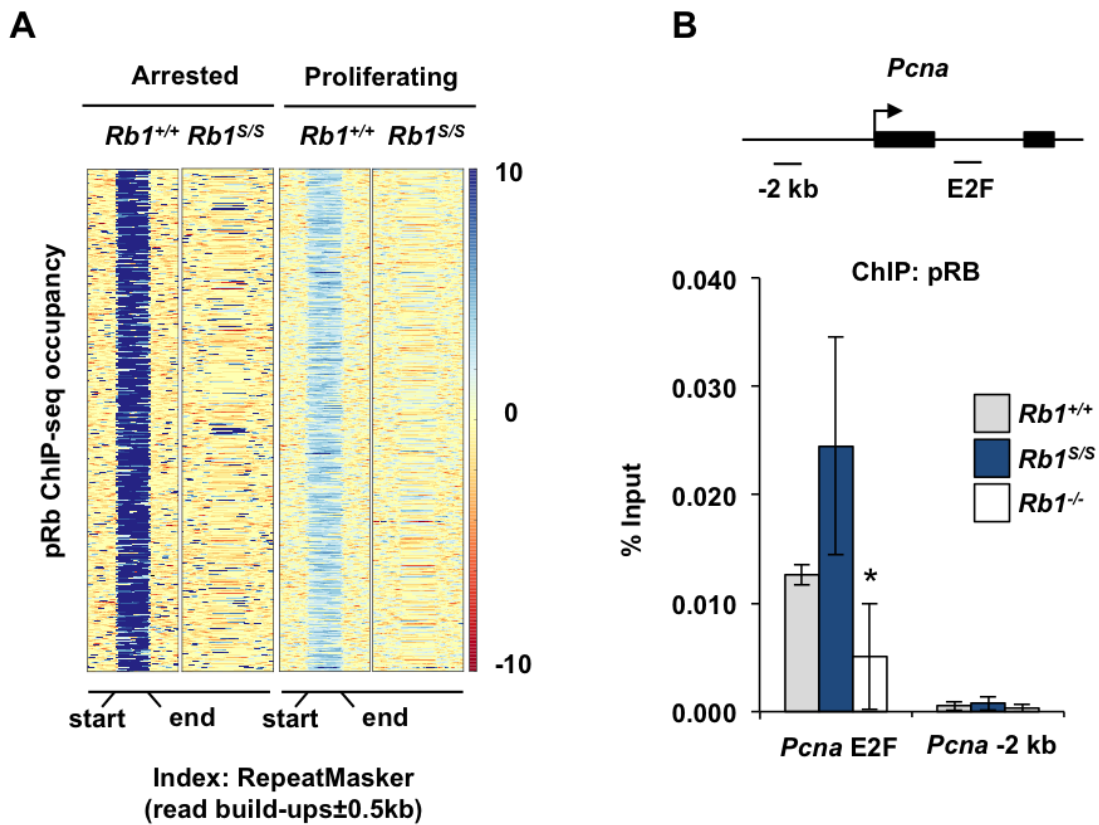


Figure 3.1: Disruption of pRB association with repetitive sequences.

(A) Heat maps display scaled pRB ChIP-seq read build ups. Wild-type pRB read build ups are shown for mm9 RepeatMasker index locations. Each row contains ± 0.5 kb of flanking sequence surrounding the scaled reads. Intensity scales on right indicate the magnitude of read enrichment over input control. Heat maps of *Rb1*^{S/S} mutant ChIP-seq reads display occupancy at the analogous wild type positions under arrested and proliferating conditions. (B) pRB ChIP-qPCR analyzing amplicons at the *Pcna* transcriptional start site (TSS) and 2 kb 5' of *Pcna*. Error bars indicate one standard deviation from the mean, and an asterisk represents a significant difference from wild type ($n = 3$, $P \leq 0.05$ by *t*-test).

the *Rb1^S* mutation permits assessment of post-G1 pRB-chromatin regulatory activities independent of E2F cell cycle gene association and regulation.

We investigated a number of broad measures of genome integrity in *Rb1^{S/S}* MEFs relative to controls. Since *Rb1^{-/-}* cells exhibit aneuploidy with increasing rounds of cell division (Srinivasan et al., 2007), we sought to determine whether loss of pRB-chromatin association at non-cell cycle genes could cause a similar effect. To assess cellular DNA content, proliferating and serum-starved MEFs were stained with propidium iodide and analyzed by flow cytometry. DNA content greater than the 4N peak was quantified to determine the proportion of aneuploid cells. In accordance with previous reports, *Rb1^{-/-}* MEFs exhibit significantly elevated levels of >4N DNA. Intriguingly, *Rb1^{S/S}* MEFs also exhibit increased levels of >4N DNA relative to wild-type MEFs under arrested and proliferating growth conditions, albeit at levels less than those of *Rb1^{-/-}* MEFs (Figure 3.2A).

Another broad manifestation of genome instability observed upon pRB loss is the emergence of γ H2AX foci in fluorescence microscopy experiments. Immunofluorescence revealed increased γ H2AX foci in proliferating *Rb1^{S/S}* MEF cultures comparable in magnitude to *Rb1^{-/-}* MEFs, with approximately 10% of nuclei displaying 5 or more foci (Figure 3.2B and 3.2C). Increased γ H2AX foci together with elevated >4N DNA content in *Rb1^{S/S}* cells suggests pRB-E2F1 complexes might mediate post-G1 functions. Post-G1, pRB reduces DNA damage through mitigation of replication stress via mechanisms that remain poorly understood (Bester et al., 2011; Coschi et al., 2014; Manning et al., 2014). To explore the effects of reduced pRB chromatin association on replication, we assessed

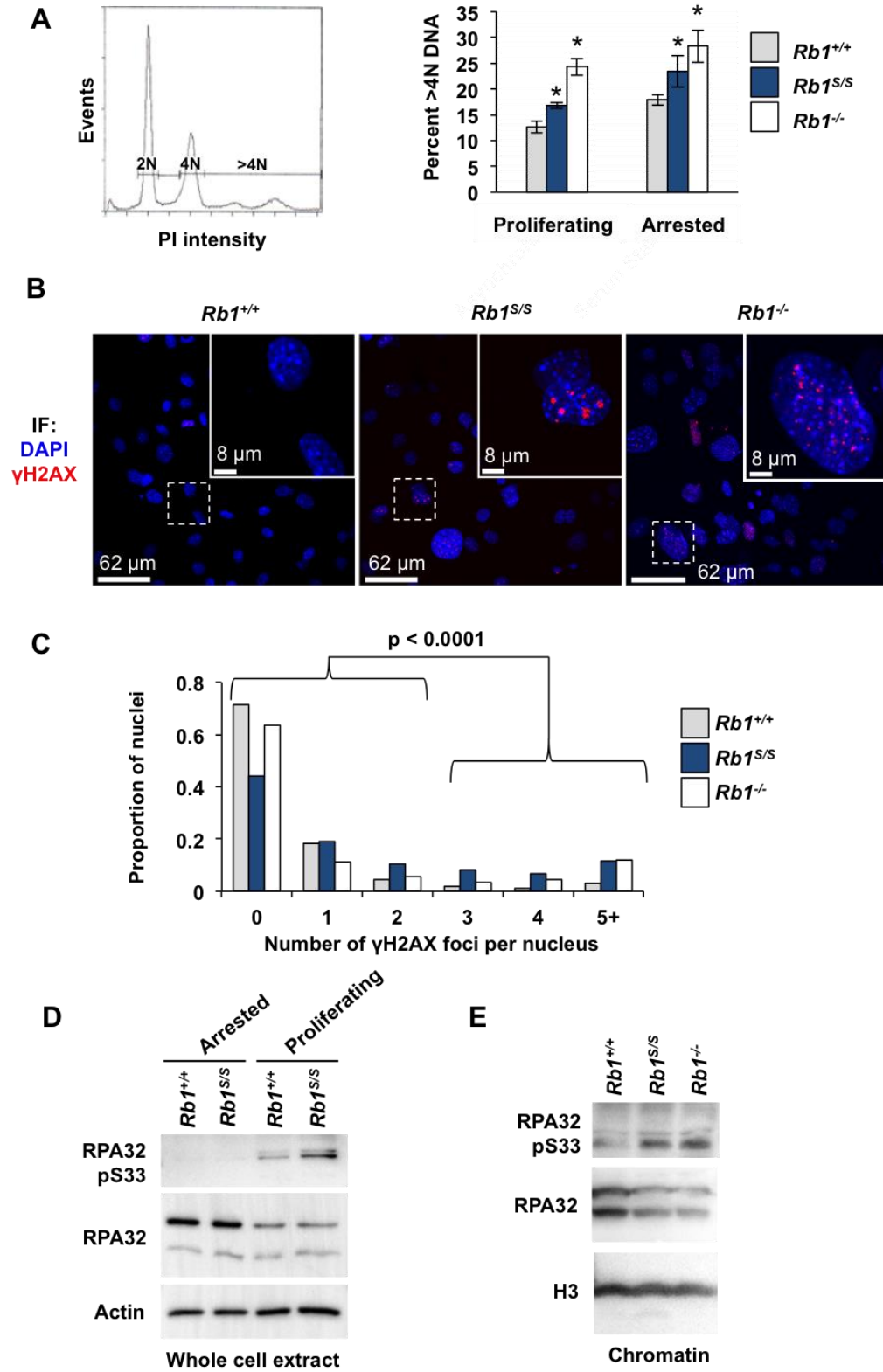


Figure 3.2: Loss of genome integrity in *Rb1*^{S/S} mutant cells.

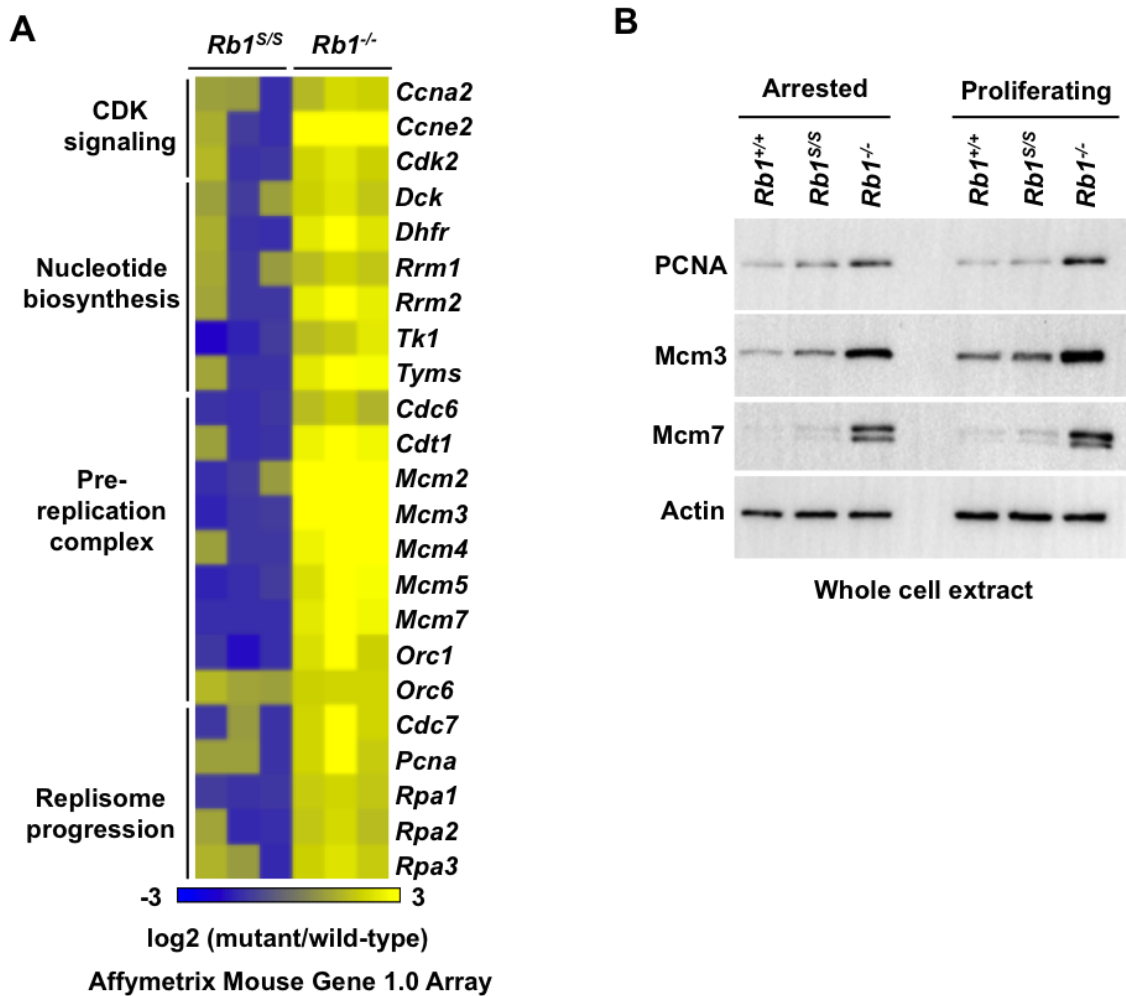
Figure 3.2: Loss of genome integrity in *Rb1*^{S/S} mutant cells.

(A) Cells were stained with propidium iodide and analyzed by flow cytometry for DNA content. The histogram shows gates to demarcate cells with >4N DNA content. 4N DNA content was determined for the indicated genotypes of cells. Error bars indicate one standard deviation from the mean, and an asterisk represents a significant difference from wild type compared within the same growth condition ($n = 3$, $P \leq 0.05$ by t -test). (B) Immunofluorescence microscopy of proliferating MEFs stained for γ H2AX (red) and DAPI (blue). White boxes indicate regions shown at increased magnification within the inset. Scale bars indicate relative magnification. (C) The number of γ H2AX foci per nucleus was quantified and compared among three biological replicates per genotype using a χ^2 test ($Rb1^{+/+}$ $n = 1054$, $Rb1^{S/S}$ $n = 744$, $Rb1^{-/-}$ $n = 602$ total nuclei analyzed). (D) Western blots show RPA32 pSer33 levels for the indicated genotypes from arrested and proliferating MEFs. The Actin blot serves as a loading control. (E) RPA32 pSer33 and RPA32 western blots of chromatin fractions from proliferating MEFs. Histone H3 blot indicates loading.

relative phosphorylation levels of the single-strand DNA binding protein RPA. Western blots of whole cell extracts reveal increased levels of RPA32 pS33 under proliferating conditions relative to arrested wild-type MEFs. This proliferation-dependent RPA32 pS33 increase appears further elevated in *Rb1^{S/S}* MEFs relative to control cells (Figure 3.2D). Strikingly, western blots of chromatin fractions revealed that the elevated RPA32 pS33 in mutant MEFs can be detected on chromatin at levels comparable to that of *Rb1^{-/-}* MEFs (Figure 3.2E).

In pRB deficient cells, misregulation of E2F transcriptional control of DNA replication components contributes to aneuploidy (Srinivasan et al., 2007). However, in accordance with pRB^S association with cell cycle promoters in ChIP experiments, microarray analysis revealed normal regulation of E2F targets involved in DNA replication in arrested *Rb1^{S/S}* MEFs (Figure 3.3A). In contrast, *Rb1^{-/-}* MEFs exhibited deregulation of DNA replication components under the same culture conditions (Figure 3.3A). Beyond mRNA levels, western blots of whole cell extracts confirmed expression levels of DNA replication components in *Rb1^{S/S}* MEFs paralleled those in wild-type MEFs under both arrested and proliferating conditions, and contrasted with the pronounced misregulation evident upon complete loss of pRB expression (Figure 3.3B).

Collectively, these observations suggest that reduced pRB-chromatin association under proliferating growth conditions increases the frequency of events that can compromise genome integrity. Expression analysis suggests that these effects in *Rb1^{S/S}* MEFs are independent of E2F transcriptional control of DNA replication genes.



3.4.2 Rb1S mutant cells exhibit defects in mitosis.

Beyond replication, pRB maintains proper chromosome segregation through coordination of multiple mitotic processes such as the regulation of E2F-activated spindle assembly checkpoint targets, and regulation of chromosome condensation (Manning and Dyson, 2012). We investigated whether the *Rb1^S* mutation affected mitosis. To visualize mitotic progression, wild-type and mutant MEFs were transduced with GFP-tagged H2B using viral delivery, and subjected them to live-cell video microscopy. Analysis of *Rb1^{S/S}* cells revealed a marked defect in chromosome condensation apparent in prophase that frequently impeded chromosome congression at metaphase (Figure 3.4A and 3.4B). We next analyzed mitotic chromosome segregation. Figure 3.4C shows examples of normal mitotic stages and cell division observed by video microscopy in wild-type MEFs. These microscopy experiments revealed numerous mitotic aberrations present in *Rb1^{S/S}* MEFs such as chromosome bridges in anaphase, partial segregation of chromosomes, as well as missegregation of all chromosomes to one daughter, or failure of cytokinesis leading to binucleated cells (Figure 3.4D and 3.4E). Ultimately, the majority of mitotic *Rb1^{S/S}* MEFs fail to faithfully segregate duplicated chromosomes to their daughter cells, while over 90% of wild-type MEFs displayed proper mitotic progression in this assay (Figure 3.4E).

Mitotic errors such as lagging chromosomes and missegregation events contribute to the generation of micronuclei (Holland and Cleveland, 2012). To determine whether mitotic errors in *Rb1^{S/S}* cells were associated with the accumulation of micronuclei, MEFs were fixed and stained with DAPI for fluorescence-based visualization. Quantification of micronuclei revealed a significant increase in *Rb1^{S/S}* cells relative to wild type (Figure

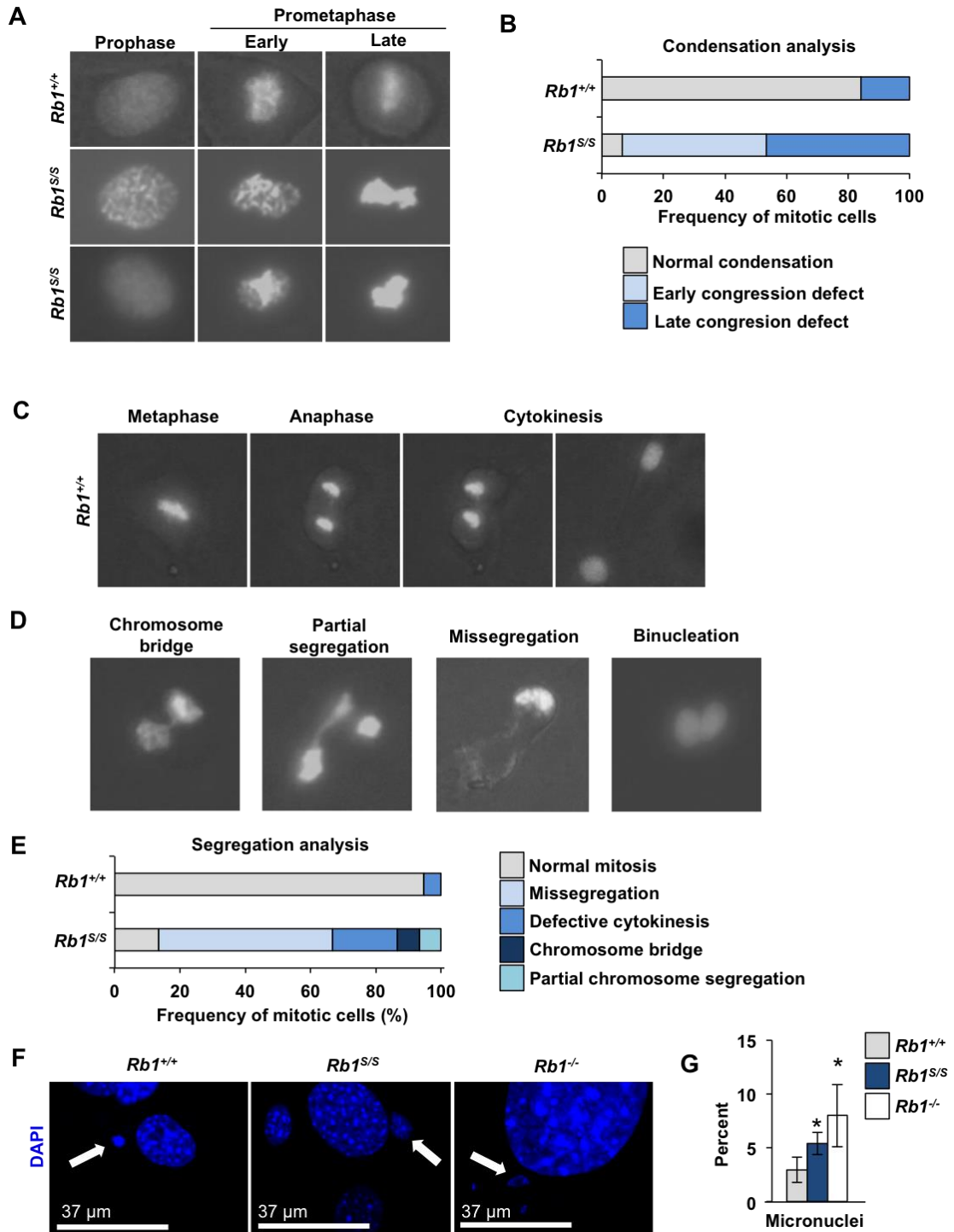


Figure 3.4: Defective mitosis in *Rb1^{S/S}* mutant cells.

Figure 3.4: Defective mitosis in *Rb1*^{S/S} mutant cells.

Mitosis was investigated by video microscopy experiments using MEFs transduced with H2B-GFP (*Rb1*^{+/+} n = 19, *Rb1*^{S/S} n = 15). **(A)** Merged images of phase-contrast and GFP channels display examples of chromosome condensation in prophase for indicated genotypes. **(B)** Quantitation of the frequency of condensation errors observed in wild type and *Rb1*^{S/S} MEFs. **(C)** Merged images of phase-contrast and GFP channels display examples of normal mitotic stages observed in wild type cells are shown. **(D)** Merged images of phase-contrast and GFP channels to demonstrate examples of defective anaphase and cytokinesis observed by video microscopy. **(E)** Quantitation of segregation events observed in wild type and *Rb1*^{S/S} MEFs. **(F)** Fluorescence microscopy of proliferating MEFs stained with DAPI (blue). White arrows demark examples of micronuclei while scale bars indicate relative magnification. **(G)** Quantitation of micronuclei frequency visualized by immunofluorescence microscopy. Error bars indicate one standard deviation from the mean, and an asterisk represents a significant difference from wild type ($P \leq 0.05$ by *t*-test, n = 3).

3.4F and 3.4G). However, the increase observed in mutant cells does not exceed the magnitude of micronuclei present in *Rb1*^{-/-} cells (Figure 3.4G).

We next assessed whether misregulation of E2F mitotic target gene expression might underlie the mitotic errors observed upon reduction of pRB-chromatin association. Akin to DNA replication components, microarray analysis revealed normal expression of E2F mitotic checkpoint targets in *Rb1*^{S/S} MEFs that contrasted with the misexpression observed in *Rb1*^{-/-} MEFs (Figure 3.5A). Western blots of whole cell extracts confirmed that expression levels of mitotic checkpoint proteins in *Rb1*^{S/S} MEFs resembled expression levels observed in wild-type fibroblasts. Accordingly, *Rb1*^{-/-} cells exhibit misexpression of E2F mitotic checkpoint targets at the protein level (Figure 3.5B). Overall, lack of mitotic checkpoint misexpression in the presence of mitotic errors suggests that pRB-chromatin association facilitates mitotic progression independently of E2F transcriptional control.

3.4.3 pRB-E2F1 recruits Condensin II to major satellites to mitigate DNA damage.

In light of the post-G1 defects apparent upon diminished pRB^S chromatin association, we sought to identify a pRB-dependent mechanism that could link increased γ H2AX, increased RPA32 pS33, and mitotic defects observed in *Rb1*^{S/S} cells. Since pRB serves as a recruitment factor for numerous chromatin regulators including Condensin II (Coschi et al., 2014; Coschi et al., 2010; Longworth et al., 2008), we investigated its recruitment to sites of γ H2AX deposition. First, to determine whether Condensin II exhibited sensitivity to diminished pRB-chromatin association, we assessed the expression of Condensin II subunits. Western blots of whole cell extracts from arrested

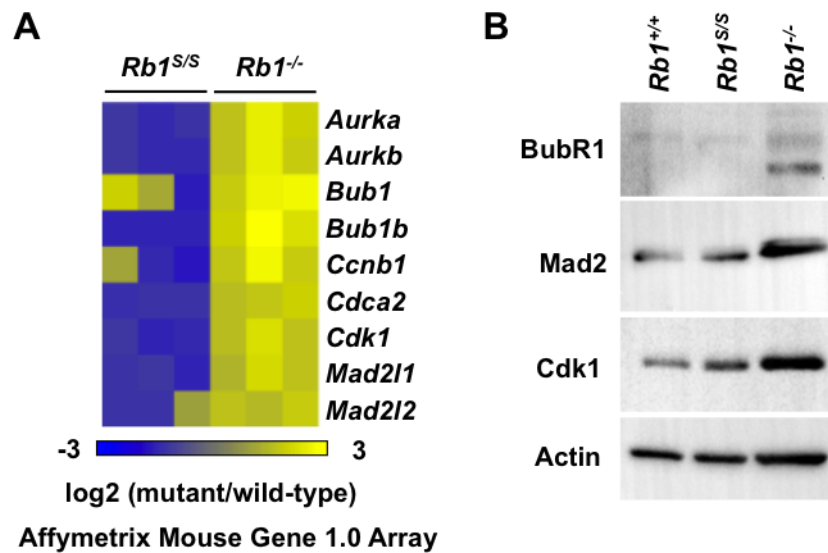


Figure 3.5: Normal expression of mitotic pRB-E2F target genes.

(A) Expression microarrays were performed with RNA from serum-starved MEFs of the indicated genotypes and wild type controls ($n = 3$). For each gene listed, corresponding log₂ values of each mutant replicate vs. wild type is shown as a heat map. (B) Western blots indicate BubR1, Mad2, and Cdk1 levels detected in whole-cell extracts from proliferating MEFs. The Actin blot serves as a loading control.

and proliferating MEFs revealed no differences in CAP-D3 and SMC2 expression in mutant cells relative to wild type controls (Figure 3.6A). We next assessed whether the *Rb1^S* mutation affected Condensin II recruitment to chromatin. Western blots of chromatin fractions revealed that relative to the arrested state, both CAP-D3 and SMC2 exhibited increased chromatin loading in proliferating wild-type MEFs. Notably, this proliferation-dependent increase in Condensin II chromatin loading is diminished in *Rb1^{S/S}* cells (Figure 3.6B). We then used ChIP-reChIP to determine whether reduced Condensin II loading on chromatin in mutant cells was due to a direct pRB-mediated recruitment mechanism. ChIP for CAP-D3 followed by ChIP for pRB confirms that CAP-D3 localizes with pRB to pericentric major satellite repeats in wild type MEFs. pRB-CAP-D3 co-recruitment is significantly reduced in *Rb1^{S/S}* MEFs, consistent with the global reduction of Condensin II loading observed in chromatin fractions (Figure 3.4C).

Condensin II-mediated regulation of replication and chromosome condensation requires chromatin loading. We hypothesized that genomic locations of pRB-dependent Condensin II association, such as pericentric repeats, would be particularly sensitive to accumulation of γ H2AX upon reduction of Condensin II recruitment. ChIP-qPCR demonstrates a relative increase in γ H2AX at major satellite repeats in proliferating *Rb1^{S/S}* MEFs, while γ H2AX levels in wild-type MEFs do not exceed background levels (Figures 3.6D). By comparison, γ H2AX ChIP-qPCR experiments demonstrated that DNA damage is not increased at LINE1 or endogenous retroviral repeats in *Rb1^{S/S}* cells (Figure 3.6E and 3.6F). This indicates that only specific genomic locations accumulate γ H2AX in response to the *Rb1^S* mutation rather than all repeat locations occupied and

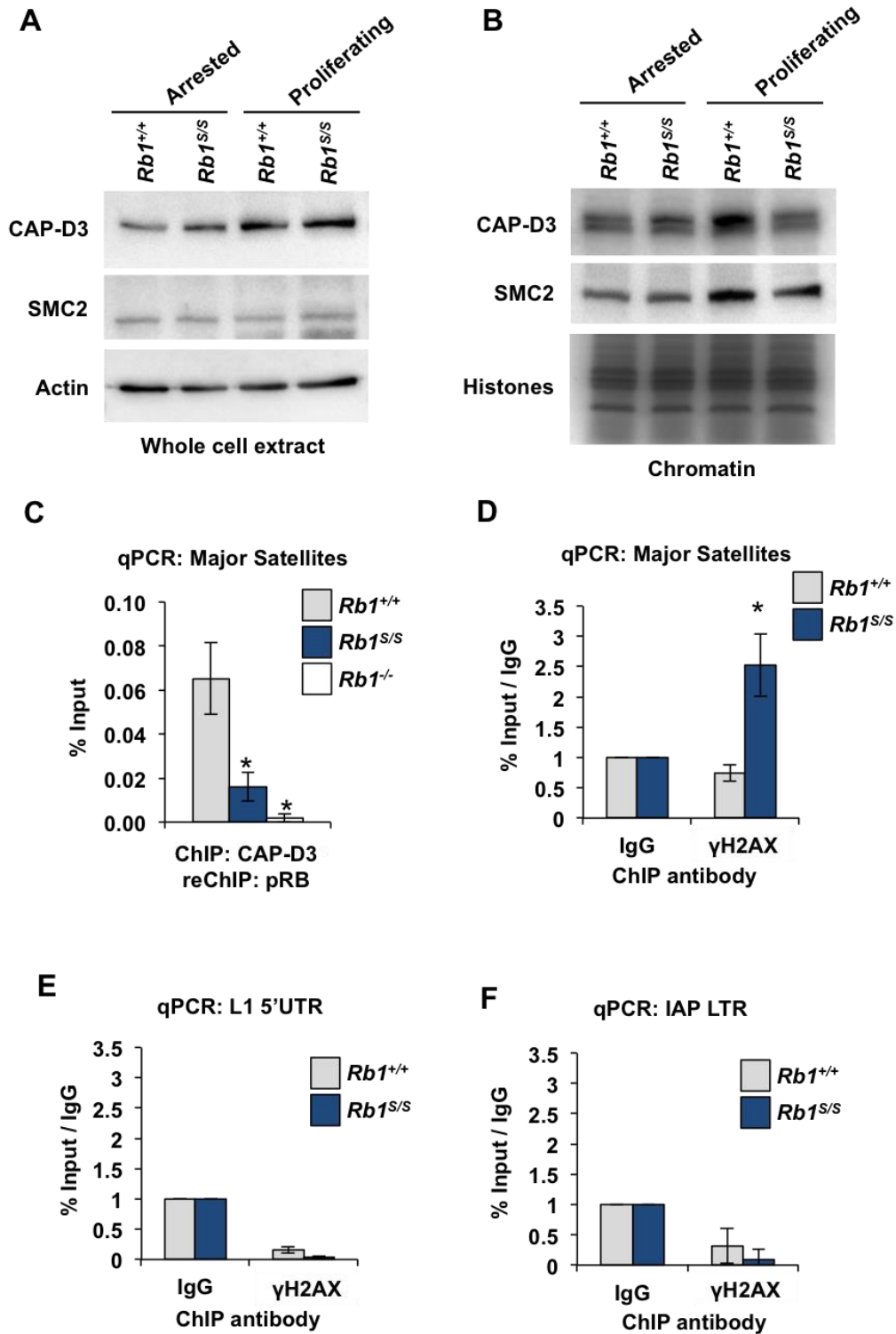


Figure 3.6: Recruitment of CAP-D3 by pRB mitigates DNA damage at pericentromeric major satellite repeats.

Figure 3.6: Recruitment of CAP-D3 by pRB mitigates DNA damage at pericentromeric major satellite repeats.

(A) CAP-D3 and SMC2 levels were detected by western blotting whole-cell extracts from arrested and proliferating MEFs. The Actin blot serves as a loading control. (B) CAP-D3 and SMC2 western blots of chromatin fractions. Coomassie-stained histones are used as a loading control. (C) CAP-D3-pRB ChIP-reChIP was performed using chromatin from proliferating MEFs and occupancy was quantified at pericentromeric major satellite repeats by qPCR. Error bars indicate one standard deviation from the mean, and an asterisk represents a significant difference from wild type ($n = 3$, $P \leq 0.05$ by t -test). (D) γ H2AX ChIP-qPCR was performed using chromatin from proliferating MEFs and quantified at pericentromeric major satellite repeats and normalized to IgG ChIP performed in parallel from same chromatin preparation. (E and F) γ H2AX ChIP-qPCR as in D except occupancy was quantitated at L1 5' UTRs and IAP LTRs.

regulated by pRB. Overall, site-specific γ H2AX accumulation at locations of pRB-Condensin II loss in *Rb1*^{S/S} MEFs suggests that the CDK-resistant pRB-E2F1 complex mediates Condensin II recruitment to pericentromeric repeats to support genome integrity. Loss of this recruitment event is associated with the onset of DNA damage and mitotic errors that are prevalent in *Rb1*^{S/S} MEFs, and the contributions of this mechanism to cancer susceptibility in *Rb1*^{S/S} mice is likely significant.

3.5 Discussion

The original null alleles of *Rb1* in mice revealed that it was indispensable to the maintenance of genome integrity (Zheng et al., 2002). However, deregulation of E2F cell cycle targets concurrent with loss of genome stability hindered the ability to assess whether pRB could maintain genome integrity independent of E2F transcriptional control. Here, we utilized a synthetic *Rb1* mutant allele that maintains pRB association at E2F cell cycle targets, but reduces overall pRB-chromatin association at intergenic regions (Ishak et al., 2016). We demonstrate that cells from these mice possess inherently unstable genomes characterized by markers of DNA damage, replication abnormalities, and aneuploidy.

Elevated RPA32 pS33 in *Rb1*^{S/S} chromatin is suggestive of DNA replication defects. pRB-E2F1-dependent Condensin II recruitment prevents many features that are characteristic of ‘under replication’ of pericentric repeats (Coschi et al., 2014; Harrigan et al., 2011; Lukas et al., 2011). It remains to be explored whether the pRB-E2F1 scaffold underlies other pRB interactions with replication components that may also contribute to spontaneous DNA damage. pRB restricts DNA replication initiation and progression

through its interaction with Mcm7 and its ability to suppress DNA polymerase α and Ctf4 recruitment to replisomes (Borysov et al., 2015). It has also been shown that pRB associates with Orc1 at replication origins (Avni et al., 2003; Mendoza-Maldonado et al., 2010). Finally, pRB can displace PCNA to halt progression of the replication fork (Braden et al., 2006). If the pRB-E2F1 scaffold mediates these interactions, it is possible that they also contribute to RPA32 pS33 and γ H2AX at pericentric repeats.

We note a significant failure of *Rb1*^{S/S} cells to condense chromosomes that precedes numerous chromosome segregation defects. These defects parallel mitotic errors observed in other models that are deficient for pRB-Condensin II recruitment to chromatin (Coschi et al., 2010; Longworth et al., 2008; Manning et al., 2010). Collectively, these data suggest that pRB-E2F1 forms a scaffold to permit Condensin II interaction with the pRB LxCxE binding cleft. Despite characterization of chromatin recruitment, mechanistic details of pRB-Condensin II association remain poorly understood. However, these phenotypes and the ensuing lymphoma in *Rb1*^{S/S} mice has intriguing similarities to recent studies examining a hypomorphic CAP-H2 mutant mouse strain (called *Nessy*) (Woodward et al., 2016), as well as lymphomas from *E2f1*^{-/-} mice (Yamasaki et al., 1996). *E2f1*^{-/-} mice frequently succumb to follicular B-lymphomas evident in the mesenteric lymph node and this is a common finding in *Rb1*^{S/S} mice (Ishak et al., 2016; Yamasaki et al., 1996). *Nessy*, or *Caph2*^{I15N} mutant mice, have lineage-specific delayed anaphase entry that manifests as aneuploid CD4^{+I0};CD8⁺;CD71⁺ thymic T-cells that develop into lymphomas in adult animals (Woodward et al., 2016). It will be interesting to understand the subtle differences in tissue tropism between the *Rb1*^{S/S} and

Nessy mice, although other pRB-E2F1 containing complexes recruited to chromatin likely underlie some of these differences.

Our observations contribute to a growing body of literature that challenges classification of pRB as ‘inactive’ beyond entry into S-phase. In addition to Condensin II, the pRB-E2F1 scaffold also recruits EZH2 to repetitive elements in cycling cells (Ishak et al., 2016). We envision that disruption of both complexes likely contributes to the cancer phenotype in *Rb1^{S/S}* mice. First, loss of Condensin II recruitment and instability phenotypes are found in *Rb1* mutant mice with defective LxCxE interactions (*Rb1^L*), but this defect is insufficient to trigger cancer on its own (Coschi et al., 2014). In this study we show that instability phenotypes found in *Rb1^{S/S}* cells are most attributable to defects in Condensin II recruitment as γ H2AX accumulates preferentially in pRB-E2F1-Condensin II locations, yet *Rb1^{S/S}* mice are cancer prone. An important difference between *Rb1^{S/S}* and *Rb1^{L/L}* mutant mice is repeat misexpression that predominantly occurs in the spleens of *Rb1^{S/S}* mice where the majority of tumors arise. Based on this reasoning, we expect that loss of both pRB-E2F1-Condensin II and pRB-E2F1-EZH2 complexes caused by the F832A mutation are both necessary to cause the cancer phenotype observed in *Rb1^{S/S}* mice. Collectively, this body of work further emphasizes the multifunctionality of pRB and how its disparate activities work together to underlie its tumor suppressor role.

3.6 References

Avni, D., Yang, H., Martelli, F., Hofmann, F., ElShamy, W.M., Ganesan, S., Scully, R., and Livingston, D.M. (2003). Active localization of the retinoblastoma protein in chromatin and its response to S phase DNA damage. *Mol Cell* 12, 735-746.

Bester, A.C., Roniger, M., Oren, Y.S., Im, M.M., Sarni, D., Chaoat, M., Bensimon, A., Zamir, G., Shewach, D.S., and Kerem, B. (2011). Nucleotide deficiency promotes genomic instability in early stages of cancer development. *Cell* 145, 435-446.

Borysov, S.I., Nepon-Sixt, B.S., and Alexandrow, M.G. (2015). The N Terminus of the Retinoblastoma Protein Inhibits DNA Replication via a Bipartite Mechanism Disrupted in Partially Penetrant Retinoblastomas. *Mol Cell Biol* 36, 832-845.

Braden, W.A., Lenihan, J.M., Lan, Z., Luce, K.S., Zagorski, W., Bosco, E., Reed, M.F., Cook, J.G., and Knudsen, E.S. (2006). Distinct action of the retinoblastoma pathway on the DNA replication machinery defines specific roles for cyclin-dependent kinase complexes in prereplication complex assembly and S-phase progression. *Mol Cell Biol* 26, 7667-7681.

Calbo, J., Parreno, M., Sotillo, E., Yong, T., Mazo, A., Garriga, J., and Grana, X. (2002). G1 cyclin/cyclin-dependent kinase-coordinated phosphorylation of endogenous pocket proteins differentially regulates their interactions with E2F4 and E2F1 and gene expression. *J Biol Chem* 277, 50263-50274.

Cecchini, M.J., Amiri, M., and Dick, F.A. (2012). Analysis of cell cycle position in mammalian cells. *Journal of visualized experiments : JoVE*.

Cecchini, M.J., and Dick, F.A. (2011). The biochemical basis of CDK phosphorylation-independent regulation of E2F1 by the retinoblastoma protein. *Biochem J* 434, 297-308.

Cecchini, M.J., Thwaites, M., Talluri, S., Macdonald, J.I., Passos, D.T., Chong, J.L., Cantalupo, P., Stafford, P., Saenz-Robles, M.T., Francis, S.M., *et al.* (2014). A retinoblastoma allele that is mutated at its common E2F interaction site inhibits cell proliferation in gene targeted mice. *Molecular and cellular biology* 34, 2029-2045.

Coschi, C., Ishak, C., Gallo, D., Marshall, A., Talluri, S., Wang, J., Cecchini, M., Martens, A., Percy, V., Welch, I., *et al.* (2014). Haploinsufficiency of an RB-E2F1-Condensin II complex leads to aberrant replication and aneuploidy. *Cancer Discov* 4, 840-853.

Coschi, C.H., Martens, A.L., Ritchie, K., Francis, S.M., Chakrabarti, S., Berube, N.G., and Dick, F.A. (2010). Mitotic chromosome condensation mediated by the retinoblastoma protein is tumor-suppressive. *Genes Dev* 24, 1351-1363.

Dyson, N.J. (2016). RB1: a prototype tumor suppressor and an enigma. *Genes Dev* 30, 1492-1502.

Harrigan, J.A., Belotserkovskaya, R., Coates, J., Dimitrova, D.S., Polo, S.E., Bradshaw, C.R., Fraser, P., and Jackson, S.P. (2011). Replication stress induces 53BP1-containing OPT domains in G1 cells. *J Cell Biol* 193, 97-108.

Hernando, E., Nahle, Z., Juan, G., Diaz-Rodriguez, E., Alaminos, M., Hemann, M., Michel, L., Mittal, V., Gerald, W., Benezra, R., *et al.* (2004). Rb inactivation promotes

genomic instability by uncoupling cell cycle progression from mitotic control. *Nature* *430*, 797-802.

Herrera, R.E., Chen, F., and Weinberg, R.A. (1996). Increased histone H1 phosphorylation and relaxed chromatin structure in Rb-deficient fibroblasts. *Proc. Natl. Acad. Sci. USA* *93*, 11510-11515.

Holland, A.J., and Cleveland, D.W. (2012). Losing balance: the origin and impact of aneuploidy in cancer. *EMBO Rep* *13*, 501-514.

Ianari, A., Natale, T., Calo, E., Ferretti, E., Alesse, E., Screpanti, I., Haigis, K., Gulino, A., and Lees, J.A. (2009). Proapoptotic function of the retinoblastoma tumor suppressor protein. *Cancer Cell* *15*, 184-194.

Ishak, C.A., Marshall, A.E., Passos, D.T., White, C.R., Kim, S.J., Cecchini, M.J., Ferwati, S., MacDonald, W.A., Howlett, C.J., Welch, I.D., *et al.* (2016). An RB-EZH2 Complex Mediates Silencing of Repetitive DNA Sequences. *Mol Cell* *64*, 1074-1087.

Jacks, T., Fazeli, A., Schmitt, E.M., Bronson, R.T., Goodell, M.A., and Weinberg, R.A. (1992). Effects of an Rb mutation in the mouse. *Nature* *359*, 295-300.

Jackson, S.P., and Bartek, J. (2009). The DNA-damage response in human biology and disease. *Nature* *461*, 1071-1078.

Longworth, M.S., and Dyson, N.J. (2010). pRb, a local chromatin organizer with global possibilities. *Chromosoma* *119*, 1-11.

Longworth, M.S., Herr, A., Ji, J.Y., and Dyson, N.J. (2008). RBF1 promotes chromatin condensation through a conserved interaction with the Condensin II protein dCAP-D3. *Genes Dev* *22*, 1011-1024.

Lukas, C., Savic, V., Bekker-Jensen, S., Doil, C., Neumann, B., Pedersen, R.S., Grofte, M., Chan, K.L., Hickson, I.D., Bartek, J., *et al.* (2011). 53BP1 nuclear bodies form around DNA lesions generated by mitotic transmission of chromosomes under replication stress. *Nat Cell Biol* *13*, 243-253.

Manning, A.L., and Dyson, N.J. (2012). RB: mitotic implications of a tumour suppressor. *Nat Rev Cancer* *12*, 220-226.

Manning, A.L., Longworth, M.S., and Dyson, N.J. (2010). Loss of pRB causes centromere dysfunction and chromosomal instability. *Genes & development* *24*, 1364-1376.

Manning, A.L., Yazinski, S.A., Nicolay, B., Bryll, A., Zou, L., and Dyson, N.J. (2014). Suppression of Genome Instability in pRB-Deficient Cells by Enhancement of Chromosome Cohesion. *Molecular cell* *53*, 993-1004.

Mendoza-Maldonado, R., Paolinelli, R., Galbiati, L., Giadrossi, S., and Giacca, M. (2010). Interaction of the retinoblastoma protein with Orc1 and its recruitment to human origins of DNA replication. *PLoS One* 5, e13720.

Oeck, S., Malewicz, N.M., Hurst, S., Rudner, J., and Jendrossek, V. (2015). The Focinator - a new open-source tool for high-throughput foci evaluation of DNA damage. *Radiation oncology (London, England)* 10, 163.

Papamichos-Chronakis, M., and Peterson, C.L. (2013). Chromatin and the genome integrity network. *Nat Rev Genet* 14, 62-75.

Ramirez, F., Dundar, F., Diehl, S., Gruning, B.A., and Manke, T. (2014). deepTools: a flexible platform for exploring deep-sequencing data. *Nucleic acids research* 42, W187-191.

Schvartzman, J.M., Duijf, P.H., Sotillo, R., Coker, C., and Benezra, R. (2011). Mad2 is a critical mediator of the chromosome instability observed upon Rb and p53 pathway inhibition. *Cancer Cell* 19, 701-714.

Srinivasan, S.V., Mayhew, C.N., Schwemberger, S., Zagorski, W., and Knudsen, E.S. (2007). RB loss promotes aberrant ploidy by deregulating levels and activity of DNA replication factors. *J Biol Chem* 282, 23867-23877.

Talluri, S., and Dick, F.A. (2012). Regulation of transcription and chromatin structure by pRB: here, there and everywhere. *Cell Cycle* 11, 3189-3198.

Thwaites, M.J., Coschi, C.H., Isaac, C.E., and Dick, F.A. (2016). Cell Synchronization of Mouse Embryonic Fibroblasts. *Methods Mol Biol* 1342, 91-99.

van Harn, T., Foijer, F., van Vugt, M., Banerjee, R., Yang, F., Oostra, A., Joenje, H., and te Riele, H. (2010). Loss of Rb proteins causes genomic instability in the absence of mitogenic signaling. *Genes & development* 24, 1377-1388.

Woodward, J., Taylor, G.C., Soares, D.C., Boyle, S., Sie, D., Read, D., Chathoth, K., Vukovic, M., Tarrats, N., Jamieson, D., *et al.* (2016). Condensin II mutation causes T-cell lymphoma through tissue-specific genome instability. *Genes Dev* 30, 2173-2186.

Yamasaki, L., Jacks, T., Bronson, R., Goillot, E., Harlow, E., and Dyson, N. (1996). Tumor induction and tissue atrophy in mice lacking E2F-1. *Cell* 85, 537-548.

Zheng, L., Flesken-Nikitin, A., Chen, P.L., and Lee, W.H. (2002). Deficiency of Retinoblastoma gene in mouse embryonic stem cells leads to genetic instability. *Cancer Res* 62, 2498-2502.

Chapter 4

4 **Disruption of the CDK-resistant pRB-E2F1 scaffold up-regulates L1 ORF2p, interferon response genes, and shifts tumor spectrum of *Trp53*^{-/-} mice**

4.1 Introduction

Misexpression of endogenous repetitive elements threatens the stability of the host genome through numerous means. To prevent such deleterious effects, host genomes employ epigenetic silencing mechanisms to repress repetitive element activity (Slotkin and Martienssen, 2007). Perturbance of these mechanisms invokes an additional layer of defenses in which endosomal toll-like receptors (TLRs) and cytosolic RIG-I-like receptors (RLRs) detect nucleic acids of foreign origin to initiate an interferon (IFN) response that culls affected cell populations (Shen et al., 2015; Young et al., 2012; Yu et al., 2012). While this cascade is generally utilized upon ectopic viral detection, specific effectors distinguish an endogenous retrovirus (ERV)-specific TLR response. TLR7 ensures production of ERV-specific antibodies, while TLR3 and TLR9 modulate ERV antibody response to propagate a type I IFN response. Mice deficient for these three TLRs succumb to T-cell acute lymphoblastic leukemia (T-ALL) that bear novel ERV re-integrations (Yu et al., 2012).

Studies using epigenetic modifiers have revealed the effect of redundancy on induction of the ERV-specific innate immune response. Observations of repetitive sequence resurrection following radiation or chemotherapy first suggested that genomic insults could suffice to disrupt repetitive sequence silencing (Vabret et al., 2016). Subsequent investigations with epigenetic inhibitors, such as inhibitors of histone de-

acetylases (HDACs) or DNA methyltransferases (DNMTs), identified redundant and non-redundant effectors of repetitive sequence silencing. It became clear that targeted disruption of these effectors could activate the ERV-specific innate immune response in a dose-dependent manner (Chiappinelli et al., 2015; Roulois et al., 2015; Saito et al., 2016). More specifically, alleviation of non-redundant silencing mechanisms enhanced the interferon response (Desai et al., 2017; Leonova et al., 2013). While this IFN response initially serves as a negative selection pressure, constitutive IFN activation becomes antagonistic towards this end, sustaining cell populations that harbour nucleic acids of foreign origin (Vabret et al., 2016). Despite extensive characterization, the mechanisms by which epigenetic effectors target mutually exclusive repeats, and the biological contexts in which they are perturbed to activate the IFN response remain poorly understood.

Recent evidence suggests that common inactivating events in cancer may disrupt chromatin organization at repetitive sequences (Levine et al., 2016). The p53 tumor suppressor protein suppresses retrotransposon expression and transposition through H3K9me3 deposition (Botcheva and McCorkle, 2014; Leonova et al., 2013; Wylie et al., 2015). Recent discovery of pRB-EZH2-mediated H3K27me3 deposition at repetitive elements and specific pRB-Condensin II-mediated mitigation of γ H2AX accumulation at major satellites merits investigation into the effects of alleviating multiple tumor-suppressor based mechanisms of chromatin-organization at repetitive sequences (Ishak et al., 2016). Notably, it remains unknown whether pRB-mediated chromatin organization at repeats presents an opportunity to enhance the immune response through drug-induced

viral mimicry (Roulois et al., 2015). If so, pRB functional status may predict efficacy of clinically relevant epigenetic modulators.

In this study, we investigate whether disruption of pRB-EZH2-mediated silencing through acute epigenetic modulation can suffice to de-repress repetitive elements. We investigate whether cells deficient for this silencing paradigm exhibit evidence of transposition, or evidence of ERV-specific innate immune responses. Finally, we explore the effects of disrupting the CDK-resistant pRB-E2F1 scaffold in a *Trp53*^{-/-} background.

4.2 Experimental Procedures

4.2.1 Cell culture and mouse colonies

Mouse embryonic fibroblasts (MEFs) were generated from E13.5 embryos using standard procedures. Cells were cultured in Dulbecco's modified Eagle's medium (DMEM) supplemented with L-glutamine (2mM), streptomycin (50µg/mL), penicillin (50U/mL), and 10% fetal bovine serum, incubated at 37°C with 5% CO₂. Generation and characterization of *Rb1*^{S/S} mice has been described previously. To ablate p53 expression, *Rb1*^{S/S} mice were crossed into a *Trp53*^{-/-} background in which *Trp53* exons 2-7 are substituted for a Neomycin cassette. The *Trp53*^{-/-} mice were obtained from The Jackson Laboratory. All animals were housed, handled, and analyzed as approved by the Canadian Council on Animal Care.

4.2.2 Determination of protein and RNA expression

Chromatin fractions whole cell extracts were prepared as previously described (Ishak et al., 2016). Antibodies used for Western blots are as follows: Ezh2 (D2C9; Cell Signaling), H3K27me3 (07-449; Millipore), H3K9Ac (06-942; Millipore), H3 (ab1791;

abcam), L1 ORF2p (M-300; Santa Cruz), tubulin (11H10; Cell Signaling), Actin (A2066; SIGMA). RNA was prepared in TRIzol as previously described. Primers used are as follows: Maj_F: GACGACTTGAAAAATGACGAAATC, Maj_R: CATATTCCAGGTCCTTCAGTGTGC, L1 5' UTR_F: CTGCCTTGCAAGAAGAGAGC, L1 5' UTR_R: AGTGCTGCGTTCTGATGATG, IAP LTR_F: CTGACAGCTGTGTTCTAAGTGGTAAACAAA, IAP LTR_R: AGAACACCACAGACCAGAATCTTCTGC.

4.2.3 EZH2 inhibition

In vivo based EZH2 inhibition was performed based upon methods modified from Beguelin *et. al* (2013). Briefly, mice received daily treatments of 150mg/kg/day of GSK343 or vehicle (Captisol) through 100 μ l intraperitoneal injections for 7 consecutive days. Splenocytes were harvested on day 8 for RNA extraction using TRIzol reagent. RNA was reverse transcribed and used for qRT-PCR.

To inhibit EZH2 in MEFs, asynchronously growing P4 MEFs at 50% confluency were treated with GSK343 or vehicle (DMSO) with treatment volumes of 0.1% of total media volume. For the 96-hour treatment course, 10 μ M were treatments were administered every 12 hours. H3K27me3 blots were performed from chromatin fractions of treated cells. For the 48-hour treatment course, treatments of 2.5 μ M or 5 μ M were administered once every 24 hours. L1 ORF2 blots were performed from whole cell extract of treated cells. GSK343 was stored at a stock concentration of 10mM in DMSO at -20°C protected from light.

4.2.4 Retrotransposition Assay

P3 MEFs seeded at 2×10^5 cells / well in a 6-well dish were co-transfected with $1 \mu\text{g}$ of an eGFP-expressing L1 reporter plasmid along with $1 \mu\text{g}$ of a Crimson-expressing plasmid. 24h post-transfection, cells were split 1:3 into 6-well dishes. Three wells per experimental group were harvested 72h post transfection for live-cell flow cytometry to measure Crimson (+) cells as a measure of transfection efficiency. To test TSA sensitive de-repression, MEFs were treated with $2.5 \mu\text{M}$ TSA or vehicle (DMSO) 6d post-transfection. 7d post-transfection, live-cell flow cytometry was conducted to measure eGFP expression as a measure of retrotransposition using a FACSCalibur. Analysis was conducted using FlowJo software. Live cells were gated, and analyzed for Crimson (+) and eGFP (+) signal. Analysis of H2B-GFP-transduced MEFs were used to gate eGFP positive cells. Background signal from untransfected controls was subtracted from all samples, and eGFP signal was normalized to Crimson (+) signal. The following plasmids were used in this study: cep99-gfp-L1SM (gift from Boeke lab, NYU), cep99-gfp-TGF21 (gift from Moran lab, U-M), pEF.myc.ER-E2-Crimson (Addgene), and pBABE-H2B-GFP (Dick lab). See Appendix E for plasmid descriptions.

4.2.5 Expression Microarray

RNA levels were determined by Affymetrix Mouse Gene 1.0 Array as previously described (Ishak et al., 2016). Average RMA expression values of all three replicates per genotype were \log_2 transformed for an ANOVA analysis to determine significant expression changes of 1.5 fold or greater with a p value of 0.05 or less in mutant cells relative to wild-type cells. GeneOntology (GO) analysis on this list of genes yielded GO enrichment scores that were plotted for the top 5 enriched categories. Annotations were

derived from Affymetrix MoGene-1 0-st-v1 Transcript Cluster Annotations, CSV, Release 32.

4.2.6 CD4 CD8 thymocyte quantification

To determine distribution of immature and mature thymocyte populations, thymocytes from 4-6 week old mice were isolated from freshly sacrificed mice, and mashed through a 40 μ m sterile cell strainer in a 10cm dish containing 3-4ml of media. Cells were then isolated, pelleted at 4°C, and incubated 5 minutes in 1x RBC lysis buffer (0.15M NH₄ Cl, 10mM KHCO₃, 0.1mM EDTA) to lyse erythrocytes. Thymocytes were washed twice in 1x PBS, then labeled with fluorescein-conjugated α -CD8, R-phycoerythrin-conjugated α -CD4, 7-AAD, and subjected to flow cytometry analysis to compare thymocyte maturation stage according to expression of CD4 and CD8 surface antigens. Percent viability was measured as proportion of total cells within the ‘live’ gate of count versus 7-AAD plots. CD4 CD8 status was quantified as proportion of total viable cells per quadrant, and then plotted as an average of the same quantification for three animals per genotype. Error bars indicate +/- 1 standard deviation.

4.3 Results

4.3.1 Disruption of the CDK-resistant pRB-E2F1 interaction deregulates L1 ORF2p expression

We sought to identify whether disruption of certain pRB interaction surfaces could permit expression of factors required for endogenous retrotransposition. Western blots of whole cell extracts from proliferating MEFs demonstrate L1 ORF2p misregulation is specific to the *Rb1*^{S/S} mutant, and not sensitive to disruption of pRB-E2F small pocket interactions in *Rb1*^{G/G} cells, or disruption pRB LxCxE binding cleft

interactions in *Rb1^{LL}* cells (Figure 4.1A). This complements previous microarray-based analysis of repetitive element transcript levels across *Rb1* synthetic mutant genotypes (Ishak et al., 2016). Importantly, since both the *Rb1^{SS}* and *Rb1^{LL}* mutants perturb Condensin II recruitment to pericentric satellites, this corroborates attribution of pRB-mediated repeat silencing to EZH2 recruitment rather than interactions with Condensin II.

4.3.2 GSK343 treatment de-represses repetitive elements in MEFs

We sought to determine whether epigenetic modulation could perturb pRB-mediated facultative heterochromatinization of repetitive sequences. Since pRB-mediated silencing is specific to EZH2 recruitment, chemical inhibitors of EZH2 function may recapitulate repetitive element deregulation observed in *Rb1^{SS}* cells. Western blots of chromatin fractions reveal reduced H3K27me3 levels following GSK343 treatment of P4 MEFs every 12 hours for 96 hours (Figure 4.2A). Upon confirmation of activity, GSK343 treatments were modified to identify minimal doses that sufficed to de-repress repeats silenced by H3K27me3 in MEFs. Increasing doses of GSK343 produced modest increases in L1 ORF2p levels in proliferating MEFs, with no overt fluctuations in H3K27me3 levels as measured by western blots (Figures 4.2B and 4.2C).

4.3.3 GSK343 treatment de-represses repetitive elements in splenocytes

Ablation of epigenetic writers results in differential effects on repetitive element silencing based on cell type and developmental stage (Rowe and Trono, 2011). Disruption of pRB-EZH2-mediated silencing resulted in pronounced deregulation of repetitive elements in adult *Rb1^{SS}* splenocytes. To determine whether targeted EZH2

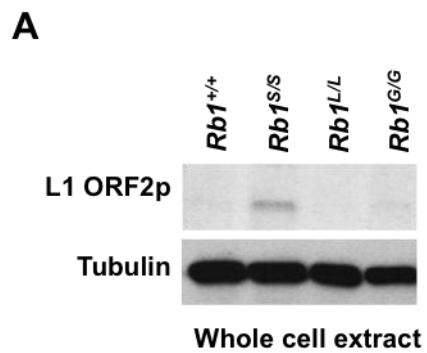


Figure 4.1: Disruption of the CDK-resistant pRB-E2F1 interaction de-represses L1 ORF2p.

(A) Western blots of whole cell extract from asynchronous P4 MEFs of the indicated genotypes demonstrate expression levels of L1 ORF2p, and tubulin as a loading control.

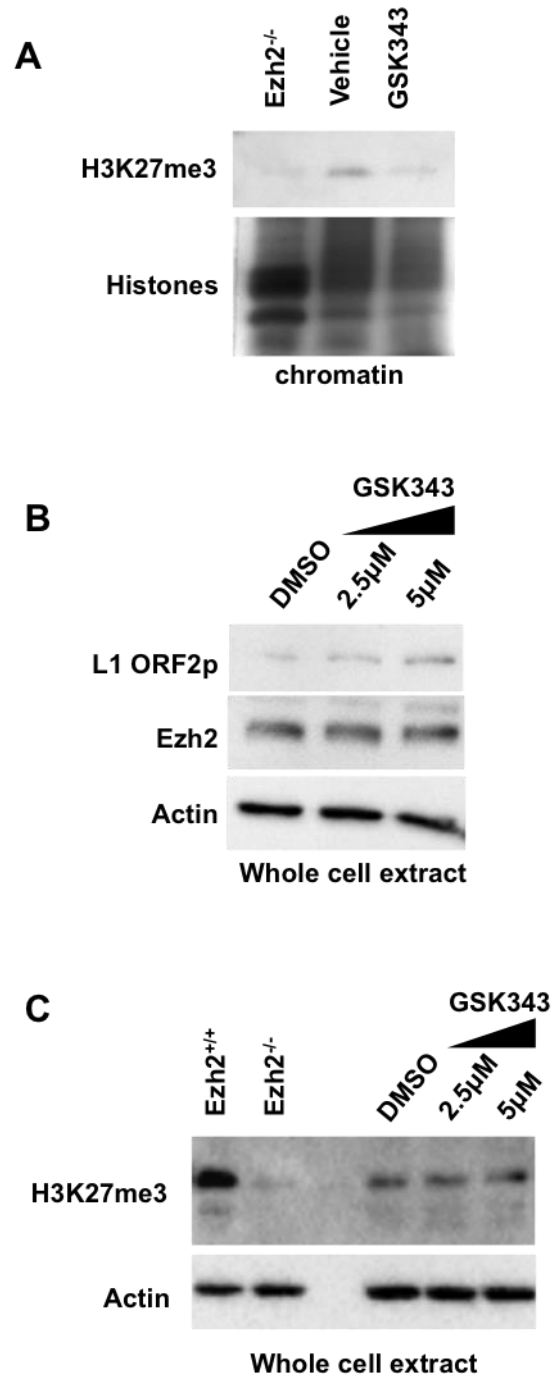


Figure 4.2: GSK343 inhibition of EZH2 de-represses repetitive elements in MEFs.

Figure 4.2: GSK343 inhibition of EZH2 de-represses repetitive elements in MEFs.

(A) Western blot for H3K27me3 from chromatin fractions of asynchronous P4 MEFs treated every 12 hours with 10 μ M of GSK343 or DMSO vehicle for 96 hours total. Coomassie-stained histones serve as a loading control, and chromatin from *Ezh2*^{-/-} MEFs serves as a control for antibody specificity. (B) Western blot for L1 ORF2p, EZH2, and Actin as a loading control from whole cell extracts of asynchronous P4 MEFs treated every 24 hours with with indicated concentrations of GSK343 or DMSO vehicle for 48 hours total. (C) Extracts from (B) blotted for H3K27me3 and Actin along with extract from *Ezh2*^{-/-} MEFs to serve as a control for antibody specificity.

inhibition could recapitulate this effect, wild-type mice received daily treatments of 150mg/kg/day of GSK343 or vehicle through intraperitoneal injections for 7 consecutive days. Splenocytes were harvested on day 8 for RNA extraction (Figure 4.3A). Strikingly, while overt tissue morphology remained unchanged, qRT-PCR revealed elevated levels of major satellites, 5' L1 UTR, and the IAP LTR in splenocytes from GSK343 treated mice only (Figures 4.3B and 4.3C). This demonstrates that acute EZH2 inhibition de-represses repetitive elements in splenocytes.

4.3.4 The CDK-resistant pRB-E2F1 complex suppresses retrotransposition of LINE1 reporters

Amongst the repetitive element families silenced by pRB-EZH2 recruitment, a subset contain members that retain the potential to mobilize throughout the genome. Detection of L1 ORF2p suggests that the components required for endogenous retrotransposition are present in *Rbl^{SS}* cells. To assess retrotransposition in cells deficient for pRB-EZH2 recruitment, we used a previously described assay in which a plasmid borne LINE1 element contains an eGFP reporter in the antisense orientation interrupted by an intron (Figure 4.4A) (Garcia-Perez et al., 2010). Only following expression, splicing, and retrotransposition can eGFP be expressed, thus serving as a read out for *bona fide* mobility of the reporter. Both a naturally occurring LINE1 (L1 Gf) and a synthetic version (L1 SM) exhibited elevated retrotransposition in *Rbl^{SS}* MEFs relative to wild-type cells (Figure 4.4B). In addition to retrotransposition, we also used this assay to analyze silencing of retroelements. Treatment of cells with Trichostatin A (TSA)

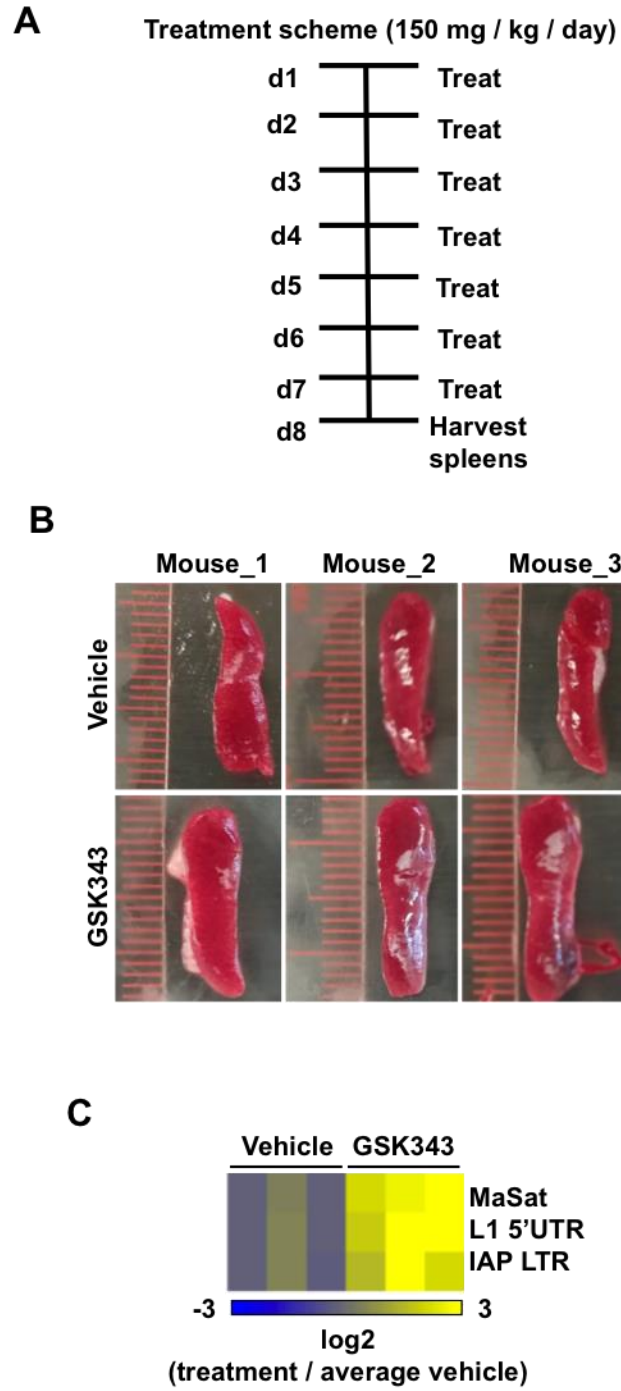


Figure 4.3: GSK343 inhibition of EZH2 de-represses repetitive elements in splenocytes.

Figure 4.3: GSK343 inhibition of EZH2 de-represses repetitive elements in splenocytes.

(A) Treatment scheme illustrates that 6-8 week-old wild-type mice received daily treatments of 150mg/kg/day of GSK343 or volume-matched vehicle for 7 consecutive days. Splenocytes were harvested on day 8. (B) Overt morphology of splenocytes upon necropsy. (C) Heat map of repeat element expression in spleens of treated mice quantified by qRT-PCR. Log₂ ratio of expression is displayed relative to the average of all vehicle-treated mice.

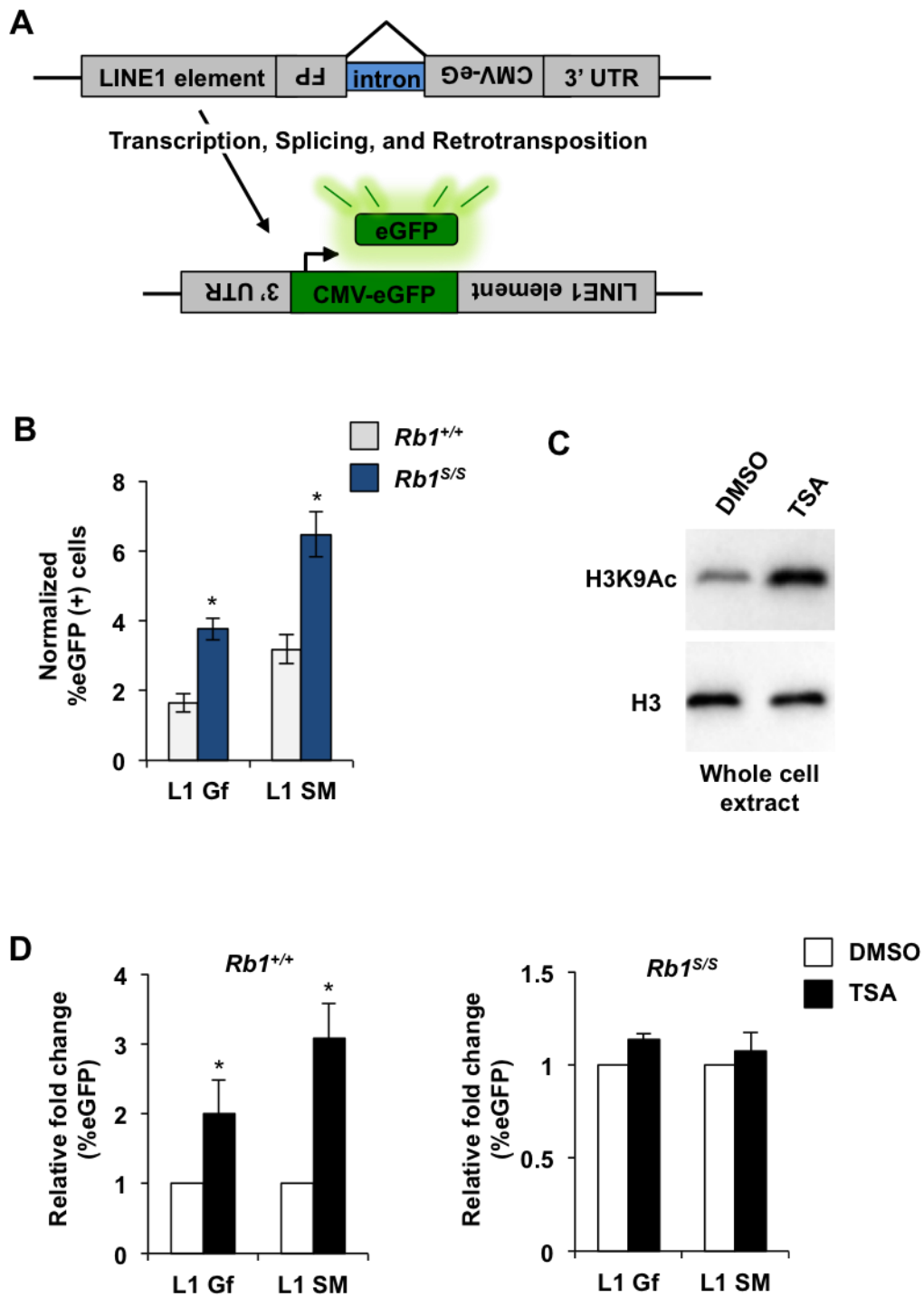


Figure 4.4: pRB suppresses retrotransposition.

Figure 4.4: pRB suppresses retrotransposition.

(A) Retrotransposition assay schematic. LINE1 reporters encode an anti-sense CMV-eGFP marker in the 3'UTR interrupted by an intron in the sense direction. Upon genomic integration, expression, intron splicing, and re-integration, the sense CMV-eGFP is expressed. (B) Percent eGFP positive MEFs per genotype determined by flow cytometry normalized to co-transfected Crimson expression plasmid to provide an unconditionally expressed marker of transfection efficiency. Reporters used encoded endogenous L1 (L1 Gf), and a synthetic L1 (L1 SM) with modified ORFs for optimized expression. Signal measured by live cell flow cytometry. (C) Whole cell extract WB of H3K9Ac, and H3 from MEFs treated 24h with 2.5 μ M TSA or DMSO vehicle. (D) Retrotransposition assay conducted with DMSO vehicle or 2.5 μ M TSA treatment 24h prior to live cell flow cytometry. Percent eGFP positive cells were expressed as fold change relative to vehicle control for each genotype and reporter. Error bars indicate one standard deviation from the mean, an asterisk represents a significant difference from wild type or untreated control ($P \leq 0.05$ using a *t*-test).

inhibits HDAC activity to increase histone acetylation as detected by western blot of H3K9Ac (Figure 4.4C). TSA treatment of reporter-transduced wild type and *Rbl*^{S/S} fibroblasts elevated the abundance of eGFP positive wild type cells, but not *Rbl*^{S/S} mutants (Figure 4.4D). This suggests that retrotransposon expression is fully de-repressed in *Rbl*^{S/S} cells such that TSA dependent de-repression can no longer lead to higher levels of eGFP reporter transposition. Considered together with the elevated levels of retrotransposon reporter events that take place in *Rbl*^{S/S} MEFs, there is a strong likelihood that loss of pRB-EZH2 occupancy and repression of repetitive sequences may be associated with endogenous transposition of mobile repetitive elements.

4.3.5 Disruption of the CDK-resistant pRB-E2F1 interaction activates innate immune components

Cells with perturbed silencing of repetitive sequences exhibit activation of the innate immune response (Roers et al., 2016). To determine transcriptional responses associated with loss of pRB-mediated repetitive element silencing, expression microarrays of arrested *Rbl*^{S/S} MEFs were analyzed (Ishak et al., 2016). Average RMA expression values of all three replicates per genotype were log transformed for an ANOVA analysis to determine significant expression changes of 1.5 fold or greater with a p value of 0.05 or less in mutant cells relative to wild-type cells. GeneOntology (GO) analysis conducted on this list of genes revealed that 3 of the top 5 GO enrichment scores corresponded to categories that were specific to immune responses (Figure 4.5A).

Up-regulated immune targets from this list were curated into tables based upon sensory or responsive roles in the immune response. Analysis of up-regulated sensory components revealed up-regulation of toll like receptors, C-type lectins, and Ig

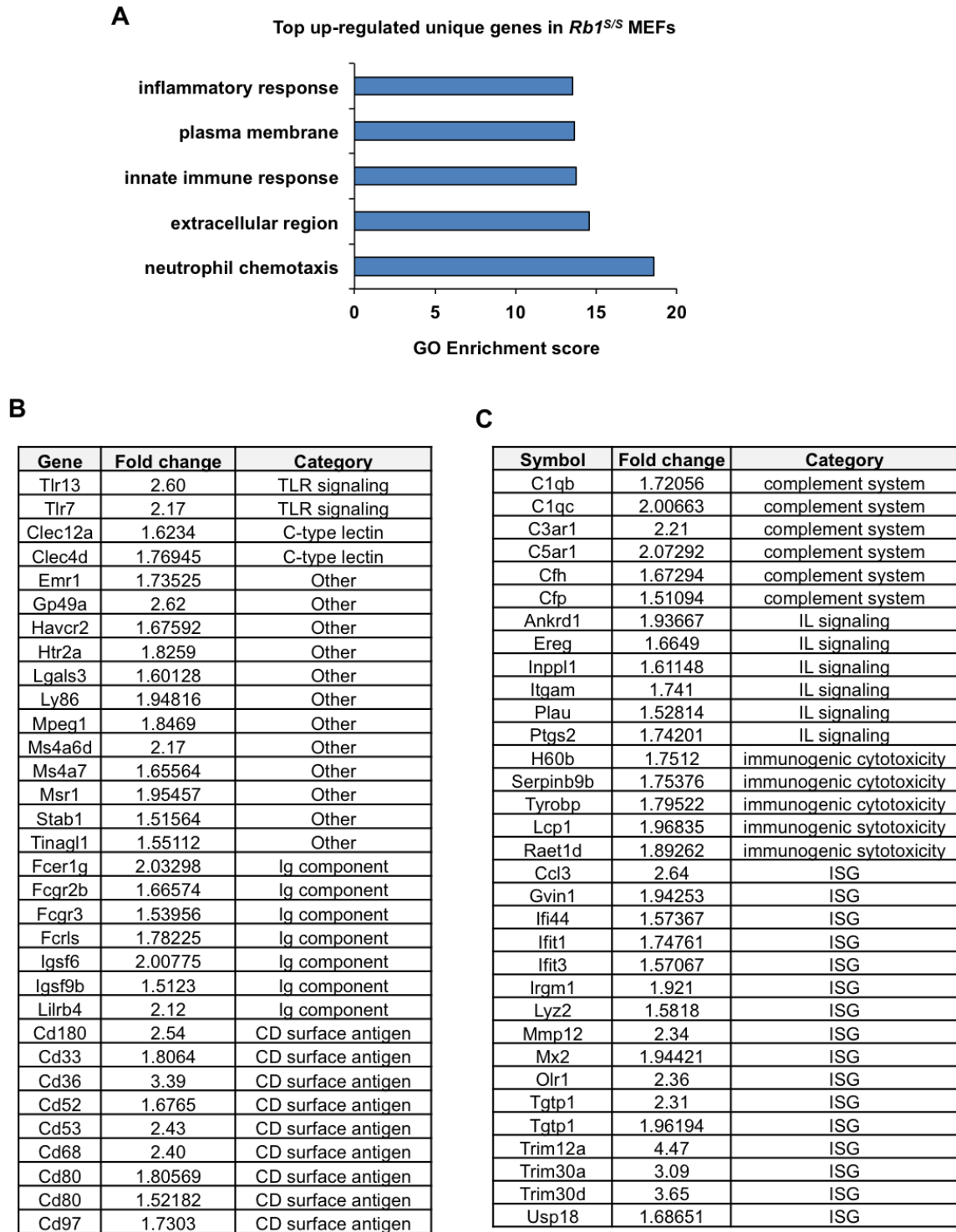


Figure 4.5: Upregulation of innate immune components upon loss of the CDK-resistant pRB-E2F1 interaction

Figure 4.5: Upregulation of innate immune components upon loss of the CDK-resistant pRB-E2F1 interaction.

(A) Average Affymetrix Mouse Gene 1.0 Array RMA expression values of all three replicates per genotype were log₂ transformed for an ANOVA analysis to determine significant expression changes of 1.5 fold or greater with a p value of 0.05 or less in mutant cells relative to wild-type cells. GeneOntology (GO) analysis on this list of genes yielded GO enrichment scores that were plotted for the top 5 enriched categories. (B) Annotations of immune targets from this list were derived from Affymetrix MoGene-1 0-st-v1 Transcript Cluster Annotations, CSV, Release 32 and plotted as tables according to ‘sensory’ functions. (C) Same analysis as (B) with ‘response’ components listed.

components, in addition to surface markers associated with immune cells (Figure 4.5B). Amongst responsive components, Trim proteins exhibited the most pronounced up-regulation, accompanied by other IFN and IL-stimulated cytokines (Figure 4.5C). Interestingly, components of the complement system downstream of antigen recognition were also enriched. Finally, components involved in immunogenic cytotoxicity were also up-regulated. Collectively, this suggests that nucleic acid sensory receptors and IFN stimulated cytokines are active in cells with disrupted pRB-EZH2-mediated repeat silencing.

4.3.6 Disruption of the CDK-resistant pRB-E2F1 interaction does not alter thymocyte maturation

Studies in embryonic stem cells demonstrate that p53, like pRB, mediates genome-wide chromatin organization. Specifically, p53 mediates H3K9me3-dependent silencing of repetitive sequences (Wylie et al., 2015). We sought to determine the effects of disrupting multiple tumor suppressor-based chromatin-organizing mechanisms. *Trp53*^{-/-} mice predominantly succumb to thymic lymphomas (Jacks et al., 1994). However, the roles of E2F1 in thymocyte apoptosis may present a potential confounding variable to any alterations in tumor phenotypes.

E2f1^{-/-} thymocytes exhibit attenuated apoptosis during negative selection as measured by CD4/CD8 surface markers (Field et al., 1996). As thymocytes mature, they progress sequentially from CD4/CD8 double negative, to double positive, and finally single positive status following selection. Elevated levels of single-positive *E2f1*^{-/-} thymocytes underscore the role of E2F1 as a pro-apoptotic transcription factor, and complement their resistance to etoposide-induced apoptosis (Field et al., 1996; Lin et al.,

2001). If pRB represses E2F1-induced apoptosis through the CDK-resistant interaction, then *Rb1^{S/S}* thymocytes may exhibit increased sensitivity to pro-apoptotic stimuli, and thus, delay or ablate onset of thymic lymphomas within a *Trp53^{-/-}* background.

To assess potential alterations in thymocyte negative selection, freshly harvested thymocytes from 4-6 week old wild-type and *Rb1^{S/S}* mice were stained for CD4/CD8 to measure thymocyte proportions per maturation stage, and 7-AAD to measure thymocyte viability. No significant differences in total viability or thymocyte maturation were noted from this analysis, suggesting that any potential differences in thymic lymphoma development within a *Trp53^{-/-}* background could not be attributed to intrinsic developmental alterations (Figures 4.6A, 4.6B and 4.6C).

4.3.7 Disruption of the CDK-resistant pRB-E2F1 complex decreases tumor-free survival of *Trp53^{-/-}* mice.

Since *TP53* inactivating mutations often accompany *RBI* inactivation in human cancers, *Trp53^{-/-}* mice were crossed with *Rb1^S* mice, and offspring were aged until animal protocol endpoints, upon which they were subjected to necropsies with portions of samples fixed for histological analysis, and the remaining sample portions frozen. Within a *Trp53^{-/-}* background, *Rb1^{S/S}* mice all succumb to tumors with decreased tumor latency relative to *Rb1^{+/+}* controls ($p = 0.032$) (Figure 4.7A). Consistent with previous studies, *Rb1^{+/+}; Trp53^{-/-}* mice predominantly succumb to thymic lymphomas or sarcomas (Figure 4.4B) (Jacks et al., 1994). A subset of *Rb1^{S/S}; Trp53^{-/-}* mice presented with lymphomas in the spleen, or axial lymph nodes, or mesenteric lymph nodes (Figures 4.7B and 4.7C). Beyond lymphomas and sarcomas, a lung adenocarcinoma and a malignant papillary

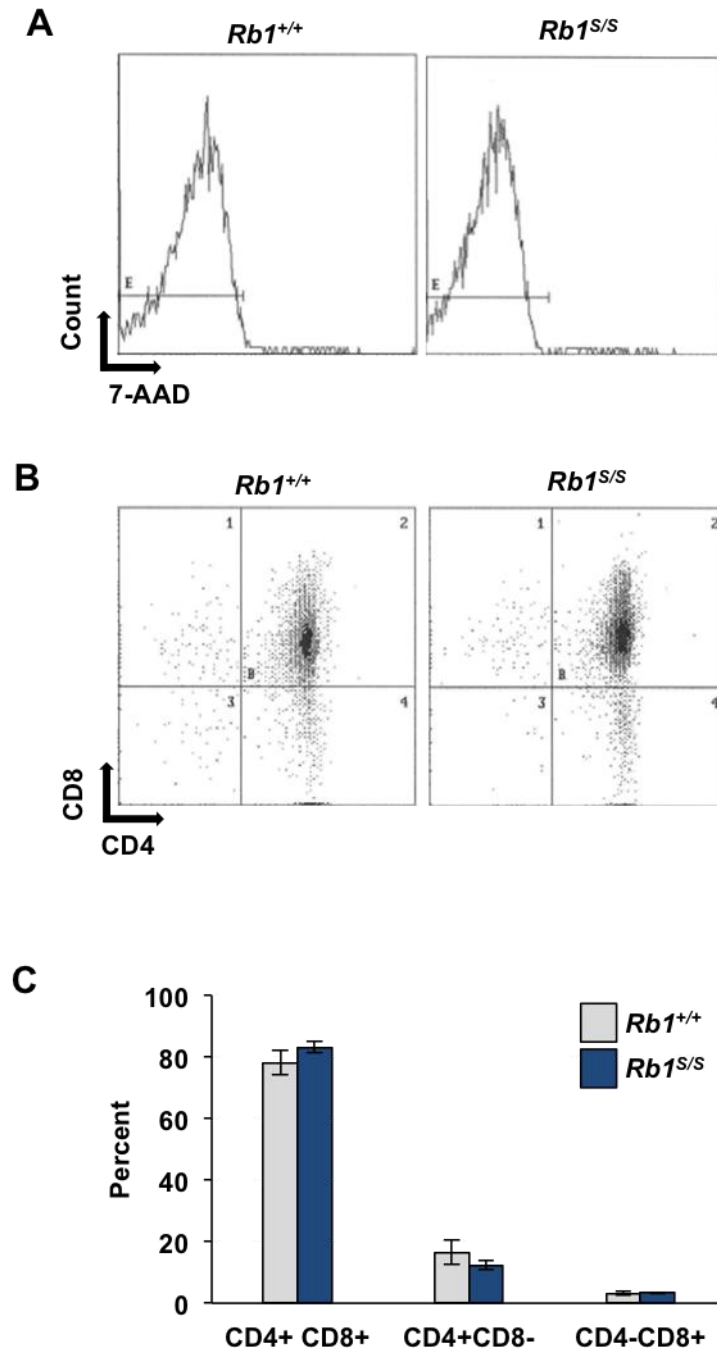


Figure 4.6: Disruption of the CDK-resistant pRB-E2F1 interaction does not alter thymocyte maturation.

Figure 4.6: Disruption of the CDK-resistant pRB-E2F1 interaction does not alter thymocyte maturation.

A) Freshly harvested thymocytes from 4-6 week-old mice were stained and subjected to live-cell flow cytometry analysis. Percent viability was measured as proportion of total thymocytes within the 'live' gate of count versus 7-AAD plots. (B) Representative CD4 versus CD8 histograms demonstrate gating used to determine positive or negative signal by flow cytometry. (C) Proportion of total viable cells per quadrant plotted as an average of the same quantification for three animals per genotype. Error bars indicate +/- 1 standard deviation.

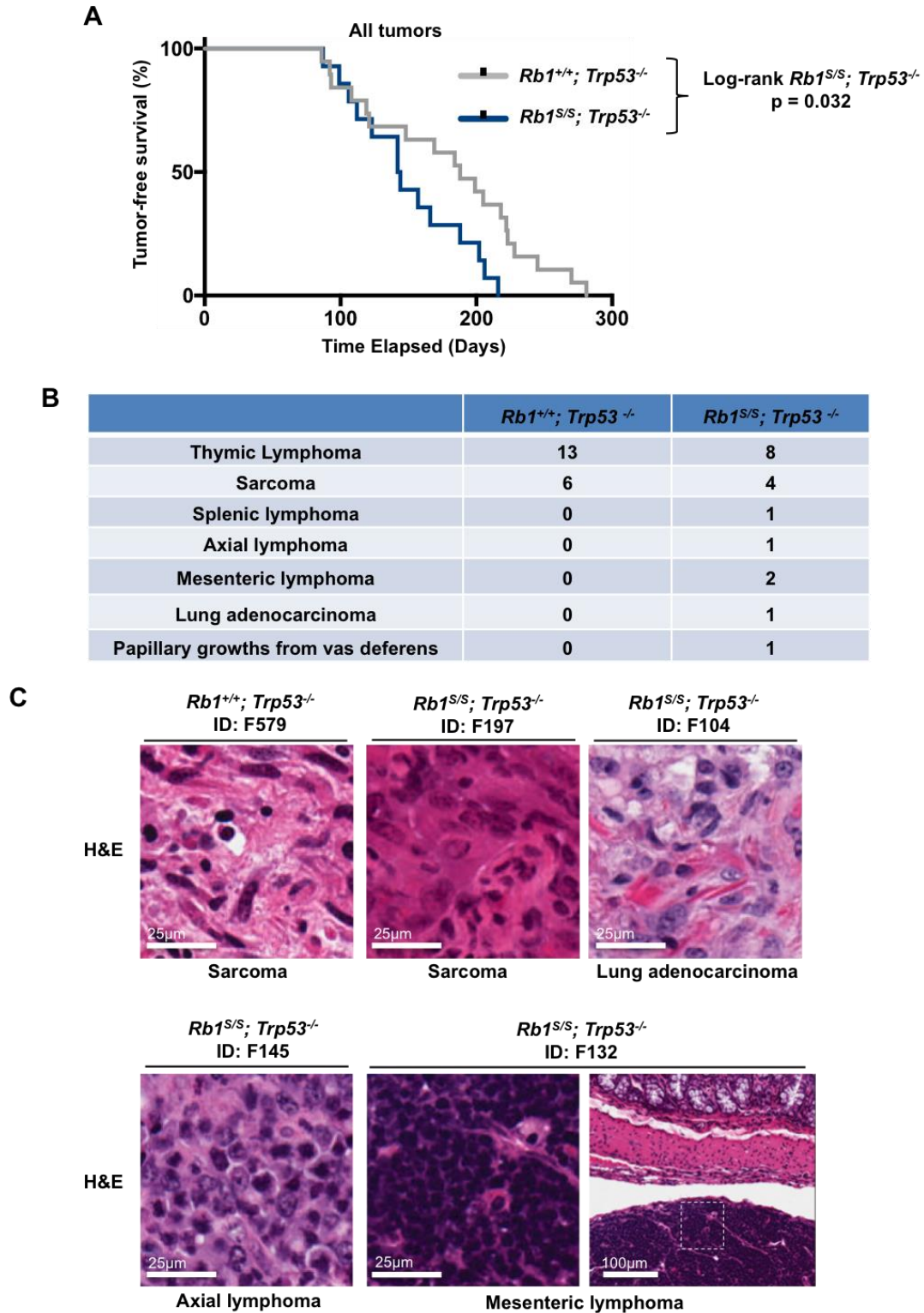


Figure 4.7: Disruption of the CDK-resistant pRB-E2F1 interaction accelerates onset of tumorigenesis in a $Trp53^{-/-}$ background.

Figure 4.7: Disruption of the CDK-resistant pRB-E2F1 interaction accelerates onset of tumorigenesis in a *Trp53*^{-/-} background.

(A) Overall tumor-free survival plotted for *Rb1*^{+/+}; *Trp53*^{-/-} (n = 18) and *Rb1*^{S/S}; *Trp53*^{-/-} mice (n = 13) as Kaplan-Meier curves with log rank test p-value indicated. (B) Table indicates occurrence per tumor type (C) H&E-stained sections exhibit histological characteristics specific to tumor type. Scale is indicated per image. For F132, a white box within an image at a lower magnification indicates the relative location of the adjacent image.

growth from the vas deferens were present amongst the *Rb1^{S/S}; Trp53^{-/-}* cohort (Figures 4.7B and 4.7C).

Since different tumor types confer different latencies to animal protocol endpoints, latency was compared amongst control and mutant animals that succumbed to thymic lymphomas. *Rb1^{S/S}; Trp53^{-/-}* mice that succumbed to thymic lymphomas exhibited a significantly reduced tumor latency relative to *Rb1^{+/+}; Trp53^{-/-}* mice that developed thymic lymphomas ($p = 0.023$) (Figure 4.8A). No differences in overt morphology of thymic lymphomas were noted upon necropsy between cohorts. Mitotic cells were readily apparent upon histological analysis that revealed no pathological differences between thymic lymphomas of compound mutants versus single mutants (Figure 8B).

4.4 Discussion

This chapter explores a number of focused questions to initiate investigations of how the pRB-E2F1 scaffold may be exploited for therapeutic purposes, and how it may contribute to tumorigenesis in combination with p53 ablation. With respect to therapeutic exploitation, we explore whether a clinically relevant epigenetic modulator can alleviate H3K27me3-based repetitive element silencing. Intraperitoneal injections of the EZH2 inhibitor GSK343 sufficed to de-repress repetitive sequences in splenocytes. De-regulation was uniform for all drug treated animals at time of harvesting. In contrast, the response of aged-matched animals is less likely to be synchronized after 6-8 weeks of immune-induced negative selection (Ishak et al., 2016).

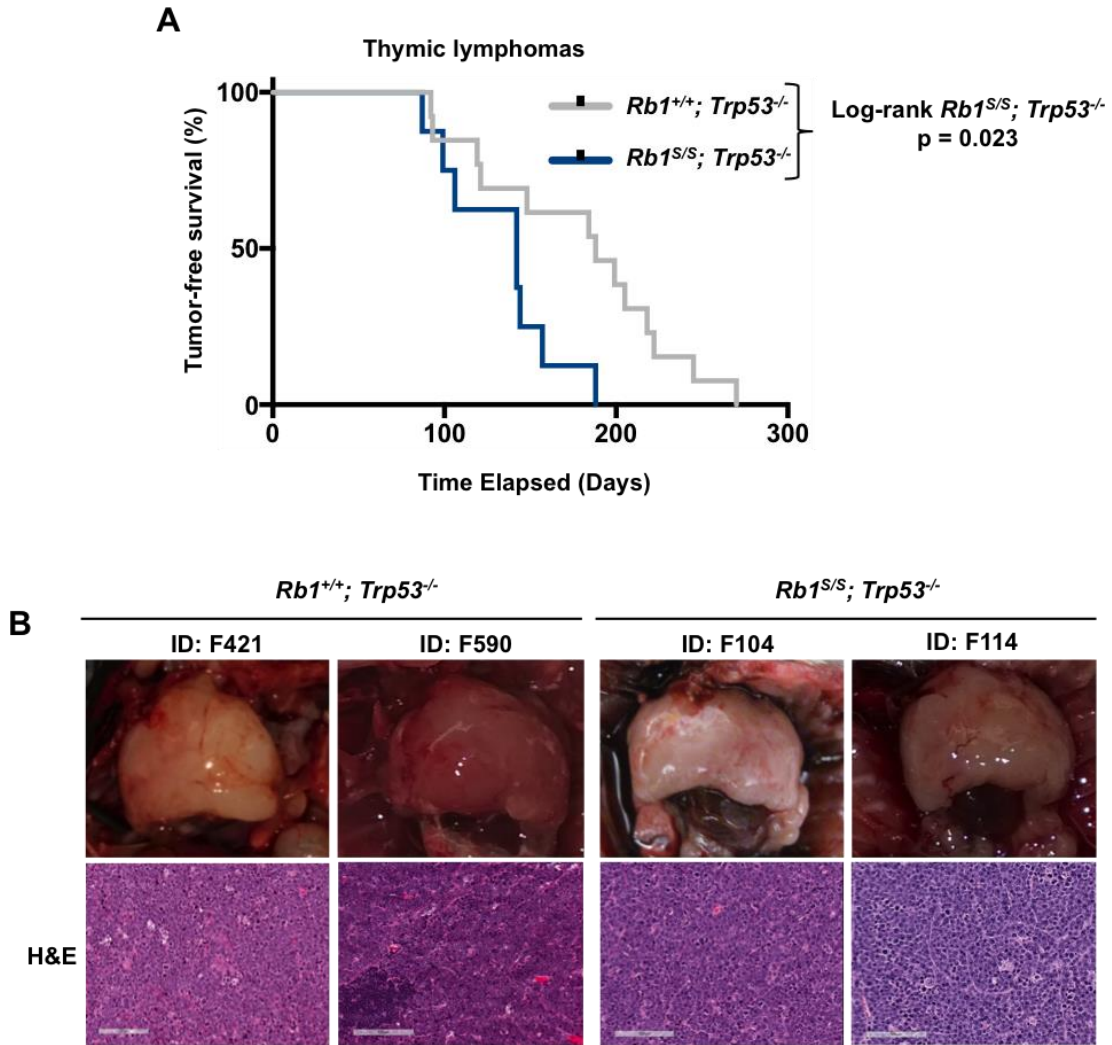


Figure 4.8: Disruption of the CDK-resistant pRB-E2F1 interaction accelerates onset of thymic lymphomas in a $Trp53^{-/-}$ background.

(A) Tumor-free survival of mice that succumbed to thymic lymphomas plotted for $Rb1^{+/+}; Trp53^{-/-}$ (n = 13) and $Rb1^{S/S}; Trp53^{-/-}$ mice (n = 8) as Kaplan-Meier curves with log rank test p-value indicated. (B) Representative images of thymic lymphomas upon necropsy accompanied by corresponding H&E stained sections. Scale bar indicates 100 μ m.

Disruption of repeat-silencing mechanisms may also permit retrotransposition of elements that retain the ability to transpose autonomously. Discovery of L1 ORF2p expression in *Rbl^{S/S}* MEFs suggests that the machinery required for endogenous retrotransposition is present in *Rbl^{S/S}* cells. Further exploration of L1 ORF2p expression in tissues of adult *Rbl^{S/S}* mice may reveal tissue-specific differences in any potential endogenous retrotransposition. Here, a transfection-based eGFP LINE reporter assay was used to assess whether pRB-EZH2-mediated silencing suppressed expression and retrotransposition in wild-type and *Rbl^{S/S}* MEFs. Reporter retrotransposition is silenced in a pRB-dependent manner. Whole genome sequencing will be required to determine whether endogenous LINE retrotransposition can be observed upon alleviation of pRB-repeat association in both experimental models, and human cancers. If so, LINE retrotransposition may be common to cancers with inactivated pRB.

Constitutive disruption of repeat silencing induces an innate immune response that begins with stimulation of endosomal toll-like receptors (TLRs) or cytosolic RIG-I-like receptors that initiate an interferon (IFN) response. Expression microarray analysis of *Rbl^{S/S}* MEFs suggests that such a response may occur in upon disruption of pRB-EZH2-mediated repeat silencing. Upon detection of repetitive transcripts, TLR7 ensures production of ERV-specific antibodies. Indeed TLR7 and immunoglobulin components were amongst the most up-regulated sensory components in mutant MEFs. Downstream of receptor stimulation, TRIM proteins propagate the response to ensure that a host of IFN-stimulated cytokines can respond and induce cytotoxicity to cull the cells if required. Transcriptional targets associated with the immune response in *Rbl^{S/S}* MEFs suggest that this response may be active upon disruption of this silencing paradigm. Accordingly, we

previously report IFN activation in splenocytes of adult *Rb1^{S/S}* MEFs (Ishak et al., 2016). However, assessing such signatures in multiple tissues of GSK343-treated adult mice may reveal additional cell types that may invoke such a response upon disruption of pRB-EZH2-mediated heterochromatinization.

Investigation of p53-deficient cells first revealed that retrotransposition and innate immune responses were sensitive to tumor suppressor-mediated repeat silencing (Leonova et al., 2013; Wylie et al., 2015). Identification of pRB-mediated H3K27me3 deposition at repeats suggested that combinatorial inactivation of both pRB and p53 may exacerbate overall heterochromatinization defects relative to those observed upon inactivation of either tumor suppressor in isolation. To assess whether this was the case, *Rb1^{S/S}* mice were crossed into a *Trp53^{-/-}* background and aged until animal protocol endpoints. Upon necropsy, *Rb1^{S/S}; Trp53^{-/-}* mice presented with a slightly more varied tumor spectrum and an overall decreased tumor latency relative to *Rb1^{+/+}; Trp53^{-/-}* mice. *Trp53^{-/-}* mice predominantly succumb to thymic lymphomas. Compound mutants that developed thymic lymphomas exhibited a significantly reduced latency relative to *Rb1^{+/+}; Trp53^{-/-}* mice. While *Rb1^{S/S}; Trp53^{-/-}* displayed an increase in lymphomas beyond the thymus, *Rb1^{L/L}; Trp53^{-/-}* display an increase in sarcoma incidence. This further distinguishes additional factors that contribute to genome instability in *Rb1^{S/S}* mice beyond disruption of Condensin II-mediated mitotic instability observed in *Rb1^{L/L}* mice. Mechanistic underpinnings of reduced latency may provide insight into yet-unidentified factors that govern tumor evolution in human cancers that lack both pRB and p53.

4.5 References

- Botcheva, K., and McCorkle, S.R. (2014). Cell Context Dependent p53 Genome-Wide Binding Patterns and Enrichment at Repeats. *PLoS ONE* 9, e113492.
- Chiappinelli, K.B., Strissel, P.L., Desrichard, A., Li, H., Henke, C., Akman, B., Hein, A., Rote, N.S., Cope, L.M., Snyder, A., *et al.* (2015). Inhibiting DNA Methylation Causes an Interferon Response in Cancer via dsRNA Including Endogenous Retroviruses. *Cell* 162, 974-986.
- Desai, N., Sajed, D., Arora, K.S., Solovyov, A., Rajurkar, M., Bledsoe, J.R., Sil, S., Amri, R., Tai, E., MacKenzie, O.C., *et al.* (2017). Diverse repetitive element RNA expression defines epigenetic and immunologic features of colon cancer. *JCI Insight* 2.
- Field, S.J., Tsai, F.-Y., Kuo, F., Zubiaga, A.M., Kaelin, J., W.G., Livingston, D.M., Orkin, S.H., and Greenberg, M.E. (1996). E2F-1 functions in mice to promote apoptosis and suppress proliferation. *Cell* 85, 549-561.
- Garcia-Perez, J.L., Morell, M., Scheys, J.O., Kulpa, D.A., Morell, S., Carter, C.C., Hammer, G.D., Collins, K.L., O'Shea, K.S., Menendez, P., *et al.* (2010). Epigenetic silencing of engineered L1 retrotransposition events in human embryonic carcinoma cells. *Nature* 466, 769-773.
- Ishak, C.A., Marshall, A.E., Passos, D.T., White, C.R., Kim, S.J., Cecchini, M.J., Ferwati, S., MacDonald, W.A., Howlett, C.J., Welch, I.D., *et al.* (2016). An RB-EZH2 Complex Mediates Silencing of Repetitive DNA Sequences. *Mol Cell*.
- Jacks, T., Remington, L., Williams, B.O., Schmitt, E.M., Halachmi, S., Bronson, R.T., and Weinberg, R.A. (1994). Tumor spectrum analysis in p53-mutant mice. *Current Biology* 4, 1-7.
- Leonova, K.I., Brodsky, L., Lipchick, B., Pal, M., Novototskaya, L., Chenchik, A.A., Sen, G.C., Komarova, E.A., and Gudkov, A.V. (2013). p53 cooperates with DNA methylation and a suicidal interferon response to maintain epigenetic silencing of repeats and noncoding RNAs. *Proceedings of the National Academy of Sciences* 110, E89-E98.
- Levine, A.J., Ting, D.T., and Greenbaum, B.D. (2016). P53 and the defenses against genome instability caused by transposons and repetitive elements. *BioEssays* 38, 508-513.
- Lin, W.C., Lin, F.T., and Nevins, J.R. (2001). Selective induction of E2F1 in response to DNA damage, mediated by ATM-dependent phosphorylation. *Genes Dev* 15, 1833-1844.
- Roers, A., Hiller, B., and Hornung, V. (2016). Recognition of Endogenous Nucleic Acids by the Innate Immune System. *Immunity* 44, 739-754.
- Roulois, D., Loo Yau, H., Singhania, R., Wang, Y., Danesh, A., Shen, Shu Y., Han, H., Liang, G., Jones, Peter A., Pugh, Trevor J., *et al.* (2015). DNA-Demethylating Agents

Target Colorectal Cancer Cells by Inducing Viral Mimicry by Endogenous Transcripts. *Cell* *162*, 961-973.

Rowe, H.M., and Trono, D. (2011). Dynamic control of endogenous retroviruses during development. *Virology* *411*, 273-287.

Saito, Y., Nakaoka, T., Sakai, K., Muramatsu, T., Toshimitsu, K., Kimura, M., Kanai, T., Sato, T., and Saito, H. (2016). Inhibition of DNA Methylation Suppresses Intestinal Tumor Organoids by Inducing an Anti-Viral Response. *Scientific reports* *6*, 25311.

Shen, Yu J., Le Bert, N., Chitre, Anuja A., Koo, Christine X.E., Nga, Xing H., Ho, Samantha S.W., Khatoor, M., Tan, Nikki Y., Ishii, Ken J., and Gasser, S. (2015). Genome-Derived Cytosolic DNA Mediates Type I Interferon-Dependent Rejection of B Cell Lymphoma Cells. *Cell Reports* *11*, 460-473.

Slotkin, R.K., and Martienssen, R. (2007). Transposable elements and the epigenetic regulation of the genome. *Nat Rev Genet* *8*, 272-285.

Vabret, N., Bhardwaj, N., and Greenbaum, B.D. (2016). Sequence-Specific Sensing of Nucleic Acids. *Trends in Immunology*.

Wylie, A., Jones, A.E., D'Brot, A., Lu, W.-J., Kurtz, P., Moran, J.V., Rakheja, D., Chen, K.S., Hammer, R.E., Comerford, S.A., *et al.* (2015). p53 genes function to restrain mobile elements. *Genes & Development*.

Young, G.R., Eksmond, U., Salcedo, R., Alexopoulou, L., Stoye, J.P., and Kassiotis, G. (2012). Resurrection of endogenous retroviruses in antibody-deficient mice. *Nature* *491*, 774-778.

Yu, P., Lübben, W., Slomka, H., Gebler, J., Konert, M., Cai, C., Neubrandt, L., Prazeres da Costa, O., Paul, S., Dehnert, S., *et al.* (2012). Nucleic Acid-Sensing Toll-like Receptors Are Essential for the Control of Endogenous Retrovirus Viremia and ERV-Induced Tumors. *Immunity* *37*, 867-879.

Chapter 5

5 Discussion

5.1 Summary of findings

My thesis investigates mechanistic links between genome integrity and pRB-mediated recruitment of chromatin organizing proteins to repetitive DNA sequences. The work here suggests that the CDK-resistant interaction between the pRB C-terminus and the E2F1 marked box domain establishes a scaffold that facilitates recruitment of multiple chromatin-organizing proteins to repetitive sequences across the genome throughout the cell cycle. The onset of lymphomagenesis evident upon disruption of this pRB-E2F1 interaction suggests that the activities of this complex constitute a previously unappreciated facet of pRB-mediated tumor suppression.

My work in chapter two identifies the enhancer-of-zeste-homologue 2 (EZH2) histone methyl transferase as one such chromatin-modifying protein recruited through this pRB-E2F1 complex. pRB-E2F1 recruit EZH2 to deposit H3K27me3 and silence repetitive elements. Germline disruption of this interaction results in pronounced misexpression of repetitive elements in splenocytes, and lymphomas that arise in the spleen, mesenteric and axial lymph nodes.

In chapter 3, the CDK-resistant scaffold is investigated as a biochemical mechanism that underlies previous observations of pRB-mediated Condensin II recruitment to pericentric heterochromatin. A portion of my investigation into this question was published in *Cancer Discovery* and it is appended to this thesis. I will consider its implications while discussing findings from chapter 3. Chapter 3

demonstrates that disruption of the CDK-resistant pRB-E2F1 interaction coincides with increased γ H2AX, aneuploidy, ppRPA32, and mitotic errors. While these functions are known to be associated with perturbed Condensin II recruitment, chromatin immunoprecipitation experiments demonstrate that γ H2AX appears to be limited to regions co-occupied by pRB-Condensin II and not regions exclusively occupied by pRB-EZH2.

In chapter 4, I explore whether functions of the pRB-E2F1 scaffold provide an opportunity for therapeutic exploitation, and whether these properties direct disease outcomes in combination with other cancer-relevant events that deregulate repetitive elements. My work demonstrates that the EZH2 inhibitor GSK343 derepresses repetitive elements in MEFs and in splenocytes. While acute derepression may be therapeutic, constitutive derepression may permit retrotransposition as determined using LINE reporter assays. Furthermore, disruption of this silencing paradigm through the *Rbl*^S mutation in concert with ablation of p53 expression decreases latency of thymic lymphomas, and increases diversity of tumor spectrum.

Collectively, my work provides a mechanistic link between tumor suppressor inactivation and repetitive element misregulation in cancer. Specifically, cell cycle independent pRB-chromatin association at repetitive regions maintains genome stability through facultative heterochromatinization of repetitive sequences, and recruitment of chromatin-condensing proteins required for fidelity of DNA replication and mitosis. Discovery of this recruitment mechanism suggests a previously unidentified means of therapeutic exploitation of pRB-positive cancers through the use of EZH2 inhibitors. Upon review of the implications of this work, it is apparent that the investigation into the

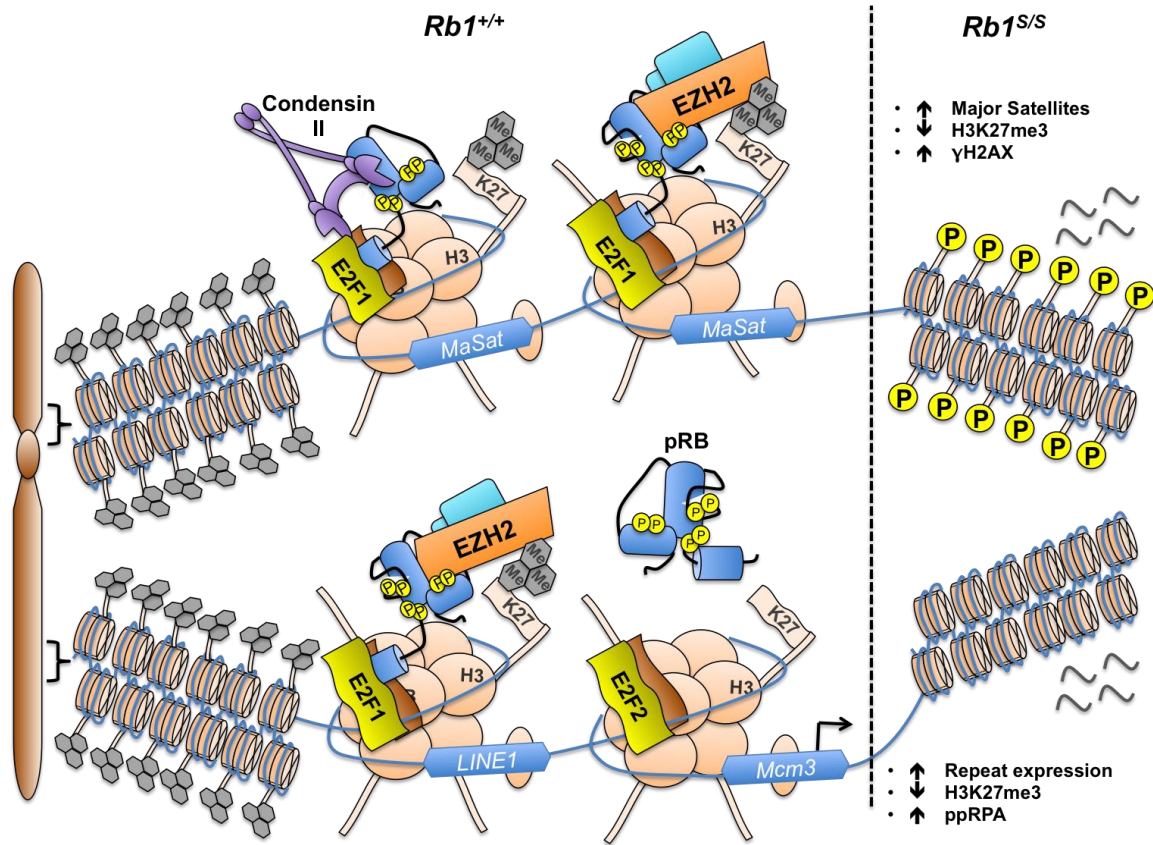


Figure 5.1: The CDK-resistant pRB-E2F1 scaffold recruits chromatin-organizing complexes to repetitive sequences.

The above model of post-G1 pRB-chromatin association depicts CDK-phosphorylated pRB, however whether CDK-phosphorylated pRB associates with repetitive elements endogenously remains to be investigated. The top half of the panel portrays pRB-E2F1-Condensin II complexes at major satellites (MaSat). Loss of this recruitment in *Rb1^{S/S}* mutant cells coincides with increased γ H2AX depicted specifically at major satellites, but not at other repetitive elements that are insensitive to loss of pRB-Condensin II interactions alone. Whether these regions account for increases in ppRPA32 remains to be explored. In addition, pRB-E2F1-EZH2 complexes are illustrated at both a major satellite and a LINE1 element to emphasize the increased repertoire of repetitive sequences occupied by this complex. Loss of pRB-dependent EZH2 recruitment coincides with loss of repressive H3K27me3 and transcriptional activation of both interspersed and tandem repetitive elements that include major satellites, IAP endogenous retroviruses, and LINE1 elements. Post-G1, pRB-E2F1 occupy repetitive sequences while pRB dissociates from E2Fs at cell cycle genes such as *Mcm3* illustrated above.

properties of the pRB-E2F1 scaffold may illuminate answers to long-standing questions in the repetitive element field regarding recruitment of epigenetic effectors to repetitive sequences, host-directed alleviation of repetitive element silencing, and misregulation of silencing associated with mitotic defects and the onset of tumorigenesis.

5.2 The CDK-resistant pRB-E2F1 scaffold recruits multiple complexes to repetitive sequences.

The use of discrete pRB synthetic mutants has permitted elucidation of two distinct pRB-E2F1 complexes. The CDK-resistant pRB-E2F1 scaffold mediates EZH2 recruitment and H3K27me3 deposition at repetitive sequences throughout the genome. In contrast, pRB-E2F1-Condensin II complexes occupy and act upon major satellite sequences, but are not functionally relevant at the L1 5'UTR or IAP LTR. Curiously, disruption of the pRB-E2F1 scaffold resulted in γ H2AX accumulation at repeats regulated by pRB-Condensin II, but not pRB-EZH2 exclusively. The attribution of repetitive element silencing to EZH2 recruitment appears consistent with another synthetic pRB mutant model that is defective for Condensin II recruitment, but does not exhibit deregulation of repetitive sequences. Proliferating *Rb1^{L/L}* MEFs exhibit reduced H4K20me3 at pericentric repeats, and reduced H3K9me3 at cell cycle promoters upon senescence induction, consistent with defective recruitment of HMTs that establish constitutive heterochromatin marks (Isaac et al., 2006; Talluri et al., 2010). In contrast, H3K27me3 levels remain unperturbed at these sites and at *Hox* genes, consistent with proper H3K27me3 levels maintained at *Hox* genes in *Rb1^{S/S}* cells (Talluri et al., 2010). This suggests that H3K27me3 deposition at these regions is likely pRB-independent. Curiously, the *D.melanogaster* CAP-D3 subunit that interacts with the *D.melanogaster*

pRB orthologue Rbf restricts transposon activity (Schuster et al., 2013). This suggests that Condensin II may participate in transposon silencing in mammals, however the means by which this may occur remains unknown, but is likely independent of pRB.

These observations give rise to questions regarding the biochemical properties that distinguish either complex. With respect to assembly, functional expression and epigenetic outputs suggest that pRB-dependent EZH2 recruitment must be independent of the LxCxE binding cleft. Since nuclear extract pulldowns with recombinant GST-RBLP^L exhibit reduced binding to the PRC2 subunit RbAp46, this suggests RbAp46 may not participate in recruitment of EZH2 by pRB (Isaac et al., 2006). Alternatively, RbAp46 may be required for non-PcG HDAC complex recruitment by pRB through the LxCxE binding cleft. Endogenous immunoprecipitations in previous data chapters assess protein-protein interactions or genome occupancy but cannot distinguish whether pRB-mediated EZH2 recruitment is direct or indirect. Furthermore, a minimal region required for this recruitment has yet to be mapped on pRB.

While Condensin II association with pRB has been characterized as LxCxE-dependent, many of the same questions that exist for EZH2 recruitment exist for Condensin II recruitment. Despite extensive characterization, it remains unknown whether interactions between pRB and certain Condensin II subunits are direct or indirect, and which subunits are essential for this interaction. Evidence of a higher-migrating CAP-D3 band that associates with pRB suggests modifications to Condensin II subunits, such as CAP-D3 phosphorylation, may facilitate interaction with pRB. Finally, properties that determine whether pRB-E2F1 will recruit Condensin II or EZH2 remain unknown. Biochemical experiments are required to determine whether this recruitment is

competitive, and whether additional co-factors or post-translational modifications are required to mediate this interaction. Development of pRB synthetic mutants that disrupt EZH2 recruitment and preserve LxCxE interactions will facilitate this endeavor.

5.3 Do E2F-consensus motifs underlie pRB-E2F1 recruitment to repetitive elements?

Occupancy of the CDK-resistant pRB-E2F1 scaffold at a diverse repertoire of repetitive elements begs the question of the molecular basis that underlies repetitive sequence recruitment. Repetitive elements must be recognized by chromatin modifying complexes in order to be silenced, or by transcription factors to serve as alternative promoters or enhancers throughout the host genome. However, mechanisms of repetitive sequence recognition remain poorly understood. Classic mechanisms of promoter-transcription factor dynamics predominantly involve the recognition of a conserved DNA motif or element within the promoter. There is some evidence to suggest that recognition of DNA sequences serves as the recruitment mechanism for a subset of proteins that bind repeats.

For example, retrotransposition assays that utilize fragments of IAPs demonstrate that the presence of the 5'UTR or a 160bp region from the gag-encoding ORF suffice to silence the reporter (Sadic et al., 2015). Certain members of the Krüppel-associated box zinc-finger proteins (KRAB-ZFPs) recognize these sequences within the 5'UTR and *gag* regions (Wolf and Goff, 2009). KRAB-ZFPs harbor varying numbers of zinc finger motifs to confer DNA binding specificity. Divergence amongst these motifs are believed to underlie extensive occupancy of a diverse repertoire of repeats by Cys2-His2 zinc finger (C2H2-ZF) transcription factors that include the KRAB-ZFP members (Najafabadi

et al., 2015). These associations are often found within heterochromatinized repeats, and corroborate mechanistic investigations that conclude KRAB-ZFPs bind TRIM28 and SETDB1 to mediate H3K9me3 of certain repetitive elements (Schmitges et al., 2016).

It appears that other DNA-binding motifs commonly found within transcription factors suffice to mediate sequence-based recognition of repetitive sequences. For example, a partial consensus motif within major satellite subrepeat 2 recognized by the homeodomain of Pax3 is required for Pax3 recruitment and deposition of H3K9me3 and H4K20me3 at pericentric satellites (Bulut-Karslioglu et al., 2012). The p53 transcription factor also associates with repetitive sequences. p53 recognizes DNA as a tetramer in which a DNA binding domain within its ‘core’ region associates with p53 recognition elements (Demir et al., 2017). p53 recognition elements in human ERV LTRs and L1 5'UTRs appear to be mediate p53 recognition (Harris et al., 2009). Paradoxically, *in vitro* reporter assays suggest p53 association with these elements activates transcription, while *in vivo* NGS profiles suggest p53 association establishes repressive heterochromatin at these elements (Wylie et al., 2016).

Investigation of E2F-based mechanisms of DNA recognition provide insights into how an E2F might recruit pocket proteins to repetitive sequences. E2F/DP heterodimers were discovered to recognize and bind the canonical E2F motif 5'TTTC[CG]CGC-3' (Boeuf et al., 1990; Kovesdi et al., 1987; Yee et al., 1987). More recent work suggests that these heterodimers along with atypical E2Fs bind the core sequence 5'-GGCGGG-3' (Jolma et al., 2013). Crystal structures of E2F4/DP2 fragments bound to DNA suggest that a winged-helix fold adopted by the DNA-binding domains of both transcription factors mediates this recognition (Zheng et al., 1999). Subsequent investigations of

atypical E2Fs reveal that the two DNA binding domains of E2F8 adopt an analogous structure upon DNA binding (Morgunova et al., 2015).

Identification of L1 ORF2p expression in MEFs deficient for all three pocket proteins first prompted investigation of E2F recognition of mammalian LINE elements. Investigation of the human L1RP 5'UTR and the murine L1Md-A2 5'UTR identified a stretch of GGCG and CGCG respectively within either 5'UTR. These sequences were considered homologous to the E2F core recognition sequence 5'-GGCGGG-3', and were attributed as the basis of E2F recruitment to these UTRs. ChIP for E2F1 yielded occupancy above IgG background levels when quantified using primers that produced an amplicon >100bp that encompassed this sequence in the L1 5'UTR (Montoya-Durango et al., 2009). However, loss-of-function approaches, such as mutagenesis of this site, were never performed. Thus, the requirement of either sequence for E2F1 occupancy of the L1 5'UTR remains unknown.

In contrast to mammalian studies, investigations in plants conclude that the pRB-E2F network is extensively governed by E2F consensus motifs that are enriched within repetitive elements. Motif enrichment analysis of the *Arabidopsis thaliana* genome indicates that 73% of all E2F recognition sequences (TTssCGssAA) intersect with transposable elements, while overlap is 85% in *Arabidopsis lyrata*. This appears to suggest extensive amplification of E2F recognition sequences through transposable element activity. Notably, analysis of ChIP-seq profiles for histone tail marks reveal that these E2F binding sites within transposable elements exhibit significant enrichment of H3K27me1 (Henaff et al., 2014).

Despite the parallels between these studies and our model of H3K27me3 deposition at repeats through the pRB-E2F1 scaffold, the absence of E2F consensus sequences within pericentric repeats suggests that pRB-E2F1 recognition must be more complex in mammalian systems. Furthermore, the inability of E2F1 to associate with major satellites independent of pRB binding strongly suggests that this association is likely conferred through a structural motif, a post-translational modification, or an interaction with an additional binding partner formed upon E2F1 binding to pRB (See appendix C) (Coschi et al., 2014). This supports electrophoretic mobility shift assay experiments that demonstrate E2F1 bound through the pRB-C-terminus exhibits reduced affinity for a DNA probe that contains the E2F consensus motif (Dick and Dyson, 2003).

Finally, sequence-dependent pRB-repeat recruitment may be mediated through E2F-independent means. Recent studies in murine osteoblasts demonstrate that CDK-phosphorylated pRB occupies the promoter regions of subtelomeric TERRA repeats. Occupancy appears to be dependent on the presence of Retinoblastoma Control Elements (RCEs) that facilitate pRB recruitment through the Sp1 transcription factor. Interestingly, reporter assays demonstrate that pRB positively regulates TERRA expression. Since TERRA forms DNA-RNA hybrids to maintain telomere length, this may be another means by which pRB maintains genome stability (Gonzalez-Vasconcellos et al., 2017). Direct roles of Sp1 in pRB-telomere requirement were not explored in this study (Kim et al., 1992). Beyond E2F1 and Sp1, it remains unknown whether other transcription factors may recruit pRB to repetitive sequences.

5.4 pRB-E2F1 repeat-recruitment independent of E2F consensus motifs?

Recruitment to sites of DNA damage suggests that pRB and E2F1 can be recruited through sequence-independent means throughout the genome (Cook et al., 2015; Vélez-Cruz et al., 2016). Recruitment to sites of DNA damage occurs through step-wise deposition of post-translational modifications that recruit additional epigenetic ‘writers’ that deposit new marks for recruitment of new effectors (Munro et al., 2012). Likewise, heterochromatinization also follows a hierarchical modification and recruitment scheme. At constitutively heterochromatinized regions, H3K9me3 is recognized and bound by HP1. Following this event, SUV4-20H1/2 histone methyltransferases catalyze H4K20me_{2/3} deposition at these regions (Saksouk et al., 2015). The participation of EZH2 in pRB-mediated silencing of repetitive sequences suggests that the pRB-E2F1 scaffold may adhere to the step-wise mechanisms of facultative heterochromatinization that underlie target site recruitment.

Facultative heterochromatin is established through the activity of Polycomb group (PcG) proteins. These proteins were first discovered in *Drosophila melanogaster* as regulators of *Hox* gene expression, and thus, normal development. PcG recruitment in *D.melanogaster* is mediated through sequence recognition of Polycomb response elements (PREs) at target sites (Bauer et al., 2015). However, the lack of PREs that predict polycomb binding in vertebrates suggests that vertebrate PcG recruitment is more complex, and may involve targeting by different co-factors, adaptors, or transcription factors that recognize histone or DNA modifications. PcG-mediated heterochromatin is established through two multi-subunit complexes. Polycomb Repressor Complex 2

methylates lysine 27 of histone H3, while Polycomb Repressor Complex 1 ubiquitylates lysine 119 of histone H2A. The interplay between these two activities has provided a foundation to explore PcG recruitment mechanisms (Margueron and Reinberg, 2011).

Early models of PcG activity suggested that H3K27me3 deposition by EZH2 or EZH1 of the PRC2 complex is recognized and bound by the PRC1 complex. Following recruitment, the RING1A or RING1B ubiquitin E3 ligases of the PRC1 complex ubiquitylate H2AK119 (Margueron et al., 2008). However, this model is challenged by recent discoveries of PRC1-mediated H2AK119Ub1 that precedes and recruits PRC2 to permit H3K27me3 deposition (Cooper et al., 2014). Following deposition, H3K27me3 recognition by EED permits PRC2-mediated H3K27me3 spreading independent of nucleation mechanisms (van der Vlag and Otte, 1999). The interplay with PRC1 remains unexplored in our model of pRB-mediated PRC2 recruitment to repetitive sequences. PRC1-mediated ubiquitylation at repetitive sequences remains relatively unexplored. However, if H2AK119Ub1 levels remain unperturbed at repetitive elements in *Rbl^{SS}* MEFs, then E2F1-pRB-EZH2 recruitment may be mediated through recognition of H2AK119Ub1. Conversely, reduced H2AK119Ub1 at repetitive elements in *Rbl^{SS}* MEFs would suggest a model of PRC2-based recruitment of PRC1 to repetitive sequences.

PcG proteins also recognize modifications that neither PRC complex deposits. For instance, the tudor domains of the substoichiometric PRC2 subunits PCL1, PCL2, and PCL3 recognize and bind H3K36me3. In addition to histone methylation, enrichment of CpG islands at regions of PcG occupancy suggests DNA methylation may recruit PcGs as well (Entrevan et al., 2016). This presents another means by which pRB-E2Fs may alter facultative heterochromatinization at repeats. Multiple E2Fs along with DP1 and

pRB have been discovered in certain PRC1 complexes within human polycomb interactome datasets (Hauri et al., 2016). If the GC-rich sequences at PcG-occupied CpG islands are recognized as E2F ‘core’ sequences, then disruption of the CDK-resistant pRB-E2F1 interaction may disrupt PRC1 recruitment in addition to PRC2 recruitment.

PcG recruitment dynamics may explain pRB-E2F1 recruitment to repetitive sequences, but exclusion of pRB-Condensin II from the L1 5'UTR and IAP LTR suggest that differential recruitment mechanisms act on different pRB-E2F1 complexes. Comparison of genome wide occupancy patterns for PcG and Condensin components will reveal the extent of this apparent mutually exclusive occupancy. If PcG components direct E2F1-pRB-EZH2 recruitment, Condensin subunits may direct E2F1-pRB-Condensin II recruitment. ESC ChIP-seq profiles for non-SMC subunits of Condensin II suggest that Condensin II localizes to promoters and enhancers in addition to pericentric repeats (Downen et al., 2013). Analysis of occupancy profiles has yet to yield a cis-regulatory motif that predicts Condensin association. Thus, *in vivo* recruitment of E2F1-pRB-Condensin localization is likely mediated through additional mechanisms beyond sequence recognition.

5.5 pRB-E2F1 functions may underlie phenotypes associated with both regulated and unregulated repetitive element reactivation

Repetitive elements are repressed through mechanisms that function cooperatively to maintain silencing throughout fluctuations in developmental or cell cycle stage. However, host genomes alleviate these mechanisms to permit repetitive element activation under certain conditions. For example, under conditions of environmental

stress, bursts of transposon activity serve as a means to increase genetic diversity within a gene pool of individuals with low genetic diversity (Rowe and Trono, 2011). The means by which stress signals propagate to epigenetic effectors that silence repeats remains unknown. In this regard, effectors of the stress response should be surveyed as possible candidates to dissociate the CDK-resistant pRB-E2F1 scaffold. Residues within the minimal interaction C-terminal interaction domain on pRB or the marked-box domain of E2F1 should be investigated for potential modifications imposed by stress response effectors. The identified dissociation mechanism should then be investigated as a means of pRB misregulation and repetitive element activation in human cancers.

Identification of how pRB-E2F1 recognizes repetitive sequences may also reveal whether pRB functions may underlie chromosome segregation defects that recur regardless of how repeat silencing is perturbed. Currently, the mechanisms that underlie these errors remain unknown. However, if DNA or histone modifications mediate pRB-Condensin II recruitment to pericentric heterochromatin, then cells with defective constitutive heterochromatinization of repeats may exhibit reduced pRB-Condensin II recruitment. Thus, pRB-Condensin II recruitment and mitotic regulation should be investigated in cells that lack mutations in *RBI* or Condensin subunits, but exhibit repetitive element mis-expression along with mitotic defects.

5.6 Exploitation of pRB functions at repetitive elements

Beyond epigenetic repression, the innate immune system serves as a form of ‘responsive’ repeat silencing (Vabret et al., 2016). This response is predominantly characterized within the context of ectopic viral infection, in which nucleic acids of

foreign origin are detected by endosomal toll-like receptors (TLRs) and cytosolic RIG-I-like receptors that initiate an interferon (IFN) response (Shen et al., 2015; Young et al., 2012; Yu et al., 2012).

Amongst endosomal pattern recognition receptors, TLR3, TLR7, TLR8, TLR9, and TLR13 sense different nucleic acids that have been endocytosed or phagocytosed (Vabret et al., 2016). TLR3 recognizes dsRNA, TLR7 and TLR8 generally recognize ssRNA, while TLR9 recognizes bacterial and viral ssDNA with unmethylated CpG regions (Jiménez-Dalmaroni et al., 2016). Specific endosomal receptors mediate the endogenous retrovirus (ERV)-specific response. TLR7 ensures production of ERV-specific antibodies, while TLR3 and TLR9 modulate ERV antibody response to propagate a type I IFN response. Mice deficient for TLR3, TLR7, and TLR9 succumb to T-cell acute lymphoblastic leukemias (T-ALL) that bear novel ERV re-integrations (Yu et al., 2012). Stimulation of these TLRs activates a type I IFN response that may result in immunogenic cell death.

The cytosolic RIG-I-like receptors (RLRs) RIG-I, MDA5, and LGP2 also contribute to nucleic acid sensory pathways that activate the innate immune response (Schlee and Hartmann, 2016). Upon detection of dsRNA, these pattern recognition receptors activate mitochondrial antiviral-signalling protein (MAVS) that induces nuclear localization of IFN regulatory factor 7 (IRF7) to initiate a type III IFN response. This response acts upon both ectopic and endogenous retroviruses. Following alleviation of DNA methylation at repetitive elements, transcripts from de-repressed endogenous retroviruses stimulate RIG-I and MDA5 that then signal through MAVS and IRF7 to a type III IFN response.

Analogous to TLR-induced IFN responses, RLR-induced IFN responses may cause immunogenic cell death (Roers et al., 2016).

The ability to induce immunogenic cell death upon activation of endogenous retroviruses presents an emerging strategy that uses epigenetic modulation as an immune enhancing therapy (Minn, 2015). This strategy, coined as ‘viral mimicry’, has been most extensively characterized within the context of DNMT inhibition. In human and murine cells, the FDA-approved DNMT inhibitor 5-aza-cytidine suffices to de-repress repetitive elements which are detected by cytosolic RIG-I-like receptors that induce an interferon response (Leonova et al., 2013). This response has been observed in human cells derived from colorectal cancers, ovarian cancers, promyelocytic leukemia, hepatocellular carcinomas, breast cancer, and in human intestinal tumor organoid models (Chiappinelli et al., 2015; Desai et al., 2017; Liu et al., 2016; Roulois et al., 2015; Saito et al., 2016).

Characterization of viral mimicry has revealed that induction of the IFN response is sensitive to a threshold of repetitive element misregulation. Cells that exhibit some degree of repetitive element expression succumb to immunogenic cell death with relatively lower doses of 5-aza-cytidine compared to cells with proper repression of repetitive sequences. For example, p53-deficient cells and cancers exhibit increased expression of repetitive elements, and increased sensitivity to lower doses of 5-aza-cytidine relative to p53-positive cells (Desai et al., 2017; Leonova et al., 2013). This is of particular clinical significance upon consideration of emerging mechanisms of tumor-suppressor based silencing of repetitive elements that include ATRX-mediated H3.3 deposition in addition to p53-mediated H3K9me3 deposition (Sadic et al., 2015; Wylie et al., 2015).

Identification of pRB-EZH2-dependent facultative heterochromatinization suggests that EZH2 inhibitors may be a yet-unidentified means of inducing viral mimicry. Indeed, my work in chapter 4 demonstrates that EZH2 inhibition through GSK343 treatment suffices to deregulate repetitive elements in wild-type MEFs and splenocytes. The next steps may be to characterize whether an IFN response is induced, and if so, whether induction is more efficient in cells with perturbed silencing of repetitive elements as a result of combinatorial treatments with chemotherapy, radiation therapy, or DNMT inhibitors. The observations from this work will determine whether tumor suppressor status may predict efficacy of viral mimicry induced from epigenetic modulators. Specifically, *RBI*-positive cancers may serve as ideal candidates for EZH2 inhibition.

In contrast to viral mimicry induced upon acute ablation of silencing, sustained deregulation of repetitive elements promotes genome instability and proves advantageous towards tumorigenesis. Independent of the mutagenic effects of endogenous retrotransposition, constitutive IFN activation gradually becomes immunosuppressive, and is associated with cancer cell resistance to chemotherapy and radiation therapy (Kassiotis and Stoye, 2016). If tumor suppressor inactivation misregulates repetitive elements, then the potentially mutagenic and immunosuppressive consequences may be underappreciated drivers of clonal evolution and overall disease outcomes. To assess whether this was the effect, *Rb1^S* mice were crossed into a *Trp53^{-/-}* background. Decreased tumor latency and a modest increase in tumor spectrum in *Rb1^{S/S};Trp53^{-/-}* relative to *Rb1^{+/+};Trp53^{-/-}* mice merit further investigation into whether a net increase in repetitive element misregulation underlies potentially increased genome instability in relevant cell-of-origin populations. The results of this work may suggest further

investigations into whether transcriptional signatures of active repetitive elements and the associated IFN response are a general property of all pRB-deficient human cancers.

5.7 Summary of pRB-E2F1 functions at repetitive elements

In summary, the work presented in this thesis represents a significant contribution towards the elucidation of pRB functions at repetitive regions of the genome. My characterization of altered pRB-E2F1 recognition dynamics at major satellites presented in appendix C initiated investigation into whether this altered recognition conferred recruitment of the CDK-resistant pRB-E2F1 complex to other repetitive elements. This investigation revealed that the pRB-E2F1 scaffold mediates recruitment of multiple chromatin regulatory proteins to repetitive sequences throughout the genome. pRB recruits EZH2 to deposit H3K27me₃ to silence repetitive elements genome wide. In addition to EZH2, pRB recruits Condensin II to major satellites to facilitate proper replication and mitotic progression. Loss of the CDK-resistant pRB-E2F1 scaffold precedes the onset of genome instability and lymphomagenesis.

This work also reveals new questions stated throughout this discussion that concern distinguishing the biochemical properties of multiple complexes that utilize the CDK-resistant pRB-E2F1 scaffold, and the recognition mechanism that underlies recruitment to repetitive sequences. In addition to these questions, future work should continue from the initial investigations presented in Chapter 4 that explore how loss of this regulatory paradigm affects tumor outcomes in a *Trp53*^{-/-} background, and whether the functions of pRB at repetitive elements prove relevant towards predicting efficacy of EZH2 inhibition in human cancers.

5.8 References

- Bauer, M., Trupke, J., and Ringrose, L. (2015). The quest for mammalian Polycomb response elements: are we there yet? *Chromosoma*.
- Boeuf, H., Reimund, B., Jansen-Durr, P., and Kédinger, C. (1990). Differential activation of the E2F transcription factor by the adenovirus E1a and E1V products in F9 cells. *Proceedings of the National Academy of Sciences of the United States of America* *87*, 1782-1786.
- Bulut-Karslioglu, A., Perrera, V., Scaranaro, M., de la Rosa-Velazquez, I.A., van de Nobelen, S., Shukeir, N., Popow, J., Gerle, B., Opravil, S., Pagani, M., *et al.* (2012). A transcription factor–based mechanism for mouse heterochromatin formation. *Nature structural & molecular biology* *19*, 1023-1030.
- Chiappinelli, K.B., Strissel, P.L., Desrichard, A., Li, H., Henke, C., Akman, B., Hein, A., Rote, N.S., Cope, L.M., Snyder, A., *et al.* (2015). Inhibiting DNA Methylation Causes an Interferon Response in Cancer via dsRNA Including Endogenous Retroviruses. *Cell* *162*, 974-986.
- Cook, R., Zoumpoulidou, G., Luczynski, M.T., Rieger, S., Moquet, J., Spanswick, V.J., Hartley, J.A., Rothkamm, K., Huang, P.H., and Mittnacht, S. (2015). Direct Involvement of Retinoblastoma Family Proteins in DNA Repair by Non-homologous End-Joining. *Cell Rep* *10*, 2006-2018.
- Cooper, S., Dienstbier, M., Hassan, R., Schermelleh, L., Sharif, J., Blackledge, N.P., De Marco, V., Elderkin, S., Koseki, H., Klose, R., *et al.* (2014). Targeting polycomb to pericentric heterochromatin in embryonic stem cells reveals a role for H2AK119u1 in PRC2 recruitment. *Cell Rep* *7*, 1456-1470.
- Coschi, C.H., Ishak, C.A., Gallo, D., Marshall, A., Talluri, S., Wang, J., Cecchini, M.J., Martens, A.L., Percy, V., Welch, I., *et al.* (2014). Haploinsufficiency of an RB–E2F1–Condensin II Complex Leads to Aberrant Replication and Aneuploidy. *Cancer Discovery* *4*, 840-853.
- Demir, O., Jeong, P.U., and Amaro, R.E. (2017). Full-length p53 tetramer bound to DNA and its quaternary dynamics. *Oncogene* *36*, 1451-1460.
- Desai, N., Sajed, D., Arora, K.S., Solovyov, A., Rajurkar, M., Bledsoe, J.R., Sil, S., Amri, R., Tai, E., MacKenzie, O.C., *et al.* (2017). Diverse repetitive element RNA expression defines epigenetic and immunologic features of colon cancer. *JCI Insight* *2*.
- Dick, F.A., and Dyson, N. (2003). pRB Contains an E2F1 Specific Binding Domain that Allows E2F1 Induced Apoptosis to be Regulated Separately from other E2F Activities. *Mol Cell* *12*, 639-649.
- Downen, Jill M., Bilodeau, S., Orlando, David A., Hübner, Michael R., Abraham, Brian J., Spector, David L., and Young, Richard A. (2013). Multiple Structural Maintenance of

Chromosome Complexes at Transcriptional Regulatory Elements. *Stem Cell Reports* 1, 371-378.

Entrevan, M., Schuettengruber, B., and Cavalli, G. (2016). Regulation of Genome Architecture and Function by Polycomb Proteins. *Trends in Cell Biology* 26, 511-525.

Gonzalez-Vasconcellos, I., Schneider, R., Anastasov, N., Alonso-Rodriguez, S., Sanli-Bonazzi, B., Fernández, J.L., and Atkinson, M.J. (2017). The Rb1 tumour suppressor gene modifies telomeric chromatin architecture by regulating TERRA expression. *Scientific reports* 7, 42056.

Harris, C.R., DeWan, A., Zupnick, A., Normart, R., Gabriel, A., Prives, C., Levine, A.J., and Hoh, J. (2009). p53 responsive elements in human retrotransposons. *Oncogene* 28, 3857-3865.

Hauri, S., Comoglio, F., Seimiya, M., Gerstung, M., Glatter, T., Hansen, K., Aebersold, R., Paro, R., Gstaiger, M., and Beisel, C. (2016). A High-Density Map for Navigating the Human Polycomb Complexome. *Cell Reports* 17, 583-595.

Henaff, E., Vives, C., Desvoyes, B., Chaurasia, A., Payet, J., Gutierrez, C., and Casacuberta, J.M. (2014). Extensive amplification of the E2F transcription factor binding sites by transposons during evolution of Brassica species. *Plant J* 77, 852-862.

Isaac, C.E., Francis, S.M., Martens, A.L., Julian, L.M., Seifried, L.A., Erdmann, N., Binne, U.K., Harrington, L., Sicinski, P., Berube, N.G., *et al.* (2006). The retinoblastoma protein regulates pericentric heterochromatin. *Mol Cell Biol* 26, 3659-3671.

Jiménez-Dalmaroni, M.J., Gerswhin, M.E., and Adamopoulos, I.E. (2016). The critical role of toll-like receptors — From microbial recognition to autoimmunity: A comprehensive review. *Autoimmunity Reviews* 15, 1-8.

Jolma, A., Yan, J., Whittington, T., Toivonen, J., Nitta, Kazuhiro R., Rastas, P., Morgunova, E., Enge, M., Taipale, M., Wei, G., *et al.* (2013). DNA-Binding Specificities of Human Transcription Factors. *Cell* 152, 327-339.

Kassiotis, G., and Stoye, J.P. (2016). Immune responses to endogenous retroelements: taking the bad with the good. *Nat Rev Immunol* 16, 207-219.

Kim, S.J., Onwuta, U.S., Lee, Y.I., Li, R., Botchan, M.R., and Robbins, P.D. (1992). The retinoblastoma gene product regulates Sp1-mediated transcription. *Molecular and Cellular Biology* 12, 2455-2463.

Kovesdi, I., Reichel, R., and Nevins, J.R. (1987). Role of an adenovirus E2 promoter binding factor in E1A-mediated coordinate gene control. *Proceedings of the National Academy of Sciences of the United States of America* 84, 2180-2184.

Leonova, K.I., Brodsky, L., Lipchick, B., Pal, M., Novototskaya, L., Chenchik, A.A., Sen, G.C., Komarova, E.A., and Gudkov, A.V. (2013). p53 cooperates with DNA

methylation and a suicidal interferon response to maintain epigenetic silencing of repeats and noncoding RNAs. *Proceedings of the National Academy of Sciences* *110*, E89–E98.

Liu, M., Ohtani, H., Zhou, W., Ørskov, A.D., Charlet, J., Zhang, Y.W., Shen, H., Baylin, S.B., Liang, G., Grønbaek, K., *et al.* (2016). Vitamin C increases viral mimicry induced by 5-aza-2'-deoxycytidine. *Proceedings of the National Academy of Sciences* *113*, 10238-10244.

Margueron, R., Li, G., Sarma, K., Blais, A., Zavadil, J., Woodcock, C.L., Dynlacht, B.D., and Reinberg, D. (2008). Ezh1 and Ezh2 maintain repressive chromatin through different mechanisms. *Mol Cell* *32*, 503-518.

Margueron, R., and Reinberg, D. (2011). The Polycomb complex PRC2 and its mark in life. *Nature* *469*, 343-349.

Minn, A.J. (2015). Interferons and the Immunogenic Effects of Cancer Therapy. *Trends in Immunology* *36*, 725-737.

Montoya-Durango, D.E., Liu, Y., Teneng, I., Kalbfleisch, T., Lacy, M.E., Steffen, M.C., and Ramos, K.S. (2009). Epigenetic control of mammalian LINE-1 retrotransposon by retinoblastoma proteins. *Mutation Research/Fundamental and Molecular Mechanisms of Mutagenesis* *665*, 20-28.

Morgunova, E., Yin, Y., Jolma, A., Dave, K., Schmierer, B., Popov, A., Eremina, N., Nilsson, L., and Taipale, J. (2015). Structural insights into the DNA-binding specificity of E2F family transcription factors. *Nature communications* *6*, 10050.

Munro, S., Carr, S.M., and La Thangue, N.B. (2012). Diversity within the pRb pathway: is there a code of conduct? *Oncogene*.

Najafabadi, H.S., Mnaimneh, S., Schmitges, F.W., Garton, M., Lam, K.N., Yang, A., Albu, M., Weirauch, M.T., Radovani, E., Kim, P.M., *et al.* (2015). C2H2 zinc finger proteins greatly expand the human regulatory lexicon. *Nat Biotech* *33*, 555-562.

Roers, A., Hiller, B., and Hornung, V. (2016). Recognition of Endogenous Nucleic Acids by the Innate Immune System. *Immunity* *44*, 739-754.

Roulois, D., Loo Yau, H., Singhanian, R., Wang, Y., Danesh, A., Shen, Shu Y., Han, H., Liang, G., Jones, Peter A., Pugh, Trevor J., *et al.* (2015). DNA-Demethylating Agents Target Colorectal Cancer Cells by Inducing Viral Mimicry by Endogenous Transcripts. *Cell* *162*, 961-973.

Rowe, H.M., and Trono, D. (2011). Dynamic control of endogenous retroviruses during development. *Virology* *411*, 273-287.

Sadic, D., Schmidt, K., Groh, S., Kondofersky, I., Ellwart, J., Fuchs, C., Theis, F.J., and Schotta, G. (2015). Atrx promotes heterochromatin formation at retrotransposons. *EMBO reports* *16*, 836-850.

- Saito, Y., Nakaoka, T., Sakai, K., Muramatsu, T., Toshimitsu, K., Kimura, M., Kanai, T., Sato, T., and Saito, H. (2016). Inhibition of DNA Methylation Suppresses Intestinal Tumor Organoids by Inducing an Anti-Viral Response. *Scientific reports* 6, 25311.
- Saksouk, N., Simboeck, E., and Déjardin, J. (2015). Constitutive heterochromatin formation and transcription in mammals. *Epigenetics & Chromatin* 8, 3.
- Schlee, M., and Hartmann, G. (2016). Discriminating self from non-self in nucleic acid sensing. *Nat Rev Immunol* 16, 566-580.
- Schmitges, F.W., Radovani, E., Najafabadi, H.S., Barazandeh, M., Campitelli, L.F., Yin, Y., Jolma, A., Zhong, G., Guo, H., Kanagalingam, T., *et al.* (2016). Multiparameter functional diversity of human C2H2 zinc finger proteins. *Genome research* 26, 1742-1752.
- Schuster, A.T., Sarvepalli, K., Murphy, E.A., and Longworth, M.S. (2013). Condensin II Subunit dCAP-D3 Restricts Retrotransposon Mobilization in *Drosophila* Somatic Cells. *PLoS Genetics* 9, e1003879.
- Shen, Yu J., Le Bert, N., Chitre, Anuja A., Koo, Christine X.E., Nga, Xing H., Ho, Samantha S.W., Khatoo, M., Tan, Nikki Y., Ishii, Ken J., and Gasser, S. (2015). Genome-Derived Cytosolic DNA Mediates Type I Interferon-Dependent Rejection of B Cell Lymphoma Cells. *Cell Reports* 11, 460-473.
- Talluri, S., Isaac, C.E., Ahmad, M., Henley, S.A., Francis, S.M., Martens, A.L., Bremner, R., and Dick, F.A. (2010). A G1 checkpoint mediated by the retinoblastoma protein that is dispensable in terminal differentiation but essential for senescence. *Mol Cell Biol* 30, 948-960.
- Vabret, N., Bhardwaj, N., and Greenbaum, B.D. (2016). Sequence-Specific Sensing of Nucleic Acids. *Trends in Immunology*.
- van der Vlag, J., and Otte, A.P. (1999). Transcriptional repression mediated by the human polycomb-group protein EED involves histone deacetylation. *Nat Genet* 23, 474-478.
- Vélez-Cruz, R., Manickavinayaham, S., Biswas, A.K., Clary, R.W., Premkumar, T., Cole, F., and Johnson, D.G. (2016). RB localizes to DNA double-strand breaks and promotes DNA end resection and homologous recombination through the recruitment of BRG1. *Genes & Development* 30, 2500-2512.
- Wolf, D., and Goff, S.P. (2009). Embryonic stem cells use ZFP809 to silence retroviral DNAs. *Nature* 458, 1201-1204.
- Wylie, A., Jones, A.E., and Abrams, J.M. (2016). p53 in the game of transposons. *Bioessays* 38, 1111-1116.

Wylie, A., Jones, A.E., D'Brot, A., Lu, W.-J., Kurtz, P., Moran, J.V., Rakheja, D., Chen, K.S., Hammer, R.E., Comerford, S.A., *et al.* (2015). p53 genes function to restrain mobile elements. *Genes & Development*.

Yee, A.S., Reichel, R., Kovesdi, I., and Nevins, J.R. (1987). Promoter interaction of the E1A-inducible factor E2F and its potential role in the formation of a multi-component complex. *The EMBO Journal* 6, 2061-2068.

Young, G.R., Eksmond, U., Salcedo, R., Alexopoulou, L., Stoye, J.P., and Kassiotis, G. (2012). Resurrection of endogenous retroviruses in antibody-deficient mice. *Nature* 491, 774-778.

Yu, P., Lübben, W., Slomka, H., Gebler, J., Konert, M., Cai, C., Neubrandt, L., Prazeres da Costa, O., Paul, S., Dehnert, S., *et al.* (2012). Nucleic Acid-Sensing Toll-like Receptors Are Essential for the Control of Endogenous Retrovirus Viremia and ERV-Induced Tumors. *Immunity* 37, 867-879.

Zheng, N., Fraenkel, E., Pabo, C.O., and Pavletich, N.P. (1999). Structural basis of DNA recognition by the heterodimeric cell cycle transcription factor E2F-DP. *Genes Dev* 13, 666-674.

Appendix A: Permissions from Molecular Cell

ELSEVIER LICENSE TERMS AND CONDITIONS

Mar 12, 2017

This Agreement between Charles A Ishak ("You") and Elsevier ("Elsevier") consists of your license details and the terms and conditions provided by Elsevier and Copyright Clearance Center.

License Number	4066790583976
License date	
Licensed Content Publisher	Elsevier
Licensed Content Publication	Molecular Cell
Licensed Content Title	An RB-EZH2 Complex Mediates Silencing of Repetitive DNA Sequences
Licensed Content Author	Charles A. Ishak, Aren E. Marshall, Daniel T. Passos, Carlee R. White, Seung J. Kim, Matthew J. Cecchini, Sara Ferwati, William A. MacDonald, Christopher J. Howlett, Ian D. Welch, Seth M. Rubin, Mellissa R.W. Mann, Frederick A. Dick
Licensed Content Date	15 December 2016
Licensed Content Volume	64
Licensed Content Issue	6
Licensed Content Pages	14
Start Page	1074
End Page	1087
Type of Use	reuse in a thesis/dissertation
Portion	full article
Format	both print and electronic
Are you the author of this Elsevier article?	Yes
Will you be translating?	No
Order reference number	
Title of your thesis/dissertation	Characterizing the role of the CDK-insensitive pRB-E2F1 complex
Expected completion date	Apr 2017
Estimated size (number of pages)	200
Elsevier VAT number	GB 494 6272 12

Appendix B: Permissions from Cancer Discovery



RightsLink®

Home

Account Info

Help



Title: Haploinsufficiency of an RB-E2F1-Condensin II Complex Leads to Aberrant Replication and Aneuploidy

Logged in as:
Charles Ishak
Account #:
3001124290

Author: Courtney H. Coschi, Charles A. Ishak, David Gallo, Aren Marshall, Srikanth Talluri, Jianxin Wang, Matthew J. Cecchini, Alison L. Martens, Vanessa Percy, Ian Welch, Paul C. Boutros, Grant W. Brown, Frederick A. Dick

LOGOUT

Publication: Cancer Discovery

Publisher: American Association for Cancer Research

Date: 2014-04-16

Copyright © 2014, ©2014 American Association for Cancer Research.

Permission Request

This reuse request is free of charge and you are not required to obtain a license.

BACK

CLOSE WINDOW

Copyright © 2017 [Copyright Clearance Center, Inc.](#) All Rights Reserved. [Privacy statement](#). [Terms and Conditions](#).
Comments? We would like to hear from you. E-mail us at customercare@copyright.com

Appendix C: Haploinsufficiency of an RB-E2F1-Condensin II complex leads to aberrant replication and aneuploidy

Published OnlineFirst April 16, 2014; DOI: 10.1158/2159-8290.CD-14-0215

RESEARCH ARTICLE

Haploinsufficiency of an RB-E2F1-Condensin II Complex Leads to Aberrant Replication and Aneuploidy

Courtney H. Coschi^{1,3}, Charles A. Ishak^{1,3}, David Gallo^{5,8}, Aren Marshall^{1,3}, Srikanth Talluri^{1,3}, Jianxin Wang⁹, Matthew J. Cecchini^{1,3}, Alison L. Martens^{1,3}, Vanessa Percy¹, Ian Welch⁴, Paul C. Boutros^{6,7,9}, Grant W. Brown^{5,8}, and Frederick A. Dick^{1,2,3}

ABSTRACT

Genome instability is a characteristic of malignant cells; however, evidence for its contribution to tumorigenesis has been enigmatic. In this study, we demonstrate that the retinoblastoma protein, E2F1, and Condensin II localize to discrete genomic locations including major satellite repeats at pericentromeres. In the absence of this complex, aberrant replication ensues followed by defective chromosome segregation in mitosis. Surprisingly, loss of even one copy of the retinoblastoma gene reduced recruitment of Condensin II to pericentromeres and caused this phenotype. Using cancer genome data and gene-targeted mice, we demonstrate that mutation of one copy of *RB1* is associated with chromosome copy-number variation in cancer. Our study connects DNA replication and chromosome structure defects with aneuploidy through a dosage-sensitive complex at pericentromeric repeats.

SIGNIFICANCE: Genome instability is inherent to most cancers and is the basis for selective killing of cancer cells by genotoxic therapeutics. In this report, we demonstrate that instability can be caused by loss of a single allele of the retinoblastoma gene that prevents proper replication and condensation of pericentromeric chromosomal regions, leading to elevated levels of aneuploidy in cancer. *Cancer Discov*; 4(7): 840–53. ©2014 AACR.

See related commentary by Hinds, p. 764.

INTRODUCTION

Fidelity of DNA replication and cell division are critical processes in multicellular organisms. Unrepaired errors can be passed on to daughter cells and contribute to cancer (1). In general, damaged DNA signals the cell cycle to arrest, and

repair is undertaken before advancement into mitosis (2). Recent evidence suggests exceptions to this rule, as damage observed before mitosis is transmitted through M-phase (3, 4). These DNA lesions are often associated with replication stress (4, 5), and their ability to evade checkpoints suggests that their impact on genome instability and cancer may be significant (6).



Replication stress can lead to fork stalling and chromosomal aberrations (7). It can create short gaps in sequence, or unresolved replication intermediates (3, 7, 8). Much of the evidence for replication stress phenotypes has been demonstrated using repetitive elements in yeast that require the Condensin complex for fidelity of replication and accurate segregation in mitosis (7, 9, 10). Mammals contain two Condensin complexes, but only Condensin II is constitutively nuclear, suggesting it may play roles in both DNA replication and chromosome condensation (11). In addition to its role in mitotic chromosome condensation, chromosome shape, and controlling recombination, Condensin II has also been implicated in DNA replication and damage repair (12). In particular, Condensin II functions in the resolution of sister chromatids immediately following replication in S-phase (13). Despite these roles for Condensin II, we know little about how it is recruited to specific genomic locations, such as repetitive sequences, to carry out these functions.

The retinoblastoma protein (pRB) is generally thought of as a regulator of the G₁ to S-phase transition (14). However, evidence suggests that pRB also contributes to functions beyond G₁. For example, pRB has been implicated in an S-phase checkpoint to repair DNA breaks and to regulate initiation of DNA replication (15–18). In addition, pRB facilitates chromosome condensation in mitosis, particularly at pericentromeres, although there is no evidence that it physically localizes to this region (19–22). pRB-deficient cells have increased genome instability characterized by spontaneous DNA breaks and chromosome missegregation in mitosis (23). Surprisingly, these outcomes have not been attributed to a specific mechanism of pRB action. For example, altered regulation of E2F transcription has been implicated in shifts in intermediary metabolism (24, 25), misexpression of spindle assembly checkpoint genes, and

imbalances in nucleotide pools (23). Thus, an in-depth understanding of pRB function in genome stability has yet to emerge, in part because these phenotypes are not mutually exclusive.

In humans, the *Rb1* gene is lost in hereditary retinoblastoma, and survivors face an elevated risk of other cancers, such as osteosarcomas, throughout their lives (26). *Rb1* loss occurs by the “two hit” model proposed by Knudson (27). Because loss of heterozygosity was the rate-limiting step in the genesis of retinoblastoma, Knudson concluded that heterozygosity likely did not contribute to tumorigenesis. This premise is recapitulated in *Rb1*^{+/-} mice that develop pituitary tumors characterized by loss of the remaining wild-type allele (28). Curiously, a number of experiments have suggested that loss of one copy of pRB may contribute to cancer progression in other contexts. Crosses between *Rb1*- and *Trp53*-deficient mice revealed that *Rb1*^{+/-};*Trp53*^{+/-} mice develop some tumors without losing the remaining *Rb1* allele (29). In addition, loss of one copy of *Rb1* in mouse osteoblasts or embryonic stem (ES) cells confers genome instability (30, 31). Consequently, phenotypes of *Rb1* heterozygosity have been previously reported, but a clear link to cancer incidence or progression is lacking. In addition, a mechanism that preserves genome stability in which the relative supply of pRB is critical has yet to be described.

pRB and Condensin II contribute to the integrity of pericentromeric heterochromatin, which is prone to the effects of replication stress. In this study, we demonstrate that *Rb1*-mutant cells experience replication stress, particularly at pericentromeric regions. We show that a complex composed of pRB, E2F1, and Condensin II localizes to pericentromeric repeats. Intriguingly, replication and chromosome structure defects were recapitulated in heterozygous *Rb1*-mutant fibroblasts, indicating that this genomic instability phenotype is gene-dosage dependent. Similarly,

RESEARCH ARTICLE

Coschi et al.

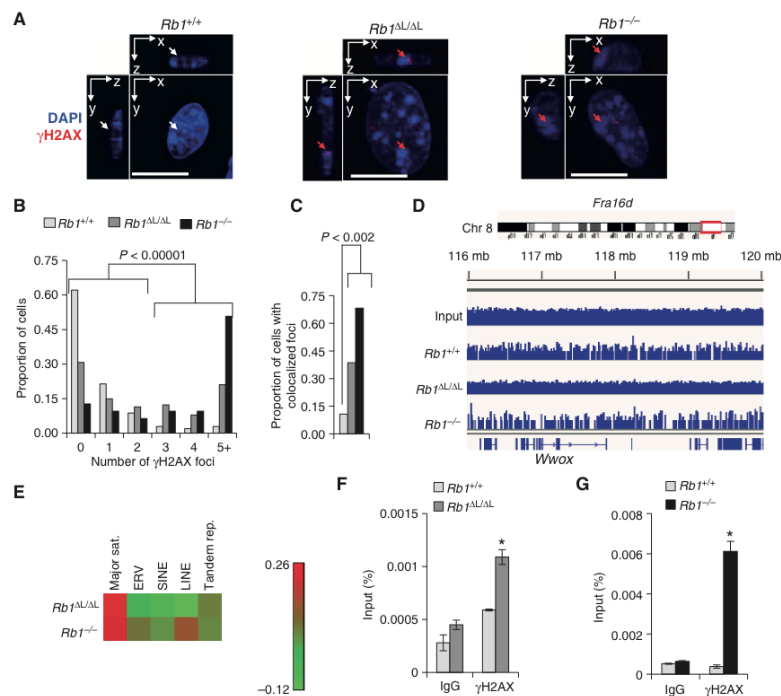


Figure 1. *Rb1*-mutant MEFs exhibit increased γ H2AX foci that are enriched at pericentromeric DNA. **A**, immunofluorescence microscopy of γ H2AX staining is shown in red and cells were counterstained with 4',6-diamidino-2-phenylindole (DAPI; blue). Red arrows, colocalization; white arrows, lack of colocalization; scale bars, 10 μ m. **B**, the quantity of foci per cell was determined for each genotype and compared using a χ^2 test. *Rb1*^{+/+}, *n* = 103; *Rb1* ^{Δ L/ Δ L}, *n* = 114; *Rb1*^{-/-}, *n* = 63. **C**, the proportion of cells with γ H2AX foci colocalizing with DAPI-rich foci was determined by confocal 3D rendering and compared using a χ^2 test. **D**, ChIP-seq analysis was performed for γ H2AX, and tracks comparing abundance at *Fra16d* among different *Rb1* genotypes are shown. A red box indicates this locus on a chromosome 8 ideogram. **E**, heatmap to show log₂ ratios of the abundance of *Rb1*-mutant γ H2AX precipitable reads per million mapped reads versus wild-type γ H2AX precipitated reads. **F** and **G**, ChIP-qPCR for γ H2AX to quantitate major satellite (major sat.) repeats. *, *P* < 0.05 using a *t* test; *n* = 3.

we demonstrate that normal *Rb1*^{-/-} fibroblasts from patients with hereditary retinoblastoma exhibit the same aberrant replication characteristics followed by mitotic errors. Using genotype and copy-number variation data from the Catalogue of Somatic Mutations in Cancer (COSMIC) database, we demonstrate that *Rb1*^{-/-} lymphoma and sarcoma cancer cell lines exhibit as much genomic instability as *Rb1*^{-/-} cell lines. Finally, using gene-targeted mice bearing a single mutant allele that is defective for recruiting Condensin II to chromatin (called *Rb1* ^{Δ L}), we demonstrate that tumors from *Rb1* ^{Δ L/+};*Trp53*^{-/-} mice have increased chromosome copy-number variation compared with *Trp53*^{-/-} controls. This provides proof-of-principle that dosage sensitivity of a pRB-E2F1-Condensin II complex compromises replication fidelity and leads to aneuploidy.

RESULTS

Defective *Rb1* Causes Deposition of γ H2AX at Pericentromeric Repeats

In normal human fibroblasts, loss of RB results in γ H2AX foci (32). We compared γ H2AX foci levels in mouse embryonic fibroblasts (MEF) from *Rb1*^{+/+} and *Rb1*^{-/-} animals (Fig. 1A). In addition, we analyzed a targeted mutant (*Rb1* ^{Δ L}) that antagonizes interactions between Condensin II and the LXCXE binding cleft region on pRB, while leaving E2F interactions and many pRB-dependent aspects of cell-cycle control intact (19, 20, 33, 34). There was a significant increase in γ H2AX foci in *Rb1*^{-/-} MEFs compared with wild-type (Fig. 1B). DAPI counterstaining produces punctate foci at pericentromeric regions. Analysis by confocal microscopy revealed that γ H2AX

accumulation was more frequent at DAPI-rich spots in *Rb1*^{-/-} MEFs than in controls (Fig. 1C). A similar, less pronounced effect was observed in *Rb1*^{Δ/Δ} cells with respect to γH2AX focus abundance and localization (Fig. 1B and C). This indicates that deficiency in pRB-LXCXE-dependent functions alone is sufficient to cause γH2AX foci.

To further investigate the localization of γH2AX deposition, we performed chromatin immunoprecipitation (ChIP)-sequence analysis in which γH2AX was precipitated from wild-type, *Rb1*^{Δ/Δ}, and *Rb1*^{-/-} chromatin. Sequence reads were mapped onto unique and repetitive genomic regions to compare their relative abundance. Analysis on a megabase scale did not reveal a particular bias of γH2AX enrichment within damage-susceptible fragile regions (Fig. 1D). Model-based Analysis of ChIP-Seq (MACS) fails to detect reproducible enrichment in *Rb1*^{Δ/Δ} and *Rb1*^{-/-} cells at this location (Supplementary Fig. S1). In accordance with elevated quantities of γH2AX foci in *Rb1*^{Δ/Δ} and *Rb1*^{-/-} MEFs, failure to detect local regions of enrichment compared with wild-type implies that γH2AX levels are uniformly increased across unique regions of the genome in *Rb1*^{Δ/Δ} and *Rb1*^{-/-} cells.

Mapping reads to nonunique regions of the genome revealed that major satellite repeats, which comprise much of the DAPI-rich pericentromeric foci, were enriched relative to other nonunique comparators (Fig. 1E). ChIP-qPCR analysis also demonstrated that γH2AX is elevated at major satellites in *Rb1*^{Δ/Δ} and *Rb1*^{-/-} genotypes compared with wild-type (Fig. 1F and G). Therefore, deficiency for pRB increases γH2AX deposition throughout the genome, with particular enrichment at pericentromeric repeats, and loss of pRB-LXCXE interactions alone contributes to this effect.

Aberrant DNA Replication in *Rb1*-Mutant MEFs

The spontaneous formation of γH2AX foci in *Rb1*-mutant cells, and their frequent association with major satellite repeats, is inconsistent with DNA double-strand breaks (35). Because *Rb1*^{-/-} cells have multiple confounding defects that contribute to genome instability, we focused on the *Rb1*^{Δ/Δ} mutant as it maintains normal G₁-S regulation during proliferation (33).

We pulse-labeled *Rb1*^{Δ/Δ} cells with CldUrd and IdUrd and stained DNA fibers to visualize replication fork progression (Fig. 2A). This revealed a net increase in fork rate in *Rb1*^{Δ/Δ} mutants compared with controls (Fig. 2B). Accelerated forks, although less common than slowed forks, are also associated with replication stress and are prone to stalling (5, 36, 37). In addition, elevated replication fork asymmetry (Fig. 2C), and elevated levels of replication protein A (RPA) 32 phosphoserine33, further suggest replication stress (Fig. 2D and Supplementary Fig. S2). Thus, from a genome-wide perspective, *Rb1*^{Δ/Δ} cells replicate their DNA abnormally and display markers of replication stress.

Because γH2AX shows greater accumulation at major satellite repeats, we investigated this region further. We used ChIP-qPCR assays of RPA to investigate its levels at major satellites in *Rb1*^{Δ/Δ} MEFs (Fig. 2E). This revealed lower levels of RPA at pericentromeres in *Rb1*^{Δ/Δ} cells, suggesting that the generation of ssDNA needed for replication or break repair is inhibited. Furthermore, ChIP-pPCR assays reveal increased levels of proliferating cell nuclear antigen (PCNA), minichromosome maintenance complex (MCM) 3, and DNA Polδ at

pericentromeres in *Rb1*^{Δ/Δ} cells (Fig. 2F-H). Together these data indicate that replication of this genomic region is defective. Investigation of γH2AX staining of mitotic cells suggests similarities between this replication phenotype and reports of under-replication (Supplementary Fig. S2). Furthermore, telomere analysis suggests no loss of integrity (Supplementary Fig. S3).

In sum, *Rb1*^{Δ/Δ} cells have abnormal replication rates and molecular markers that are consistent with replication stress. Although not entirely consistent with phenotypes generated by treating cells with hydroxyurea, reduced RPA levels at pericentromeres and elevated levels of replication machinery and γH2AX further suggest that replication in this region is impaired. The simplest explanation for γH2AX deposition at major satellite repeats is that they are the result of replication stress.

pRB, E2F1, and Condensin II Form a Complex at Pericentromeres

A similar phenotype of spontaneous γH2AX foci has been reported for a number of known pRB-interacting proteins with roles in replication. Increased γH2AX has been reported in cells deficient for the Condensin II subunit structural maintenance of chromosome protein 2 (SMC2; 38) and E2F1 (39). Notably, loss of other activator E2Fs did not cause γH2AX foci (39). In MEFs, shRNA depletion of CAP-D3 (a Condensin II subunit) caused similar patterns of γH2AX foci as described above (Supplementary Fig. S4). We also discovered similar γH2AX staining in *E2f1*^{-/-} cells (Supplementary Fig. S4).

Because of these similarities, we investigated whether pRB, E2F1, and CAP-D3 localize to pericentromeric heterochromatin in interphase cells. ChIP-qPCR for major satellites in chromatin precipitated with pRB, CAP-D3, and E2F1 antibodies revealed that they are all present at these repeats (Fig. 3A and B). Furthermore, CAP-D3 recruitment was dependent on E2F1 and pRB because its binding was diminished in *E2f1*^{-/-}, *Rb1*^{-/-}, and *Rb1*^{Δ/Δ} MEFs (Fig. 3B and C). To better understand Condensin II recruitment to chromatin and its relationship to pRB, we performed ChIP-seq for CAP-D3 in wild-type and *Rb1*^{Δ/Δ} MEFs. This revealed 8,056 peaks of local enrichment for CAP-D3 within unique genome sequences, and 6,979 of these were lost in the *Rb1*^{Δ/Δ} cells. Intriguingly, CAP-D3 was not recruited to the promoters of well-known pRB-E2F transcriptional targets such as Cyclin E1 (*Ccne1*), *Mcm3*, and p107 (*Rbl1*; Fig. 3D). However, it was recruited to the *Lmnb2* replication origin in a pRB-dependent manner (Fig. 3D). This is significant because pRB and E2F1 are known to localize to this origin (16, 18), even though it does not possess a canonical E2F DNA sequence element.

We isolated the putative pRB-E2F1-Condensin II complex to investigate its properties. We generated a biotinylated major satellite repeat probe, and mixed it with nuclear extract from wild-type and *Rb1*^{-/-} cells. Major satellite-associated complexes were collected on streptavidin beads, and proteins were detected by immunoblotting. SMC2, CAP-D3, pRB, and E2F1 were isolated together from wild-type extracts, but none of these components interacted with the major satellite sequence when pRB was absent (Fig. 4A). Major satellites were bound in a sequence-dependent manner as a control probe failed to precipitate them, and their interaction was sensitive to competition by exogenous major satellite sequences (Fig. 4B). We

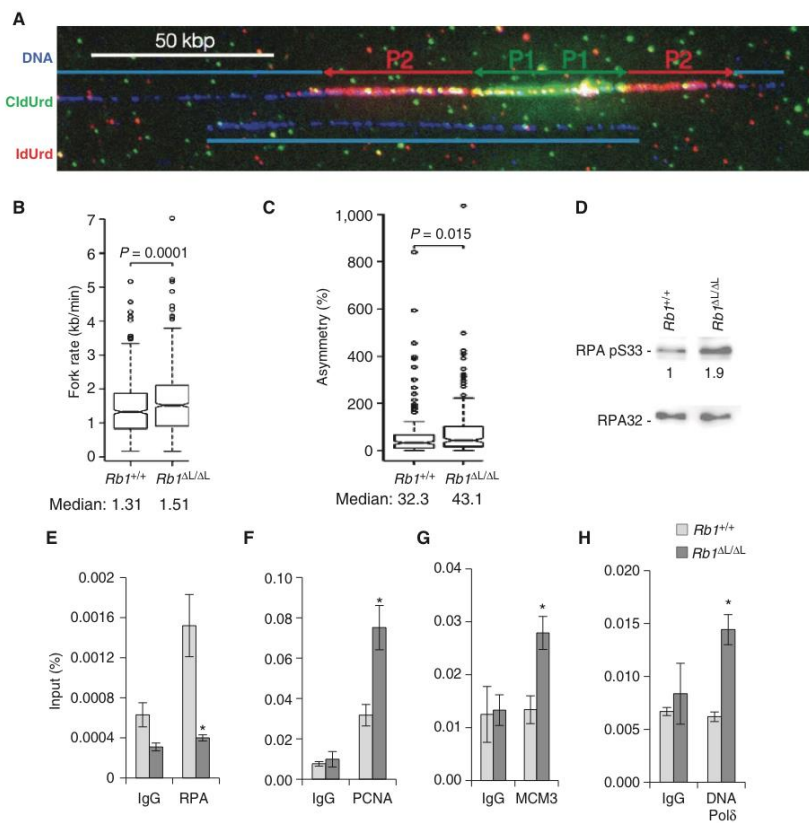


Figure 2. Replication abnormalities in *Rb1*-mutant cells. **A**, fluorescence microscopy of a replicating fork is shown by CldUrd labeling (P1, green) and IdUrd (P2, red), and light blue bars mark unlabeled DNA. **B**, fork rates were measured for *Rb1*^{+/+} ($n = 718$) and *Rb1*^{ΔL/ΔL} ($n = 855$). Median values were compared using the Mann-Whitney *U* test. **C**, diverging forks, as shown in **A**, were measured and the percentage asymmetry was determined. *Rb1*^{+/+} ($n = 141$) and *Rb1*^{ΔL/ΔL} ($n = 174$). Median values were compared as in **B**. **D**, extracts were blotted for RPA and the indicated phosphorylated RPA-S33. Relative intensity of RPA pS33 is shown below each lane. **E**, ChIP-qPCR analysis of RPA at major satellite repeats in *Rb1*^{+/+} and *Rb1*^{ΔL/ΔL} MEFs. *, $P < 0.05$ using a *t* test; $n = 3$. **F-H**, ChIP-qPCR analysis of PCNA, MCM3, and DNA Polδ occupancy at major satellites.

also reconstituted this complex using nuclear extracts from human C33A cells that express HA-E2F1/HA-DP1 (Fig. 4C). Major satellite probes were mixed with extract that contained GST-RB Large Pocket (LP). Figure 4D demonstrates that neither E2F1 nor CAP-D3 was recruited to the major satellite probe without GST-RBLP. This suggests that E2F1's ability to interact with these sequences is not autonomous, as it is in the recognition of cell-cycle target genes, but requires a cooperative contribution from pRB. Furthermore, ChIP of E2F1 from *Rb1*^{-/-} MEFs revealed cooperativity *in vivo* as E2F1 binding was diminished in the absence of pRB (Fig. 4E).

Previous reports indicate that binding of E2F1 to pRB through an alternate configuration called the "specific" interaction changes the sequence specificity of E2F1, reducing affinity for canonical E2F recognition sequences (40). We used MEFs from two new *Rb1*-mutant mouse lines to investigate whether the "specific" interaction explains cooperative DNA binding at major satellites by pRB and E2F1. *Rb1*^{ΔG} contains two amino acid substitutions (R461E and K542E) that prevent binding to activator E2Fs to regulate transcription at cell-cycle promoters; however, it maintains the ability to bind to E2F1 through the separate "specific" mechanism

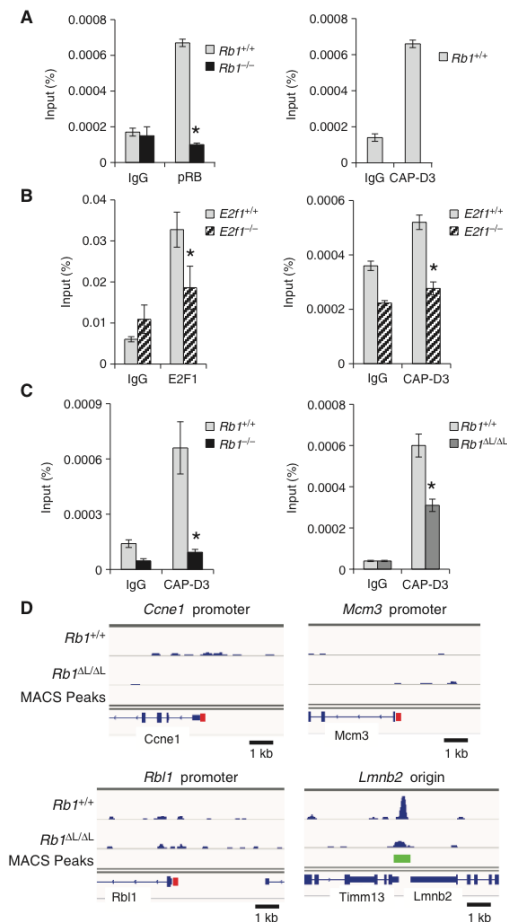


Figure 3. pRB, E2F1, and Condensin II localize to pericentromeric DNA. **A**, ChIP-qPCR for major satellite repeats using antibodies against pRB and CAP-D3. *, $P < 0.05$ using a t test; $n = 3$. **B**, chromatin was precipitated with E2F1 and CAP-D3 antibodies and major satellite repeats were amplified. **C**, ChIP-qPCR using a CAP-D3 antibody to precipitate major satellite repeats in *Rb1*^{-/-}, *Rb1*^{ΔL/ΔL}, and *Rb1*^{ΔL/ΔL} MEFs. **D**, ChIP-seq was performed for CAP-D3 using chromatin from *Rb1*^{+/+} and *Rb1*^{ΔL/ΔL} MEFs and tracks are shown for selected genomic regions. E2F binding sites present in the promoters of *Ccne1*, *Mcm3*, and *Rb1* are indicated by red boxes, and regions of significant enrichment (MACS peaks) are indicated in green.

(41, 42). Conversely, *Rb1*^{ΔS} is unable to bind E2F1 through the "specific" interaction because of an F832A substitution, but it maintains its ability to bind activator E2Fs in a manner that regulates canonical E2F transcription (42, 43). ChIP for CAP-D3 in *Rb1*^{ΔG/ΔG} MEFs demonstrated no change in its loading at pericentromeric heterochromatin, whereas in *Rb1*^{ΔS/ΔS} cells, CAP-D3 was absent (Fig. 4F).

This indicates that pRB, E2F1, and Condensin II form a stable complex with major satellite repeats, and other unique loci in the genome such as the *Lmnb2* origin (Supplementary Fig. S5). On the basis of phenotypic similarities of

γ H2AX focus location, we suggest that these proteins form a complex to facilitate DNA replication and chromosome condensation, and its absence preferentially affects major satellite repeats.

γ H2AX Distribution, Replication Stress Markers, and Recruitment of Condensin II Are Sensitive to *Rb1* Gene Dosage

Major satellites account for 3% of the mouse genome, suggesting that gene dosage of *Rb1* may be important for supplying enough of this complex to ensure stability

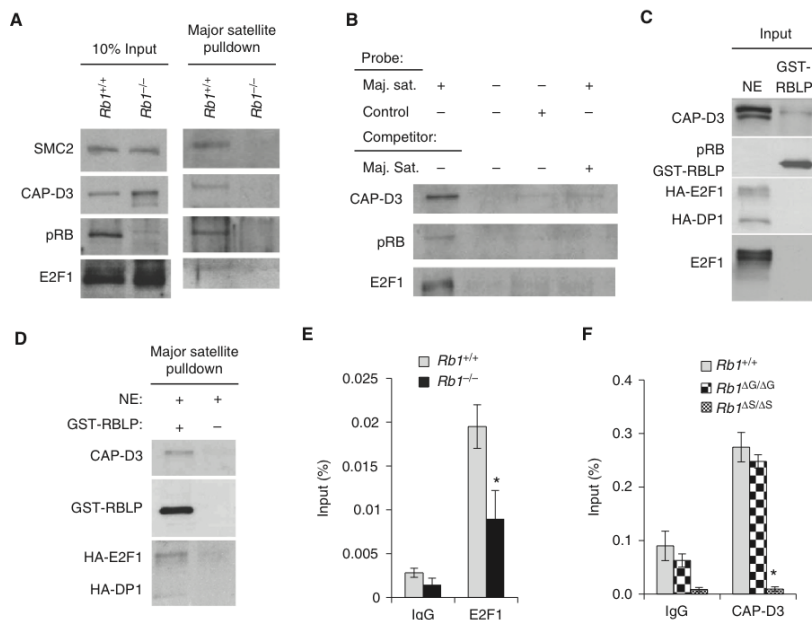


Figure 4. pRB, E2F1, and Condensin II form a complex on pericentromeric DNA. **A**, nuclear extracts (NE) were mixed with streptavidin beads and a biotinylated major satellite (maj. sat.) repeat containing probe. Precipitated proteins were analyzed by SDS-PAGE and Western blotting. **B**, wild-type nuclear extracts were mixed with the indicated probes and/or competitor DNA. **C**, *Rb1*-deficient C33A cells were transfected with HA-E2F1 and HA-DP1 expression vectors and nuclear extracts were prepared. Western blots of relevant proteins are shown. **D**, nuclear extracts were mixed with streptavidin beads and biotinylated major satellite probes, either with or without GST-RBLP. Associated proteins were precipitated and analyzed by Western blotting. **E** and **F**, ChIP-qPCR for E2F1 was performed, and major satellite repeat DNA was amplified by real-time PCR. *, $P < 0.05$ using a *t* test; $n = 3$. **F**, ChIP-qPCR using a CAP-D3 antibody was performed to precipitate major satellite repeats from *Rb1*^{+/+}, *Rb1*^{AG/AG}, and *Rb1*^{AS/AS} MEFs.

of these repeats. Fluorescence microscopy revealed a significant increase in γ H2AX foci in both *Rb1*^{+/−} and *Rb1*^{ΔL/+} MEFs compared with the wild-type control (Fig. 5A and B). Moreover, γ H2AX foci were found at pericentromeric heterochromatin in *Rb1*^{+/−} and *Rb1*^{ΔL/+} MEFs more frequently than in *Rb1*^{+/+} controls, and were almost as abundant as their homozygous mutant counterparts (Fig. 5C). Western blotting revealed elevated γ H2AX levels in *Rb1*^{ΔL/ΔL}, *Rb1*^{+/−}, and *Rb1*^{−/−} MEFs relative to *Rb1*^{+/+} (Fig. 5D). Similarly, phosphorylated RPA-S33 displays increased abundance in all *Rb1*-mutant genotypes (Fig. 5E). As with *Rb1*^{+/−} and *Rb1*^{ΔL/ΔL}, ChIP-seq analysis of the distribution of γ H2AX in *Rb1*^{ΔL/+} MEFs also revealed enrichment at major satellites (Fig. 5F). Using ChIP-seq data from all three *Rb1*-mutant genotypes, we compared the reproducibility of enrichment among repeat elements (Supplementary Fig. S6). This revealed that major and minor satellites have a greater proportion of reads than wild-type. This is noteworthy because minor satellites are adjacent to major satellites at

the centromere. To extend our investigation of *Rb1* gene dosage sensitivity, we performed ChIP-qPCR for CAP-D3 at pericentromeric heterochromatin in *Rb1*^{ΔL/+} cells and determined that it was reduced at major satellites in *Rb1*^{ΔL/+} MEFs relative to wild-type control (Fig. 5G). This suggests that loss of LXCXE interactions in even one copy of *Rb1* reduced the supply of this complex at these repeats. In addition, heterozygous *Rb1*-mutant MEFs displayed anaphase bridges, tangled centromeres, and aneuploidy as reported previously for homozygous *Rb1* mutants (Supplementary Fig. S7 and S8).

These data demonstrate that single *Rb1* null and *Rb1*^{ΔL} alleles compromise the ability to prevent γ H2AX foci and aneuploidy. γ H2AX and phosphorylated RPA-S33 levels are similar between heterozygous and homozygous genotypes, and these translate into a similar frequency of mitotic errors. On the basis of these direct comparisons of homozygous mutant, heterozygous, and wild-type genotypes, we describe *Rb1* as haploinsufficient for this function.

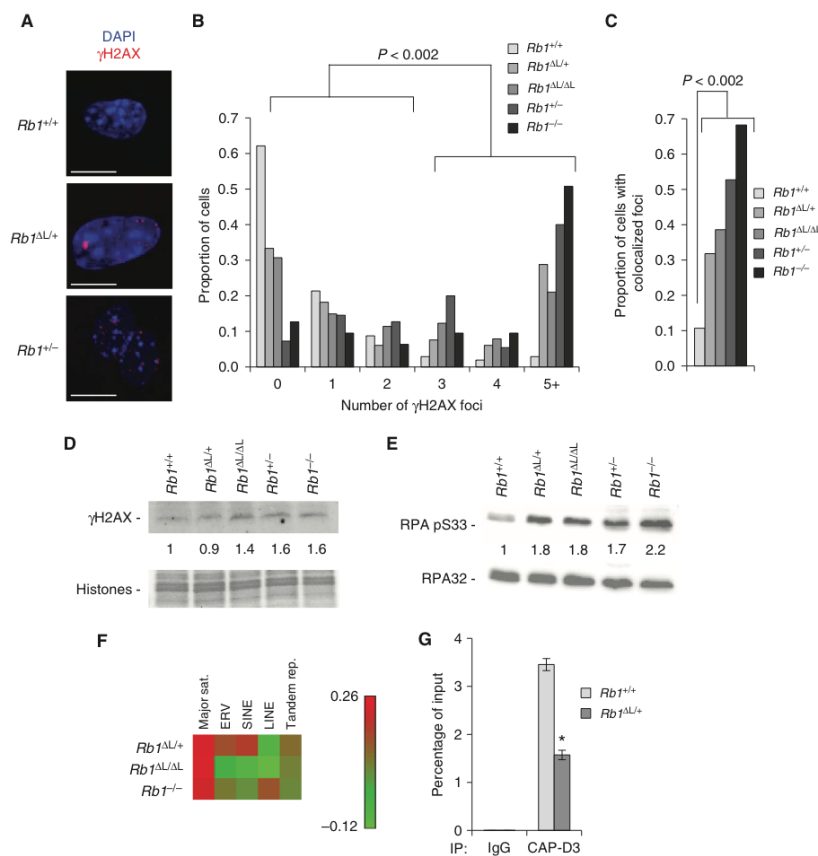


Figure 5. *Rb1* heterozygous MEFs have elevated γ H2AX and underloading of CAP-D3 at major satellites. **A**, immunofluorescence microscopy of γ H2AX staining in *Rb1*^{+/+}, *Rb1*^{ΔL/+}, and *Rb1*^{-/-} MEFs is shown. Scale bars, 10 μ m. **B**, the quantity of γ H2AX foci per cell was determined for *Rb1*^{+/+}, *Rb1*^{ΔL/+}, and *Rb1*^{-/-} MEFs and compared with homozygous mutants from Fig. 1. The quantity of foci was compared using a χ^2 test. *Rb1*^{ΔL/+}, *n* = 114; *Rb1*^{-/-}, *n* = 63. **C**, quantification of DAPI foci colocalization with γ H2AX foci by confocal microscopy. The proportion of colocalization was compared using a χ^2 test. **D**, γ H2AX levels were detected by Western blotting and Coomassie staining of histones was used as a loading control. Relative intensity of γ H2AX is shown below. **E**, RPA32 and RPA32 phospho serine 33 levels were detected by Western blotting. Relative intensity of RPA pS33 is shown below. **F**, heatmap depicting \log_2 ratios of γ H2AX precipitated sequence tags in the indicated mutants relative to wild-type control. **G**, ChIP-qPCR using a CAP-D3 antibody in *Rb1*^{+/+} and *Rb1*^{ΔL/+} MEFs was used to detect major satellite repeats. *, *P* < 0.05 using a *t* test; *n* = 3.

Human *RB1*^{+/-} Cells Exhibit γ H2AX Foci, Phosphorylated RPA-S33, Mitotic Defects, and Aneuploidy

The kinetics of *RB1* loss in retinoblastoma gave rise to the now famous “two-hit” hypothesis (27). However, our data on haploinsufficiency in *Rb1*-mutant mouse fibroblasts motivated

us to determine whether a similar phenotype is present in normal fibroblasts from patients with hereditary retinoblastoma (*RB1*^{+/-}). We obtained patient fibroblasts, confirmed their heterozygous status by sequencing (Supplementary Fig. S9), and compared them with unrelated human fibroblast cells (IMR90, BJ, and WI38). This revealed that patient fibroblasts exhibited increased γ H2AX foci (Fig. 6A and B).

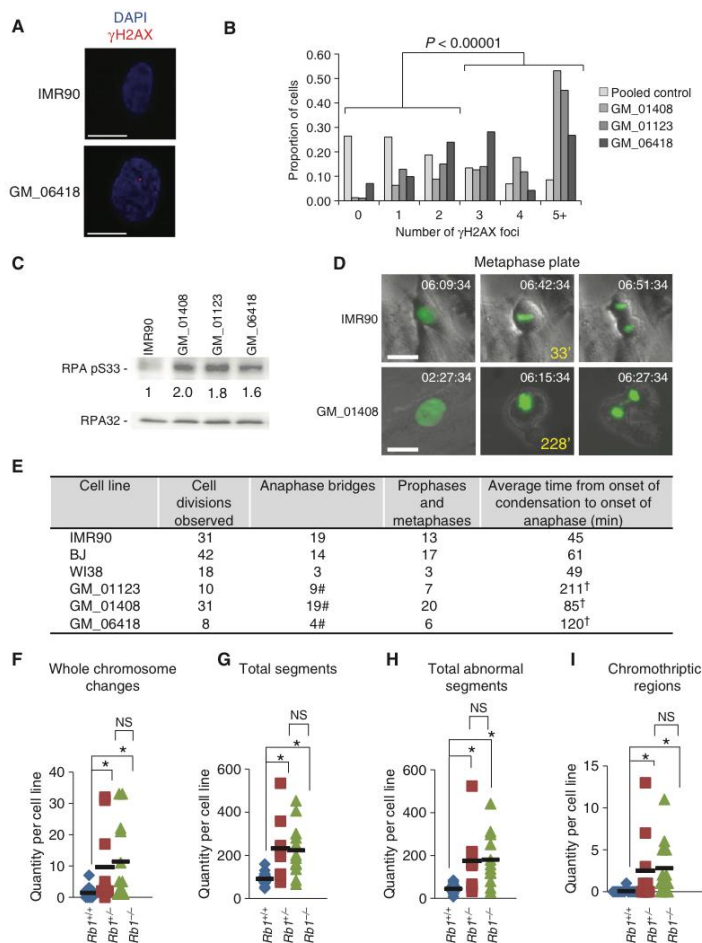


Figure 6. Normal $Rb1^{-/-}$ cells have elevated γ H2AX foci, mitotic errors, and aneuploidy. **A**, immunofluorescence microscopy for γ H2AX in control and $Rb1^{-/-}$ patient fibroblasts. Scale bars, 10 μ m. **B**, quantitation of γ H2AX foci in control and each patient fibroblast isolate. Foci were compared for patient fibroblasts against pooled control data (IMR90, BJ, and WI-38) using a χ^2 test. Pooled control, $n = 246$; GM_01408, $n = 79$; GM_01123, $n = 93$; GM_06418, $n = 71$. **C**, Western blotting was used to detect phosphorylated RPA pS33 and total RPA32. Relative intensity of RPA pS33 is displayed. **D**, cells were transfected with H2B-GFP, and video microscopy was performed to capture phase contrast and GFP images over 15 hours. The left-most image shows the onset of prophase, and the middle image is of the metaphase plate just before the onset of anaphase (elapsed time since the onset of prophase is shown in yellow). The right-most image shows cells in telophase. Scale bars, 50 μ m. **E**, summary of video microscopy data showing the number of divisions observed along with the number that contained anaphase bridges. Similarly, the number of cells observed to complete prophase and metaphase is shown along with the average length of these two phases. Each patient fibroblast is compared with pooled control data. #, $P < 0.05$, χ^2 test; †, $P < 0.05$, t test. **F-I**, quantitation of genomic abnormalities in mesenchymal-derived cancer cell lines that are wild-type ($n = 15$), hemizygous ($n = 10$), or null ($n = 12$) for $Rb1$. Means were compared using a t test. *, $P < 0.05$. NS, not significant.

As with heterozygous mouse fibroblasts, they also contained elevated levels of phosphorylated RPA-S33 compared with control (Fig. 6C). We also used video microscopy of H2BGFP-expressing cells to search for mitotic defects (Fig. 6D). All three patient fibroblast lines exhibited a significant delay in progression to metaphase from the onset of chromosome condensation (Fig. 6E). Finally, patient cells also showed a significant increase in mitoses with anaphase bridges (Fig. 6E). Taken together, these experiments suggest that normal human fibroblast cells heterozygous for *RBI* are characterized by replication and mitotic errors similar to our mouse data.

Given the direct impact of haploinsufficiency for *RBI* on γ H2AX abundance and mitotic errors, we sought evidence for aneuploidy in *RBI*^{+/−} cancers. Using copy-number variation data from COSMIC (44), we asked whether cancer-derived cell lines heterozygous for *RBI* exhibit increased levels of genomic abnormalities. Because retinoblastoma survivors are highly prone to second primary neoplasms that are of mesenchymal origin (26), we compared copy-number data for *RBI*^{+/+}, *RBI*^{+/−}, and *RBI*^{−/−} cell lines from this germ layer. We sorted genomic abnormalities into four categories: whole-chromosome gains and losses, total genomic segments, total abnormal genomic segments, and chromothripic regions. *RBI*^{+/−} and *RBI*^{−/−} cancers exhibited significantly more whole-chromosome changes than cell lines retaining both wild-type copies of *RBI* (Fig. 6F). Importantly, *RBI*^{+/−} lines exhibited as many whole-chromosome changes as *RBI*^{−/−} cells. This trend was observed for the other measures of instability as *RBI*^{+/−} and *RBI*^{−/−} lines exhibited significantly more abnormalities than wild-type and were not statistically different from each other (Fig. 6G–I). To confirm these results, we obtained representative lines to verify *RBI* copy number and expression of pRB (Supplementary Fig. S9).

These data indicate that loss of one copy of *RBI* may exhibit haploinsufficiency in humans, namely through the ability of pRB to prevent the accumulation of γ H2AX foci, phosphorylated RPA-S33, and mitotic errors. Moreover, this is associated with increased chromosomal abnormalities in cell lines at a level comparable with that found in *RBI*^{−/−} cells. A number of possibilities exist that may connect replication and chromatin structure defects at pericentromeric sequences with common chromosomal aberrations found in cancer, and they are discussed below.

Haploinsufficiency of Rb1 Contributes to Aneuploidy in a Mouse Model of Cancer

We also sought evidence for haploinsufficiency *in vivo* using mouse models. Because *Rb1*^{−/−} mice are inviable, comparisons between heterozygous, homozygous mutant, and wild-type populations are not possible. However, *Rb1*^{Δ/Δ} mice are viable and can therefore be used to study whether haploinsufficiency in *Rb1*^{Δ/+} may contribute to oncogenesis. We crossed *Rb1*^{Δ/+} mice with *Trp53*^{−/−} mice as previously reported (19). *Rb1*^{Δ/+};*Trp53*^{−/−} mice exhibited a significant decrease in survival compared with *Trp53*^{−/−} controls (Fig. 7A), which was not statistically different from previously reported *Rb1*^{Δ/Δ};*Trp53*^{−/−} mice (19). PCR amplifica-

tion of the wild-type and *Rb1*^Δ alleles in tumor DNA from *Rb1*^{Δ/+};*Trp53*^{−/−} mice showed retention of the wild-type allele (Fig. 7B). Thymic lymphomas from *Rb1*^{Δ/+};*Trp53*^{−/−} mice demonstrated a more aggressive histology compared with *Trp53*^{−/−} controls as evidenced by smaller cytoplasmic-to-nuclear area (Fig. 7C). This is very similar to the histology described in *Rb1*^{Δ/Δ};*Trp53*^{−/−} thymic lymphomas (19), and *Rb1*^{Δ/+};*Trp53*^{−/−} mice exhibited a shift in tumor spectrum from thymic lymphoma, commonly reported in *Trp53*^{−/−} mice, toward sarcomas (Supplementary Fig. S10). Thus, one defective copy of *Rb1* can have similar effects on disease progression as mutation of both alleles. Because thymic lymphomas were common among all genotypes, we investigated their relative levels of chromosome gains and losses. Figure 7D shows log₂ ratio plots from a male versus female control hybridization and representative *Rb1*^{Δ/+};*Trp53*^{−/−} tumors. The number of whole-autosome gains and losses in thymic lymphomas from *Rb1*^{Δ/+};*Trp53*^{−/−} mice was greater than *Trp53*^{−/−} controls, and statistically indistinguishable from *Rb1*^{Δ/Δ};*Trp53*^{−/−} tumors (Fig. 7E).

Earlier experiments demonstrated that one *Rb1*^Δ allele can cause replication and chromosome structure-associated phenotypes. Taken together with this tumor study, our data suggest that gene dosage-sensitive effects on replication and mitotic chromosomes have the potential to compromise pRB function *in vivo* leading to aneuploidy.

DISCUSSION

The pRB–E2F1–Condensin II complex identified in this study affects chromatin from S-phase to mitosis. Our findings suggest how replication and structural defects at pericentromeres may be connected to common chromosomal abnormalities in cancer. Reduced occupancy by this complex at pericentromeric repeats may lead to unresolved replication intermediates and compromise the integrity of centromeres and kinetochores. Misshapen kinetochores can lead to merotelic microtubule attachments, lagging anaphase chromosomes, and ultimately gains and losses of whole chromosomes in daughter cells (45). Alternatively, centromere fusions or recombination with other chromosomes (7, 8) may lead to gains or losses of whole chromosome arms, and these are the most common segmental chromosome changes in human cancer (46). Finally, lagging chromosomes created by these mechanisms are more likely to become incorporated into micronuclei and undergo chromothripsis in subsequent cell cycles (47). In this way, defects in pericentromeric chromosomal regions may have the ability to cause a wide spectrum of chromosomal abnormalities, similar to those found in *RBI*^{+/−} and *RBI*^{−/−} cancer cell lines. Intriguingly, augmentation of Cohesin function can suppress replication and chromosomal abnormalities caused by loss of *RBI* function. This suggests that these chromosomal defects may potentially be suppressed therapeutically (48).

We were surprised to discover that pRB's function with E2F1 and Condensin II was sensitive to gene dosage. Knudson's hypothesis, that both copies of *RBI* are lost during tumorigenesis (27), has greatly shaped our genetic understanding of cancer. In humans, hereditary retinoblastoma survivors

RESEARCH ARTICLE

Coschi et al.

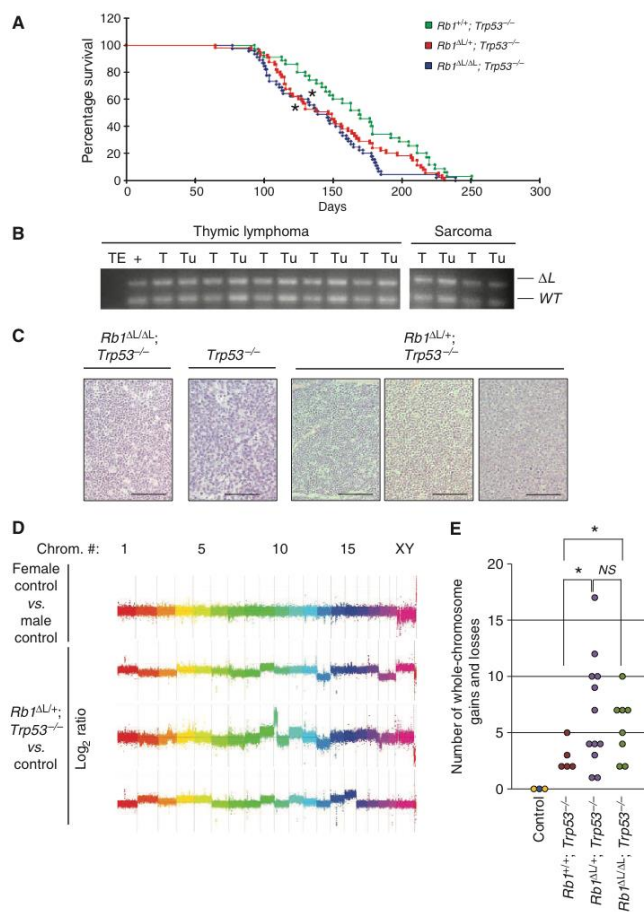


Figure 7. Haploinsufficiency of *Rb1* contributes to aneuploidy. **A**, Kaplan-Meier survival proportions are shown for *Rb1*^{ΔL/+};*Trp53*^{-/-} mice (*n* = 52). Previously reported data for *Rb1*^{ΔL/ΔL};*Trp53*^{-/-} and *Trp53*^{-/-} mice is included as a comparison. Asterisks indicate populations that are significantly different from the *Trp53*^{-/-} control (log-rank test, *P* < 0.05). **B**, *Rb1* tumor genotypes (Tu) were determined by PCR; matched tail DNA (T) is shown as a comparison. **C**, representative images of H&E-stained tumors from *Trp53*^{-/-} control, *Rb1*^{ΔL/ΔL};*Trp53*^{-/-}, and *Rb1*^{ΔL/+};*Trp53*^{-/-} compound mutants. Scale bars, 100 μm. **D**, control, or tumor DNA, was used for array comparative genomic hybridization (CGH). Representative graphs show log₂ ratio values plotted against chromosome number. Individual chromosomes are shown in different colors. **E**, whole-chromosome changes (among autosomes) for *Rb1*^{ΔL/+};*Trp53*^{-/-} tumors is plotted against their genotype. Previously reported control, *Trp53*^{-/-}, and *Rb1*^{ΔL/ΔL};*Trp53*^{-/-} data are shown for comparison. The control male versus control male hybridization is shown in blue; the male versus female hybridizations are shown in yellow. The means were compared between genotypes using a t test. *, *P* < 0.05. NS, not significant.

acquire early-onset second primary cancers more frequently than the general population (26). Thus, it is interesting to speculate that the underlying genomic instability we observe in *RBI*^{+/−} patient fibroblasts could contribute to this increased penetrance. The secondary tumors in retinoblastoma survivors are often sarcomas (26,49), which is consistent with the genome instability characteristics of mesenchymal cancers highlighted in this study.

Our data bring together concepts of replication and mitosis and demonstrate how abundance of a pRB-E2F1-Condensin II complex may link them. *RBI*^{+/−} patient fibroblasts are haploinsufficient in their ability to prevent the accumulation of γ H2AX and mitotic errors, suggesting that *RBI* haploinsufficiency in this functional context may contribute to tumorigenesis in humans.

METHODS

Cell Lines and Culture Methods

Primary MEFs were prepared and cultured according to standard methods. *Rb1*^{MGV/MG} and *Rb1*^{AS/AS} introduce R461E/K542E and F832A coding substitutions into the murine *Rb1* gene, respectively (41, 42). The generation of *Rb1*^{AS/AS} mice will be published elsewhere. Mitotic chromosome spreads were prepared and H2BGFP transduction of MEFs was as before (19). For DNA combing, cells were pulse-labeled for 30 minutes with CldUrd, followed by 30 minutes of IdUrd as described previously (50).

Primary patient fibroblasts were obtained from the Coriell Institute for Medical Research (Camden, NJ) and cultured as recommended. *RBI* genotyping was performed by Impact Genetics Inc. We created a FUtfw lentiviral vector that expresses H2BGFP for analysis of human fibroblasts. All cell lines and their culture conditions are described in the Supplementary Methods.

Staining and Microscopy

Stained cells were examined on an Olympus Fluoview FV1000 confocal microscope system, and z stacks at intervals of 7 μ m were collected using the Olympus Fluoview FV1000 Viewer. Collapsed and 3D rendered images were used to determine whether colocalization of γ H2AX foci coincided with pericentromeric DNA.

Live-cell microscopy was carried out as described previously (19). FISH analysis of aneuploidy and telomeres was carried out using previously reported methods (33). CldUrd and IdUrd staining of DNA fibers was carried out as described previously (50) with modifications described in the Supplementary Methods. Fork velocity was calculated as IdUrd length/time. Percentage asymmetry is [(long IdUrd track – short IdUrd track) – 1] \times 100.

ChIP and Analysis

Cycling cells were fixed in 1% formaldehyde, except ChIP experiments to detect PCNA, MCM3, and DNA Pol δ that were fixed in 1% formaldehyde and ethylene glycol bis[succinimidylsuccinate] (EGS). ChIP methods and the source of PCR primers are described in the Supplementary Methods. For ChIP-seq experiments, γ H2AX and CAP-D3 antibodies were used to precipitate chromatin, and 150 ng of DNA was used for library preparation and sequenced on an Illumina Hi-Seq 2000 at The Centre for Applied Genomics (Sick Kids, Toronto, ON, Canada). Unique sequence reads were aligned to the mm9 genome assembly or repeat containing indexes and analyzed as described in the Supplementary Methods. Raw sequence data are available in the Gene Expression Omnibus (GEO; GSE55041).

Western Blotting and Analysis of pRB, E2F1, and Condensin II

Nuclear extracts from the indicated cells were prepared as described previously (42). For isolation of pRB-E2F1-Condensin II complexes, a major satellite repeat probe was generated by PCR using a biotinylated primer. Extracts were mixed with the probe and complexes were precipitated using streptavidin dynabeads. Western blotting identified captured proteins. GST pull-downs were carried out by standard methods. Antibodies used in this study can be found in the Supplementary Methods.

Tumor Incidence and Genomic Analyses

The *Rb1*^{AS}-mutant strain (*Rb1*^{tm17ad}) has been previously described (33). The *Trp53*^{−/−} mice were obtained from The Jackson Laboratory. All animals were housed, handled, and analyzed as previously described (19). Tissues were processed for staining according to standard methods. Array comparative genomic hybridization (CGH) data were processed as previously reported (19), and are available in GEO (GSE51876). A list of cell line data analyzed from COSMIC is present in the Supplementary Methods.

Disclosure of Potential Conflicts of Interest

No potential conflicts of interest were disclosed.

Authors' Contributions

Conception and design: C.H. Coschi, F.A. Dick

Development of methodology: C.H. Coschi, C.A. Ishak, A. Marshall, S. Talluri, J. Wang, V. Percy, I. Welch, P.C. Boutros, F.A. Dick

Acquisition of data (provided animals, acquired and managed patients, provided facilities, etc.): C.A. Ishak, D. Gallo, S. Talluri, M.J. Cecchini, A.L. Martens, V. Percy, I. Welch

Analysis and interpretation of data (e.g., statistical analysis, biostatistics, computational analysis): C.H. Coschi, C.A. Ishak, D. Gallo, A. Marshall, S. Talluri, J. Wang, I. Welch, P.C. Boutros, G.W. Brown, F.A. Dick

Writing, review, and/or revision of the manuscript: C.H. Coschi, C.A. Ishak, P.C. Boutros, G.W. Brown, F.A. Dick

Administrative, technical, or material support (i.e., reporting or organizing data, constructing databases): C.A. Ishak, A. Marshall

Study supervision: P.C. Boutros, F.A. Dick

Acknowledgments

The authors thank Nathalie Bérubé and Kristin Kernohan for discussions and advice.

Grant Support

C.H. Coschi was a member of the Cancer Research and Technology Transfer (CaRTT) training program and was a Canadian Institutes of Health Research (CIHR) doctoral award recipient. D. Gallo was supported by an NSERC (PGS-D) award. A. Marshall holds a Natural Sciences and Engineering Research Council (NSERC) CGS-M fellowship. C.A. Ishak, S. Talluri, and M.J. Cecchini are also members of CaRTT, and M.J. Cecchini was supported by a CIHR MD/PHD award. F.A. Dick is the Wolfe Senior Fellow in Tumor Suppressor Genes. This study was conducted with support from the Ontario Institute for Cancer Research to P.C. Boutros through funding from the Government of Ontario and the CIHR to G.W. Brown (MOP79368) and F.A. Dick (MOP64253 and MOP89765).

The costs of publication of this article were defrayed in part by the payment of page charges. This article must therefore be hereby marked *advertisement* in accordance with 18 U.S.C. Section 1734 solely to indicate this fact.

RESEARCH ARTICLE

Coschi et al.

Received February 27, 2014; revised April 8, 2014; accepted April 12, 2014; published OnlineFirst April 16, 2014.

REFERENCES

- Harper JW, Elledge SJ. The DNA damage response: ten years after. *Mol Cell* 2007;28:739–45.
- Jackson SP, Bartek J. The DNA-damage response in human biology and disease. *Nature* 2009;461:1071–8.
- Torres-Rosell J, De Piccoli G, Cordon-Preciado V, Farmer S, Jarmuz A, Machin F, et al. Anaphase onset before complete DNA replication with intact checkpoint responses. *Science* 2007;315:1411–5.
- Lukas C, Savic V, Bekker-Jensen S, Doil C, Neumann B, Pedersen RS, et al. 53BP1 nuclear bodies form around DNA lesions generated by mitotic transmission of chromosomes under replication stress. *Nat Cell Biol* 2011;13:243–53.
- Aguilera A, Gomez-Gonzalez B. Genome instability: a mechanistic view of its causes and consequences. *Nat Rev Genet* 2008;9:204–17.
- Burrell RA, McClelland SE, Endesfelder D, Groth P, Weller MC, Shaikh N, et al. Replication stress links structural and numerical cancer chromosomal instability. *Nature* 2013;494:492–6.
- Dulev S, de Renty C, Mehta R, Minkov I, Schwob E, Strunnikov A. Essential global role of CDC14 in DNA synthesis revealed by chromosome underreplication unrecognized by checkpoints in *cdc14* mutants. *Proc Natl Acad Sci U S A* 2009;106:14466–71.
- Chan KL, Palmal-Pallag T, Ying S, Hickson ID. Replication stress induces sister-chromatid bridging at fragile site loci in mitosis. *Nat Cell Biol* 2009;11:753–60.
- Clemente-Blanco A, Mayan-Santos M, Schneider DA, Machin F, Jarmuz A, Tschochner H, et al. Cdc14 inhibits transcription by RNA polymerase I during anaphase. *Nature* 2009;458:219–22.
- Ide S, Miyazaki T, Maki H, Kobayashi T. Abundance of ribosomal RNA gene copies maintains genome integrity. *Science* 2010;327:693–6.
- Losada A, Hirano T. Dynamic molecular linkers of the genome: the first decade of SMC proteins. *Genes Dev* 2005;19:1269–87.
- Wang BD, Eyre D, Basrai M, Lichten M, Strunnikov A. Condensin binding at distinct and specific chromosomal sites in the *Saccharomyces cerevisiae* genome. *Mol Cell Biol* 2005;25:7216–25.
- Ono T, Yamashita D, Hirano T. Condensin II initiates sister chromatid resolution during S phase. *J Cell Biol* 2013;14:518–28.
- Bertoli C, Skotheim JM, de Bruin RA. Control of cell cycle transcription during G₁ and S phases. *Nat Rev Mol Cell Biol* 2013;14:518–28.
- Knudsen KE, Booth D, Naderi S, Sever-Chroneos Z, Fribourg AF, Hunton IC, et al. RB-dependent S-phase response to DNA damage. *Mol Cell Biol* 2000;20:7751–63.
- Avni D, Yang H, Martelli F, Hofmann F, ElShamy WM, Ganesan S, et al. Active localization of the retinoblastoma protein in chromatin and its response to S phase DNA damage. *Mol Cell* 2003;12:735–46.
- Wells J, Yan PS, Cechvala M, Huang T, Farnham PJ. Identification of novel pRB binding sites using CpG microarrays suggests that E2F recruits pRB to specific genomic sites during S phase. *Oncogene* 2003;22:1445–60.
- Mendoza-Maldonado R, Paolinelli R, Galbiati L, Giadrossi S, Giacca M. Interaction of the retinoblastoma protein with Orc1 and its recruitment to human origins of DNA replication. *PLoS ONE* 2010;5:e13720.
- Coschi CH, Martens AL, Ritchie K, Francis SM, Chakrabarti S, Berube NG, et al. Mitotic chromosome condensation mediated by the retinoblastoma protein is tumor-suppressive. *Genes Dev* 2010;24:1351–63.
- Longworth MS, Herr A, Ji JY, Dyson NJ. RBF1 promotes chromatin condensation through a conserved interaction with the Condensin II protein dCAP-D3. *Genes Dev* 2008;22:1011–24.
- Manning AL, Longworth MS, Dyson NJ. Loss of pRB causes centromere dysfunction and chromosomal instability. *Genes Dev* 2010;24:1364–76.
- van Harn T, Foijer F, van Vugt M, Banerjee R, Yang F, Oostra A, et al. Loss of Rb proteins causes genomic instability in the absence of mitogenic signaling. *Genes Dev* 2010;24:1377–88.
- Manning AL, Dyson NJ. RB: mitotic implications of a tumour suppressor. *Nat Rev Cancer* 2012;12:220–6.
- Nicolay BN, Gameiro PA, Tschop K, Korenjak M, Heilmann AM, Asara JM, et al. Loss of RBF1 changes glutamine catabolism. *Genes Dev* 2013;27:182–96.
- Reynolds MR, Lane AN, Robertson B, Kemp S, Liu Y, Hill BG, et al. Control of glutamine metabolism by the tumor suppressor Rb. *Oncogene* 2014;33:556–66.
- Abramson DH, Ellsworth RM, Zimmerman LE. Nonocular cancer in retinoblastoma survivors. *Trans Sect Ophthalmol Am Acad Ophthalmol Otolaryngol* 1976;81:454–7.
- Knudson AGJ. Mutation and cancer: statistical study of retinoblastoma. *Proc Natl Acad Sci U S A* 1971;68:820–3.
- Jacks T, Fazeli A, Schmitt EM, Bronson RT, Goodell MA, Weinberg RA. Effects of an Rb mutation in the mouse. *Nature* 1992;359:295–300.
- Williams BO, Remington L, Albert DM, Mukai S, Bronson RT, Jacks T. Cooperative tumorigenic effects of germline mutations in Rb and p53. *Nat Genet* 1994;7:480–4.
- Zheng L, Flesken-Nikitin A, Chen PL, Lee WH. Deficiency of retinoblastoma gene in mouse embryonic stem cells leads to genetic instability. *Cancer Res* 2002;62:2498–502.
- Gonzalez-Vasconcellos I, Anastasov N, Sanli-Bonazzi B, Klymenko O, Atkinson MJ, Rosemann M. Rb1 haploinsufficiency promotes telomere attrition and radiation-induced genomic instability. *Cancer Res* 2013;73:4247–55.
- Pickering MT, Kowalik TF. Rb inactivation leads to E2F1-mediated DNA double-strand break accumulation. *Oncogene* 2006;25:746–55.
- Isaac CE, Francis SM, Martens AL, Julian LM, Seifried LA, Erdmann N, et al. The retinoblastoma protein regulates pericentric heterochromatin. *Mol Cell Biol* 2006;26:3659–71.
- Talluri S, Isaac CE, Ahmad M, Henley SA, Francis SM, Martens AL, et al. A G₁ checkpoint mediated by the retinoblastoma protein that is dispensable in terminal differentiation but essential for senescence. *Mol Cell Biol* 2010;30:948–60.
- Kim JA, Kruhlik M, Dotiwala F, Nussenzweig A, Haber JE. Heterochromatin is refractory to gamma-H2AX modification in yeast and mammals. *J Cell Biol* 2007;178:209–18.
- Dominguez-Sanchez MS, Barroso S, Gomez-Gonzalez B, Luna R, Aguilera A. Genome instability and transcription elongation impairment in human cells depleted of THO/TREX. *PLoS Genet* 2011;7:e1002386.
- Lossaint G, Larroque M, Ribeyre C, Bec N, Larroque C, Decaillet C, et al. FANCD2 binds MCM proteins and controls replisome function upon activation of S phase checkpoint signaling. *Mol Cell Biol* 2013;33:678–90.
- Samoshkin A, Dulev S, Loukinov D, Rosenfeld JA, Strunnikov AV. Condensin dysfunction in human cells induces nonrandom chromosomal breaks in anaphase, with distinct patterns for both unique and repeated genomic regions. *Chromosoma* 2012;121:191–9.
- Chong JL, Wenzel PL, Saenz-Robles MT, Nair V, Ferrey A, Hagan JP, et al. E2F1-3 switch from activators in progenitor cells to repressors in differentiating cells. *Nature* 2009;462:930–4.
- Dick FA, Dyson N. pRB contains an E2F1-specific binding domain that allows E2F1-induced apoptosis to be regulated separately from other E2F activities. *Mol Cell* 2003;12:639–49.
- Cecchini MJ, Thwaites M, Talluri S, Macdonald JJ, Passos DT, Chong JL, et al. A retinoblastoma allele that is mutated at its common E2F interaction site inhibits cell proliferation in gene targeted mice. *Mol Cell Biol* 2014;34:2029–45.
- Cecchini MJ, Dick FA. The biochemical basis of CDK phosphorylation-independent regulation of E2F1 by the retinoblastoma protein. *Biochem J* 2011;434:297–308.
- Julian LM, Palander O, Seifried LA, Foster JE, Dick FA. Characterization of an E2F1-specific binding domain in pRB and its implications for apoptotic regulation. *Oncogene* 2008;27:1572–9.
- Forbes SA, Tang G, Bindal N, Bamford S, Dawson E, Cole C, et al. COSMIC (the Catalogue of Somatic Mutations in Cancer): a resource

- to investigate acquired mutations in human cancer. *Nucleic Acids Res* 2010;38:D652-7.
45. Gordon DJ, Resio B, Pellman D. Causes and consequences of aneuploidy in cancer. *Nat Rev Genet* 2012;13:189-203.
 46. Beroukhi R, Mermel CH, Porter D, Wei G, Raychaudhuri S, Donovan J, et al. The landscape of somatic copy-number alteration across human cancers. *Nature* 2010;463:899-905.
 47. Crasta K, Ganem NJ, Dagher R, Lantermann AB, Ivanova EV, Pan Y, et al. DNA breaks and chromosome pulverization from errors in mitosis. *Nature* 2012;482:53-8.
 48. Manning AL, Yazinski SA, Nicolay B, Bryll A, Zou L, Dyson NJ. Suppression of genome instability in pRB-deficient cells by enhancement of chromosome cohesion. *Mol Cell* 2014;53:993-1004.
 49. Friend SH, Horowitz JM, Gerber MR, Wang XF, Bogenmann E, Li FP, et al. Deletions of a DNA sequence in retinoblastomas and mesenchymal tumors: organization of the sequence and its encoded protein. *Proc Natl Acad Sci U S A* 1987;85:2234-8.
 50. Yang J, O'Donnell L, Durocher D, Brown GW. RMI1 promotes DNA replication fork progression and recovery from replication fork stress. *Mol Cell Biol* 2012;32:3054-64.

Appendix D: List of primers used

Primer	Primer Sequence (5'-3')	Primer Use	Source
Maj_F1	GACGACTTGAAAAATGACG AAATC	qRT-PCR, qPCR	(Martens et al., 2005)
Maj_R1	CATATCCAGGTCCTTCAGT GTGC	qRT-PCR, qPCR	(Martens et al., 2005)
IAP LTR_F	TTGATAGTTGTGTTTTAAGT GGTAAATAAA	qRT-PCR, qPCR	(Martens et al., 2005)
IAP LTR_R	AAAACACCACAAACCAAAA TCTTCTAC	qRT-PCR, qPCR	(Martens et al., 2005)
L1 5' UTR_F	CTGCCTTGCAAGAAGAGAGC	qRT-PCR, qPCR	(Montoya-Durango et al., 2009)
L1 5' UTR_R	AGTGCTGCGTTCTGATGATG	qRT-PCR, qPCR	(Montoya-Durango et al., 2009)
L1 ORF1_F	AGATCTGGAACCATAGATG	qRT-PCR	(De Cecco et al., 2013)
L1 ORF1_R	TTCTCATTGTGTCCTGGATT	qRT-PCR	(De Cecco et al., 2013)
L1 ORF2_F	ACTTCCCAAATCTTAAA	qRT-PCR	(Puszyk et al., 2013)
L1 ORF2_R	AAAAGTCTGGTGTAATT	qRT-PCR	(Puszyk et al., 2013)
IFN α _F	TGCAATGACCTCCATCAGCA	qRT-PCR	(Schneider et al., 2008)
IFN α _R	TTCCTGGGTCAGAGGAGGTT C	qRT-PCR	(Schneider et al., 2008)
IFN- β 1_F	CTGGAGCAGCTGAATGGAA AG	qRT-PCR	(Schneider et al., 2008)
IFN- β 1_R	CTCCGTCATCTCCATAGGGA TCT	qRT-PCR	(Schneider et al., 2008)
β -act_9F	CTGGCTCCTAGCACCATGAA GATC	qRT-PCR	(Matsui et al., 2010)

β -act_5R	TGCTGATCCACATCTGCTGG	qRT-PCR	(Matsui et al., 2010)
Ccne1_F1	AGCGAGGATAGCAGTCAGC C	qRT-PCR	(Pandit et al., 2012)
Ccne1_R1	GGTGGTCTGATTTTCCGAGG	qRT-PCR	(Pandit et al., 2012)
Ccna2_F1	CTTCTTCCTTTTCCCTTGCC	qRT-PCR	(Pandit et al., 2012)
Ccna2_R1	TTTCAGAGTCCCAGTGACCC	qRT-PCR	(Pandit et al., 2012)
Rbl1_F	TTCCTGTGAAGAAGTTATAT TCCCT	qRT-PCR	(Pandit et al., 2012)
Rbl1_R	CTGTAGCGCTCATGGACAGA	qRT-PCR	(Pandit et al., 2012)
Cdt1_F1	ACAGCCGGGCAAGATCCCCT	qRT-PCR	(Pandit et al., 2012)
Cdt1_R1	GGCTCCCAACTTCCGTGCC	qRT-PCR	(Pandit et al., 2012)
Mcm6_F1	CCTGTGAATAGGTTCAACGG C	qRT-PCR	(Pandit et al., 2012)
Mcm6_R1	CATTTTCCTGAGGTGGAGCA C	qRT-PCR	(Pandit et al., 2012)
Mcm3_TSS_F	ATCCAGGAAGTCCAAGTAGT CTCTC	qPCR	(Cecchini et al., 2014)
Mcm3_TSS_R	TTGAAGTGGTTAGCCAATCA TAACG	qPCR	(Cecchini et al., 2014)
Mcm3_-2kb_F	GCCAAGGCAAAACAACAAT TTCTAC	qPCR	(Cecchini et al., 2014)
Mcm3_-2kb_R	CTATCTCTTTGATTTTGGGTG GCTG	qPCR	(Cecchini et al., 2014)
Gapdh_F	GAGCCAGGGACTCTCCTTTT	qPCR	(Cecchini et al., 2014)
Gapdh_R	CTGCACCTGCTACAGTGCTC	qPCR	(Cecchini et al.,

			2014)
H19_ICR_d_F	CTGCAAACAATTCTGAAACT GC	qPCR	(Kernohan et al., 2010)
H19_ICR_d_R	TCTGCTTTTAACAAGGCTCT CC	qPCR	(Kernohan et al., 2010)
IAP_F1	TTGATAGTTGTGTTTTAAGT GGTAAATAAA	Bisulfite	(Lane et al., 2003)
IAP_R1	AAAACACCACAAACCAAAA TCTTCTAC	Bisulfite	(Lane et al., 2003)
IAP_F2	TTGTGTTTTAAGTGGTAAAT AAATAATTTG	Bisulfite	(Lane et al., 2003)
IAP_R2	CAAAAAAAAAACACACAAACC AAAAT	Bisulfite	(Lane et al., 2003)
L1_F1	AGAAGAGAGTTTGTGTGTAG AGA	Bisulfite	this study
L1_R1	ACACCTAAAATTCTCTCTTC CA	Bisulfite	this study
L1_F2	AGAAGAGAGTTTGTGTGTAG AGA	Bisulfite	this study
L1_R2	TCATTTCCATCACCTATTTAA CT	Bisulfite	this study
PCNA_E2F_F	CAGAGTAAGCTGTACCAAG GAGAC	qRT-PCR	(Cecchini et al., 2014)
PCNA_E2F_R	CGTTCCTCTTAGAGTAGCTC TCATC	qRT-PCR	(Cecchini et al., 2014)
PCNA_-2kb_F	CATCAGTGAATACGTCTCTG TTCCA	qRT-PCR	(Cecchini et al., 2014)
PCNA_-2kb_R	CTGCTTCTCAGTTGTTTTAGG AAGG	qRT-PCR	(Cecchini et al., 2014)

Appendix E: List of plasmids used

Plasmid Name	Source	Description
cep99-gfp-L1SM	Jef Boeke	full-length synthetic mouse LINE element (SM L1)
cep99-gfp-TGF21	John Moran	full-length endogenous L1
pEF.myc.ER-E2-Crimson	Addgene	Crimson reporter
pBABE-H2B-GFP	Fred Dick	H2B-GFP Mammalian Expression vector, Retroviral
pBSK-Rb25	Fred Dick	<i>Rbl</i> ^S targeting vector encoding an F832A substitution in <i>Rbl</i> exon 24, and a floxed PGK-neomycin cassette.

Appendix F: List of antibodies used

Antibody	Target	Source	ChIP (Ab:Chr)	WB	IP (Ab:extract)
C-15	pRb	Santa Cruz	5 µg : 80 µg		
M-153	pRb	Santa Cruz	5 µg : 80 µg	1:1000	
M-136	pRb	(Cecchini et al., 2014)	5 µg : 80 µg		5 µg : 1 mg
S855	pRb	(Cecchini et al., 2014)(Cecchini et al., 2014)	5 µg : 80 µg	1:1000	
Hyb4.1	pRb	Developmental Studies Hybridoma Bank	500 µl : 80 µg		
D2C9	Ezh2	Cell Signaling	5 µg : 80 µg	1:1000	4 µg : 1.5 mg
D39F6	Suz12	Cell Signaling		1:1000	
C-19	Hdac1	Santa Cruz		1:1000	
06-942	H3K9Ac	Millipore	4 µg : 30 µg	1:1000	
07-449	H3K27me3	Millipore	4 µg : 30 µg		
07-442	H3K9me3	Millipore	4 µg : 30 µg		

07-463	H4K20me3	Millipore	4 µg : 30 µg		
ab1791	H3	abcam		1:2000	
M-300	L1_ORF2p	Santa Cruz		1:1000	
C-20	p130	Santa Cruz		1:1000	
C-18	p107	Santa Cruz		1:1000	
4012S	Mcm3	Cell Signaling		1:1000	
H432	Cyclin A	Santa Cruz		1:1000	
A2066	Actin	SIGMA		1:3000	
11H10	Tubulin	Cell Signaling		1:2000	
05-636	H2A.X pSer139	Millipore			
A300-244A	RPA32	Bethyl labs		1:1000	
A300-246A	RPA32 pSer33	Bethyl labs		1:1000	
F-2	PCNA	Santa Cruz		1:1000	
C-20	BubR1	Santa Cruz		1:1000	
ab7953	Cdk1	abcam		1:1000	
C-19	Mad2	Santa Cruz		1:1000	
	CAP-D3	Dick lab	5 µg : 80 µg	1:1000	
	SMC2	Dick lab		1:1000	

Appendix G: PCR Conditions

PCR Conditions *p53*

Master Mix per reaction

- 1 μ L MgCl₂ (50mM)
- 2.5 μ L dNTPs (2mM)
- 2.5 μ L 10X PCR Buffer (200mM Tris pH8, 500mM KCl)
- 0.62 μ L 20 μ M AM3 primer
- 0.62 μ L 20 μ M AM4 primer
- 0.27 μ L 20 μ M neo-sense primer
- 0.27 μ L 20 μ M neo-antisense primer
- 11 μ L Water
- 0.5 μ L Taq (5units/ μ L)
- Total 18 μ L
- + 2 μ L DNA sample

Reaction Conditions

Program – P53 New

- | | | |
|----|-------------------------|-------|
| 1. | 94°C | 2:30 |
| 2. | 94°C | 0:30 |
| 3. | 58°C | 0:30 |
| 4. | 72°C | 1:10 |
| 5. | Go to Step #2, 29 times | |
| 6. | 72°C | 10:00 |
| 7. | 12°C | hold |

Expected Results:

Mutant (**Null**) = 424 bp
Wild type = 548 bp

Primers

AM3: ATAGGTCGGCGGTTTCAT
AM4: CCCGAGTATCTGGAAGACAG
Neo-sense:
GGAAGGGACTGGCTGCTATTG
Neo-antisense:
CAATATCACGGGTAGCCAACG

PCR Conditions *Rb1^S*

Master Mix per reaction

- 0.5 μ L MgCl₂ (50mM)
- 2 μ L dNTPs (2mM)
- 2 μ L 10X PCR Buffer (200mM Tris pH8, 500mM KCl)
- 1 μ L 20 μ M Rb1S_F
- 1 μ L 20 μ M Rb1S_R
- 11 μ L Water
- 0.5 μ L Taq (5units/ μ L)
- Total 18 μ L
- + 2 μ L DNA sample

Reaction Conditions

Program – Rb1S_GENO

- | | | |
|----|-------------------------|------|
| 1. | 94°C | 2:00 |
| 2. | 94°C | 0:45 |
| 3. | 57°C | 0:45 |
| 4. | 72°C | 0:45 |
| 5. | Go to Step #2, 39 times | |
| 6. | 72°C | 5:00 |
| 7. | 12°C | hold |

Expected Results:

Mutant = 254 bp
Wild type = 153 bp

Primers

Rb1S_F:
ATGCATAGCTGCTGTCATCC
Rb1S_R:
GACTGTTGGCCAGTTTGGTT

Curriculum Vitae

CHARLES ALLAN ISHAK

EDUCATION

PhD Candidate **2011 - 2017**

Biochemistry

Western University Department of Biochemistry

PhD Supervisor: Dr. Fred Dick

H.BSc **2006 - 2010**

Specialist: Molecular Biology; Minor: Chemistry

University of Toronto

Honors Thesis Supervisor: Dr. Danton O'Day

Honors Thesis: Exploring the role of calcium in the regulation of nuclear number in *Dictyostelium discoideum*

AWARDS AND SCHOLARSHIPS

Lucille & Norton Wolf Publication Award: Epigenetics **2017**

Lawson Health Research Institute (\$1000)

Lawson Leadership Impact Award **2017**

Lawson Health Research Institute (\$1000)

WORLDiscoveries Scholarship for Commercialization and Entrepreneurship **2016**

WORLDiscoveries (\$500 project grant and research translation consultation)

Strategic Training Program in Cancer Research and Technology Transfer **2013 -**

Canadian Institute of Health Research (\$21,000/year)

2015

Dean's MSc to PhD Transfer Scholarship **2012 -**

Schulich School of Medicine and Dentistry (\$5000/year)

2016

University of Toronto Entrance Scholarship **2006**

University of Toronto (\$1000)

PUBLICATIONS

Ishak CA, Marshall AE, Passos DT, White CR, Kim SJ, Cecchini MJ, Ferwati S, MacDonald WA, Howlett CJ, Welch ID, Rubin SM, Mann MRW, Dick FA. An RB-EZH2 complex mediates silencing of repetitive DNA sequences. *Molecular Cell*. 2016 Dec;64(6):1074-87.

Cecchini MJ, **Ishak CA**, Passos DT, Warner A, Palma DA, Howlett CJ, Driman DK, Dick FA. Loss of the retinoblastoma tumor suppressor correlates with improved outcome in patients with lung adenocarcinoma treated with surgery and chemotherapy. *Human Pathology*. 2015 Dec;46(12):1922-34.

Ishak CA, Dick FA. Conditional haploinsufficiency of the retinoblastoma tumor suppressor gene. *Molecular & Cellular Oncology*. 2014 Oct 30;2(1):e968069.

Coschi CH, **Ishak CA**, Gallo D, Marshall A, Talluri S, Wang J, Cecchini MJ, Martens AL, Percy V, Welch I, Boutros PC, Brown GW, Dick FA. Haploinsufficiency of an RB-E2F1-Condensin II complex leads to aberrant replication and aneuploidy. *Cancer Discovery*. 2014 Jul;4(7):840-53.

Forristal C, Henley SA, MacDonald JI, Bush JR, Ort C, Passos DT, Talluri S, **Ishak CA**, Thwaites MJ, Norley CJ, Litovchick L, DeCaprio JA, DiMattia G, Holdsworth DW, Beier F, Dick FA. Loss of the mammalian DREAM complex deregulates chondrocyte proliferation. *Molecular and Cellular Biology*. 2014 Jun;34(12):2221-34.

MANUSCRIPTS IN REVIEW/SUBMITTED

Ishak CA, Coschi CH, Roes M, Dick FA. Disruption of CDK-resistant chromatin association by pRB causes DNA damage, mitotic errors, and reduces Condensin II recruitment. (In review at *Cell Cycle*)

Ishak CA, Cecchini MJ, Dick FA. Analysis of the retinoblastoma protein by Immunohistochemical techniques. (Submitted to *Methods in Molecular Biology*)

INTERNATIONAL AND NATIONAL MEETINGS

Ishak CA, Marshall AE, Passos DT, White CR, Cecchini MJ, Ferwati S, MacDonald WA, Mann MRW, Dick FA. The E1A-insensitive pRB-E2F1 complex silences endogenous retroviruses. ICEGB DNA Tumor Virus Meeting, Trieste, Italy
*Selected for oral presentation

2015

Ishak CA, Passos DT, Ferwati S, Marshall AE, Dick FA. Alternate pRB-E2F1 complexes silence repetitive elements. The 2nd Canadian Conference on Epigenetics: Epigenetics, Eh! London, ON, Canada **2014**
 *Selected for oral presentation

LOCAL MEETINGS

Ishak CA, Passos DT, Coschi CH, Ferwati S, Marshall AE, Dick FA. Alternate pRB-E2F1 complexes regulate repetitive genomic elements to preserve genome stability. Department of Oncology Research and Education Day. London, ON, Canada **2014**
 *Selected for poster award

Ishak CA, Passos DT, Dick FA. Alternate pRB-E2F1 complexes regulate repetitive genomic elements to preserve genome stability. Department of Oncology Research and Education Day. London, ON, Canada **2013**
 *Selected for oral presentation

Ishak CA, Passos DT, Dick FA. Alternate pRB-E2F1 complexes regulate repetitive genomic elements to preserve genome stability. London Health Research Day. London, ON, Canada **2013**
 *Selected for oral presentation

Ishak CA, Passos DT, Dick FA. Investigation of a unique pRB-E2F1 complex in development and disease. Department of Oncology Research and Education Day. London, ON, Canada **2012**
 *Selected for poster award

PROFESSIONAL ACTIVITIES AND LEADERSHIP

Department of Oncology Strategic Planning Steering Committee **2016**

- Sole basic research trainee selected to meet consultants, clinicians, scientists
- Organized trainee focus group to identify deficits in training resources
- Ensured trainees' infrastructure concerns addressed by research task force
- Efforts will culminate in the creation of a 5-10 year steering committee plan

Keynote Speaker Session Chair **2014, 2016**

- Department of Oncology Research and Education Day Meeting
- Identified and recruited high-profile speaker on behalf of selection committee
- Worked with administration to plan travel, accommodations, and itinerary
- Introduced speaker and chaired question period during keynote session
- Speakers hosted: Dr. Douglas Levine, Dr. Elaine Mardis

- Victoria Research Laboratories Bioinformatics Group (co-founder)** **2016-**
- Co-founded group to improve bioinformatics resources and support off campus
 - Organized meetings attended by both trainees and principle investigators
 - Extended collaboration amongst analogous groups at multiple institutions
- Canadian Cancer Society Research Information Outreach Team** **2013-2017**
- Published ‘Promise & Progress in Research’ news article on funding outcomes
 - Assisted with ‘Let’s Talk Cancer’ genomics tutorial for high school students
 - Interviewed for televised ‘Promise in Cancer: Young Researcher Series’
- Undergraduate Student Mentorship** **2008-2017**
- Led graduate school webinar at Michael Power – St. Joseph high school
 - Directly guided student throughout entire undergraduate research placement
 - Served as an exam proctor for the Department of Biochemistry at Western
 - Laboratory technician assistant for the University of Toronto Dept. of Biology
 - Prepared of practicums and maintained laboratory glassware
 - University of Toronto Dept. of Psychology PSY100 teaching lab volunteer
 - Assisted students with troubleshooting computer-based modules